Seismic Hazard Analysis using Mapping Techniques for Underground, Narrow-Vein Metal Mines

by

Eliot Reimer

A thesis submitted in partial fulfillment
of the requirements for the degree of
Master's of Applied Science (M.A.Sc)
in Natural Resources Engineering

Faculty of Graduate Studies,
Laurentian University
Sudbury, Ontario, Canada

THESIS DEFENCE COMMITTEE/COMITÉ DE SOUTENANCE DE THÈSE
Laurentian Université/Université Laurentienne
Faculty of Graduate Studies/Faculté des études supérieures

Title of Thesis Titre de la thèse	Seismic Hazard Analysis using Mapping Techniques for Underground, Narrow-Vein Metal Mines
Name of Candidate Nom du candidat	Reimer, Eliot
Degree Diplôme	Master of Science
Department/Program Département/Programme	Engineering
Date of Defence Date de la soutenance	February 09, 2018

APPROVED/APPROUVÉ

Thesis Examiners/Examinateurs de thèse:

Dr. Marty Hudyma
(Supervisor/Directeur de thèse)

Dr. Ming Cai
(Committee member/Membre du comité)

Dr. Eugene Ben-Awuah
(Committee member/Membre du comité)

Dr. John Henning
(External Examiner/Examinateur externe)

Approved for the Faculty of Graduate Studies
Approuvé pour la Faculté des études supérieures
Dr. David Lesbarrères
Monsieur David Lesbarrères
Dean, Faculty of Graduate Studies
Doyen, Faculté des études supérieures

ACCESSIBILITY CLAUSE AND PERMISSION TO USE

Thesis Abstract

This thesis investigates the ability to forecast the occurrence of large events through node-based hazard mapping at KGHM's Morrison Mine located in Levack, ON. Node-based hazard maps function by pasting a heat-map onto a solid model of mine workings to identify, visually, the areas that have experienced high levels of seismicity. The notion within this research is that it is possible to forecast the occurrence of large seismic events with a reasonable degree of effectiveness using a trailing period of 6-months and a forecast period of the following 2-months. Using the following parameters, each hazard map has been analyzed over three different forecast periods:

- Cumulative Seismic Energy
- Cumulative Seismic Moment
- Number of Events > Defined Magnitude
    - M > 0
    - M > -0.5
    - M > -1
- Number of Events > Apparent Stress, 80^{th} percentile

The forecast periods analyzed were April – June 2016, June – August 2016, and August – October 2016 with a success rate (the number of events successfully forecasted) between 38% and 67% and false alarm rates (the number of denoted hazard areas that did not experience large events in the forecast period) between 41% and 65%.

Keywords: Seismicity, Mining, Seismic Energy, Seismic Moment, Apparent Stress, Seismic Hazard, Seismic Hazard Mapping,

Acknowledgements

I would like to thank Dr. Marty Hudyma for the opportunity to conduct this research. Without his guidance and support, this body of work would not have been possible.

Additional thanks are extended to the mine personnel at Morrison Mine for their support and the allowance to spend time on-site in the ground control department. This helped establish the foreknowledge needed to conduct this research.

Financial support was provided by KGHM, the Natural Sciences and Engineering Research Council of Canada (NSERC), the Australian Centre for Geomechanics (ACG), and the Goodman School of Mines.

Table of Contents

Table of Figures

List of Tables

1 Introduction

The old adage states 'If it's not grown, it has to be mined'-Unknown. A 2015 estimate provided by the World Mining Congress states that approximately 17 billion tonnes of mineral raw materials were extracted that year (Reichl, Schatz and Zsak, 2017). In Canada as of 2014, there were 1209 active mines, including metal and non-metal operations. In terms of metal mines, Quebec has the most at 26 and Ontario following with 19 active metal mines (Marshall, 2015). As near-surface deposits are depleted, mines around the world are moving deeper where stresses in the rock are greater and overall conditions are poorer. Mines such as Vale's Creighton Mine, Glencore's Kidd Creek Mine, and Agnico Eagle's LaRonde Mine are currently approaching 3km deep and each experience significant problems in terms of ground conditions. One major component within the assessment of ground conditions, as is the responsibility of the mines' ground control department, is the recording and analysis of dynamic rock mass failure or seismic activity. The focus of this thesis is hazard assessment using seismic data from KGHM's Morrison Mine located in Levack, Ontario.

1.1 Seismic Activity in a Mining Context

In mines that are deep, extensive, and/or geologically complex, seismic activity is unavoidable. Much of the seismicity observed in mines is induced either directly or indirectly through mining activity. As excavations are created in the rock mass, the local state of stress around mine openings is altered. In this case the state of stress around an opening is the sum of the ambient stress (corresponding to the weight of overburden) and stresses induced by mining (Gibowicz and Kijko, 1994).

Induced seismicity can be the result of numerous activities including surface quarrying, deep-level mining, the filling of water reservoirs behind dams, and the injection and/or extraction of fluids into or out of the rock mass. In the interest of safety, out of the causes previously listed, mining-induced seismic activity is the most severe and can manifest as violent ejections of rock from the roof, walls, and floor of mine excavations (Cook 1976;

cited in Gibowicz and Kijko, 1994). This problem is compounded as mines plunge deeper into Earth's crust.

With the advent of seismic monitoring technology, the ability for mining operations to assess seismicity is possible. With a proper, functional seismic system, data can be collected and further analyzed to assess the current and past states of seismic activity as well, in the interest of mine planning, the likelihood in space and time of the occurrence of seismicity above a certain magnitude. This is known as seismic hazard and the assessment of such is the focus of this thesis.

1.2 Research Scope

This thesis aims to use hazard assessment as a tool for forecasting the occurrence of a 'large' seismic event. For the purposes of this research, a large event is defined as being above 0 Moment Magnitude (M_w). The data used in this thesis is taken from KGHM's Morrison Mine in Sudbury Ontario; a relatively deep, narrow-vein copper operation. The means by which hazard is assessed is both numerically and visually with an emphasis on the latter. In the interest of visual assessment, hazard mapping using the Australian Centre for Geomechanics (ACG) mXrap™ program is used and is discussed at length in Chapter 2 (Section 2.6.3) and Chapter 4 (Section 4.1.2). The premise in forecasting is to use a defined trailing time period and in the case of this thesis the trailing periods used are 6months in length, the justification for which is given in Chapter 4 (Section 4.1.1). The forecast period has been defined as being 2 months which is also presented in Chapter 4 (Section 4.1.1).

1.3 Research Approach

The approaches used to assess seismic hazard, in the interest of forecasting are outlined below:

1. A counting approach: Using moment magnitude and apparent stress above the mine-wide 80th percentile, the number of events above a certain magnitude and the number above the 80th percentile of apparent stress are assessed over a

trailing period, within a search radius to define a value to indicate whether or not an event above 0 moment magnitude will occur in the forecast period

2. A cumulative approach: Using ∑energy and ∑moment, each value is assessed over a trailing period, within a search radius to define a value to indicate whether or not an event above 0 moment magnitude will occur in the forecast period

The rationale for using such approaches is further discussed in Chapter 4 (Section 4.3.2) and the results of these analysis techniques are discussed in Chapter 5 (Section 5.1).

1.4 Thesis Structure

The structure of this thesis is as follows:

Chapter 1 frames the need for this type of research and describes the scope and purpose of this thesis.

Chapter 2 is a review of the literature pertinent in understanding this body of work. Concepts such as rock stress and mining-induced seismicity are discussed along with the basic seismic source parameters. Seismic data analysis techniques are presented along with seismic hazard assessment as well as the focus of this thesis, seismic hazard analysis through mapping techniques.

Chapter 3 provides a background of Morrison Mine including the mine's history, geology and mining methods. General trends in seismicity at the mine are also discussed.

Chapter 4 describes hazard assessment methodologies used namely the concept of an event count and cumulative value in terms of a seismic parameter mapped onto mine workings for hazard forecasting. The parameters chosen for hazard assessment (energy, moment, magnitude, and apparent stress) are discussed along with a justification for the choice in parameter. Further to this, examples of each methodology are provided.

Chapter 5 is a discussion of the results including the core results of each hazard map, the effects of varying the trailing and forecast time windows, the impact of mining on the hazard maps, and the ability to forecast large seismic events using the present methodologies as discussed in Chapter 4.

Chapter 6 provides a summary of the thesis.

2 Literature Review

2.1 Rock Stress and Seismic Events

Stress is a term used to describe the intensity of internal forces in a body due to applied surface or outside forces, in this case within a rock mass (Brady and Brown, 2004). Stress is the measure of force per unit area called Pascals (N/m^2). There are numerous causes for stress most notably the weight of the overlying rock which creates a vertical stress that is proportional to depth. There is also a horizontal component to stress that is a result of Poisson's Effect, $\sigma_v/(m-1)$, where σ_v is the vertical stress and 'm' is the Poisson's ratio (Morrison, 1970). Other effects such as orogenic tectonics and the conditions during the formation of the host rock also play a role in determining the orientations of the principal stresses. These principal stresses are classified as major ($\sigma1$), intermediate ($\sigma2$), and minor ($\sigma3$) (Brady and Brown, 2004).

Numerous studies over the last 40 years in the Sudbury Basin have been undertaken to determine the regional stress tensor, or principal stress orientations and gradient. Understanding the orientations of these stresses is a key input in mine design. Research conducted by Grabinsky (1997), cited in Suorineni and Malek (2014) indicates that historical in situ stress measurements carry errors in magnitude of +/- 15 to 30% and in orientation of +/- 15 to 30°. R ecent investigations by Suorineni and Malek (2014) indicate that the evaluation of the Sudbury Basin stress tensor is still a work in progress, yet from this body of work a number of conclusions can been made regarding the Sudbury Basin stress tensor. First, $\sigma3$ is likely sub-vertical and is significantly less in magnitude than originally thought. Second, $\sigma1$ is oriented sub-horizontally at around N82°E, compared from older estimates at N65°E (Suorineni and Malek 2014). The following figure shows roughly the stress directions acting on an excavation in the Sudbury Basin (see Figure 1):

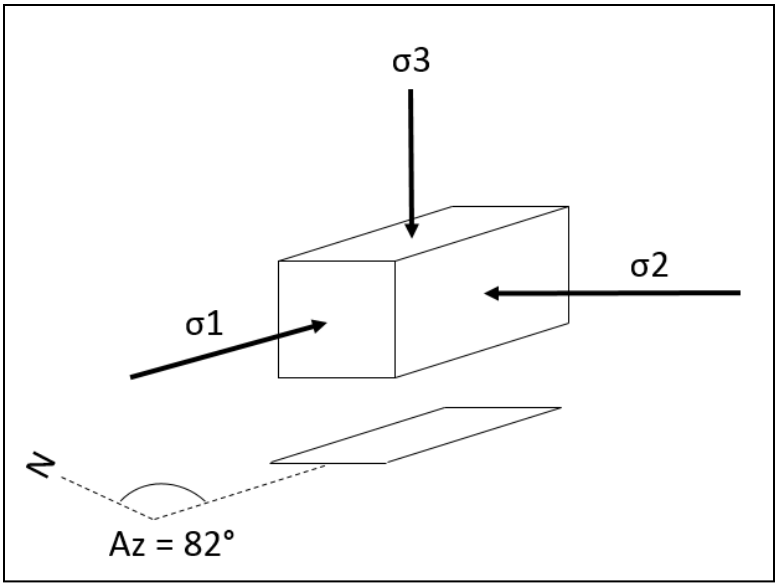

Figure 1 The Sudbury Basin Tensor showing Principal Stress Orientations (Adapted from: Suorineni and Malek, 2014)

2.1.1 Seismic Events

A seismic event can be thought of as a small earthquake which occurs due to a release of energy in the earth's crust. Common sources of these occurrences are movements along faults. These earthquakes are referred to as tectonic earthquakes (Richter, 1958). The occurrence of seismic events is measured in the waves that propagate from the location of the earthquake. Two main types of waves are of interest for seismicity in mines. P-waves or 'primary waves' travel longitudinally meaning parallel the direction of energy propagation through earth's crust. S-waves or 'secondary waves' travel slower than P-waves and oscillate normal to the direction of travel of the emitted energy (MTU, 2016). The following figures show both P and S-waves (see Figure 2):

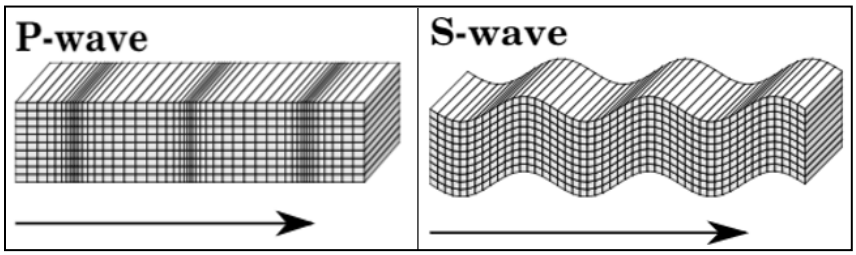

Figure 2 P-Wave and S-Wave Propagations through Media (Mendecki, 2013)

There are two other types of waves that are emitted, both are surface waves: Rayleigh and Love waves. Since underground mines operate below surface, these waves are omitted

from analyses. These waveforms are picked up by seismic sensors and the amplitudes are analyzed for further analysis. Some example waveforms are shown in the following figure (see Figure 3):

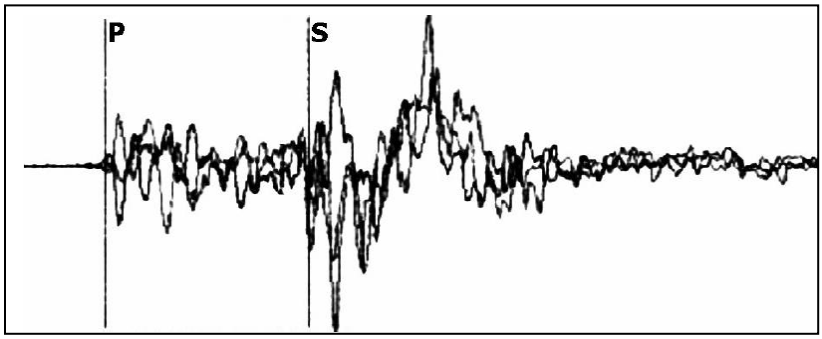

Figure 3 Waveform of a Typical Seismic Event (Hudyma, 2008)

2.2 Seismic Monitoring in Underground Mining

Seismic monitoring comprises the design, installation, and operation of seismic systems. These systems are comprised of seismic sensors and data acquisition servers. In mining, seismic sensors are installed in boreholes. When a seismic event occurs, the sensors pick it up as an analog signal. The analog data is relayed to a digitizer which then sends the digital signal to a server, usually on surface (Rebuli, Goldswain and Lynch, 2016). A diagram of this system is shown in the following figure (see Figure 4):

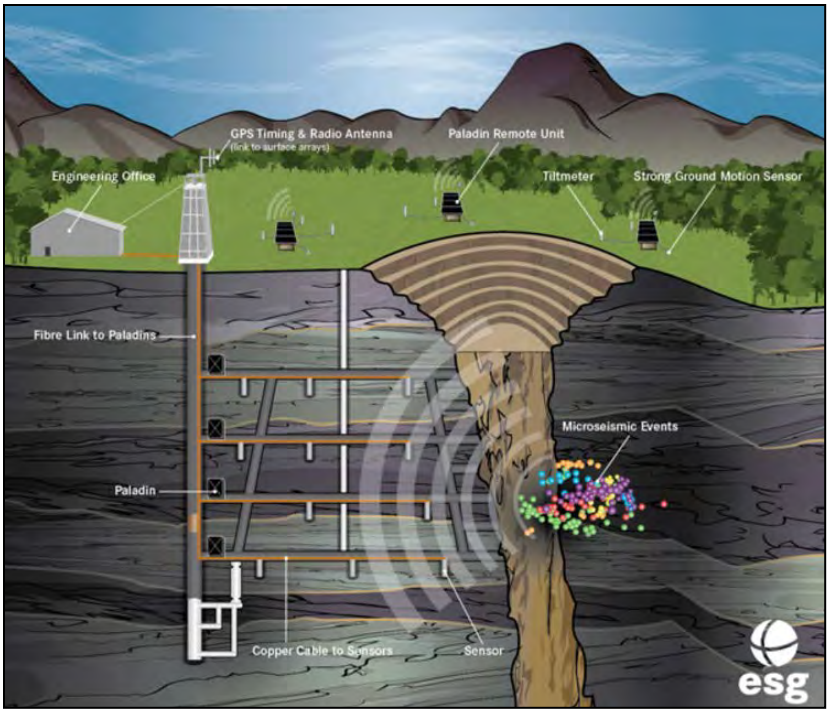

Figure 4 Diagram of a Typical Mine Seismic System showing the Main Components (ESG, 2017)

The ability of a seismic system to do this effectively depends on a number of factors including the types of sensor installed and the distribution of the sensors. In the ideal scenario, the sensor array will surround the orebody or area of interest (Heal *et al*, 2008). In most situations, mine infrastructure is developed in the footwall of the orebody. However in certain cases, there is access from the hanging wall side allowing for sensor placement there. For cases where hanging wall sensors are not possible, the overall sensor array should be 3-dimensional. This ensures good quality data as opposed to an array that is more planar or 2-dimensional (Heal *et al*, 2008).

2.2.1 The Purposes of Routine Seismic Monitoring

Seismic monitoring is not an arbitrary pursuit. Routine seismic monitoring can be used to evaluate exposure to seismicity and to analyze potential precursory activity that may lead to rockbursting. Seismic monitoring can also be used in open pit mines to monitor slope stability (Mendecki, Lynch and Malovichko, 2010). There are five objectives within this field as it pertains to mining (Mendecki *et al*, 1996):

1. Routine seismic monitoring can be used in rescue efforts in the event of a rockburst through locating the damaging seismic event

2. Seismic monitoring can be used to compare the observed versus expected seismic activity in response to mining operations. When the two do not align, which can be seen in the seismic data, mine design changes can be enacted to reduce the risk of damaging seismic events
3. Routine seismic monitoring can be used to establish a hazard rating system based on certain parameters. These ratings can be assigned to active areas of the mine to give an indication of the hazard posed by mining in that area
4. Through seismic monitoring, alerts can be given by comparing seismic activity with established thresholds or hazard ratings. These can be used by both engineering and operations in planning/scheduling
5. The final objective in routine seismic monitoring is to be able to perform back-analysis. Going back in time and analyzing trends in seismic data can be used to establish benchmarks moving forward. For example, if the magnitudes of seismic events in an area have been increasing over the last 6 months, the level of seismic hazard can be said to be increasing (Mendecki, Lynch and Malovichko, 2010)

2.3 Seismic Source Parameters

When a seismic event is recorded by a seismic sensor array, five independent source parameters can be gleaned through spectral analysis: time, location, source size, seismic energy and seismic moment. These spectrally defined seismic parameters are independent, from them a series of dependent parameters can be calculated. An expanded definition of each independent parameter is given in the following sections.

2.3.1 Event Time and Location

The time (t) of occurrence of a seismic event can be used to help determine the source mechanism. For example, events occurring close to blast times are likely blast induced. The closer in time the event is to the blast, the stronger the causal relation between mining activity and seismicity (Hudyma, 2010). Since seismic sensors are installed throughout the mine, the first 'hit' of a seismic event at the sensor occurs at different times depending on the sensor's proximity to the event. Using the arrival times and the coordinates of each sensor, the location of the seismic event can be approximated using

triangulation. The goal in seismic monitoring as it pertains to mining is to glean the location, time, and seismic source parameters of a seismic event (Rebuli, Goldswain and Lynch, 2016).

2.3.2 Seismic Energy

Seismic energy is defined as the total radiated energy emitted from the source location of a seismic event. This energy is released in the form of waves (as described in Section 2.1) from which energy is calculated using the following equation:

$$E = 4\pi\rho c R^2 \frac{Jc}{Fc^2} \quad (1)$$

Where E = total radiated seismic energy (J), ρ = rock density (kg/m^3), c = velocity of the wave in rock (m/s), R = the distance from the seismic source (m), Jc = the integral of the square of ground velocity

2.3.3 Seismic Moment

Seismic moment is a measure of the strength of an earthquake (Gibowicz and Kijko, 1994). It is commonly used to measure the size of slip-type seismic events (Hudyma, 2010). Gibowicz and Kijko (1994) use the following equation to calculate seismic moment:

$$M_o = 4\pi\rho c^3 R \frac{\Omega_0}{F_c} \quad (2)$$

Where M_o = seismic moment (Nm^2), ρ = rock density (kg/m^3), c = velocity of the wave in rock (m/s), R = the distance to the seismic source (m), Ω_0 = the low-frequency plateau on the frequency spectrum of a seismic waveform (mm·s), F_c = an empirically derived radiated pattern coefficient

2.3.3.1 A Note on the Waveform Frequency Spectrum

The waveform frequency spectrum is used in spectral analysis for the derivation of seismic source parameters. The displacement spectrum, using a Fourier transform, is evaluated to determine the Ω_0 plateau and the corner frequency (f_o). Essentially there is a level, in terms of spectral density (mm·s), for long period displacement of the waveform (Ω_0) prior to a high frequency decay. The point at which the high frequency decay begins to occur is known as the corner frequency (f_o) (Mendecki, 2013). A figure is shown below of this type of chart (see Figure 5):

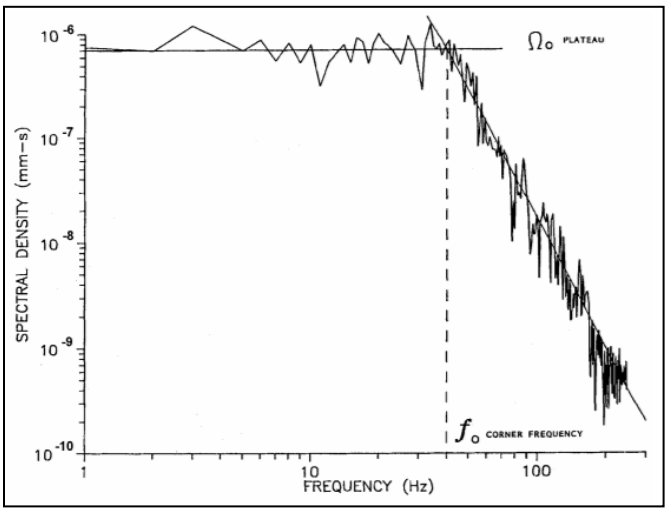

Figure 5 Frequency-Wave Spectrum Chart (Hedley, 1992)

2.3.4 Source Size

The source size of a seismic event defines the dimension of the failure surface. It is assumed circular in shape and is represented as a diameter or radius (i.e. source radius) (Hudyma, 2010). The equation for source size is given below:

$$l = \frac{c}{fo} \tag{3}$$

Where l = source size (m), c = a model-dependent constant, f_o = the corner frequency on the spectral density chart (as shown in Section 2.3.3.1) for that specific event

2.3.5 Event Magnitude

Magnitude is a measure of the strength of an earthquake and is essentially a quantification of the energy emitted over a fixed frequency band (Gibowicz and Kijko, 1994). In the analysis of earthquake magnitude, numerous scales have been developed. There are some limitations in using magnitude scales as opposed to seismic moment (Mo) such as saturation and discrepancies between different scales (Gibowicz and Kijko, 1994).

One of the most recognizable magnitude scales is the local magnitude (M_L) scale developed in California by Charles Richter (1935) whom the Richter magnitude scale is named after. The equation for local magnitude is given below:

$$M_L = \log A(\Delta) - Log\ A_0(\Delta) \quad (4)$$

Where M_L = local magnitude, A = maximum traced amplitude (μm), A_0 = a standard maximum traced amplitude measured 100km from the source (μm), Δ = distance from the source

Another popular magnitude scale used as a measure of the strength of large earthquakes is the moment magnitude scale (M_w). Hanks and Kanamori (1979) presented the following equation in the determination of moment magnitude:

$$M_w = \frac{2}{3}\log(M_o) - 6.0 \quad (5)$$

Where M_w = moment magnitude, Mo = seismic moment (Nm)

It should be noted that magnitude scales are logarithmic in nature. This means that a single-fold increase in magnitude value is a tenfold increase in earthquake strength. In mines, the magnitudes experienced are generally smaller than that of well-known earthquakes. Much of mining seismicity is in the range of -2 to $2M_R$. A practical description of event magnitude versus what it feels like underground to the observer was put forward by Hudyma (1995) and is shown in the following table (see Table 1):

Table 1 Richter Magnitudes in Underground Mines and Associated Qualitative Descriptions of Each (after Hudyma, 1995)

Richter Magnitude (approximated)	Qualitative Description
-3	Small bangs or bumps, typical activity following development rounds, too small for most seismic systems to register
-2	Ground shaking felt close to the source of the event, felt as small rumbles, typically picked up by most seismic systems
-1	Significant ground shaking felt close to the event, felt by most workers underground
0	Vibrations felt hundreds of meters away, bumps typically felt on surface as that of a development round
+1	Felt and heard very clearly on surface, vibrations similar to that of a production blast
+2	Vibrations larger than that of production blasts, these events are usually picked up by the Canadian Geologic Survey
≥ +3	Largest seismic events recorded in mines within Canada, picked up by provincial earthquake monitors

2.3.6 Apparent Stress

Apparent stress can be considered as a measure of the change in stress at a seismic source (Wyss and Brune 1968; cited in Young, 2012). The following equation was proposed by Wyss and Brune (1968) to calculate apparent stress:

$$\sigma_a = \frac{GE}{M_o} \tag{6}$$

Where σ_a = apparent stress (Pa), G = the shear modulus of the rock (N/m^2), E = seismic energy (J), Mo = seismic moment (Nm)

Seismic waveforms do not provide an absolute value for the state of stress in the rock mass, in terms of a MPa value, but rather a dynamic stress drop at the source. However, through numerous studies and underground observations, evidence suggests that apparent stress can be used as a reasonable indicator of the local stress conditions in the rock mass (Mendecki, 1993).

2.4 Seismic Activity in Mines

The mining process is primarily concerned with the removal of commodity-containing material from the ground. As excavations are created, the in-situ or prior-existing conditions are changed. A simple analogy of this is a naturally flowing stream. If one were to place a stone into the stream, the waters would divert around the obstruction creating areas of high flow around the corners of the object. In underground mining, when an excavation is opened i.e. a stope, the ground stresses are diverted around the shape. This is due to the fact that stress cannot propagate through voids or backfilled excavations (Cook 1976; cited in Gibowicz and Kijko 1994). A figure of this scenario in Section 2.1 (see Figure 6).

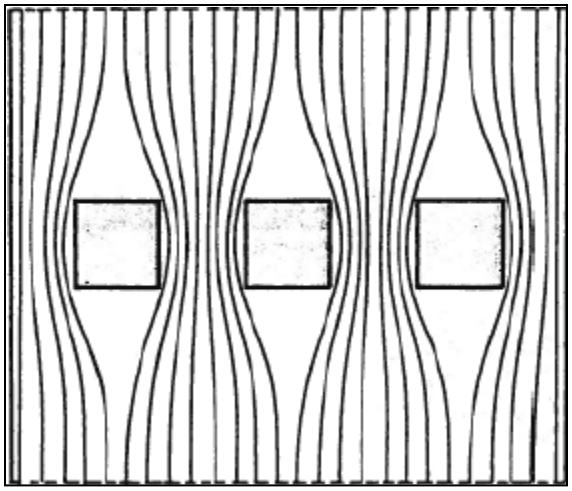

Figure 6 Stress Field Disturbance caused by Underground Voids (Hoek and Brown, 1980)

Essentially, seismic activity in mines is mainly driven by convergence of excavations in response to material extraction. The smaller magnitude events are generally well correlated with mining while the larger magnitude events may be correlated to mining activity, however, they are more commonly correlated to past mining activity as it pertains to the overall layout of excavations in an area (Mendecki, 2016). For example, as mining progresses on one side of a known fault, the stresses acting on the structure are changed and can cause fault-movement resulting in a large magnitude event.

2.5 Seismic Source Mechanism and Seismic Data Analysis

The seismic source mechanism is the rock mass mode of failure at the source of the event. This concept should not be confused with rock mass damage mechanism which can occur at varying distances away from the source (Hudyma, 2014). There are a number of different source mechanisms which fall under either stress-induced or shear-induced. The following mechanisms have been proposed by Ortlepp (1992) and are listed in the following table (see Table 2):

Table 2 Seismic Events by Type, Mechanism, and Magnitude (after Ortlepp, 1992)

Seismic Event	Source Mechanism	Magnitude Range (Local Mag)
Stress-induced fracture	Energy dissipation through the creation of new fractures	-3.0 to -1.0
Strain bursting	Superficial spalling with violent ejection of fragments	-0.2 to 0
Buckling	Outward expulsion of larger slabs parallel to opening	0 to 1.5
Pillar of face-crush	Sudden collapse of stope pillar, or violent expulsion of rock from tunnel face	1.0 to 2.5
Shear Rupture	Violent propagation of shear fracture through intact rock mass	2.0 to 3.5
Fault Slip	Movement on existing fault	2.5 to 5

Although the magnitude range, in actuality, may vary from the values in Table 2, the source mechanisms are important to note. The following figure is illustrative of some of the common localized seismic source mechanisms found in mines (see Figure 7):

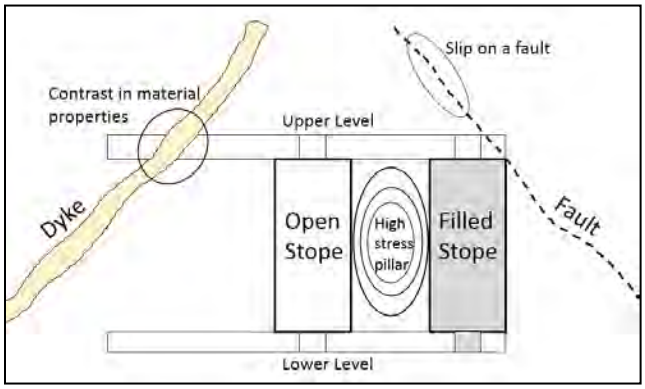

Figure 7 Seismic Source Mechanisms in Hardrock Mines (adapted from: Hudyma, 2008)

2.5.1 Magnitude-Time-History

A magnitude-time-history (MTH) chart is a plot of event magnitude versus date with the cumulative number of events plotted on a secondary y-axis. This type of chart is shown in the following figure (see Figure 8):

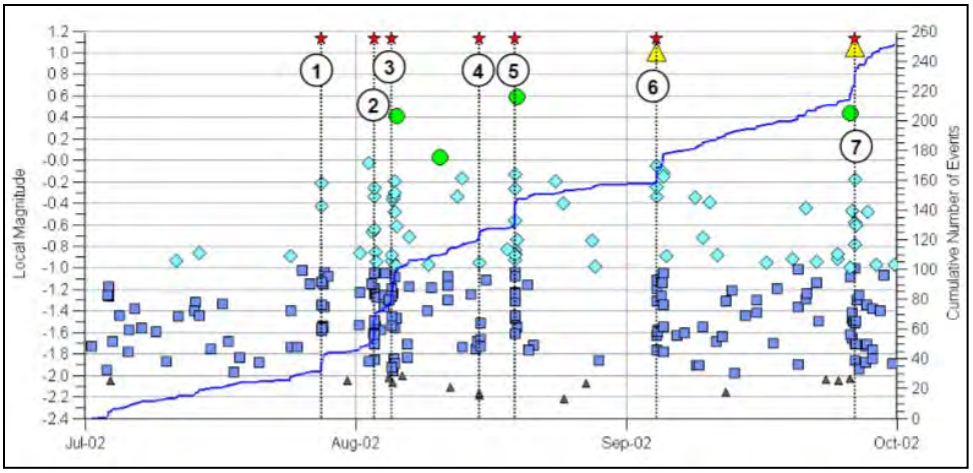

Figure 8 Magnitude-Time-History Chart showing Mine Blasts (Hudyma, 2010)

From the chart above, the numbered lines indicate blasts during the time period. These can be seen in the thick 'bands' of event markers and the vertical 'steps' in the cumulative events line. Aside from the blasts and subsequent seismic activity, time periods between blasts could be said to be exhibiting another seismic mechanism. This can be seen by the spread-out distribution of events between blasts and the more constant slope of the cumulative events line. Fault-activity may be responsible in this case, however it is not entirely clear 100%. As a general rule, a gradual sloping events line is indicative of fault-related seismic activity and a step-riddled line is indicative of mining-related activity (blasting). Shown below is a MTH chart of a cluster of seismicity along a known mine-fault (see Figure 9):

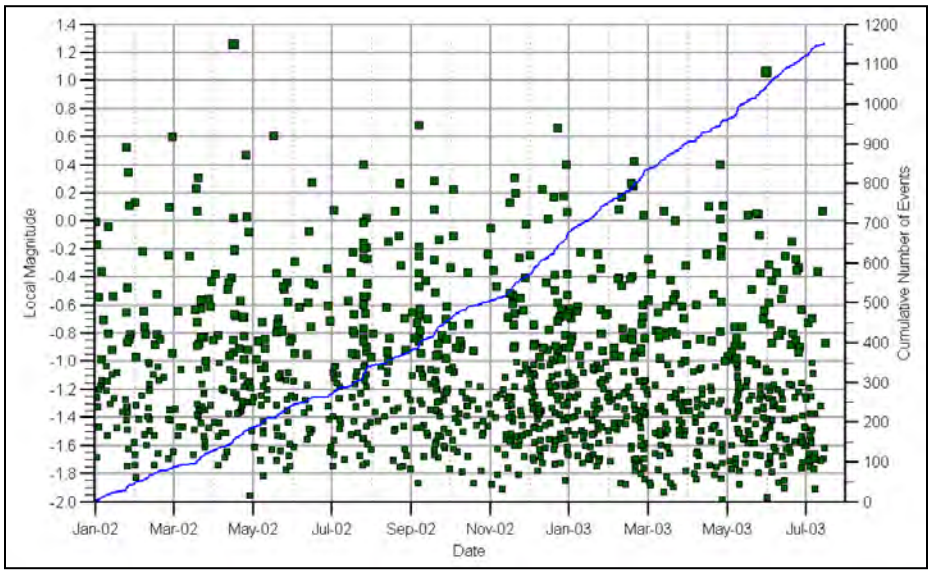

Figure 9 Magnitude-Time-History Chart showing Fault-Driven Seismicity (Hudyma, 2010)

In the case illustrated in the previous figure, mining activity was consistent throughout the 18-month period shown, however the effect of blasting on the fault appears to be minimal. This indicates that fault activity in this instance is not heavily influenced by mining.

2.5.2 Frequency Magnitude Relation

The Gutenberg-Richter Frequency-Magnitude relation (Gutenberg and Richter, 1944) is derived from earthquake seismology which displays the magnitude of seismic events versus the frequency of occurrence in a cumulative distribution. The trend-line plotted follows a logarithmic scale relation in the form:

$$\log N = a - bM \tag{7}$$

Where N = number of events, a = a parameter related to the level of seismicity, b = the slope of the trend-line related to seismic source, M = magnitude

It has been shown that the parameter 'b' behaves in a characteristic way with stress changes in the rock. Essentially, 'b' decreases as stress increases (Gibowicz and Kijko 1994). As a rule of thumb, b-values greater than 1.0 are indicative of stress-fracturing related seismicity while b-values less than 1.0 are indicative of shear driven seismicity (Hudyma, 2014). The lower the b-value, the shallower the slope of the trend-line, ergo, the further to the right the x-intercept is meaning large magnitude events. Shown below is a sample comparing distributions from mining activity and from fault activity (see Figure 10):

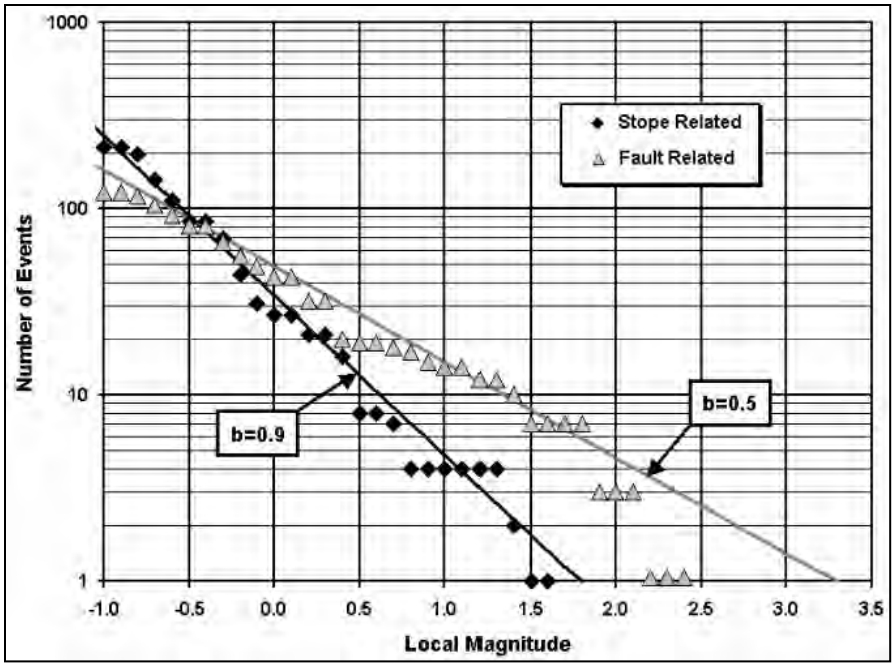

Figure 10 Frequency-Magnitude Relations for 2 Different Seismic Data Populations (Hudyma, 2010)

In the above figure, populations indicating mining and faulting are shown for comparison. With available data, comparing the frequency magnitude relations to the MTH charts adds credibility to seismic source determination. This practical comparison is shown below (see Figure 11):

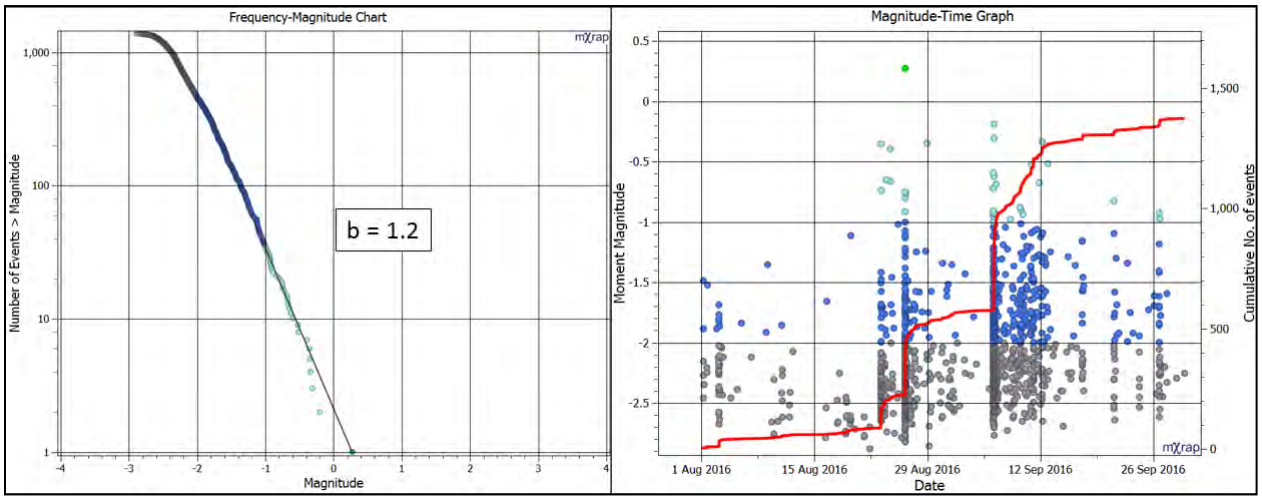

Figure 11 A Comparison between the Frequency-Magnitude and Magnitude-Time-History Charts for a Seismic Data Population

2.5.3 Diurnal Charts

Diurnal, or time-of-day analysis is used to determine when events occur during the day (Cook, 1976). This is done primarily to determine the influence of blasting on seismicity. The number or rate of events is graphed against the hour of the day, this chart is shown below (see Figure 12):

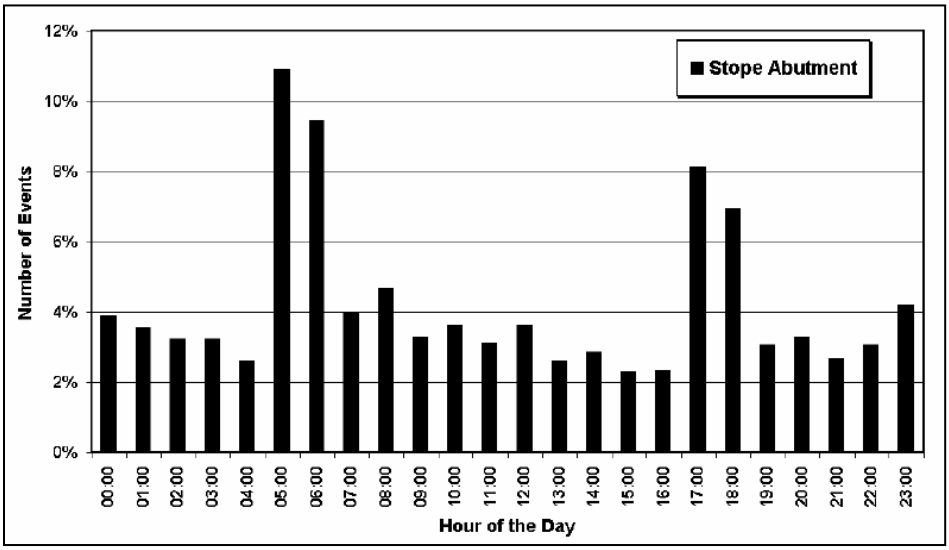

Figure 12 A Diurnal Chart for a Seismic Population along a Known Stope Abutment (Hudyma, 2010)

In the previous chart, large amounts of events occur between 05:00 - 07:00 and 17:00 – 19:00. This is in-line with the blast times at the mine. As indicated in the upper right-hand portion of the chart, this chart is representative of a stope abutment area. These areas define the lateral extremities of mining and tend to be areas of high stress, and as a consequence, experience large amounts of seismicity with mine blasts (Hudyma, 2010). Diurnal charts can also be used to determine if fault activity is affected by mining. Shown below is a diurnal chart for a cluster of events along a known mine fault (see Figure 13):

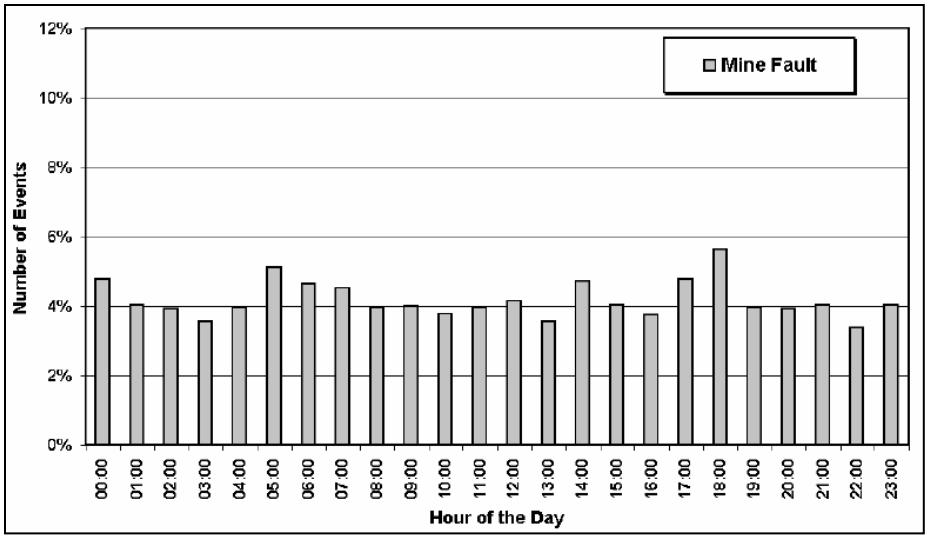

Figure 13 A Diurnal Chart for a Seismic Population on a Known Mine-Fault (Hudyma, 2010)

As can be seen in the above chart, seismic activity occurs at a fairly constant rate throughout the day. There is some influence of blasting, however the effect is minimal at only around 1 – 2% more active than non-blasting times in the mine.

2.5.4 ES:EP Charts

As its name suggests, the ES:EP or simply S:P ratio is the energy emitted from the s-wave divided by the p-wave energy. The most common way to display this ratio is by using a cumulative distribution. Past research indicates, as a rule of thumb, that S:P < 3 are stress-induced events (Urbancic *et al*, 1992) and S:P > 10 are shear-induced events (Boatwright and Fletcher, 1984). This type of chart is shown in the following figure (see Figure 14):

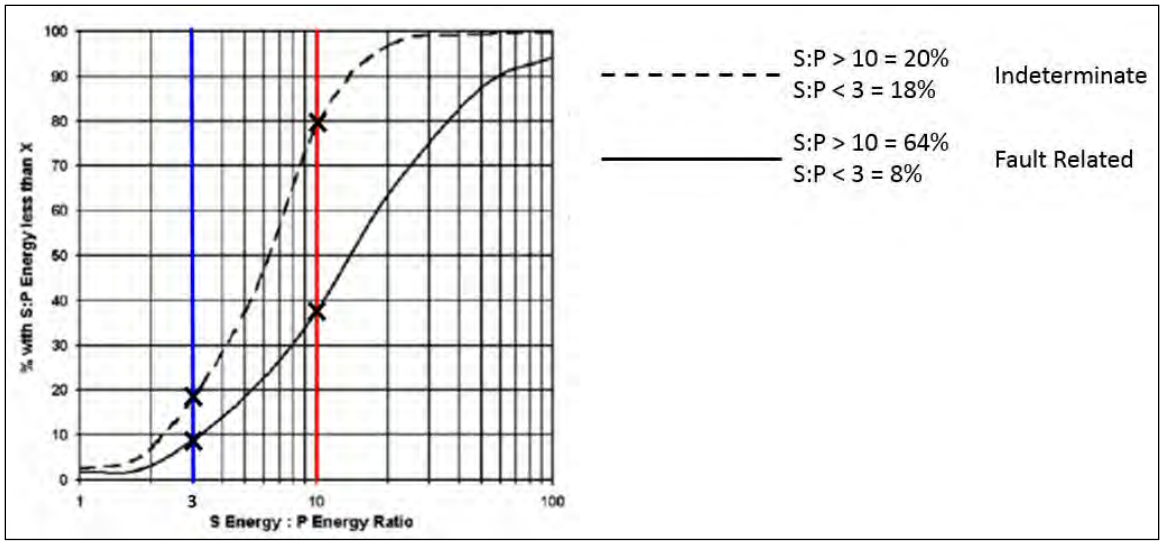

Figure 14 ES:EP Chart Showing Two Seismic Populations of Differing Source Mechanisms (adapted from Hudyma, 2010)

Shown in the figure above are two populations shown by the dashed and solid lines. The key numbers in these charts are the percentage of events with an S:P ≤ 3 and S:P ≥ 10. With the dashed-line population, 18% of events have S:P ≤ 3 and 20% of events, 62% of events are between 3 and 10 therefore the mechanism is indeterminate. For the solid-line population, 8% of events have S:P ≤ 3 and 64% of events have S:P ≥ 10, 28% of events are between 3 and 10 therefore the mechanism is likely shearing or fault-related.

2.5.5 Seismic Data Analysis Using mXrap™

As discussed in the previous subsections, it is possible to undertake meaningful seismic data analysis using parameters that are recorded by the mine seismic system. To make complex data analysis faster and more user-friendly, the Australian Centre for Geomechanics developed the Mine Seismicity Risk Assessment Program (MS-RAP™) which has been recently changed to mXrap™ (Harris and Wesseloo, 2015). This software program provides a development platform for which a range of apps can be used to analyze seismic data and new apps can be created and shared by users of the program based on more specific needs (Harris and Wesseloo, 2015). Essentially, charts and tables that would otherwise take upwards of an hour to produce can be generated with the click of a button leaving more time for the actual interpretation of the data.

2.6 Seismic Hazard

Seismic hazard, as it pertains to underground mining, is defined as the likelihood of an event occurring of certain magnitude in a location within a mine or a geographical area (in the case of earthquake seismology) (Gibowicz and Kijko, 1994). Understanding seismic hazard in a mine can give both engineering and operations insight into which areas put the workers at greater risk and using the data can indicate ways to mitigate the risk i.e. changing mining method and/or sequence.

2.6.1 Seismic Hazard Assessment

Seismic hazard assessment is the means by which the largest expected magnitude of a hazardous phenomenon is determined. Statistical methods are usually applied using data collected by the mine's seismic system. The types of hazard assessment generally fall under empirical and/or probabilistic methodologies.

2.6.1.1 Empirical Hazard Assessment

Empirical hazard assessment as its name suggests involves inputs that do not exhibit randomness. The emphasis in these types of analyses is placed on observation. A common empirical means of hazard assessment is the estimation of the maximum expected event magnitude which was presented by Kijko and Funk (1994):

$$M_{max} = X_{max} + (X_{max} - X_{n-1}) \tag{8}$$

Where M_{max} = the maximum expected event size, X_{max} = the largest magnitude event in the data set, X_{n-1} = the second largest magnitude event in the data set.

The maximum expected event size is not the only way to assess hazard, other seismic parameters can be used. Magnitude is merely the simplest and most recognizable. Parameters such as apparent stress can give indication of areas under high stress or increasing stress regimes (Brown, 2015). This can be compared to the magnitudes of events occurring in those high stress areas which can be used to validate the predictions.

2.6.1.2 Probabilistic Hazard Assessment

Probabilistic hazard assessment, as it relates to seismicity, aims to estimate the frequency of ground motion that can be reached or exceeded at a given point of interest, in a future time. The analysis incorporates all magnitudes of potential seismic events, frequency of

occurrence, and distance from the source using a ground-motion-prediction-equation or GMPE. This gives an estimate of the combined probability of exceedance at a location (X) for different time periods (ΔT) (Mendecki, 2016).

For mining applications, this type of assessment is limited to estimating the probability that a large event ≥ log P (where P = seismic potency), will occur in a specific volume or area (ΔV) in a future time (ΔT) or while extracting a given volume of rock (ΔV_m) (Mendecki, 2016). Seismic potency (P) is a source parameter found using the product of average slip (u) and source area (A). The generic probability of the occurrence of a large event occurring is illustrated in the following notation (Mendecki, 2016):

$$\Pr[\geq log\, P(\Delta V), \Delta T \; or \; \Delta V_m] \tag{9}$$

The probability statement above is valid for mines where the linear size of the target event (log P) is proportional to the size of the mine (Mendecki, 2016).

2.6.2 Routine Seismic Hazard Assessment

As discussed in the previous section, the methodology for assessing seismic hazard can be probabilistic or empirical. To do a standalone analysis of hazard is in itself useful, however conditions within mines change over time in terms of percent extraction, ground stresses, the frequency of occurrence of large seismic events etc. Therefore, the concept of performing seismic hazard assessment on a semi-regular basis becomes pertinent. The main question arises: over what time period or periods should seismic hazard be evaluated? The concept of varying time periods for hazard assessment was put forth by van Aswegen (2005) who suggested long, medium, and short term assessments.

Long term hazard assessment is defined as a time span, sufficiently long enough for changes to mine design to be made, typically in the range of several months to a few years (van Aswegen, 2005). This method of hazard assessment is in line with the fact that many mines, especially deep mines rely on numerical modelling to make design decisions and having a defined seismic hazard level adds more credibility to the mine design (van Aswegen, 2005). Medium term hazard assessment is related to the monthly planning cycle and as such is recommended to be 1 month or so. Short term refers to a

time period of hours or days. This reflects the daily and/or weekly schedule at the mine (van Aswegen, 2005). Short term hazard assessment would give an ability to undertake changes to the daily and/or weekly schedule. It should be noted that the length of time should be chosen such that there are no major changes in mining activity.

2.6.3 Seismic Hazard Mapping

In the interest of seismic hazard assessment, reporting results is made easier when one can visualize the scenario. For example, if hazard is evaluated using a given seismic source parameter, a heat map may be produced that is plotted in space to show which areas of the mine have an elevated hazard level. One such method of mapping, known as grid-based, function using a defined grid with a set spacing and search radius. The basic principle behind this analysis technique is to assign a seismic parameter to grid points in space based on nearby seismic events (based on the search radius) to glean information on the variation of said parameter in space (Wesseloo, Woodward and Pereira, 2014). The data can be evaluated based on a number of parameters and usually a heat map is generated using ranges of values. This analysis technique can be conducted using programs such as mXrap™ (Harris and Wesseloo, 2010). The following figure shows a grid map of the b-value for an Australian Mine using mXrap™ (see Figure 15):

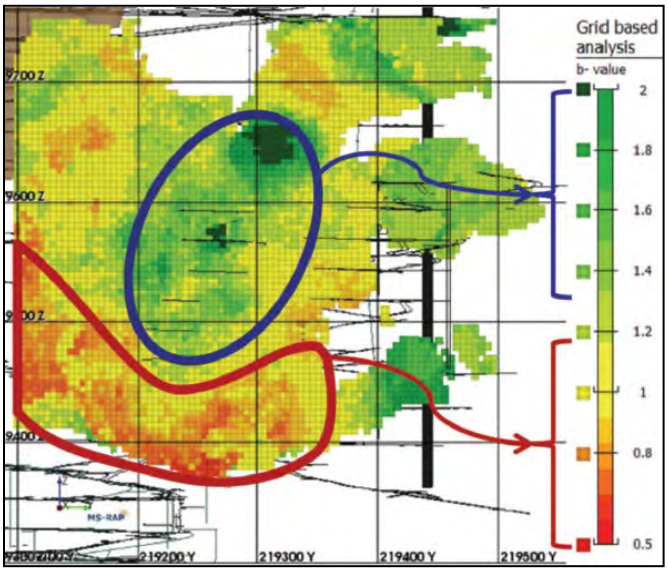

Figure 15 Grid-Based Hazard Mapping using the B-Value for a Stope Block in an Australian Underground Mine (Wesseloo, Woodward and Perreira, 2014)

The b-value is indicative of seismic source mechanism be it shearing or stress. Low b-values ($b < 1$) are indicative of shearing while higher values ($b > 1$) are indicative of stress fracturing (Wesseloo, Woodward and Pereira, 2014). The red outline encompasses an abutment while the blue outline encircles a stoping zone. In this case, the abutment is experiencing shearing while the stoping zone is experiencing stress related seismic activity.

Another method of hazard mapping is node-based mapping. In this technique, rather than mapping hazard values onto grid points in 3D space, the heat-map is smeared onto a solid model of mine workings using established nodes and a search radius around each node. An example of this is the Apparent Stress Ratio (ASR) hazard map proposed by Brown (2015) where the ratio of the 80th percentile of apparent stress is divided by the 20th percentile to give the ASR value. Essentially, an increasing ASR value indicates an increase in stress which can lead to larger seismic events (Brown, 2015). In the context of a heat-map, the warmer the color, the higher the ASR value. The following figure shows this hazard map for a mining level at Agnico Eagle's LaRonde Mine (see Figure 16):

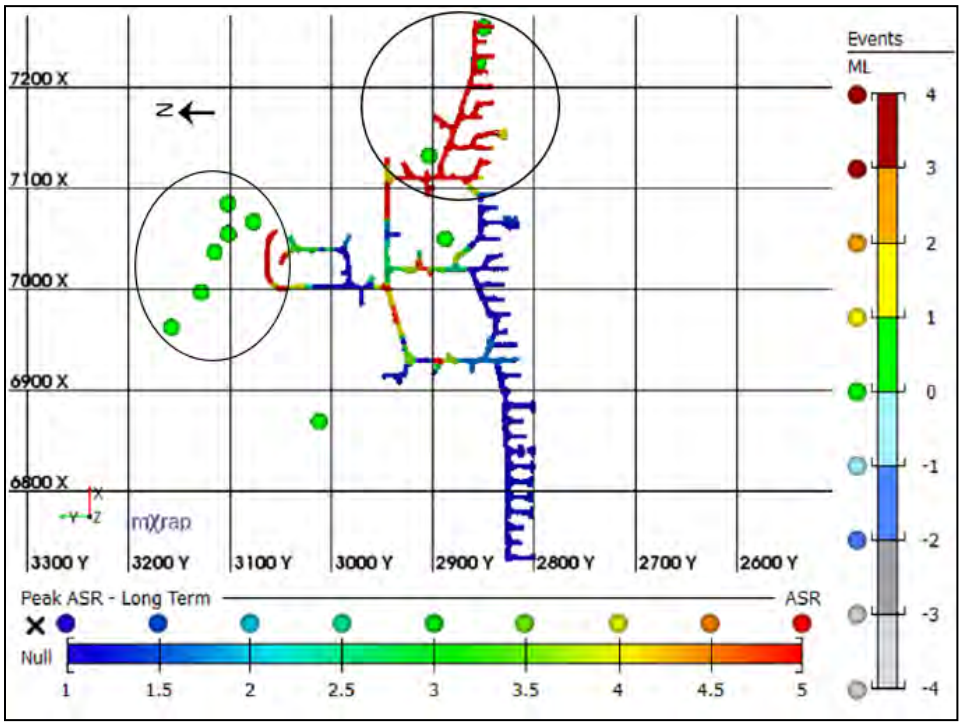

Figure 16 ASR Hazard Map for a Production Level at LaRonde Mine (Brown, 2015)

2.7 Literature Review: Summary

Due to tectonic forces and the sheer weight of the overlying rock, stresses exist in rock mass around mine openings exist and can lead to seismic events. This fact becomes of particular importance as mines progress deeper into the earth's crust and stress levels increase towards the ultimate strength of the host rock. The way in which mines record seismic data is through seismic monitoring accomplished through a mine seismic system. These systems are comprised of sensors connected to digitizer units which relay the data to surface through either copper of fibre optic cables.

Seismic source parameters recorded using the mine's seismic system are useful in determining what is causing the seismic activity be it blast-related or fault-related. In this vein numerous analysis techniques exist. The basic ones are the magnitude-time-history chart, frequency-magnitude relation, diurnal charts, and ES:EP charts.

Taking seismic source analysis a step further, techniques exist to evaluate what is known as seismic hazard; the likelihood of an event of a certain size occurring in a defined area in a given time period. Seismic hazard can be used to delineate which areas of the mine are at risk of experiencing a large event in the near future. To visually represent hazard analysis, mapping techniques such as grid-based mapping and node-based mapping can be used with such programs as ACG's mXrap™. Node-based hazard mapping using the ACG's mXrap program is the focus of this thesis and this type of hazard mapping is further discussed in Chapter 4.

3 Background and Mine Details

3.1 The Sudbury Basin

The Sudbury Basin is a geologic structure situated between 3 geologic provinces: it lies within the Southern Province, near the Superior Province to the northwest, and the Grenville Province to the southeast. The rock types that make up the basin are Whitewater Group and are early Proterozoic in age. These rocks are unique to the Sudbury Basin (Rousell, 1983). There are 3 distinct formations within the basin and are listed from oldest to youngest: the Onaping Formation, Onwatin Formation, and the Chelmsford Formation. The Onaping Formation consists of massive upward-fining breccia. Upward-fining meaning that the brecciated fragments decrease in size in the upward direction. The breccia is made up of gneiss, granite, quartzite, and gabbro (Rousell, 1983). The Onwatin Formation consists of argillite and siltstone. The Chelmsford Formation is mainly comprised of greywacke with some argillite and siltstone. The Whitewater Group rocks contain large amounts of carbonaceous material which gives a characteristically dark color (Rousell, 1983). The following figure shows the basin in plan-view with notation given to the various formations mentioned previously (see Figure 17):

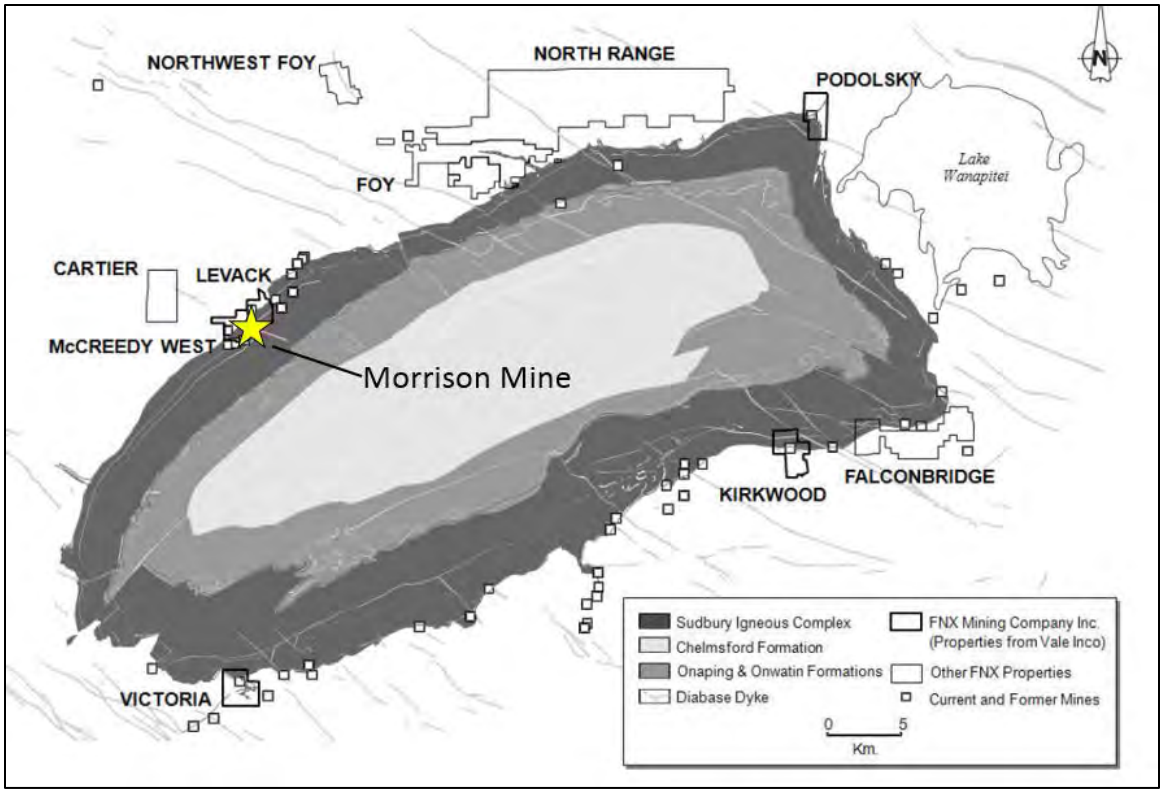

Figure 17 The Sudbury Basin Showing Geologic Formations (adapted from FNX Mining Company, 2009)

The Sudbury basin was formed by an impact event between 1.6 to 1.8 BYa. During the impact, the metals were displaced along the edges of the Sudbury Igneous Contact with the ore mineralization being deposited along the footwall of the Onaping Formation. This can be seen in the distribution of metal mines in the Sudbury area. There are also dykes that radiate outwards from the edges of the basin some of which bear mineral deposits as in the Copper Cliff Offset Dyke which is shown in the following figure (see Figure 18):

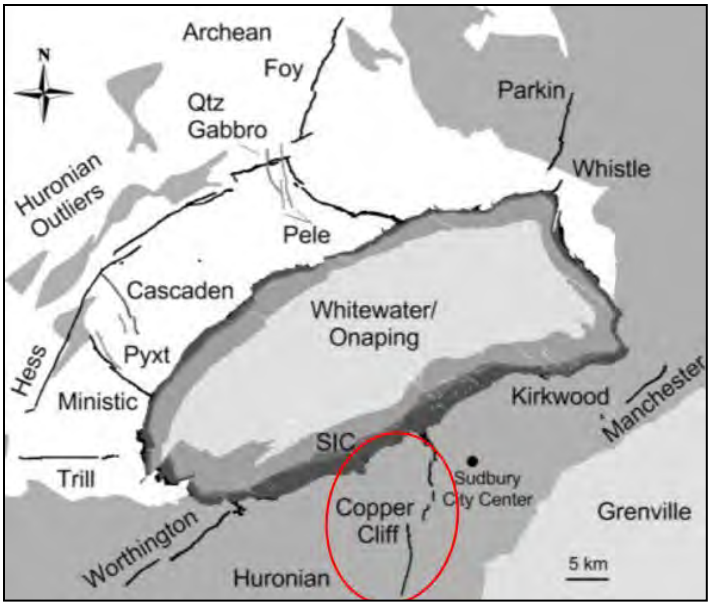

Figure 18 The Sudbury Basin showing General Geology and Major Offset Dykes with the Copper Cliff Dyke circled in Red (adapted from Smith, Bailey and Pattison, 2013)

In the previous figure, the major offset dykes are shown. The Copper Cliff Offset is host to Copper Cliff Mine (North and South) and the Worthington Offset is host to Totten Mine and the historical Victoria Mine.

3.2 Morrison Mine

KGHM's Morrison Mine is located in Levack ON, about 55km northwest of Sudbury ON. The deposit lies along the north-western edge of the Sudbury Basin. This area has been mined extensively since the early 1900s with 11 mines having operated within a 10km strike length. The mine location is shown in the following figure (see Figure 19):

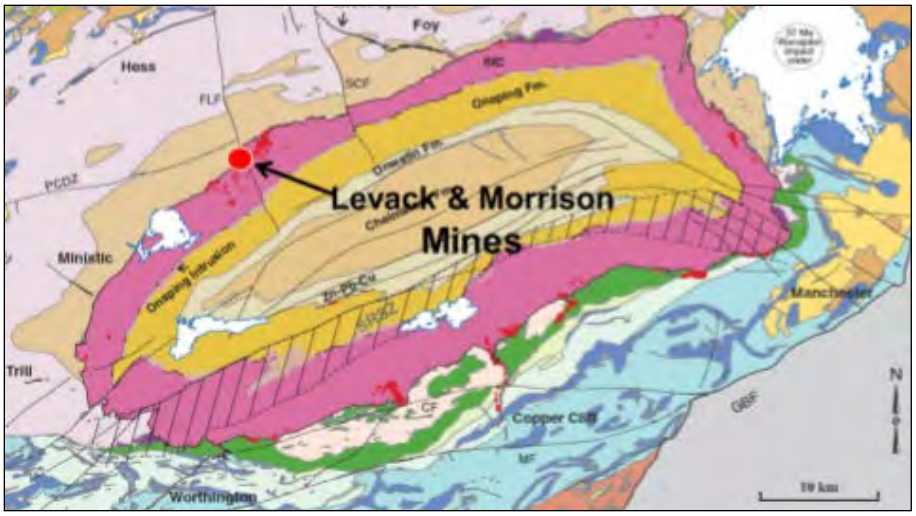

Figure 19 Morrison Mine Location shown relative to the Sudbury Basin (Milner *et al*, 2013)

The mine is located between the historic Levack Mine and Glencore's Craig Mine (closed in 2009). KGHM (formerly Quadra FNX) currently leases the Craig Mine infrastructure from Glencore and uses the Craig shaft as a primary means of access and ore haulage. The deposit is also accessible from the Levack Mine No.2 shaft. The mine is of similar depth in comparison to other operating mines in the area (Fraser and Coleman) mining between 3000 and 5000ft depth. The deposit itself is the footwall deposit of the former Levack Mine and was formerly known as the Levack footwall deposit as shown below:

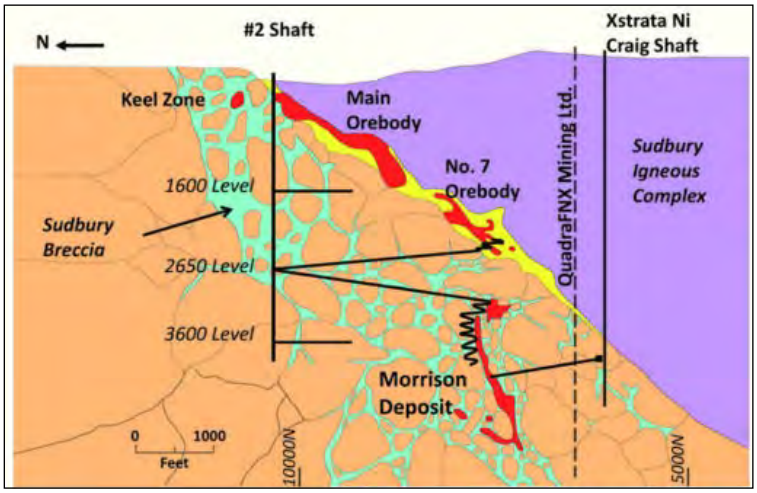

Figure 20 Section View of Morrison Mine (QuadraFNX Mining Ltd., 2011)

To give more perspective on the location of Morrison relative to the historic Levack Mine a long-section looking north is shown in the following figure along with the approximate dates of mining in the various zones of both mines (see Figure 21):

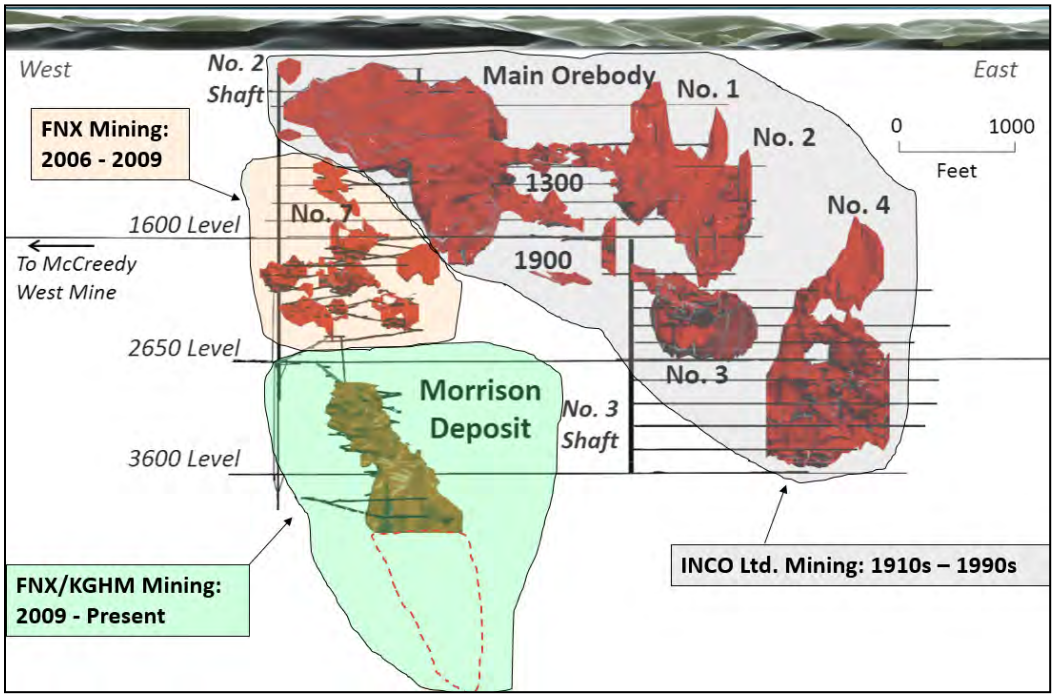

Figure 21 Strike view of Morrison Mine and the historic Levack Mine (adapted from FNX Mining, 2011)

The Morrison deposit itself is shown in the following figure in both north and westward looking views (see Figure 22):

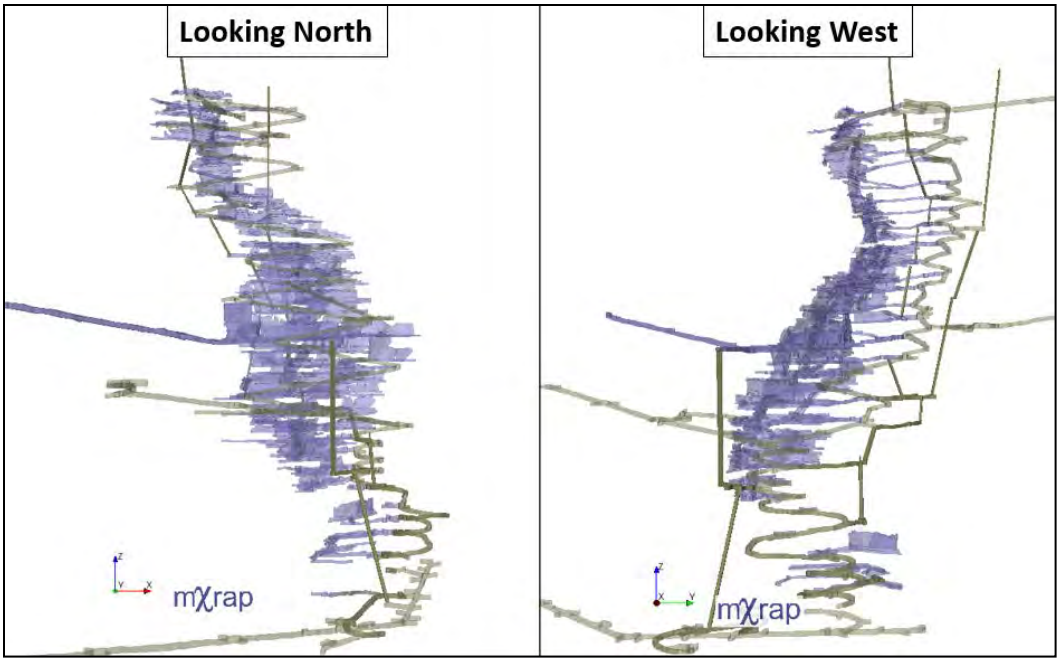

Figure 22 Morrison Mine Workings shown looking North (on left side) and looking West (on right side)

3.2.1 Mine Geology

The Morrison orebody is a Sudbury footwall, Cu-Ni-PGE deposit and is an amalgamation of the Rob's footwall and Levack footwall deposits (FNX Mining Company, 2009). This mineralization is characteristic of the Sudbury Basin and is classified as a narrow-vein copper stockwork deposit located within the brecciated zone surrounding the northwest section of the Sudbury Igneous Complex (SIC). These formations are denoted by erratic veins varying in width and dip. The veins are primarily chalcopyrite and also host cubanite, minor pyrrhotite, pentlandite, millerite, and magnetite (FNX Mining Company, 2009). The host rocks at Morrison are Sudbury breccia, meta-gabbro, granodiorite-gneiss, and mafic-gneiss ranging from 175 to 230 MPa in strength (Milner *et al*, 2013). The ore veins are comparably softer to the host rock and very brittle. The erratic nature of the veins is depicted in Figure 23from the nearby Strathcona Mine which has been mining ore of a similar nature using the cut-and-fill method since the late 1970s.

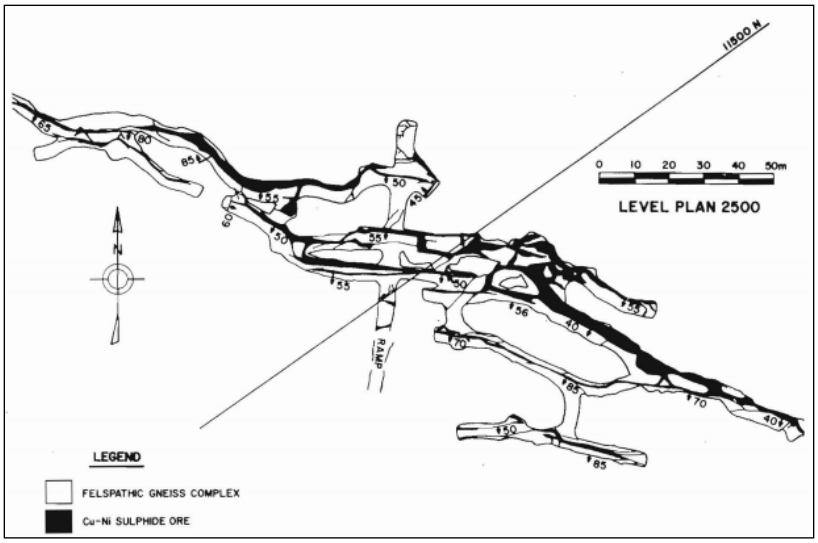

Figure 23 Strathcona Mine, 2500 Level shown in Plan-View (Abel, 1980)

Shown below is a figure of the uppermost level of Morrison Mine (2900 Level) (see Figure 24):

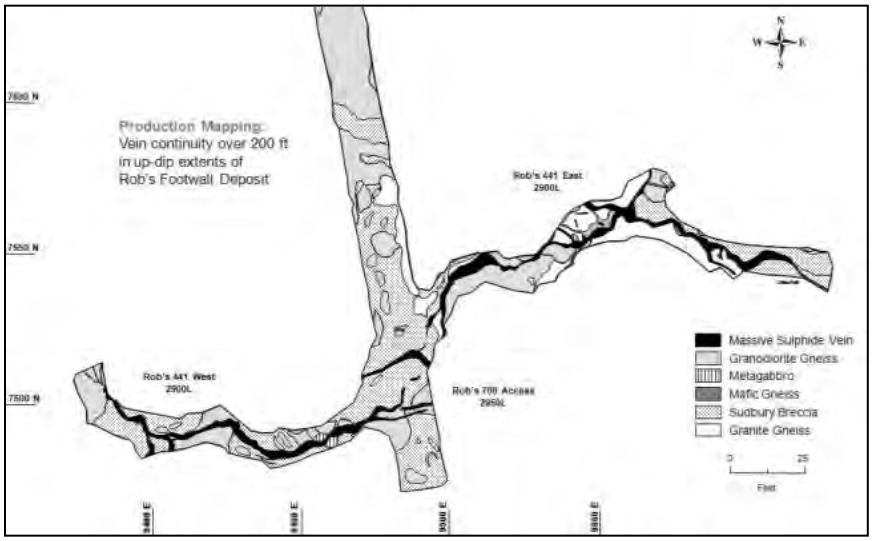

Figure 24 Morrison Mine, 2900 Level shown in Plan-View (FNX Mining, 2009)

Because Morrison is a narrow vein mine, the headings are referenced by the vein that is being extracted. The mine can be separated into logical zones based on the veins present. Therefore, locations referenced in this thesis, be it hazard locations or event locations the vein reference is used. For example, the mine is separated into the following sections:

- MD1: Levels 2900 – 3270, Veins X, Y, and Z
- MD2: Levels 3330 – 3510, Veins A and Z

- MD3: Levels 3570 – 4340, Veins A, B, C, D, E, F, G, H
- MD4: Levels 4400 – 4640, Veins F, G, H, I
- MD5: Levels 4700 – 5020, Veins G and K

A series of figures is shown in the following pages illustrating the different veins and their respective orientations (see Figure 25):

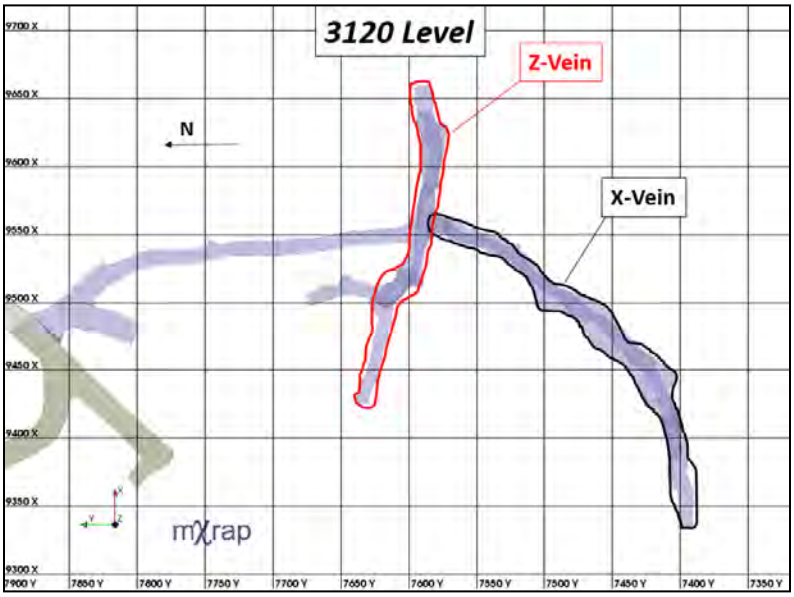

Figure 25 Morrison Mine, 3120 Level shown in Plan-View depicting Principal Vein Orientations

The previous figure is of 3120 Level which lies within the MD1 zone of the mine. As can be seen, there are 2 principal veins. Z-vein runs Northwest/Southeast and X-vein is roughly orthogonal to Z-Vein running Northeast/Southwest. Y-Vein is present in the figure as well as a splay off of Z-Vein.

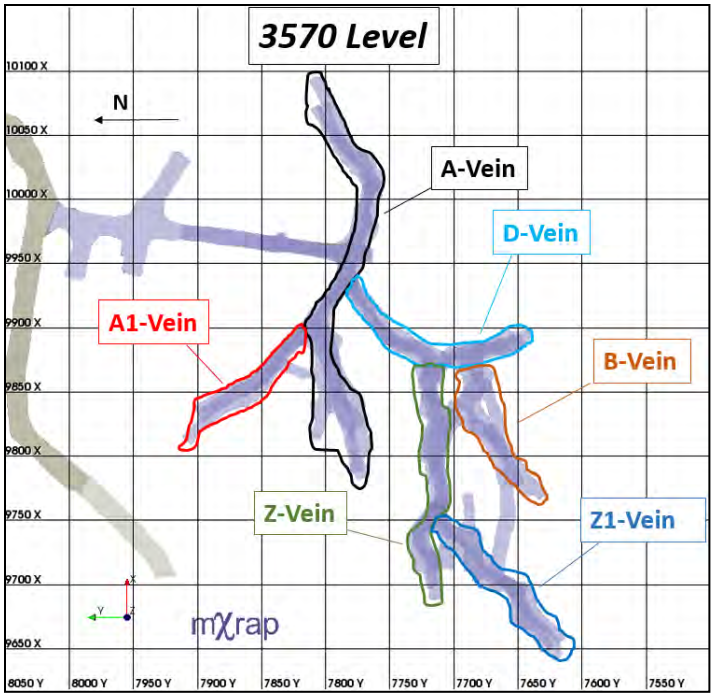

Figure 26 Morrison Mine, 3570 Level shown in Plan-View depicting Principal Vein Orientations

The figure above is of 3570 Level, located in MD3. This level is the most complex in terms of vein orientations.

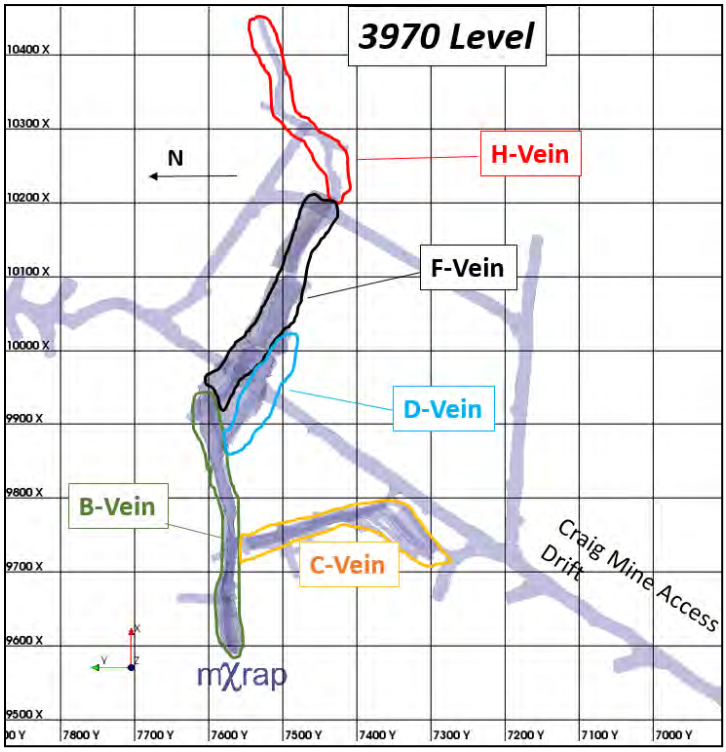

Figure 27 Morrison Mine, 3970 Level shown in Plan-View depicting Principal Vein Orientations

Figure 27 is a plan view of 3970 Level which is located in MD3. This is roughly the heart of the orebody with access from Levack Mine and Craig Mine. As of September 2016, this level is fully extracted. The veins present are listed below with their approximated orientations. 3970 Level, along with 2900 Level were two of the first explored areas of Morrison Mine. The access to 3970 was driven in 2008 and crosscutting along the vein was completed in that year as well (FNX Mining Company, 2009). This is shown in the following figure (see Figure 28):

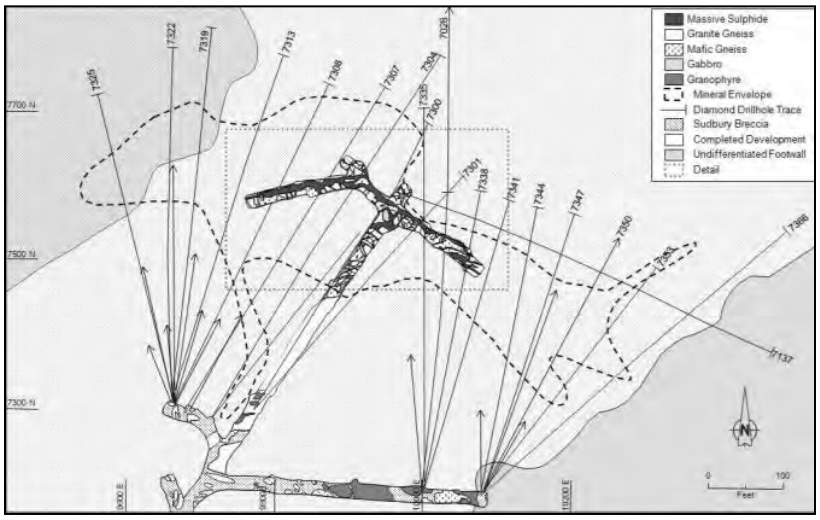

Figure 28 Morrison Mine, Initial Bulk sample on 3970 Level shown in Plan-View (FNX Mining, 2009)

Moving lower in the orebody, the following figure shows 4150 Level and the respective veins (see Figure 29):

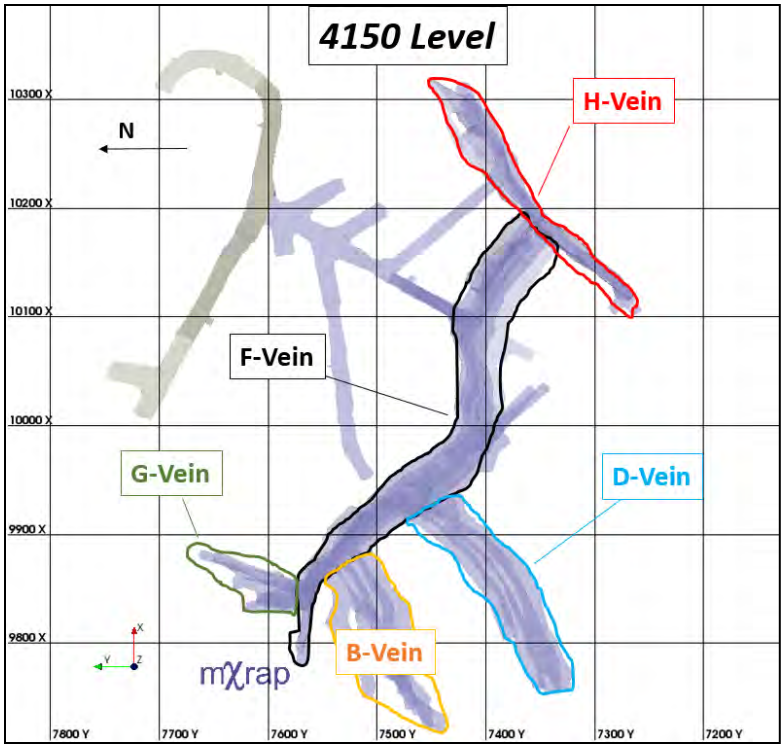

Figure 29 Morrison Mine, 4150 Level shown in Plan-View depicting Principal Vein Orientations

Moving lower into MD4, a plan view of 4400 Level is shown in the following figure (see Figure 30):

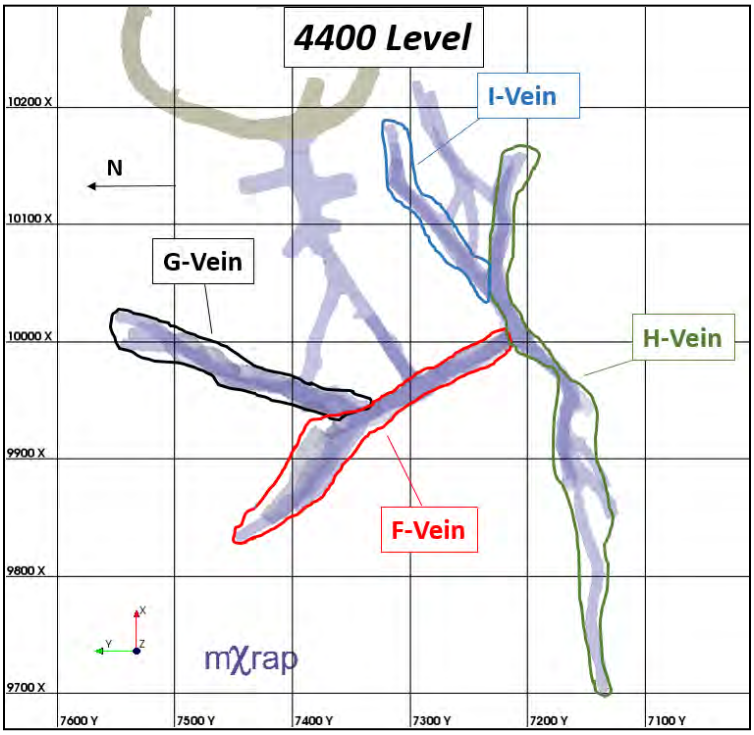

Figure 30 Morrison Mine, 4400 Level shown in Plan-View depicting Principal Vein Orientations

3.2.2.1 Faults at Morrison Mine

There are a number of faults at Morrison mine. Many of the faults are host to the ore veins. Two faults have been named and are F-Fault and H-Fault which are shown in the figure below (see Figure 31):

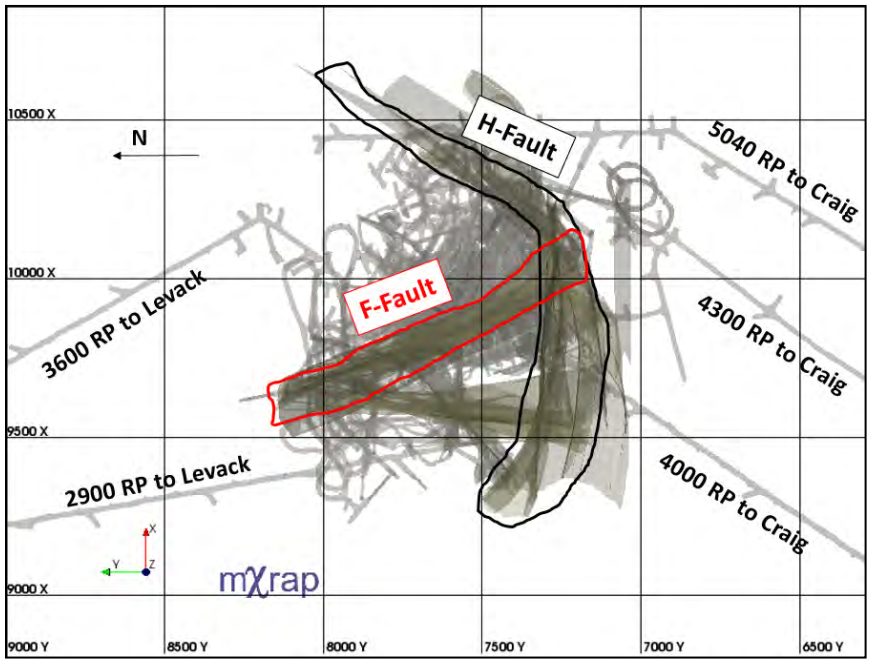

Figure 31 Morrison Mine, Plan-View showing Major Faults

3.2.3 Mining Methods at Morrison Mine

Since the veins are erratic in nature, definition of the orebody is difficult. Therefore, to effectively mine the veins, selective mining methods are more amenable. This involves following the vein using geological mapping of every round. The veins are mapped in the walls, face and back. The back mapping creates a projection of the vein for the next cut. The wall and face mapping allow operations to decide the direction of advance laterally on the current cut. Since diamond drilling results are spotty, this type of mapping 'fills in' the gaps. An example of this is shown in the following figure at the nearby Strathcona Mine (now Fraser Copper) (see Figure 32):

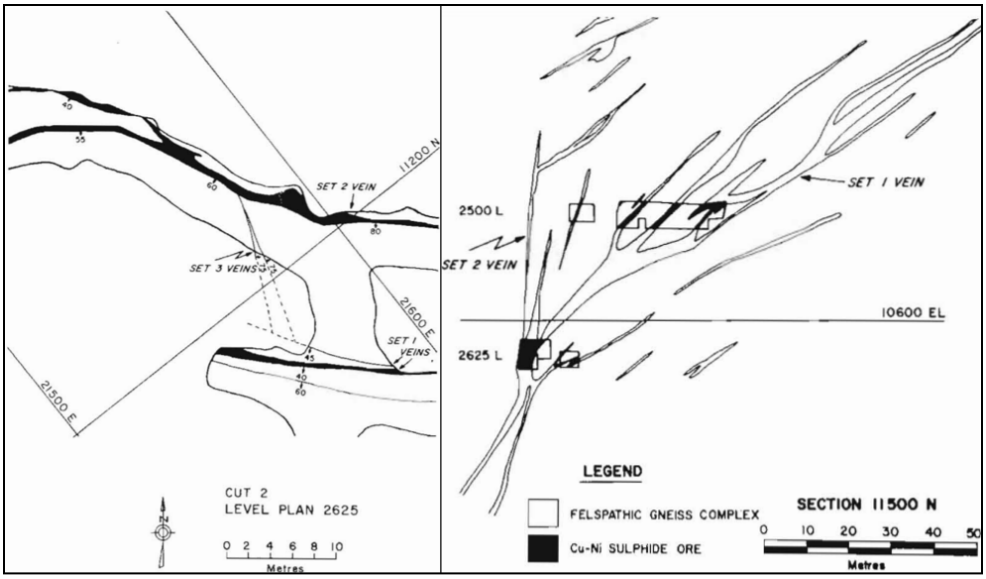

Figure 32 Strathcona Mine, 2625 Level shown in Plan-View (on Left) and Section View of 2500 and 2625 Levels (on Right) (Abel, 1980)

Similar to Strathcona Mine and Coleman Mine, the main mining methods used at Morrison include overhand cut-and-fill and longhole uppers stoping. Conventional mining methods have also been used in the past at the mine including shrinkage stoping and captive cut-and-fill. The nominal sub-level spacing used is 18m or 60ft. This amounts to 6, 10ft high cuts of cut-and-fill. The following figure set illustrates how each mining method is carried out (see Figure 33 & 34):

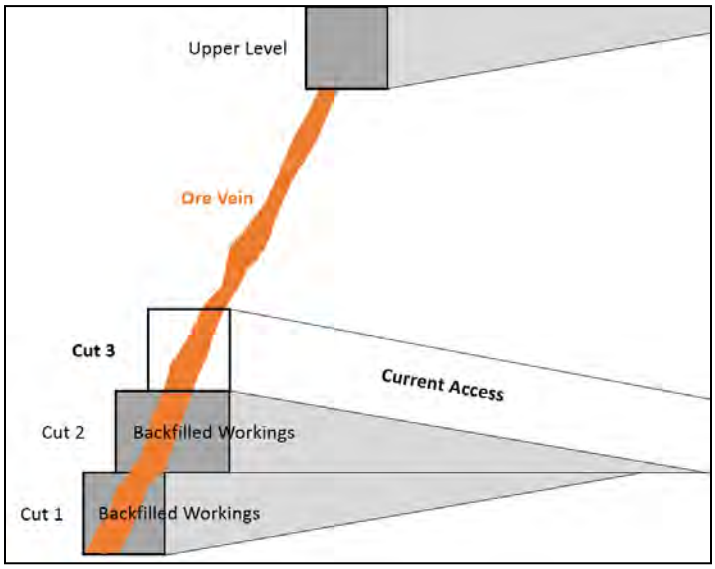

Figure 33 Generic Section View of the Overhand Cut-and-Fill Mining Method

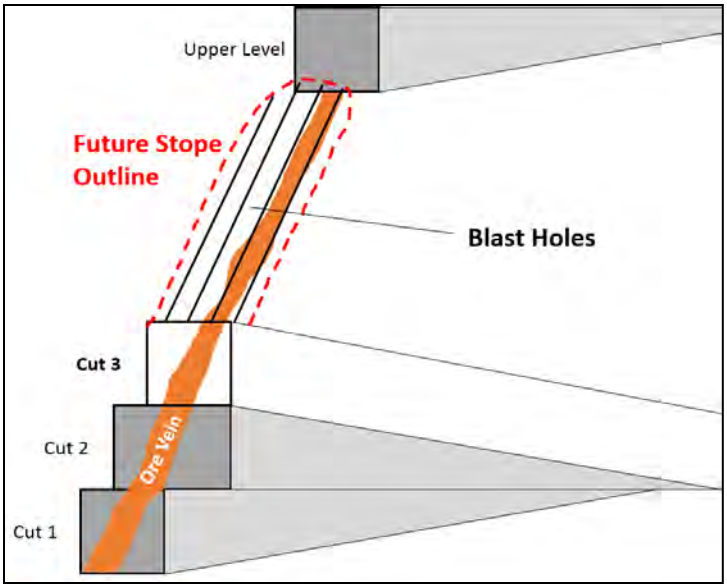

Figure 34 Generic Section View of the Longhole Stope Mining Method Using Up-Hole Drilling

The *modus operandi* currently for Morrison Mine, is to mine 3 cuts overhand, then extract the remaining 3 cuts using longhole uppers stoping retreating towards the main access point. This retreat sequence is shown in the following figure with stopes numbered according to the order of extraction (see Figure 35):

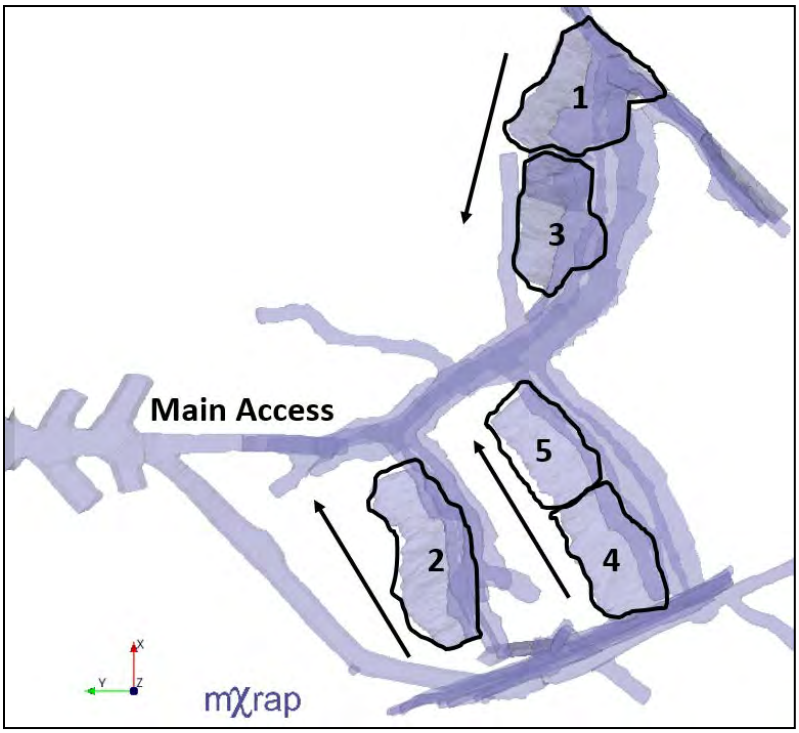

Figure 35 Plan view of a Typical Stope Extraction Sequence at Morrison Mine

Further to the standard mining sequence, some variations have also been done and are discussed below:

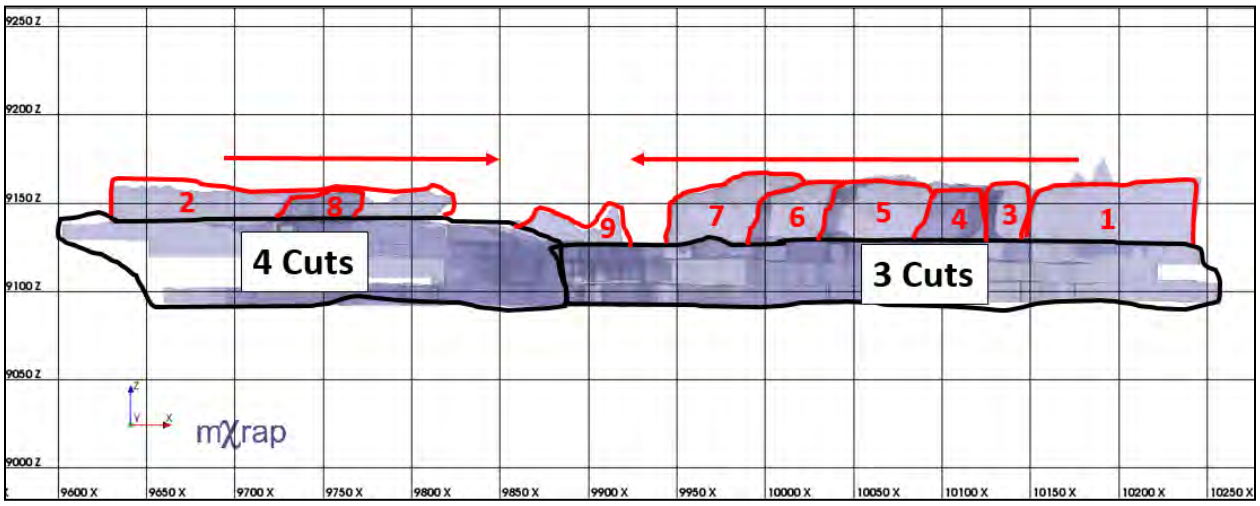

Figure 36 Morrison Mine, Section-View of 4030 Level, Looking North Showing the Extraction Sequence of that Specific Sub-Level

The case shown above is 4030 level which was mined 3 cuts overhand. A 4th cut was taken on the west side of the orebody where the vein geometry is more complex. Following the completion of the 4th cut, longhole stopes were mined back towards the main access point.

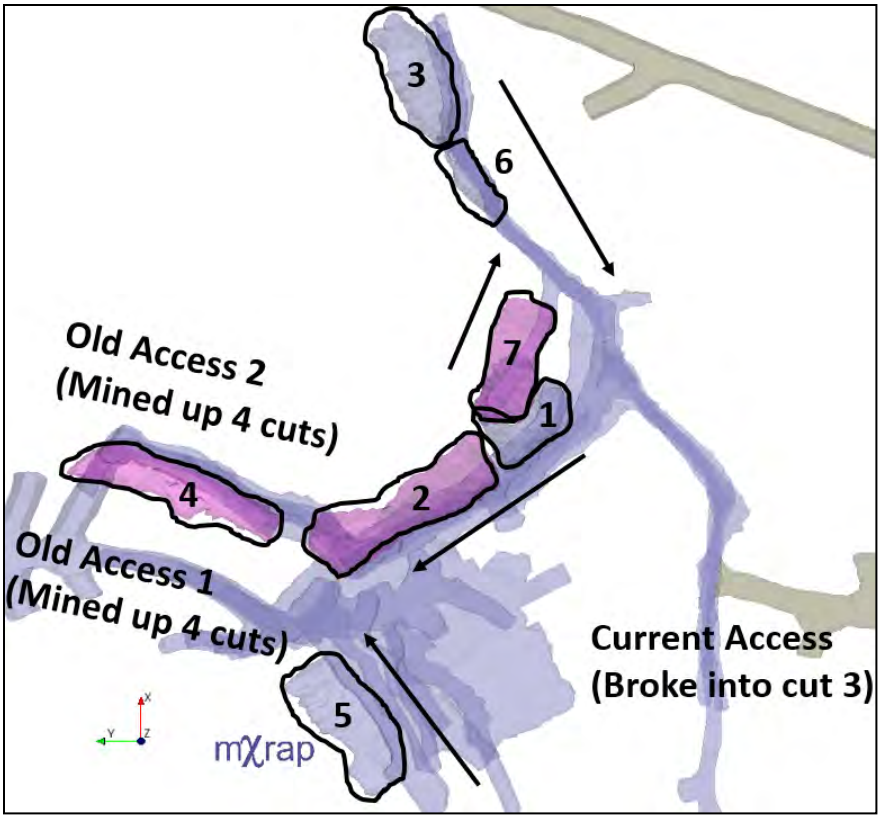

Figure 37 Morrison Mine, 4280 Level shown in Plan-View depicting the Extraction Sequence on that level

The case highlighted the previous figure is 4280 level. The level was initially mined in 4 cuts from the old access 1. Cuts 2 to 4 were mined from both old access points. H-vein was mined in 3 cuts from old access 2. The current access was driven and broke into cut 3 on H-vein where longhole stopes have been mined towards the current access point. Since this retreat sequence involves taking open stopes along abutment created by past mining, this area has experienced some of the most seismically active blasts in the mine history.

3.2.4 Mine Seismic System

Morrison Mine utilizes a micro-seismic system with sensors placed around the boundary of the mine in strategic locations. This is done in order to obtain the most accurate event locations. The sensors used are as follows: 18 uniaxial accelerometers (underground), 2, 15Hz triaxial geophones (underground), 2, 4.5Hz geophones (strong motion sensors on surface) (Taghipoor *et al*, 2016). A figure is given below showing the sensor distribution in relation to the mine (see Figure 38):

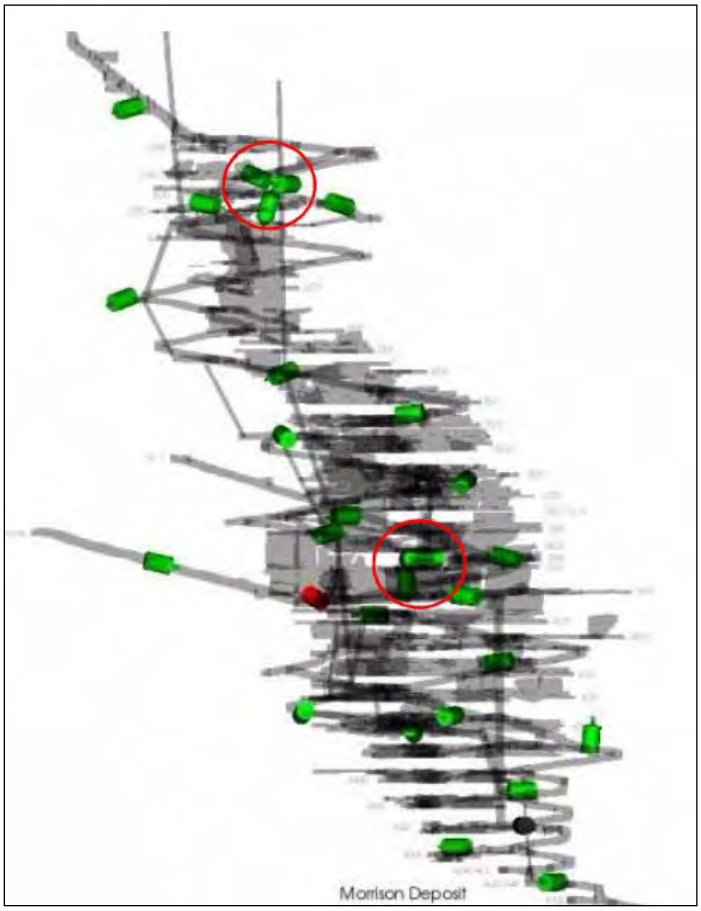

Figure 38 Morrison Mine Seismic Sensor Array with Sensors shown in Green (Taghipoor *et al*, 2016)

Due to the fact that Morrison Mine is accessible from both the hanging wall (Craig Mine) and footwall (Levack Mine), this allows for sensor coverage in both areas. This dual-sided sensor coverage allows for more accurate event locations and seismic parameters.

3.3 Seismicity at Morrison Mine

3.3.1 Magnitude Scale

In order to determine the optimal magnitude scale to be used, a series of comparisons were made between the reported Richter magnitudes from the Sudbury Regional Seismic Network and the magnitudes derived from the micro-seismic system in place at Morrison. The comparisons are summarized in the following table (see Table 3) and are also shown in the graphs below (see Figure 39):

Table 3 Magnitude Scale Comparisons between the Local, Moment, and Richter Scales

Comparison of Magnitudes	Relation	R-squared Value
ESG Moment Mag vs SRSN Richter Mag	MoMag = 0.5331*Richter + 0.0072	0.3225
ESG Local Mag vs SRSN Richter Mag	LocalMag = 1.1697*Richter - 0.2658	0.3618

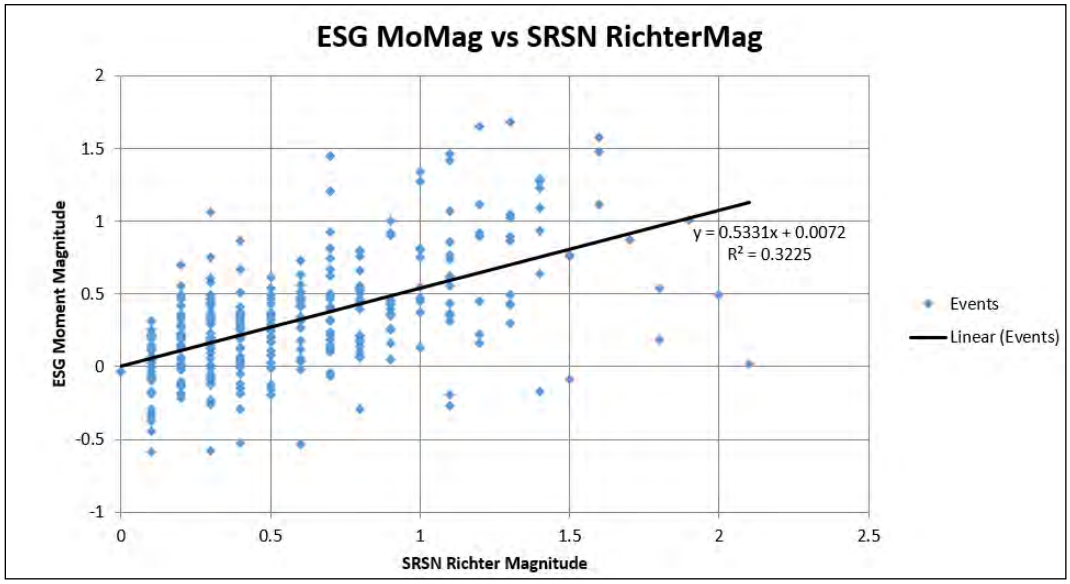

Figure 39 Magnitude Scale Comparison between Moment and Richter Magnitudes

Referring to Table 3, the r-squared values give an indication of the relation between the magnitude scales being compared. R-squared values close to 1.0 indicate a linear relationship while values close to 0.0 indicate non-linear relationships. In this case, the moment magnitude scale has been chosen primarily even though its r-squared value is further away from 1.0 than the value for the local magnitude scale. This scale was chosen primarily because the mine-site is already using that scale. Also, when examined over time, the moment magnitude is better behaved than the local magnitude which exhibited bimodal behavior.

3.3.1.1 A Note on the Sudbury Regional Seismic Network

Since 2008, a regional seismic network has been active in Sudbury. Created by Marty Hudyma of Laurentian University, this system features 28 sensors located across the entire Sudbury Basin (Hudyma, 2016). This is done in order to provide a more accurate interpretation of seismic activity in Sudbury. Since underground seismic systems saturate

very quickly due to strong ground motions of large events, the advantage of having the lower frequency regional seismic sensors is that they often retrieve accurate magnitudes for the larger events. A figure is shown below illustrating the locations of the sensors (see Figure 40):

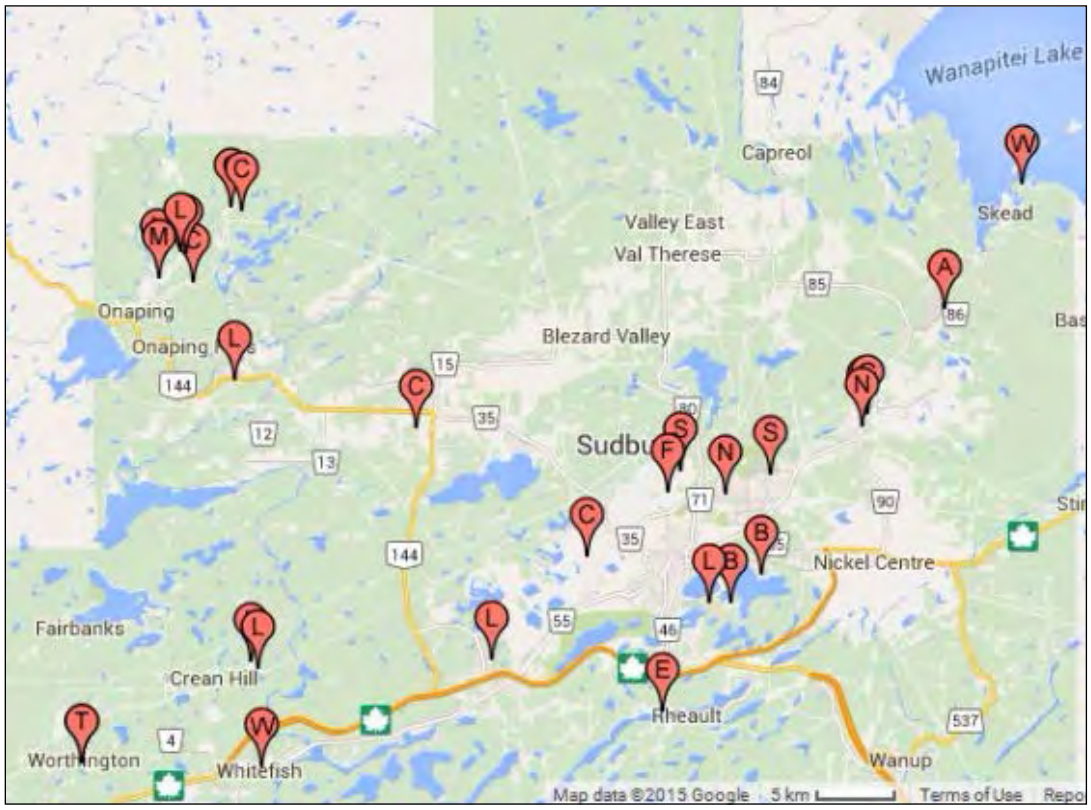

Figure 40 Sudbury Regional Seismic Network Sensor Locations (Hudyma, 2016)

The SRSN is designed to pick up events and blasts greater than Richter Mag +1.0. In some parts of the array, events and blasts smaller than Richter Mag +1.0. Since its inception in 2008/09 over 5000 mining induced events and over 14000 blasts have been recorded by the system (Hudyma, 2016). The system is used to generate weekly reports of large events and blasts that are distributed to local mines.

3.3.2 The Impact of Mining Activity on Seismicity at Morrison

As discussed in Section 3.2.3, the principal mining methods used are overhand cut-and-fill and longhole-uppers open stoping. Since the extraction sequence begins with taking successive cuts upwards, the amount of solid ground between sublevels decreases. As well, as stopes are taken in a retreating sequence towards a central access, the zone of

solid ground decreases in the horizontal dimension as well. Early on in the mine life, before the installation of the microseismic system, cut-and-fill was the predominant mining method. However, as mining fronts have approached the 3rd and sometimes 4th cut, the amount of extraction through stoping has increased. A time-history chart is shown below for all events from 2013 to 2017 (see Figure 41):

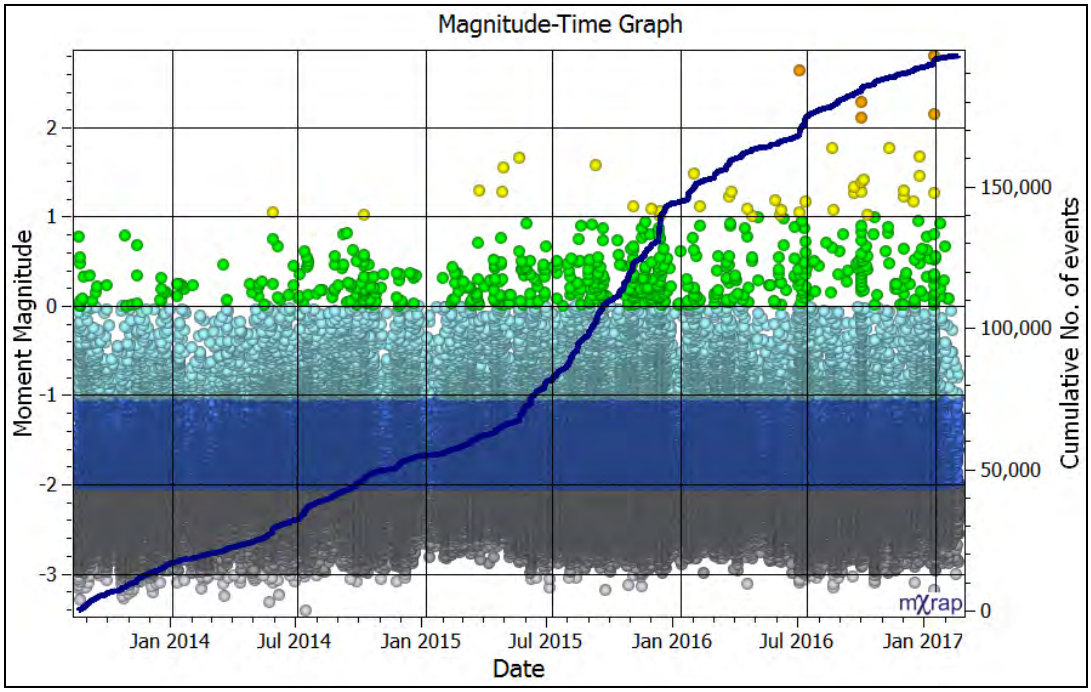

Figure 41 Magnitude-Time-History Chart of the Entire Seismic Record at Morrison Mine

The previous chart shows the seismic activity in the entire mine to date. As mentioned in Chapter 2, an important feature of the magnitude-time-history chart in the cumulative events line. Blasts can be seen as major steps in the line itself while an increase in seismic activity caused by increased production can be seen as a change in the slope of the cumulative. As previously mentioned, Morrison is essentially 2 deposits: Rob's Footwall and the Levack Footwall orebody. As well, for organizational purposes, the mine is separated into MD1, MD2, MD3, MD4, and MD5 (see Section 3.2.1). To further analyze historical seismic activity, magnitude-time-history are provided for each domain of the mine.

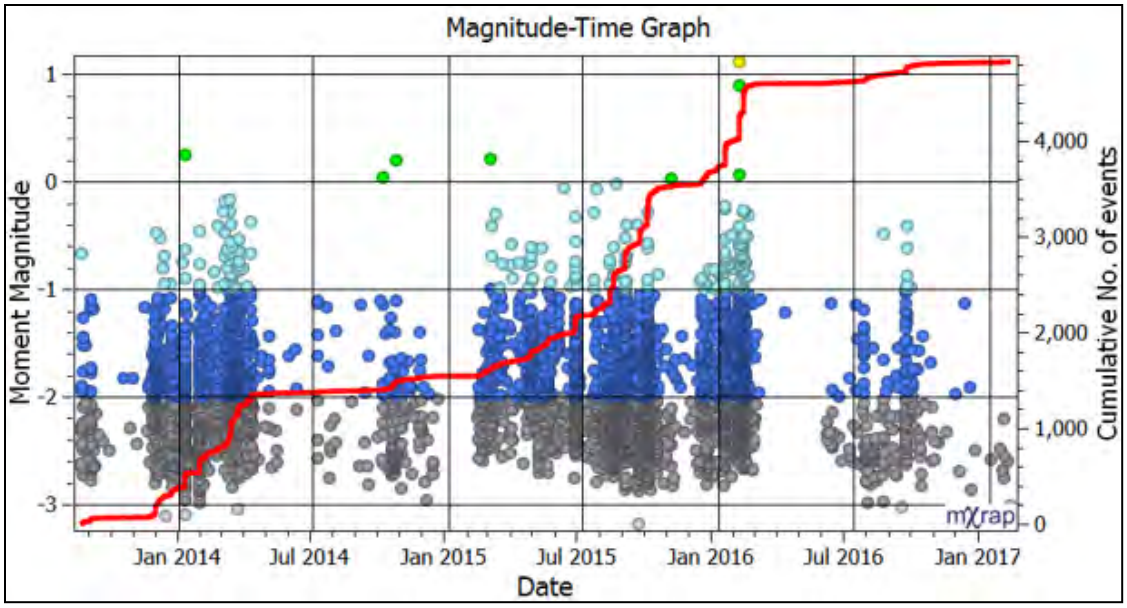

Figure 42 Morrison Mine, Magnitude-Time-History Chart for the MD1 Zone

The previous figure shows the seismic activity in MD1 to date. Examining the time-history chart, it is evident that production ramped up in late 2013/early 2014. There was a lull through 2014 until early 2015 where production increased through early 2016. At this point the majority of MD1 was extracted. The final stope was taken in September 2016 which can be seen in the time-history chart.

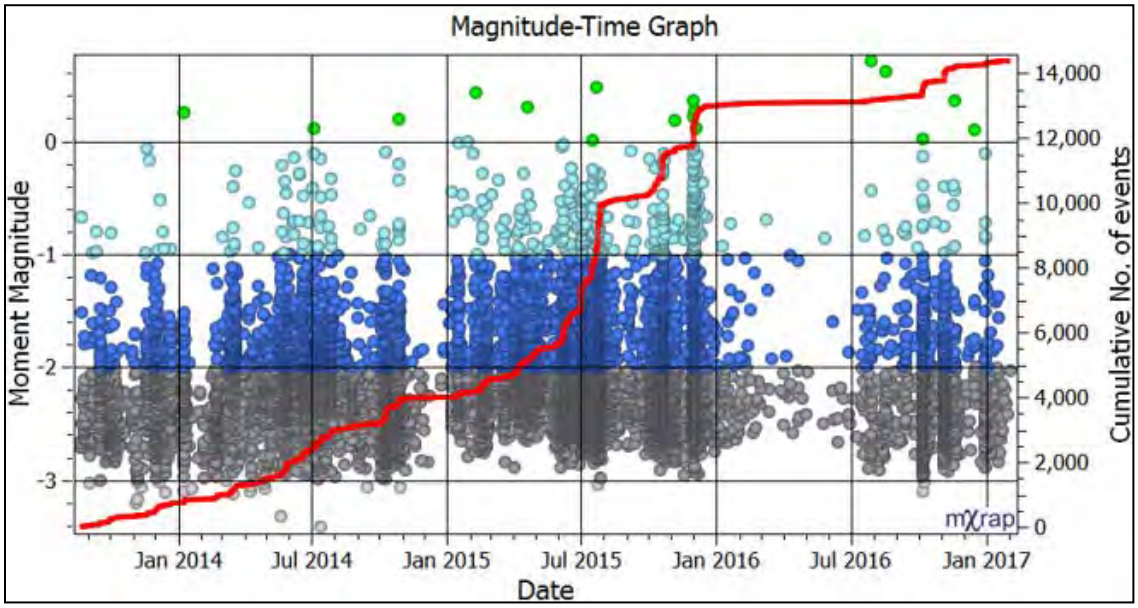

Figure 43 Morrison Mine, Magnitude-Time-History Chart for the MD2 Zone

The chart above shows the seismic activity in MD2 to date. One can see fairly consistent production through early 2015. March 2015 saw a rapid increase in stope production through December 2015 then a lull through to July 2016. In July/August 2016, production resumed on 3570 Level to begin extracting the 3510/3570 sill pillar.

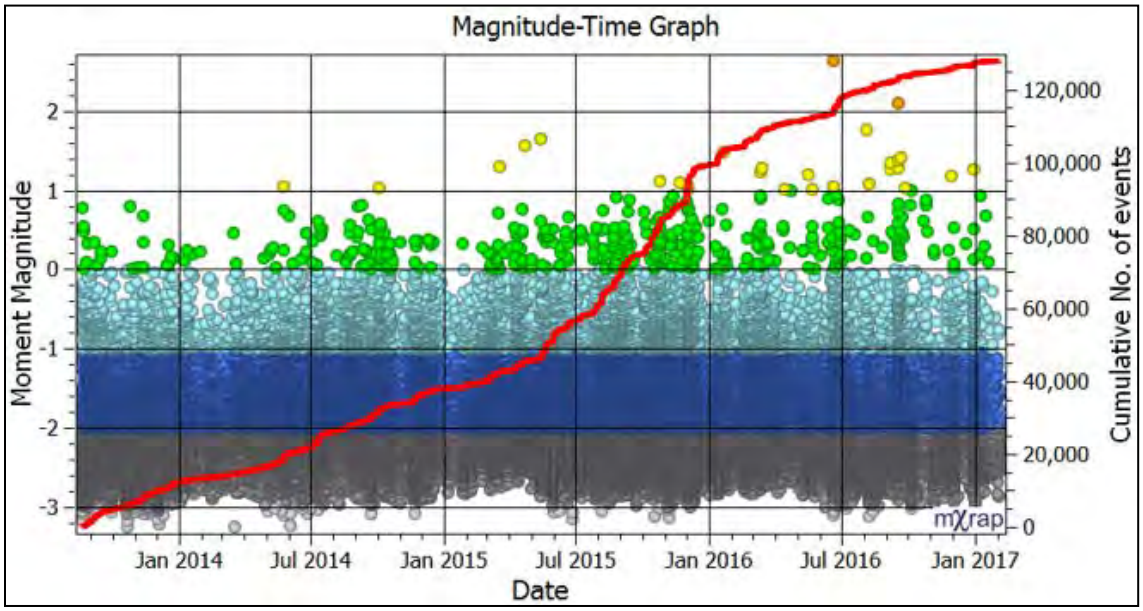

Figure 44 Morrison Mine, Magnitude-Time-History Chart for the MD3 Zone

Figure 44, shows the seismicity in MD3 to date. This zone is the largest in the mine and therefore has the largest production profile and the most seismic activity. Production through mid-2015 was fairly consistent with an increase in production from June to December 2015. During this time most of the cut-and-fill activity was finished and open stope production increased. The rate of production decreased in early 2016 and has remained fairly constant. The largest events in MD3 and in the history of Morrison mine occurred in mid-2016.

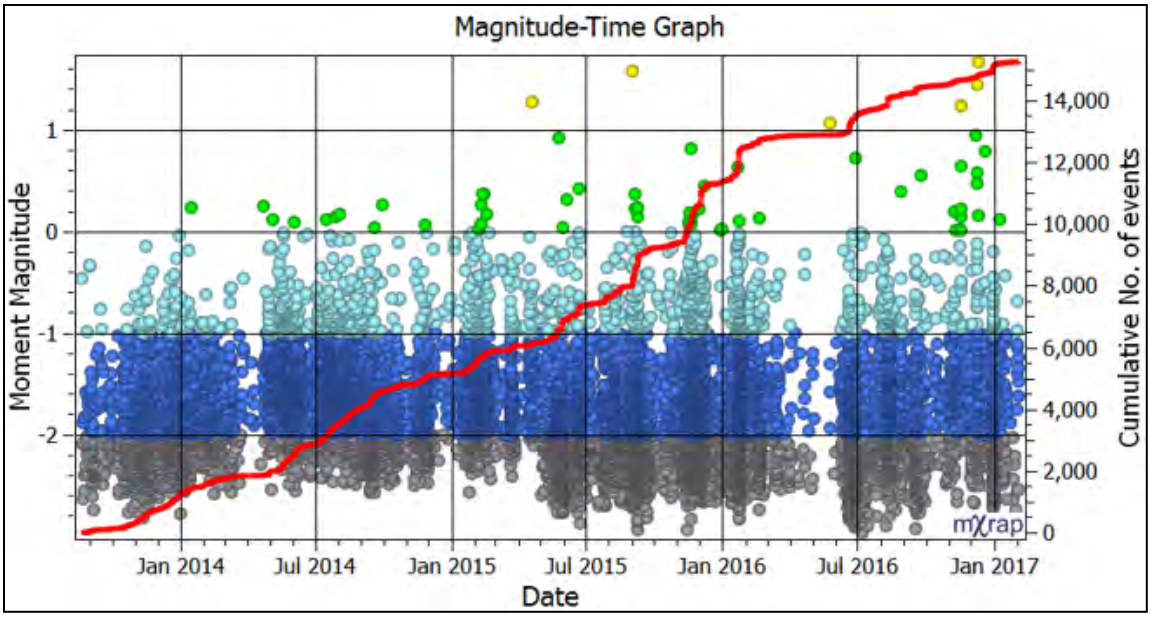

Figure 45 Morrison Mine, Magnitude-Time-History Chart of the MD4 Zone

Figure 45 shows the seismicity occurring in MD4 to date. Production was consistent through to July 2015 with an increase from July 2015 to February 2016. There was a distinct lull in production until June 2016 with mining activities resuming on 4340 and 4460 Levels.

The locations of large events in the mine are shown and are grouped by assumed mining activities including: cut-and-fill, sill extraction, and late-stage sill extraction. This was done using stope production records. From these records, the date of blasting, stope ID, location, and planned tonnage. Stopes are numbered sequentially along the vein that is being extracted. It is assumed that prior to Stope 1 on a given vein, the mining method is cut-and-fill. An example of the production data used is shown in the following table (see Table 4):

Table 4 Morrison Mine, 3030 Level Production Data

Date	Stope ID	Blast No.	Planned tons (diluted)
Feb-23-15	3030 Cut#2 Z East, Stope 1	1	764
Feb-28-15	3030 Cut#2 Z East, Stope 1	2	1198
Apr-18-15	3030 Cut#2 Z East, Stope 2	1	505

Apr-21-15	3030 Cut#2 Z East, Stope 2	2	1089
Jun-20-2015	3030 Cut#2 Z East, Stope 3	1	2607

The large event locations for each year are shown in the following figures (see Figures 46 & 47):

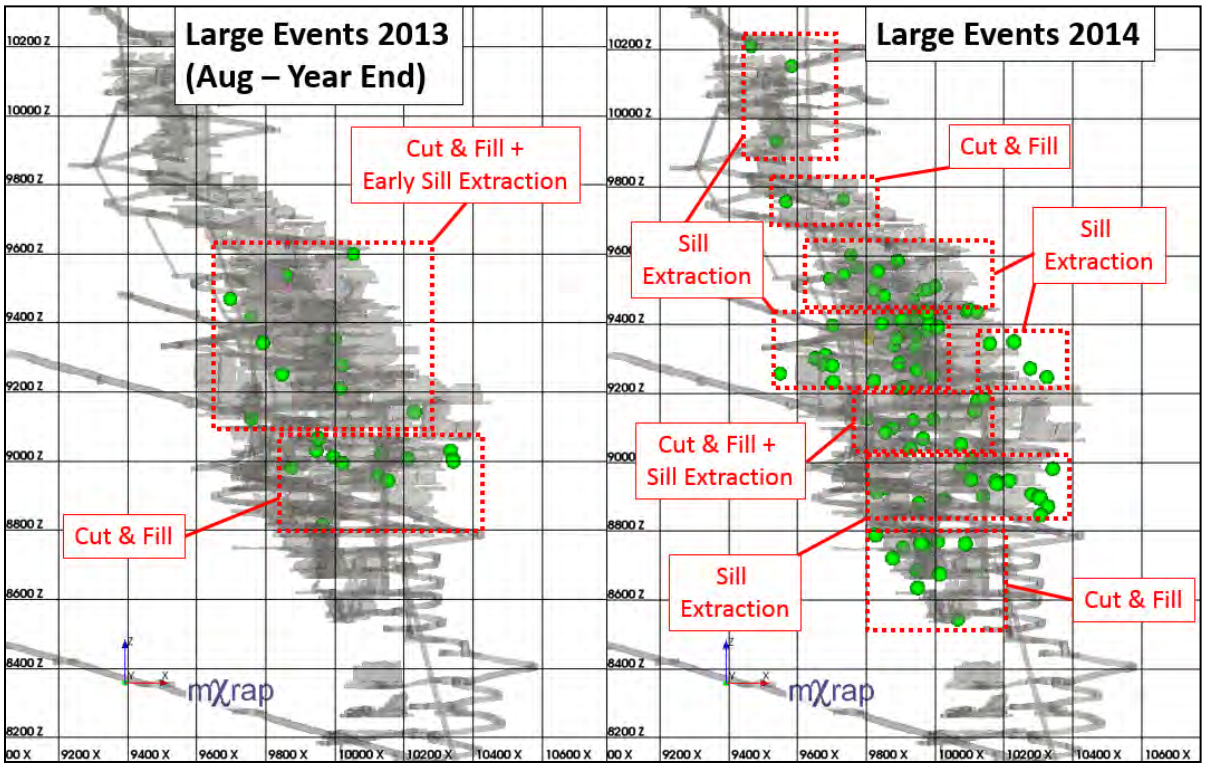

Figure 46 Large Event Locations (M > 0) for 2013 (on Left) and 2014 (on Right)

Looking at the previous figure it is important to note that the seismic data for 2013 is only inclusive from August onwards. As well, there is no available blast record for 2013. Therefore it is assumed that the majority of mining was cut-and-fill with some longhole stope extraction.

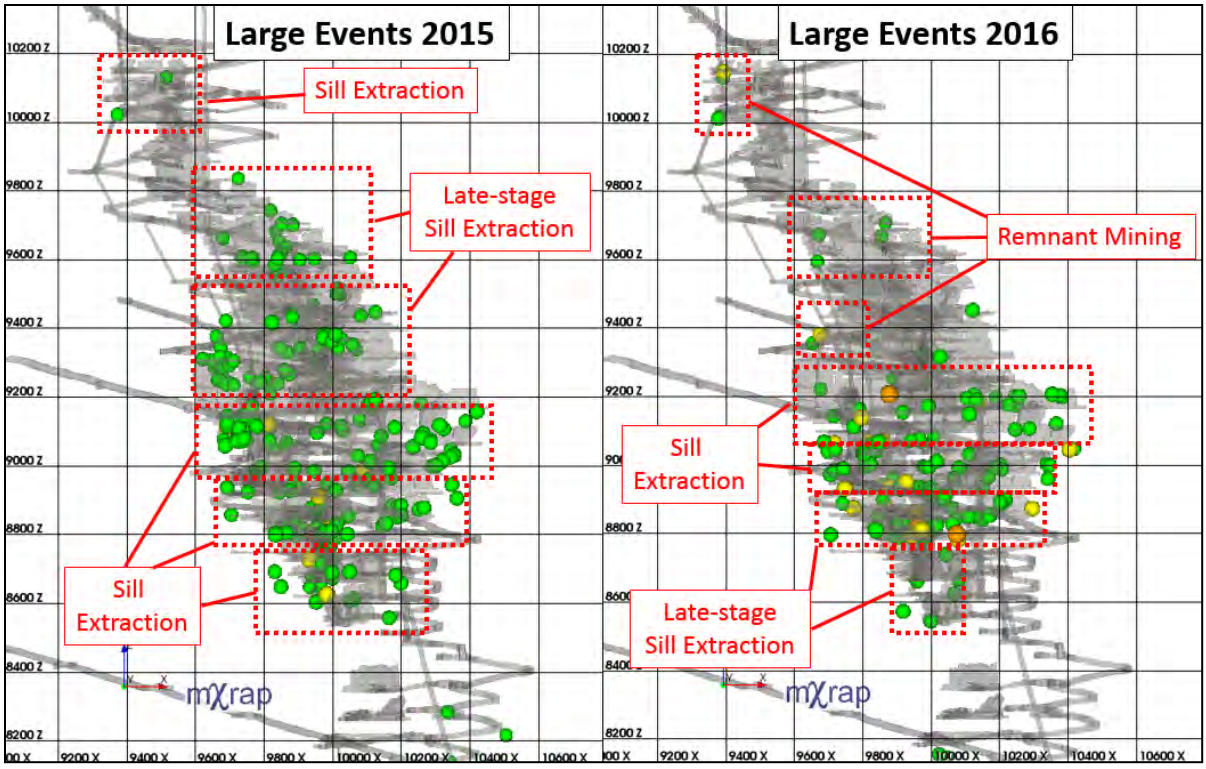

Figure 47 Large Event Locations (M > 0) for 2015 (on Left) and 2016 (on Right)

Examining 2015 and 2016, it is evident that as sill extraction progresses, the amount and sizes of events increase. As well, since the upper portion of the mine is nearing exhaustion, the seismic activity is migrating in to the lower reaches of MD3 and MD4 as sill extraction increases on those levels. To better illustrate the effect of mining, namely stope blasting a figure is shown for 4280 Level with all seismic activity occurring between August 2013 and February 2017 (see Figure 48):

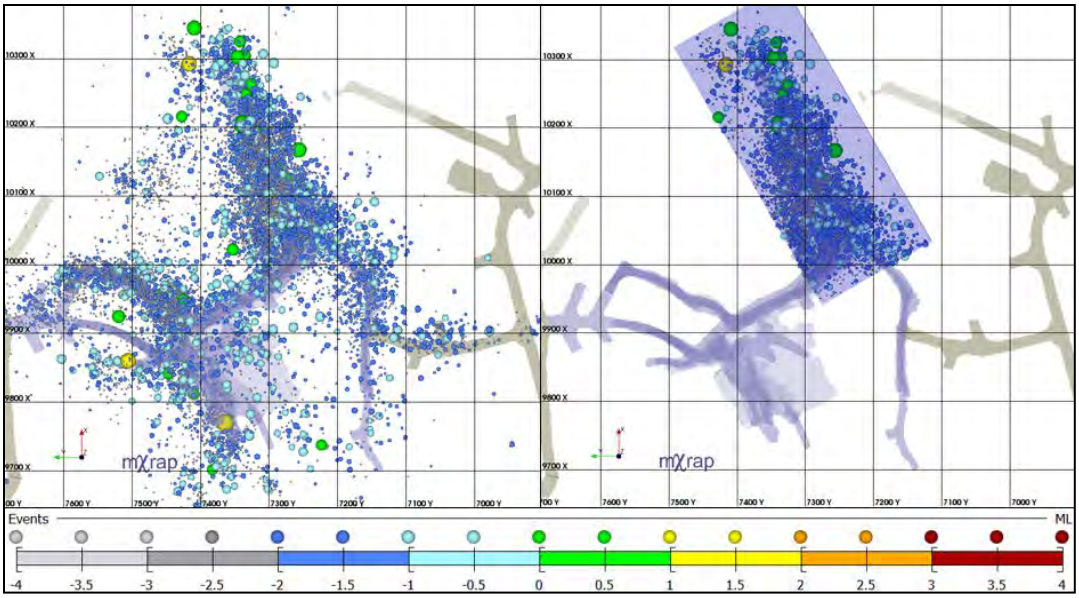

Figure 48 Morrison Mine, 4280 Level Plan-View Showing Seismic Activity from August 2013 to February 2017

With the application of a filter (in this case a volume filter in mXrap), the seismicity for specific areas can be analyzed and interpreted. A magnitude-time-history chart is shown below for 4280 Level, H-vein where significant seismic activity has occurred (see Figure 49):

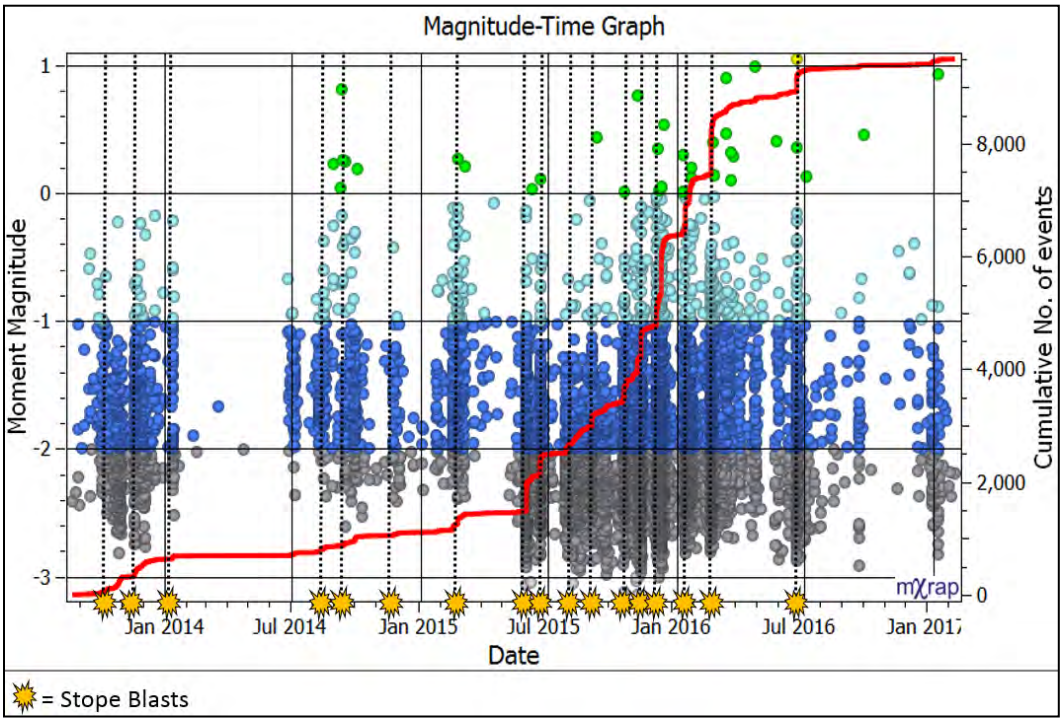

Figure 49 Magnitude-Time-History Chart of 4280 Level with Blasts Denoted

What is evident is that the severity of seismic activity increases from July 2014 through to July 2016. This is in line with increased stope production on the level and level above (4210 Level). This is also evident in the step-like nature of the cumulative events line. Also of interest, when stope blasting stops in June 2014, the rate of seismicity decreases dramatically and the number of large seismic events decreases in the same fashion. A diurnal chart is shown below to illustrate the time of day when large events have occurred (see Figure 50):

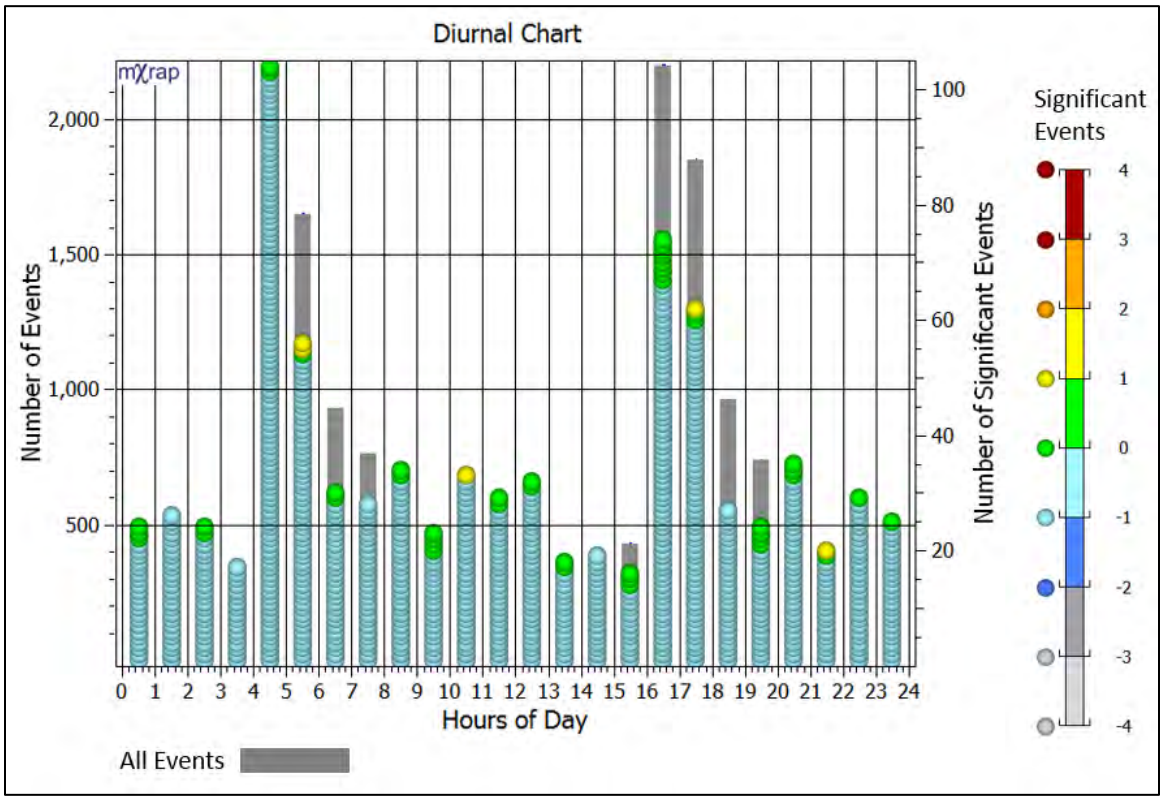

Figure 50 A Diurnal Chart of the Seismic Activity To-Date on 4280 Level

Referring to the previous chart, significant events are those above -1.0 M_w. There are distinct increases in the number of significant events between 04:00 to 06:00 and 16:00 to 18:00. This lines up well with the blast times at Morrison Mine which are around 04:45 and 16:45. Referring to the large events, those > 0 M_w, most occur in the morning within 6 hours of blasting. It should be noted that large events occur throughout the day. Even so, the effect of mining is clear in the spikes of the amount of events occurring around blast times.

3.3.2.1 Impact of Mining Activity on Large Event Occurrence

From the previous section, it is apparent that mining activity has a large impact on the amount and severity of seismic activity. To establish any relation between stope blasting and the occurrence of large events, the following parameters have been compared using events > 0 M_w and stope blasts for the hazard periods analyzed (April-June 2016; June-August 2016; August-October 2016): date/time, XYZ location, largest event magnitude, blast size (planned tons, diluted), and the distance between event and stope blast. These relations are graphed in the following figure (see Figure 51):

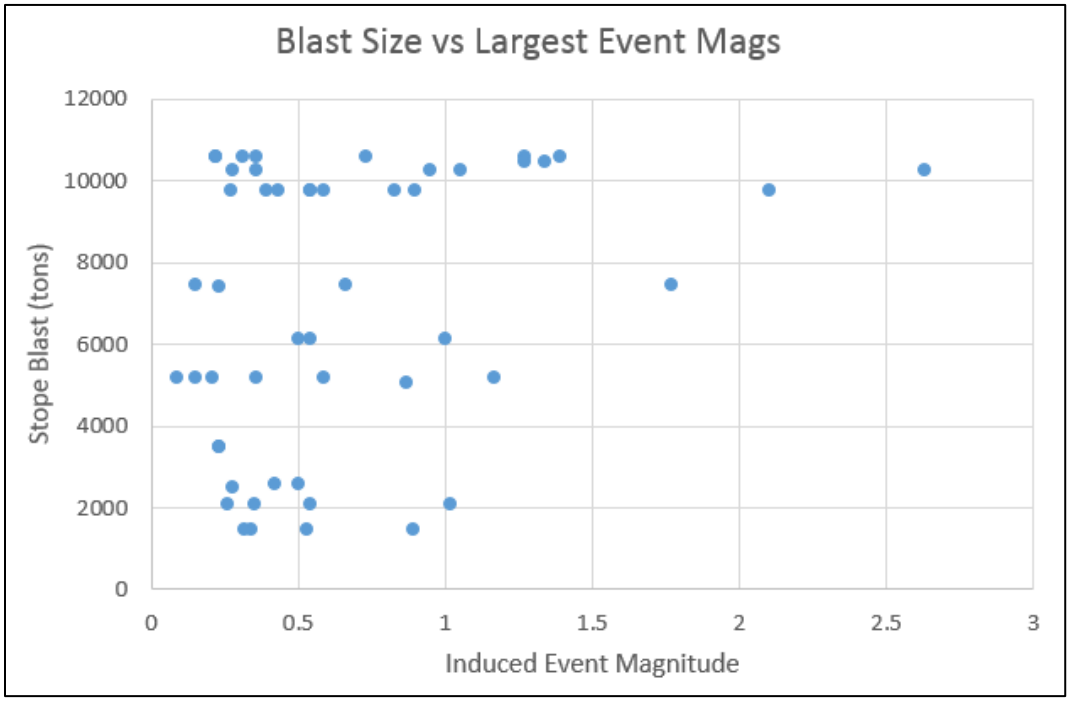

Figure 51 Blast Size versus Largest Event Magnitude

Referring to the previous chart, the likelihood of occurrence of events > 0.5, 1, and 2 M_w for logical ranges based on blast size have been calculated and are shown in the following table (see Table 5):

Table 5 Blast Size versus the Probability of the Occurrence of an Event of a Certain Size

Blast Size (tons)	P > 0.5	P > 1	P > 2
0 - 2000	40%	0%	0%
2000 - 5000	33%	11%	0%
5000 - 8000	57%	21%	0%
> 8000	61%	30%	9%

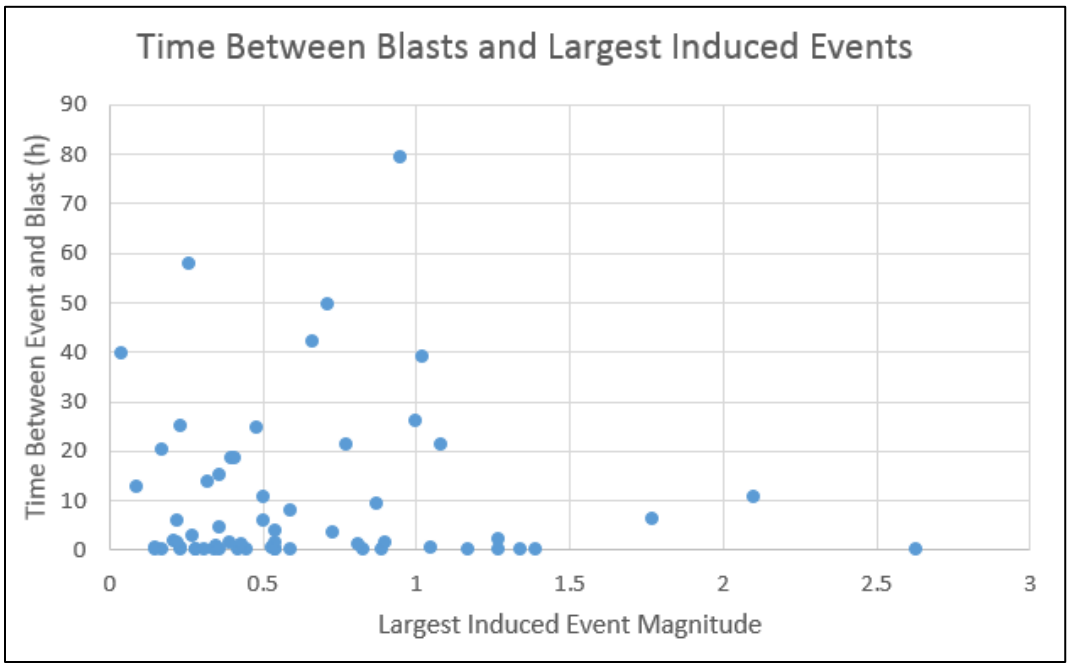

Figure 52 Time between Blasts and Possible Induced Seismic Events

Referring to the previous chart, the likelihood of occurrence of events > 0.5, 1, 2 M_w have been calculated based on logical ranges of time difference and are shown in the following table (see Table 6):

Table 6 Time Difference between Blasts and Largest Induced Events versus the Probability of Occurrence of an Event above a Certain Size

Time Difference (hrs)	P > 0.5	P > 1	P > 2
0 - 6	19%	7%	1%
6 to 12	86%	29%	14%
12 to 24	25%	13%	0%
> 24	56%	22%	0%

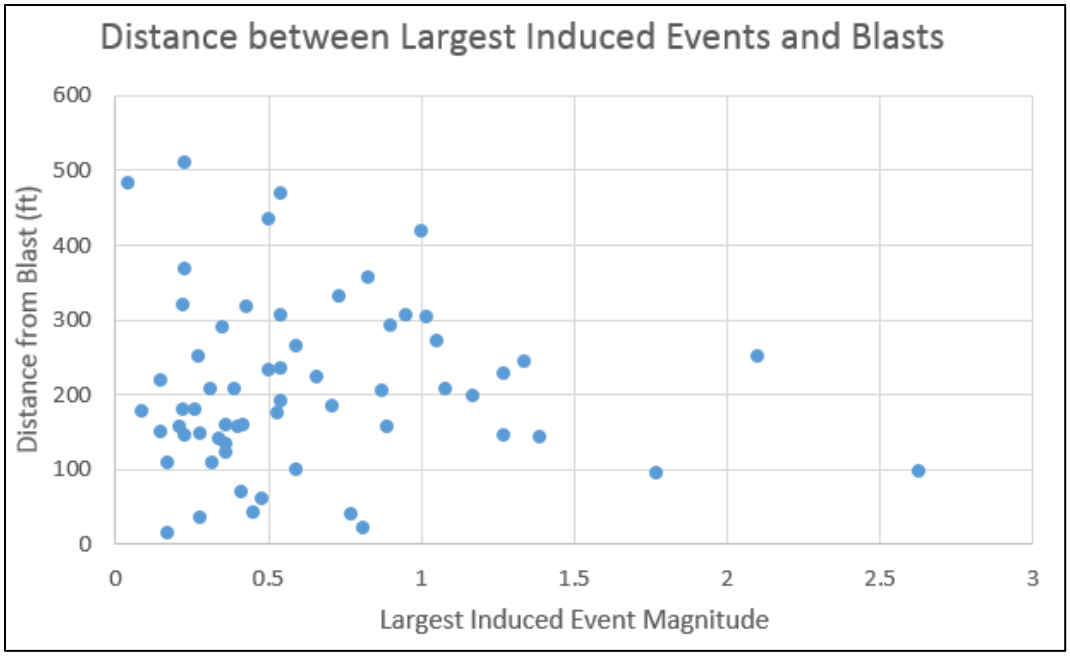

Figure 53 Distance between Blasts and Largest Induced Event Magnitudes

Referring to the previous chart, the likelihood of occurrence of events > 0.5, 1, 2 M_w have been calculated based on logical ranges of distance from the stope blast to the event and is shown in the following table (see Table 7):

Table 7 Distance from Event to Blast versus the Probability of Occurrence of and Event above a Certain Size

Distance from Blast (ft)	P > 0.5	P > 1	P > 2
0 - 100	50%	20%	10%
100 to 200	32%	14%	0%
200 to 300	69%	31%	6%
> 300	62%	15%	0%

The results of each analysis based on the behavior of likelihood, be it increasing or decreasing, are summarized in the following table (see Table 8):

Table 8 Summary of Probabilistic Behavior

Relation	P > 0.5 behavior	P > 1 behavior	P > 2 behavior	Comments
Blast Size vs Mag	General increase	Direct increase	General increase	Reasonable relation
Time Diff vs Mag	No pattern	No pattern	No pattern	No strong relation
Distance vs Mag	No pattern	No pattern	No pattern	No strong relation

From the previous table, it is evident that the blast size has the most impact on the size of the induced event.

3.3.3 Fault Activity at Morrison Mine

Through previous investigations at Morrison Mine, the majority of seismicity is blast-induced. Essentially, when there is no blasting, there are no large events. However, there is also evidence of fault-related seismic activity. As stated previously in Section 3.2.1.1, many of the faults at Morrison are host to the various ore-veins. The 2 main faults are F-fault and H-fault. Historically speaking, H-fault is the most active having been host to some of the largest events in the mine's history. The following figure shows 3970 Level where the separation between the mining-induced and fault events is the most apparent (see Figure 54):

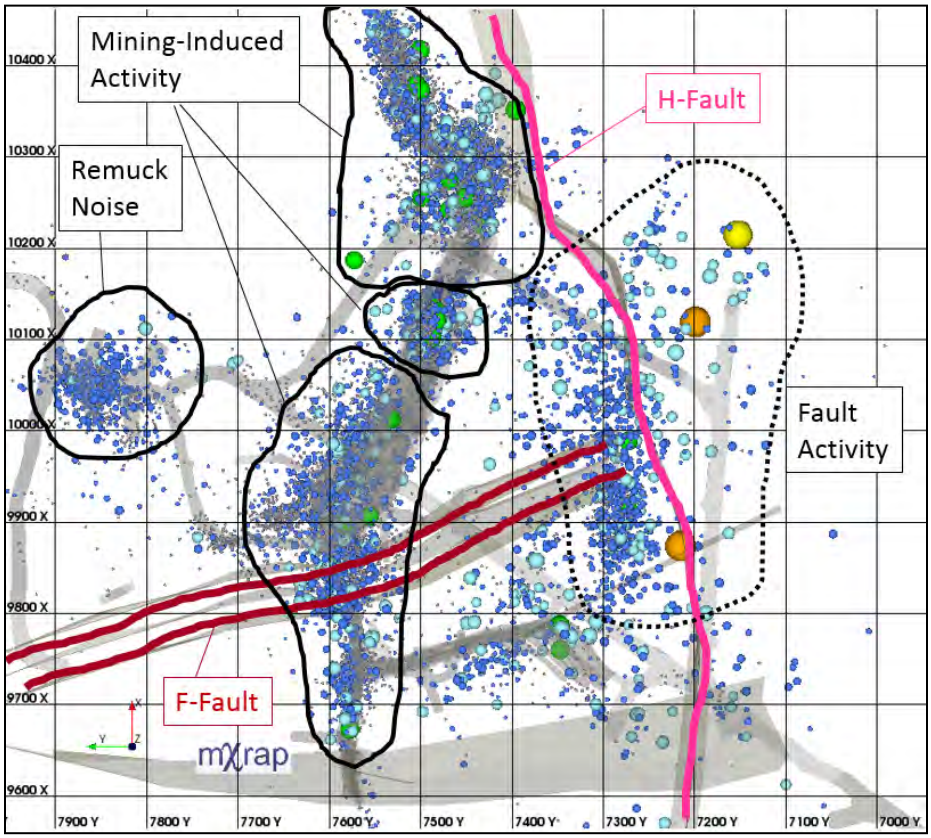

Figure 54 Fault Orientation compared to the Distribution of Seismic Activity

The following figure shows the fault activity isolated (see Figure 55):

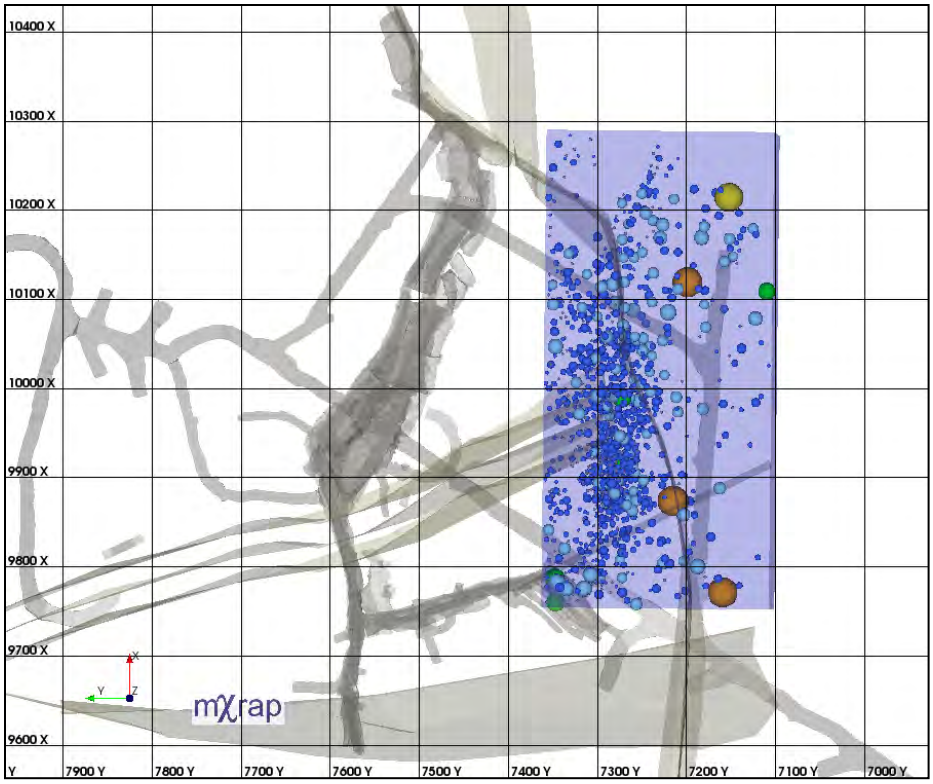

Figure 55 Seismic Activity Occurring in Proximity to H-Fault

Shown for further analysis is a magnitude-time-history of that cluster of events shown in the previous figure (see Figure 56):

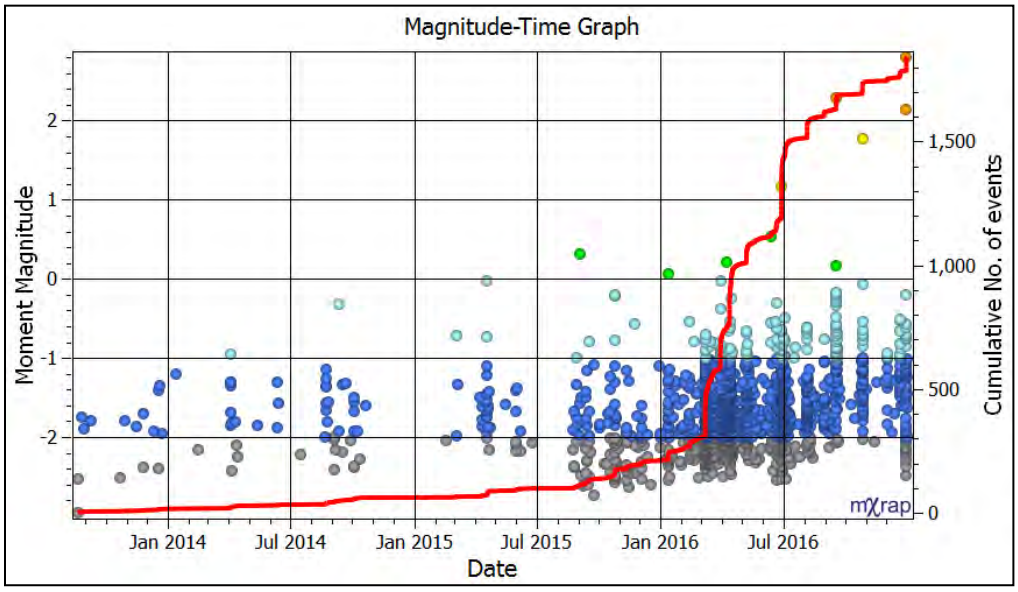

Figure 56 Magnitude-Time-History Chart of Seismic Activity Occurring in Proximity to H-Fault

From late-2013 to September 2015 the activity in the area is sporadic. From September 2015 to July 2016, activity increases and is more tied to mining activity as indicated by the cumulative events line (in red). A diurnal chart is shown below for the same cluster (see Figure 57):

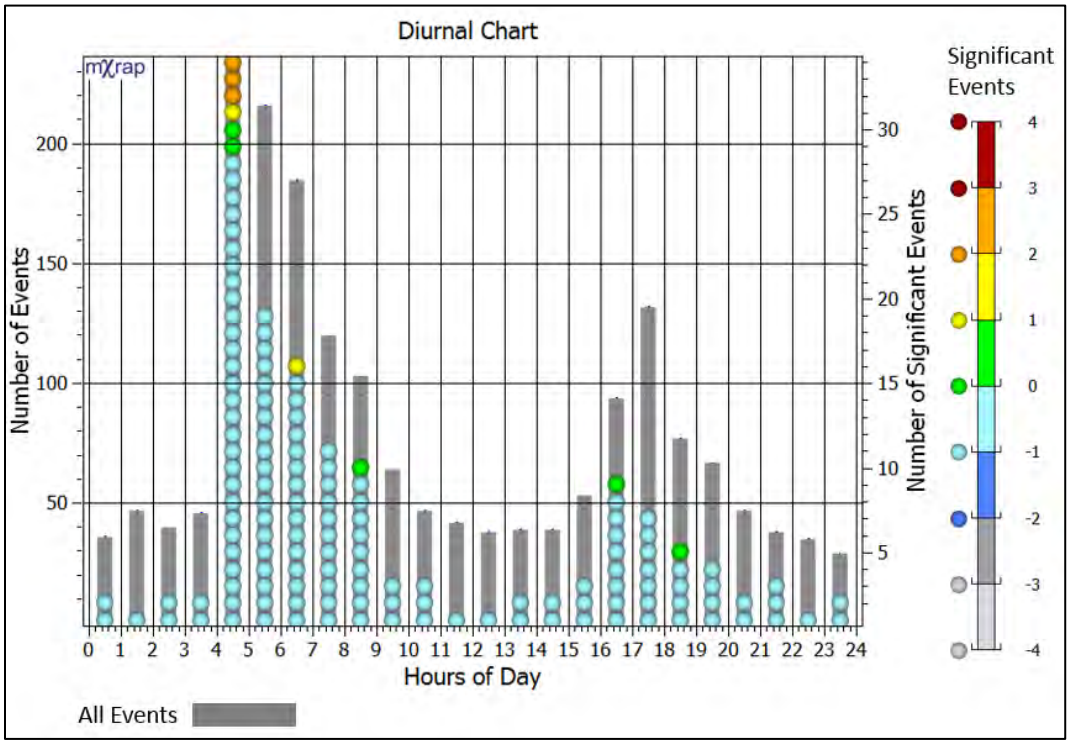

Figure 57 Diurnal Chart of Seismic Activity Occurring in Proximity to H-Fault

From examination of the above chart, the majority of significant events (Mag > -1) occur around the morning and afternoon blast times. Therefore, the activity is occurring along H-fault but is closely tied to blasting. Since H-fault has a large surface area and these events tend to occur in random locations along the fault, this type of seismic activity is difficult to analyze as to whether or the events are behaving in slip or unclamping of the fault. To further determine whether or not these events are slip or not, an S:P chart is shown below (see Figure 58):

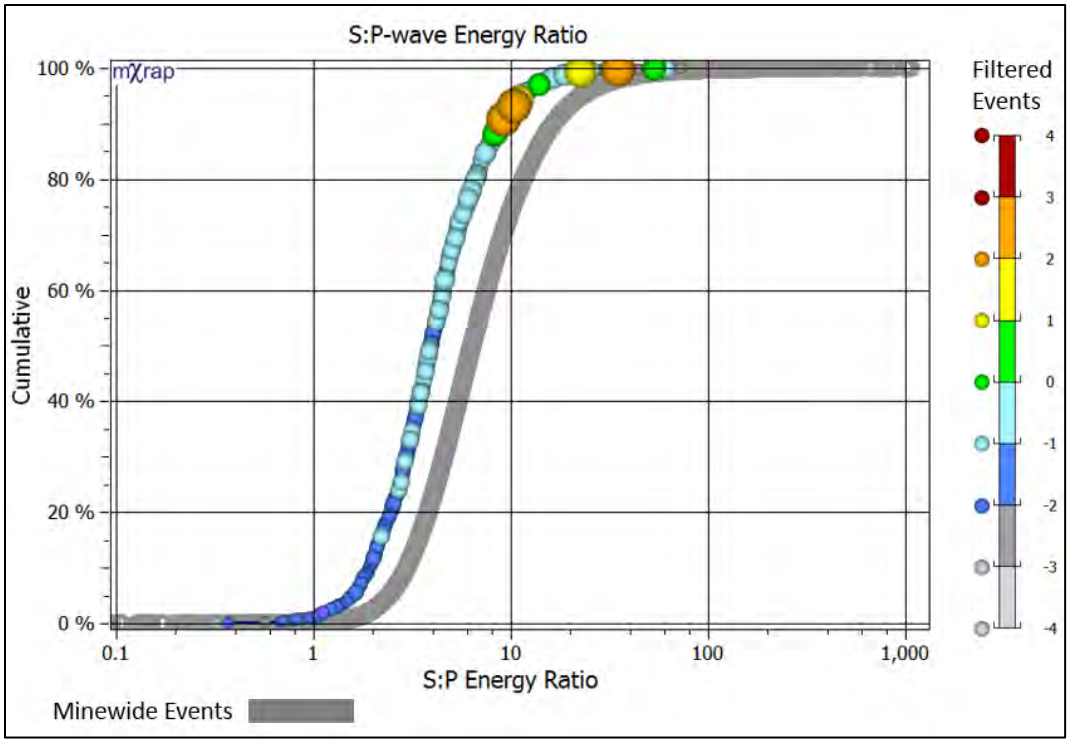

Figure 58 ES:EP Chart of Seismic Activity Occurring in Proximity to H-Fault

In the above chart, the grey curve is all the data, the colored curve with magnitude spheres is the data from the specific cluster. Referring to section, S:P > 10 is indicative of shearing i.e. fault-slip, and S:P < 3 is indicative of stress-induced i.e. caused by blasting. In the above figure almost all of the large events (Mag > 0), have an S:P > 10. Therefore, it is reasonable to assume that fault-slip is occurring due to mining near and on the fault and is generating large events.

4 Methodology for Hazard Assessment

Seismic hazard, simply defined is the likelihood of an event of certain size occurring in an area in a given time period (Gibowicz and Kijko, 1994). This is known as quantitative seismic hazard in that a probabilistic value is assigned in terms of likelihood. The techniques for hazard assessment laid out in this thesis do not incorporate probabilistic analyses. Therefore, the methodology of hazard assessment used in this thesis can be referred to as empirical or qualitative.

The level of hazard in this thesis is defined by magnitude in that the occurrence of an event above 0 M_w is considered hazardous. The rationale for using events above 0 M_w, using previous research done by Hudyma (2004) and Morissette (2015), is that this is smallest magnitude above which visible rock mass damage occurs.

4.1 Thesis Approach to Hazard Assessment

The overarching premise of this research is that past seismicity is a strong indicator of future seismicity. This statement is reasonably accurate assuming that future mining activity progresses at a comparable rate to past activity (Hudyma, 2010). Proceeding with this notion, it follows logically that the occurrence of larger events could be predicated on the occurrence of past events (Simser *et al*, 2003). In fact the occurrence of large events is more closely tied to past mining activities and the overall layout of excavations in an area (Mendecki, 2016). Therefore, it is reasonable to assume that a level of seismic hazard in a certain area could be used as a forecasting tool for future activity. In this regard, the question arises: in the interest of routine seismic hazard assessment, how far back in the data does one have to look to give an accurate forecast of future activity? This is further discussed in the next section (see Section 4.1.1).

4.1.1 Trailing Window vs Forecast Window

For the purposes of this research, the trailing window is defined as the time period (up to t_0) leading up to the forecast period or forecast window which proceeds from t_0. This is shown in the following figure (see Figure 59):

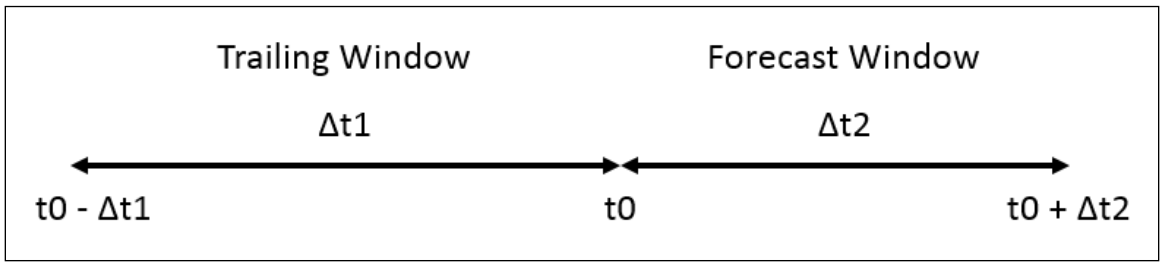

Figure 59 Time Windows for Seismic Hazard Forecasting

The objective in using a trailing, and subsequent forecast period, is to perform routine hazard analysis. This is done due to the fact that conditions in mines change. The notion of using varying time periods for hazard assessment was notably put forth by van Aswegen (2005) who suggested long, medium, and short term analyses. Long term was defined as a time period sufficiently long enough to allow changes in mine design. Medium term was defined as a time period reflecting the monthly planning cycle and short term refers to hours and days (van Aswegen, 2005). The period of hazard assessment, be it long, medium or short, depends on the purposes of the user. For example, one may use the previous 6 months to forecast the following 2 months. There are logical pros and cons to choosing an acceptable trailing and forecast windows. An important fact to consider when doing so is that seismic hazard levels change, and within that, the level of hazard may eventually decrease (Hudyma, 2008).

Using incredibly long trailing periods result in an ever-increasing hazard level. Conversely, using very short trailing periods can misrepresent hazard as being low when it may not be as the seismicity and/or mining in the recent trailing period may not accurately reflect the seismic response to mining at a particular location. Therefore it stands to reason that a trailing window that lies somewhere between medium and long-term needs to be sufficiently long enough to capture significant activity to give an accurate level of hazard. In keeping with this notion, a test of varying the trailing and forecast time windows was undertaken. Based on this test, it was decided to use a 6 month trailing window and a 2 month forecast window yielded sufficiently decent results. Details of this test are further discussed in Chapter 5. The following figure showcases the increase and subsequent decrease of seismic hazard in an area of a mine (see Figure 60):

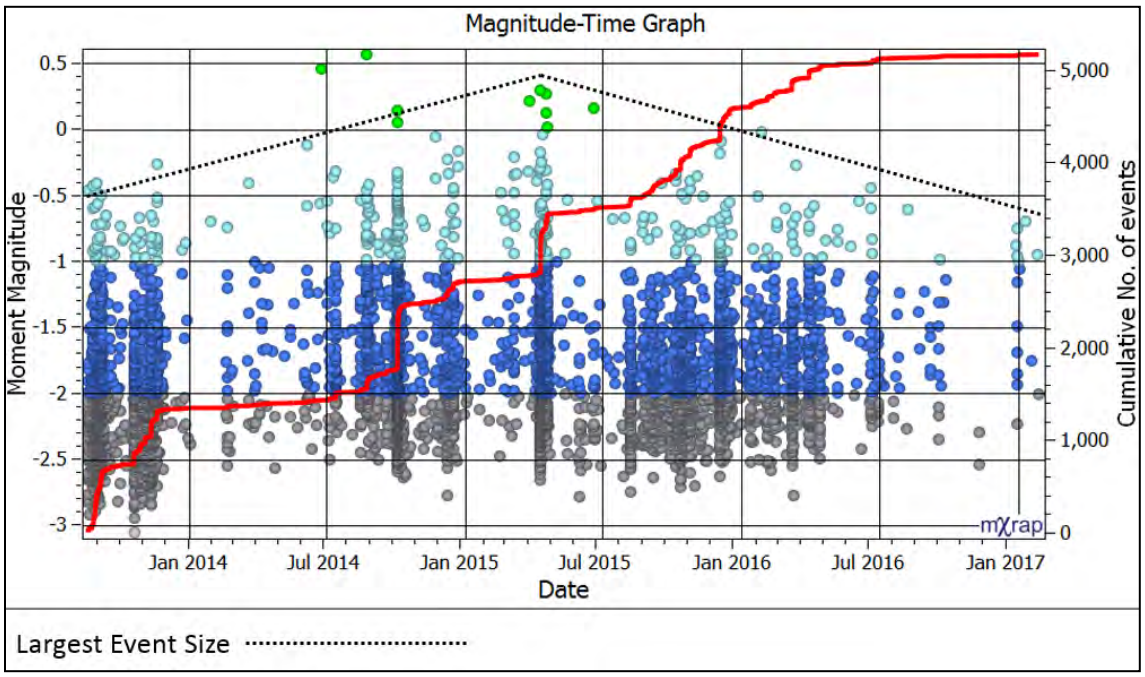

Figure 60 Magnitude-Time-History Chart Showing the Trend in Occurrence of the Largest Events

In the above figure, if one defined seismic hazard as the largest event that has occurred, it can be seen that hazard increases from late-2013 to mid-2015. Beyond that point, the level of hazard decreases. The specific situation that this chart is capturing is the eventual failure and unloading of a local mine pillar through subsequent stoping. If the entire data stream were to be used to assess hazard moving forward through February 2017, an uncharacteristically high level of hazard would be estimated. It is clear from the above chart that hazard is decreasing.

It should be noted as well that mining is not spontaneous. Stresses are being induced, through blasting, at a particular rate and at a specific time (Mendecki and Lötter, 2011). As well, the intensity of mining activity can vary over time. This can be due to mine planning and production scheduling. As a result, the rate of loading of the local rock mass is variable and is correlated to extraction. Therefore, when deciding on an appropriate time period, the past and future planned mining activities must be accounted for, or at the very least, noted. This is further expounded upon in the discussion of the scorecard used to evaluate hazard maps in Section 4.4.1.

4.1.2 Node-based Hazard Mapping

In Section 2.6.3, the concept of hazard mapping was introduced. This, in its simplest form is a method by which the user may easily assess hazard visually. The notion of grid-based and node-based hazard mapping was introduced as well in Chapter 2. Using mXrap™, a solid model of the mine workings was imported and a mine-node file created; in node-based hazard mapping, the XYZ location of the mine-node defines the center-point of the search radius. These nodes are simply points to denote the location of mine workings (which is shown in Figure 61). All the seismic events that locate within the search radius in a defined time period are used in the generation of hazard maps. A function can then applied to the captured data within the search radius be it a summation, the count of a certain type etc. The results are plotted as a color that makes up a heat-map i.e. cool to hot colors. Generally, areas of the mine with hotter colors are at greater risk of large events occurring. The rationale of what constitutes high-risk is based on the definition of a hazard threshold, this is discussed in Section 4.3. The following figure illustrates the concept of node-based hazard maps (see Figure 61):

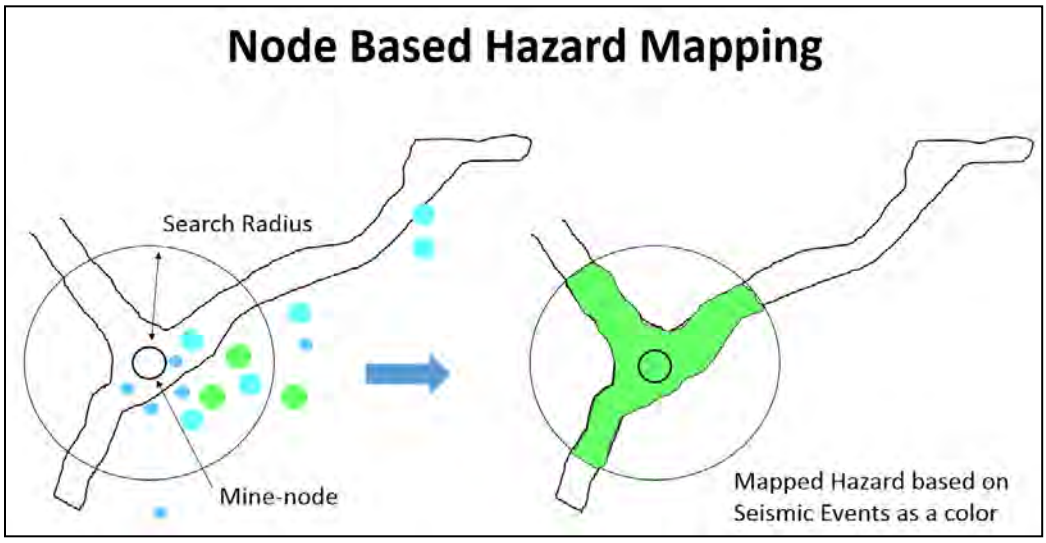

Figure 61 Node Based Hazard Mapping Illustration Showing, Generally, How these Types of Maps are Produced

From the figure above, a h azard level has been determined based on a d efined methodology. Moving forward in time, it is expected that the activity would fall within that hazard level. For example, if the hazard is defined by the largest expected magnitude and the hazard map indicates an expected magnitude from 0 to 1, if an event occurs

within the vicinity in the forecast period it is considered a successful forecast. This is shown below (see Figure 62):

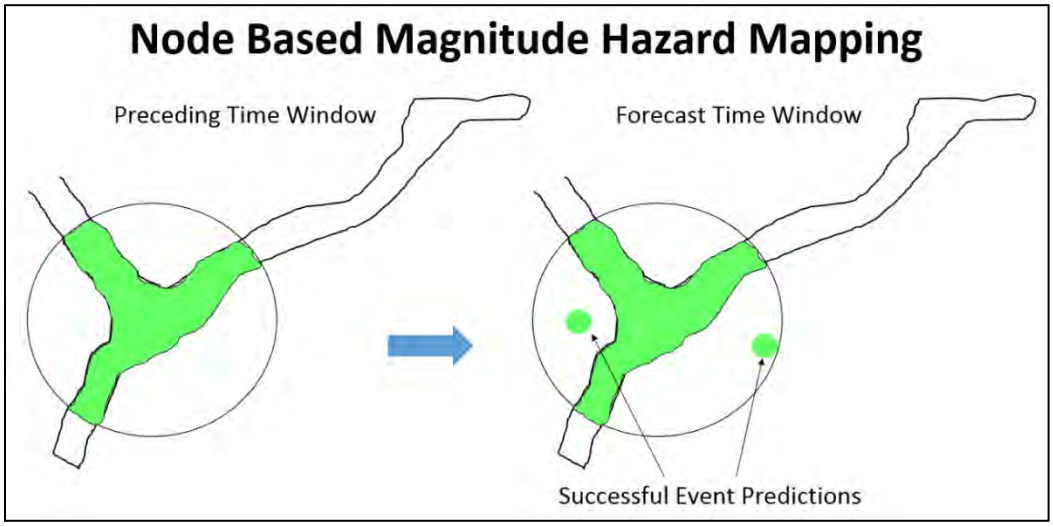

Figure 62 Node Based Hazard Map Forecasting Showing the Rationale for Hazard Forecasting

From the figure above, two events occurred within the vicinity of the hazard area and are therefore counted as successes. When plotted the results may not be clear-cut and should be subject to some scrutiny. The result is shown in the following figure (see Figure 63):

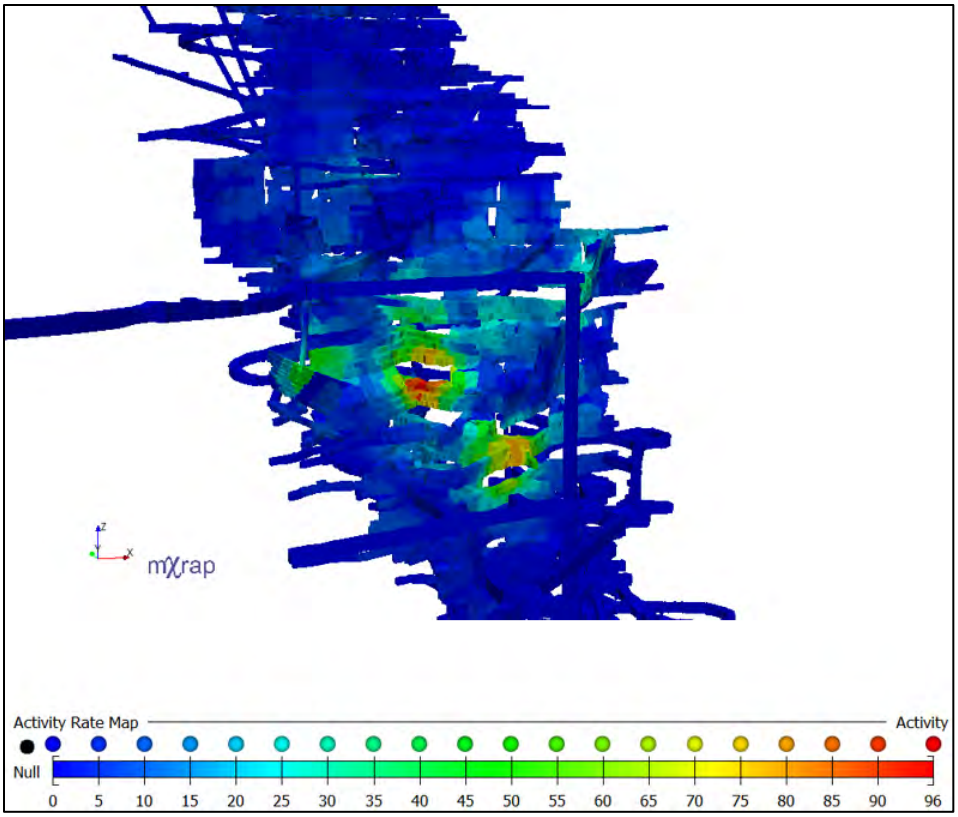

Figure 63 Morrison Mine, Mine-Wide Hazard Map Plotted as a Heat Map with Warmer Colors Indicating Higher Hazard Areas

Looking at the hazard map in the above figure areas of elevated hazard can be seen denoted by warmer colors. Since colors are plotted onto the mine model, node based hazard maps are generally easier to use and simpler in a visual sense. The question in using these maps is beyond what hazard value should the area be considered high hazard? Discussed in Section 4.3 is how one sets a threshold that defines the hazard map.

4.1.3 Search Radius Chosen

As stated previously, the mine-node defines the center point of a sphere with a size defined by the search radius. Previous work done by Brown (2015) indicates that a search radius approximately equal to the mine's sub-level spacing is often a good starting point for a search radius. Since Morrison Mine uses an 18m (≈ 60ft) sublevel spacing, the search radius used is 60ft. Selecting smaller search radii may be useful in further discretizing the results. This depends on how accurate one wants or needs to be for the analysis. It should be noted that event locations derived from seismic monitoring are not 100% precise, there is an error residual associated with the location of each event. With

this in mind, choosing a small radius, for example 30ft, may exclude relevant data. Referring to the accuracy of event locations, when the Morrison seismic data is plotted as a cumulative chart using the error residual or location error, one can see, from the following figure that the mean value (50%) is 15ft. This is shown in the Figure 64.

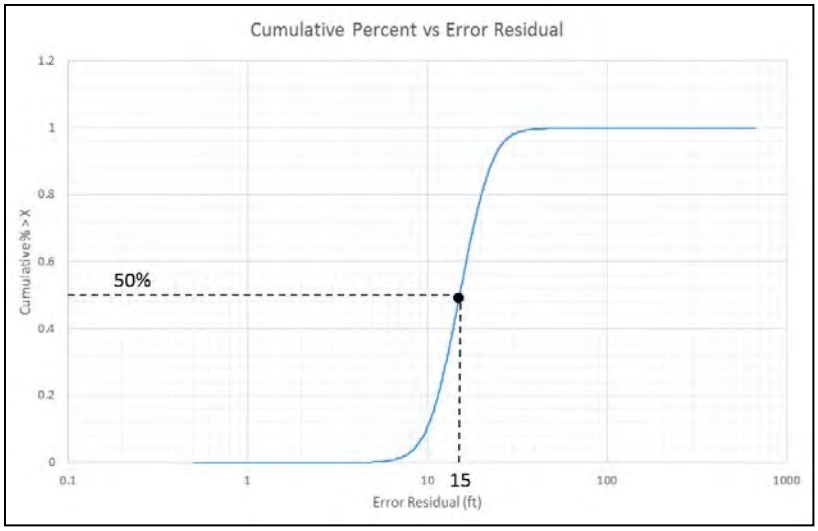

Figure 64 Location Error Residual Plotted as a Cumulative Chart Showing the Error at 50% of all Seismic Data

When evaluating the hazard maps (as discussed in Section 4.4) a certain amount of user discretion needs to be applied. This is in regards to the distance away from a hazard site the event in the forecast period is. Although a search radius of 60ft was used in the generation of the hazard map, as long as the event is within 100ft of the hazard area, it is considered a success. Therefore the search radius can be expressed as 60ft +/- 40ft to allow for location errors. This was done to be more lenient. Varying the search radius will be discussed further in Chapter 5.

4.2 Seismic Source Parameters Chosen for Hazard Assessment

This section presents a discussion into the selection of 4 different source parameters chosen for hazard mapping. The specific derivations of these parameters have been covered in the literature review (see Ch.2). The parameters used are energy, moment, apparent stress, and moment magnitude and the justification for using such parameters is given in the following sections.

4.2.1 Energy

Seismic energy is one of five independent seismic source parameters. It is a well-recognized measure of event size and represents the total radiated elastic energy of an event (Gibowicz and Kijko, 1994). Areas of high stress tend to release more energy, comparative to other parameters such as seismic moment. This is a result of high clamping forces which do not allow for significant rock mass deformation (Simser *et al.*, 2003). Therefore, when examining mining-induced seismicity, areas with high amounts of released energy may potentially be interpreted as high stress environments. As stated in Section 4.1, the hazard defining parameter chosen for this research is moment magnitude, namely the occurrence of an event above 0 M_w. In this respect, seismic energy is a well-suited parameter. The following figure illustrates the scaling between energy and magnitude (see Figure 65):

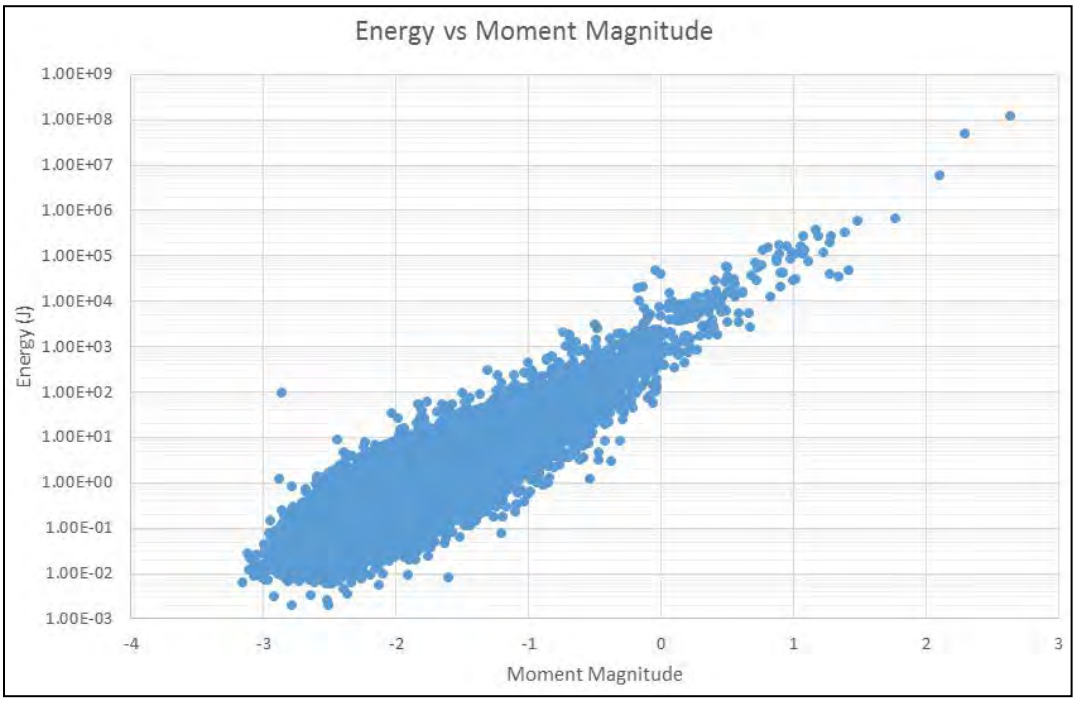

Figure 65 Total Radiated Energy-Moment Relation

It can be seen in the above figure that total radiated energy is well correlated with magnitude in that the larger the magnitude, the larger the amount of radiated energy. Shown below is a time-history plot of seismic energy to give an indication of how this parameter behaves over time (see Figure 66):

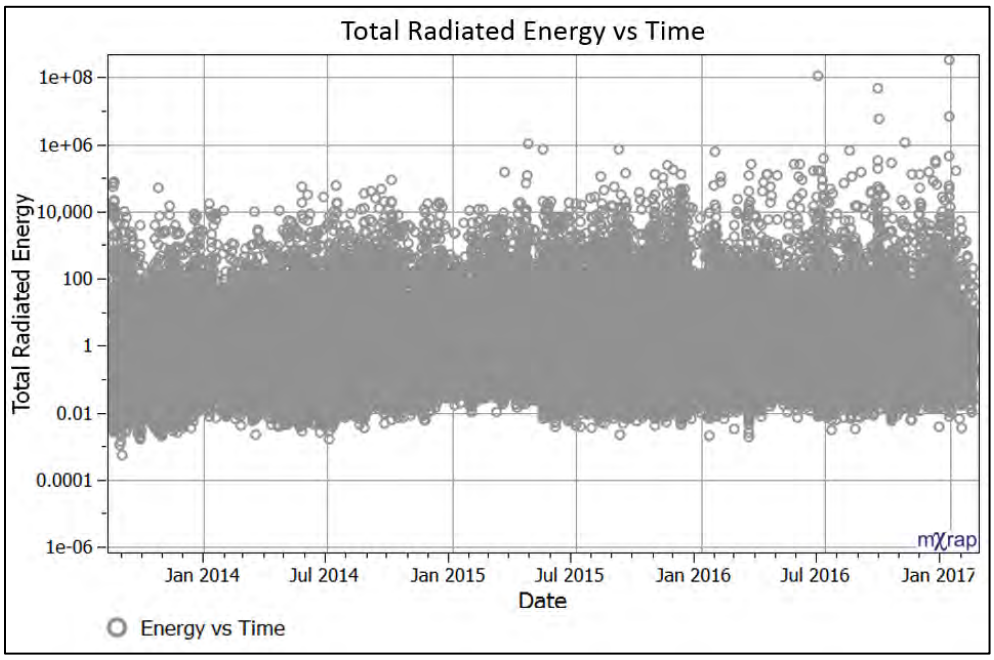

Figure 66 Energy-Time-History Chart

To indicate whether or not a parameter is well behaved, one can examine the lower limit over time. Major steps in the lowest value recorded or gaps in the data are indicators of poorer quality information. As seen in the previous figure, there are only minor steps in the lower bound and a few minor gaps, therefore energy can be said to be reasonably well-behaved and potentially well suited for hazard assessment. There is some minor inconsistency in regards to the segregation of event magnitudes vs energy, this can be seen in the imperfect banding in colors on the chart. This is because energy is not perfectly correlated to moment magnitude as seen in Figure 66.

4.2.2 Moment

Seismic moment is an independent seismic source parameter that is commonly used as a measurement of the strength of a seismic event (Gibowicz and Kijko, 1994). Since moment is calculated using the shear modulus, shear distance, and slip area, it is related to the amount of co-seismic deformation. Shown below is time-history plot for moment to illustrate this parameter's behavior over time (see Figure 67):

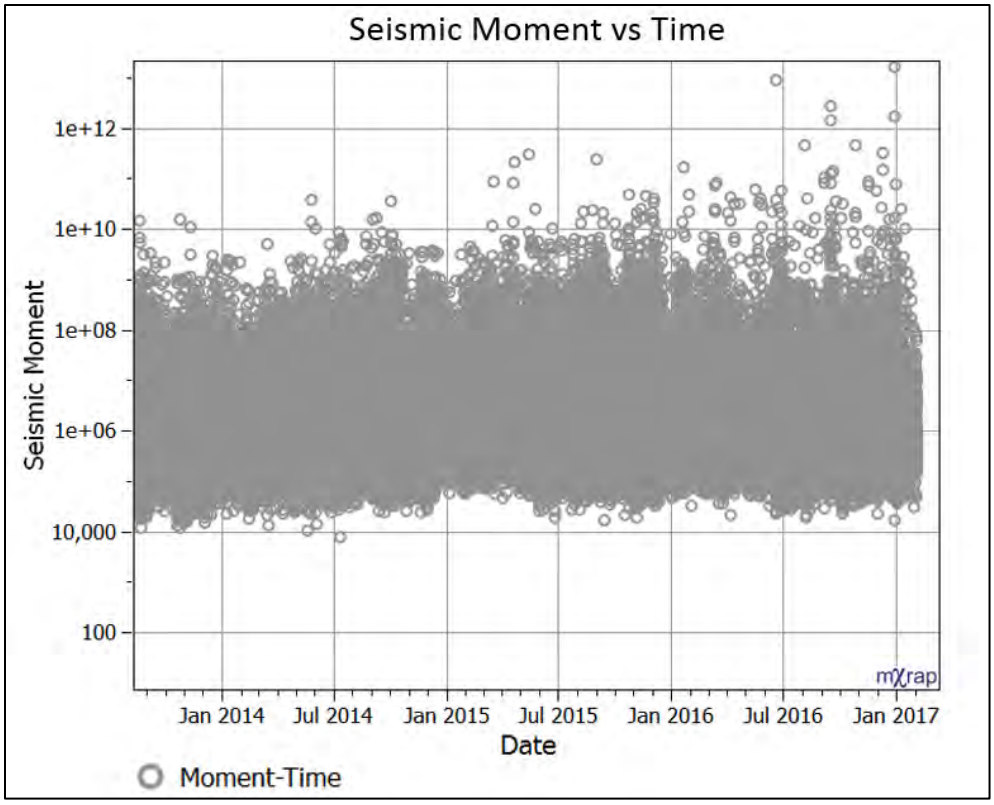

Figure 67 Moment-Time-History Chart

There are no major steps in the lower bound of moment in the above figure, as well there are no major gaps in the record. Moment can be considered to be well behaved over time and potentially well-suited for hazard assessment. Essentially areas that have experienced large amounts of co-seismic deformation should also exhibit large values in cumulative seismic moment.

4.2.3 Apparent Stress

Apparent stress is a dependent seismic source parameter derived from energy, the shear modulus of the rock, and seismic moment. Apparent stress essentially represents the amount of seismic energy per unit of volume of inelastic co-seismic deformation. High apparent stress values are indicative of increasing local stress conditions in the rock mass (Mendecki, 1993). High apparent stress, for the purposes of this thesis has been defined as being above the 80^{th} percentile for the mine at 0.028 M Pa. This is shown in the following figure (see Figure 68):

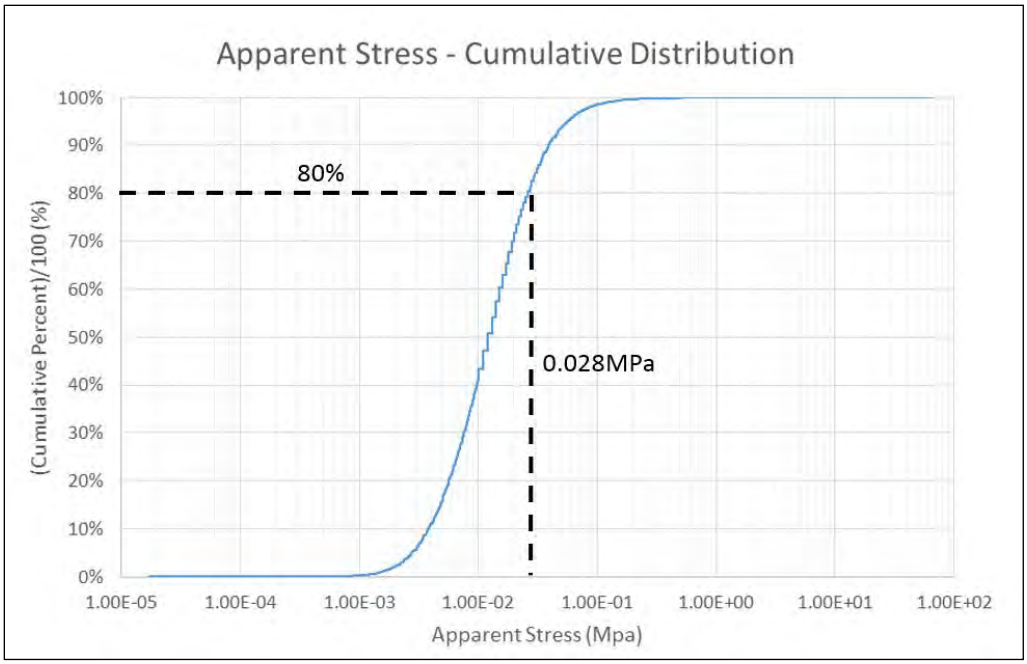

Figure 68 Cumulative Distribution of Apparent Stress Showing the Stress Level at the 80th Percentile

Previous work done by Brown (2015) indicates that an increasing 80th percentile of apparent stress is indicative of high apparent stress. Since numeric values define the 80th percentile, by setting a general threshold value, values above said threshold are considered high stress. The following figure illustrates the relation between apparent stress and moment magnitude (see Figure 69):

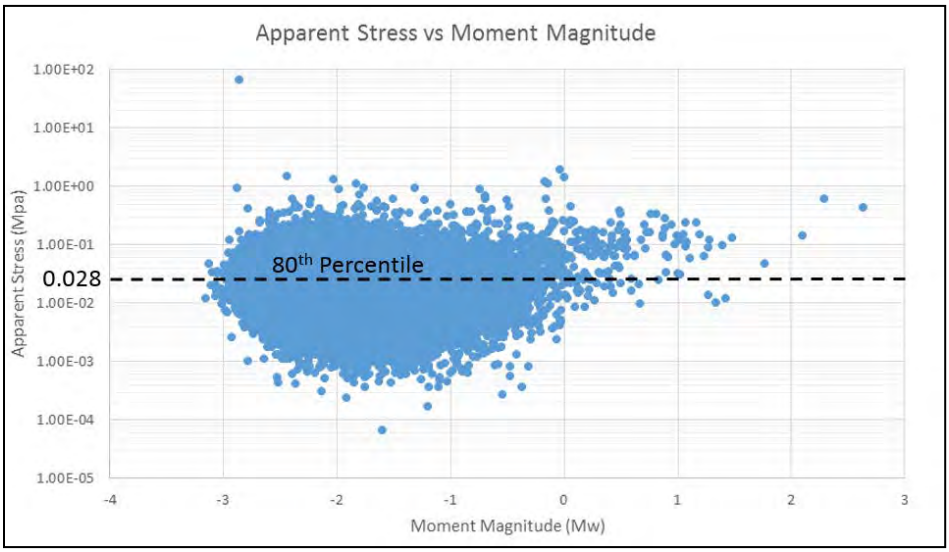

Figure 69 Apparent Stress versus Moment Magnitude

As can be seen in the above figure, apparent stress, specifically the 80th percentile does not correlate well with moment magnitude. Given the equation for apparent stress, energy is divided by moment. If an event is high energy and low moment it would have a high apparent stress value and given the scaling between energy and magnitude, it could be a large event. Conversely if an event had high moment and low energy, it would have a lower apparent stress value. Given the absence of a correlation between moment magnitude and apparent stress (in the previous figure) although the event has a low apparent stress value, it could still have a large magnitude. Despite this discrepancy, since apparent stress has been used in previous hazard assessments at LaRonde Mine by Brown (2015) this parameter may also be well-suited for hazard assessment at Morrison Mine.

4.2.4 Magnitude

As stated previously, the magnitude scale chosen for this thesis is moment magnitude. Magnitude, regardless of scale type, is a representation of the size of a seismic event. The scale is logarithmic meaning that for every 1 unit increase of magnitude, the strength of the event increases 10-fold. Out of the plethora of seismic parameters, magnitude is arguably the most recognizable and simple to use. Therefore, in the interest of practical hazard analysis, the use of magnitude is appropriate. Shown below is a magnitude-time-history for Morrison Mine (see Figure 70):

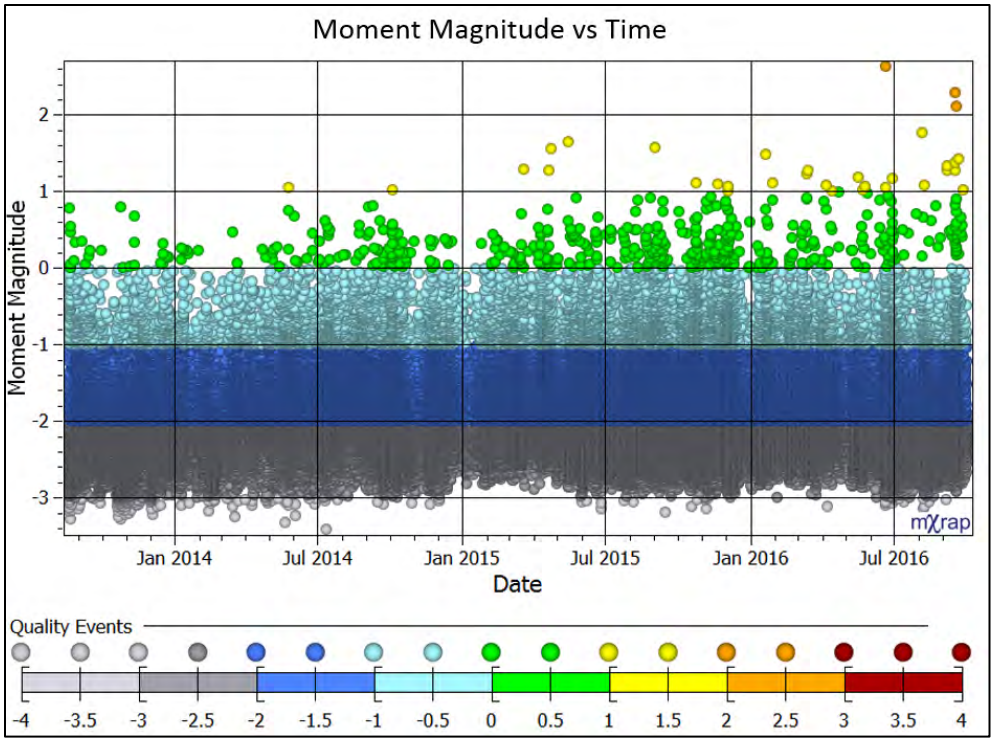

Figure 70 Magnitude-Time-History Chart

As can be seen in the previous figure, there are some steps in the lower bound of recorded magnitude and a few minor gaps in the seismic record. These are attributable to adjustments to the micro-seismic system and brief system downtimes. Despite these inconsistencies, moment magnitude can be said to be reasonably well-behaved over time. Referring to Section 3.3.2, the majority of seismic activity at Morrison Mine, namely events above magnitude 0, is closely related to mine blasting. Due to this fact, mining activity, namely stope blasting, is considered in the hazard assessments of not only magnitude but also energy, moment, and apparent stress. This is further discussed in Section 4.4.

4.3 Setting a Parametric Threshold

4.3.1 Rationale

In hazard analysis, a situation is commonly considered hazardous if a threshold or limit is exceeded. For example, in hazard assessment of the interaction between workers and contaminants, the TLV® or Threshold-Limit-Value is defined as the 'do-not exceed' concentration of a detrimental substance to human health (IUPAC, 2001). During operations, if the TLV® is exceeded, it constitutes an alarm and the suspension or

tailoring of work activities in the interest of worker safety. In this context, that of seismic hazard assessment, the threshold is defined for a seismic parameter. This is not to say that this is the same as the TLV® developed by the ACGIH, but merely a relatable concept. As mentioned in the previous section, the parameters assessed are moment magnitude, seismic energy, seismic moment, and apparent stress. Seismic energy and seismic moment are assessed by cumulative values i.e. the total sum of energy or moment in an area defined by a search radius. Magnitude and apparent stress are assessed as an event count i.e. the number of events above a certain magnitude or apparent stress value within a defined search radius. The rationale for which is further discussed in Section 4.3.2.

The time period examined in this thesis spans the middle of 2016, from April to October. All events above 0 M_w during this 6month period have been included in the determination of a threshold. This amounts to 99 events > 0 M_w. For each 'large' event that has occurred, data from 6 months leading up to the event occurrence, within a 60ft search radius, was used to determine a threshold. The idea is to try to establish pre-cursory activity/conditions to the occurrence of large events. This method is shown graphically in the following figure (see Figure 71):

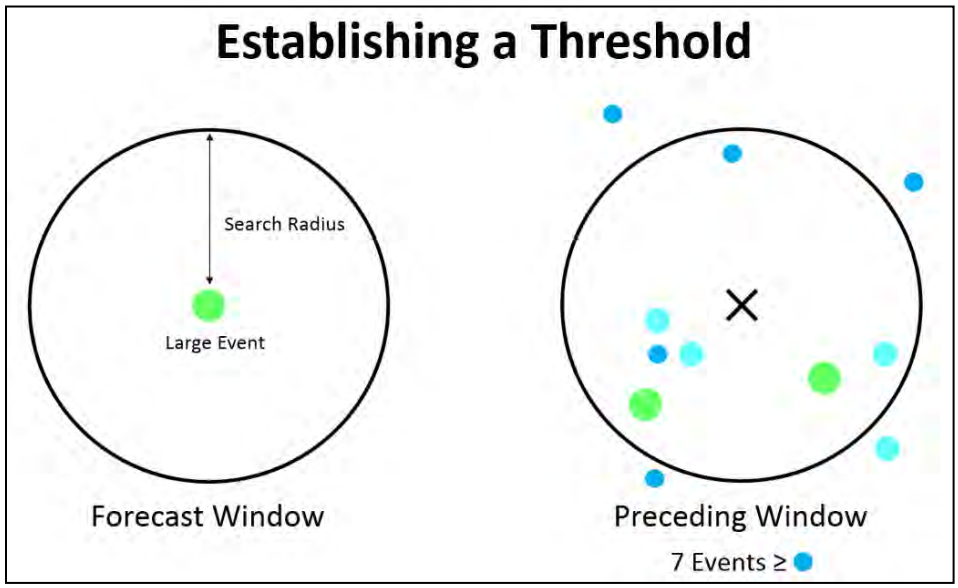

Figure 71 Parametric Threshold Establishment Using a Search Radius Around a Large Seismic Event

The results are then tabulated in Excel and graphed, an example of which is shown in figure. For example, if one was using -1 M_w as a lower bound, one would be counting the number of events above this magnitude within 60ft of each large event occurring in the trailing time period. The following figure shows the established threshold using -1 M_w as a lower bound for hazard assessment (see Figure 72):

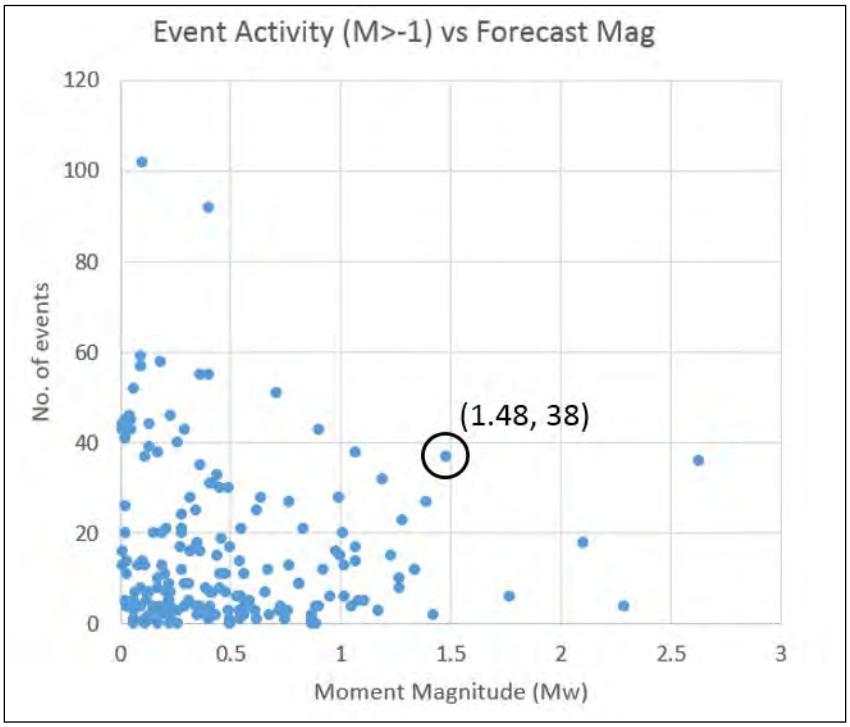

Figure 72 Event Activity in the Trailing Period versus Event Magnitude Occurring in the Forecast Period

Referring to the previous figure, the x-axis is the magnitude that occurred in the future time period. The y-axis is the number of events that occurred within 60ft of that event in the previous time period. For example, the circled event on the chart was 1.48 M_w and in the past 6 months, 38 events above -1 M_w had occurred within 60ft of that event.

The idea in choosing a desirable threshold is to minimize the amount of false estimates or 'false alarms'. If the threshold is set too low, the number of hazardous areas will be quite high with a lower success rate. However, if one adjusts the threshold to an appropriate level i.e. one that spans most of the magnitude range, the number of false alarms will be

lower and success rates should increase. This threshold is indicated by the dashed line in Figure 73.

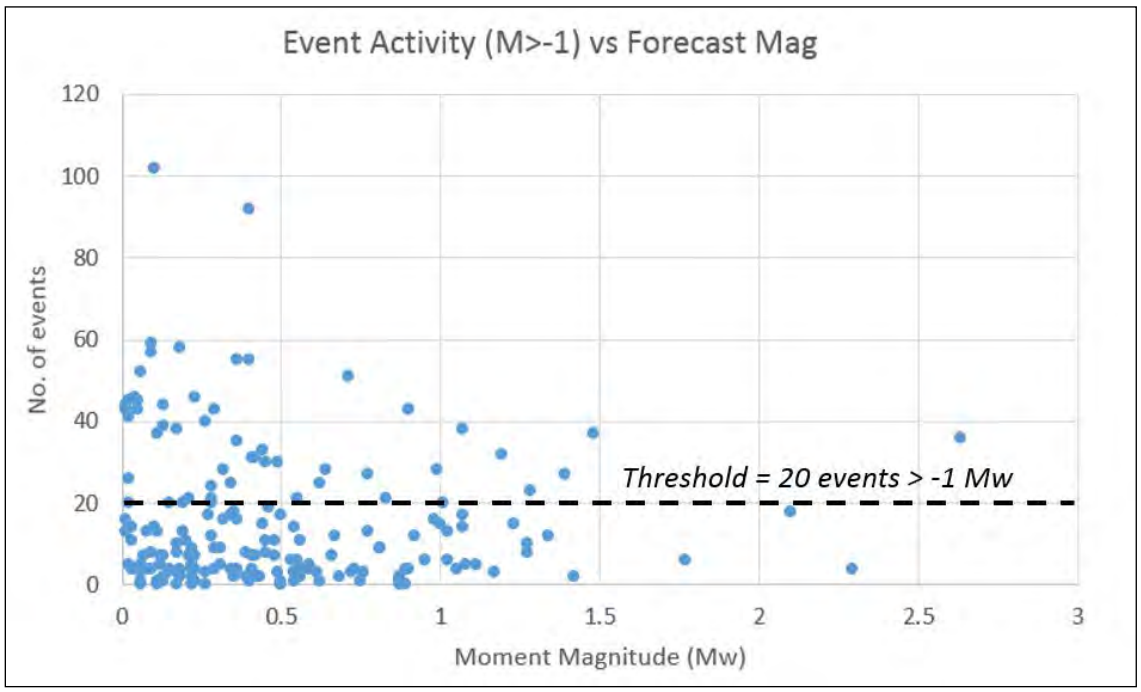

Figure 73 Event Activity in Trailing Period versus Event Magnitudes Occurring in the Forecast Period with a Defined Threshold

For example, the chart shown in Figure 73 was generated using -1 M_w. In this case a threshold value of 20 events was chosen. This is because it covers most of the forecast magnitude range while ignoring trailing time periods with limited seismic activity. This means that, for this hazard map, areas that have experienced more than 20 events > -1 M_w in the past 6 months will experience a large event in the following two months. The results of the hazard maps used, with reference to set parametric thresholds, are discussed in Chapter 5.

4.3.2 Parametric Hazard Analyses – Cumulative vs Counting Approaches

The assessment methods, pertaining to threshold definition, are a cumulative approach and a counting or Incremental approach (after Alcott, 1998). Cumulative values are simply the sum of a parameter. Therefore the threshold in this case is an accumulation

limit of a p arameter. Counted or incremental values represent the number of events, defined by a parameter, that exceed threshold.

Radiated energy as stated previously, is indicative of strain within the rock mass and therefore can be considered a proxy for increasing stress conditions. Moment on the other hand is related to rock mass deformation and is indicative of the local rock mass shedding stress. Assessing these two parameters cumulatively can give either an indication of the level of stress, as with energy, or a representation of total deformation, as with moment.

Both apparent stress and magnitude have been assessed using a count above threshold. In regards to apparent stress, it relies on both radiated energy and moment. As discussed in Section 4.2.3, the apparent stress for a large event can be either high or low since energy is divided by moment to obtain apparent stress. To better illustrate this, a chart of apparent stress vs moment magnitude is shown on the following page (see Figure 74):

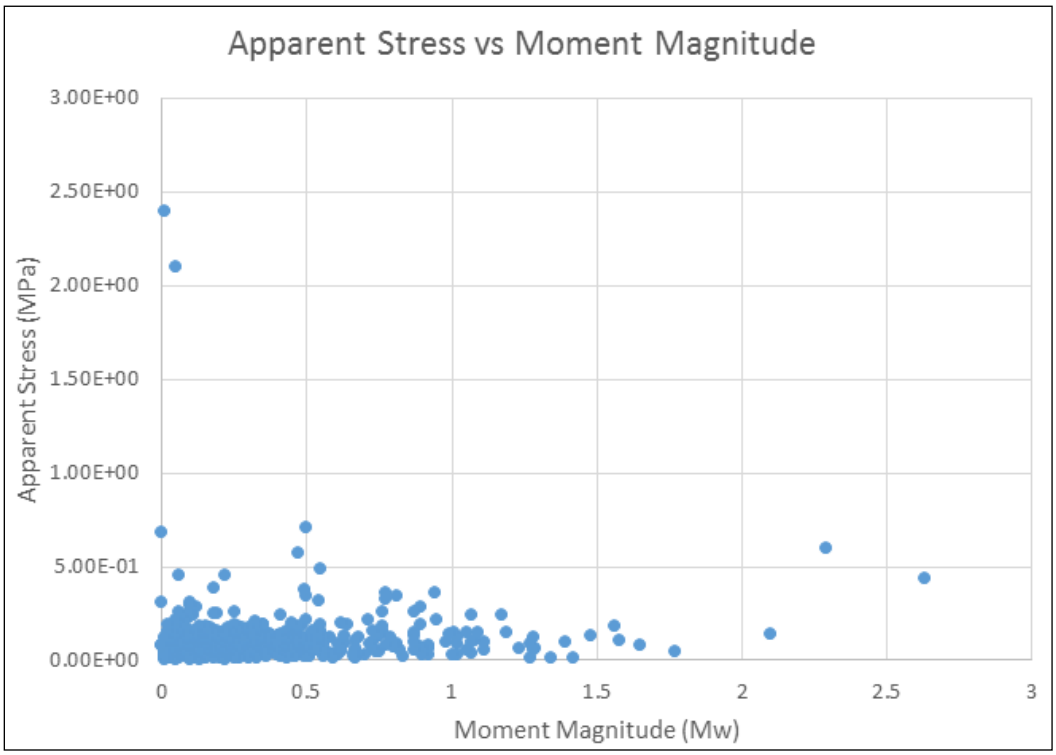

Figure 74 Apparent Stress Above the 80th Percentile versus Moment Magnitude

What is evident in the previous figure is that there is no well-defined correlation between apparent stress and magnitude. This being the case, rather than using a cumulative value, the number of events with apparent stress above the mine wide 80th percentile is counted and compared to a defined threshold. In the case of magnitude, since it is essentially a dimensionless value, assessing hazard with cumulative magnitude would not be very meaningful. As well, it would difficult to interpret.

Therefore magnitude has been assessed as a count above threshold with a lower bound applied. The logic behind this is that areas that have experienced larger events in the past will continue to experience large events assuming similar mining/activity rates. Applying a lower bound to magnitude helps to eliminate areas from assessment that may have experienced many events but have not had any larger events. An example of this are remucks which are areas of muck storage. When muck is removed using an LHD, the bucket strikes the walls and back which may register small seismic events. This is shown in the figure below (see Figure 75):

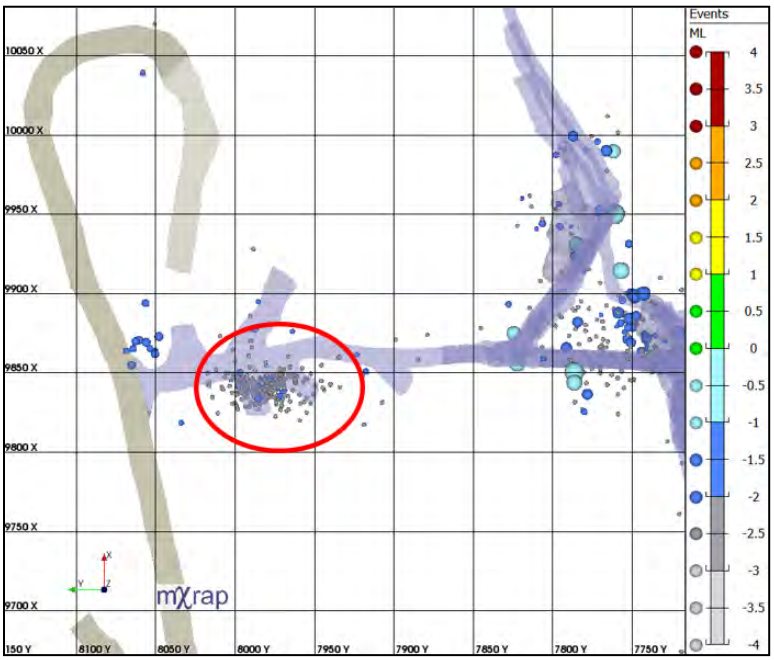

Figure 75 Possible LHD Operation Registering as Small Seismic Events in a Mine-Remuck

As seen in the above figure, the red circled area is a remuck on a production level. There is a cluster of about 100 events registered during muck removal, it is notable that most

events are between -3 and -2 M_w denoted by the color scheme. Three different lower bounds of magnitude have been chosen: -1, -0.5, and 0 M_w. The idea is to test each to choose the most appropriate value.

Aside from the theoretical interpretations of these chosen parameters, the choice to do both a cumulative and counting approach is to showcase different parameters for hazard assessment. There are potential pros and cons for each method. Cumulative values can be useful tools for examining trends in source parameters however, if a sufficiently large event occurs it will alter the cumulative value i.e. making it much larger (Alcott, 1998). In this case it would not be caused by large amounts of activity but rather a few larger events. Using counted values are not particularly useful in determining trends, as well they are very simplistic and are more or less related to blasting, which is the main mechanism at Morrison. Therefore in cases of fault-slip seismicity, these counted thresholds may not be very effective.

4.3.2.1 Established Thresholds

Using the method discussed in Section 4.3.1, thresholds were determined for magnitude, apparent stress, energy, and moment. These are expressed in the following table (see Table 9):

Table 9 Defined Parametric Thresholds

Parameter	Thresholds within a 60ft Search Radius	
	Cumulative Threshold	Incremental/Counted Threshold
M > 0	N/A	1 event in the last 6 months
M > -0.5	N/A	3 events in the last 6 months
M > -1	N/A	20 events in the last 6 months
AS-80	N/A	20 events in the last 6 months
Energy	10000 J released in the last 6 months	N/A
Moment	2.0×10^9 Nm^2 in the last 6 months	N/A

4.3.3 Defining Success

As mentioned in Section 4.1, the purpose of this type of hazard assessment is to be able to forecast seismic activity. In this case, the occurrence of an event or events above 0 M_w. Success is defined as a state where the specific hazard assessment parameter (see Section 4.2) has exceeded threshold in the preceding time window and one or more events above

0 M_w occur in the same vicinity, in the forecast time window. An example of this is given in the following figures (see Figures 76 & 77):

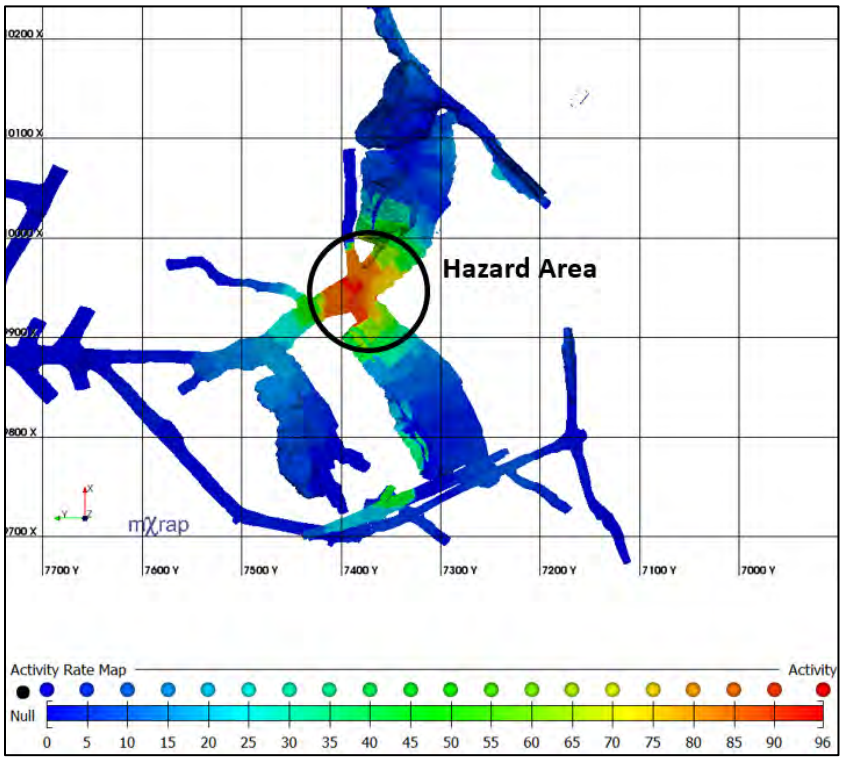

Figure 76 Seismic Hazard Forecasting Using -1.0 Mw as a Lower Bound for the Previous 6 Months

In the above figure, the hazard area is located within a retreat pillar with an elevated activity value above -1.0M_w (approximately 90 events in the past 6 months). This was caused by the mining of a large long-hole stope on the level above and 2 smaller stopes on the same level near the vicinity of the hazard area. The seismic activity in the forecast period is shown in the following figure (see Figure 77)

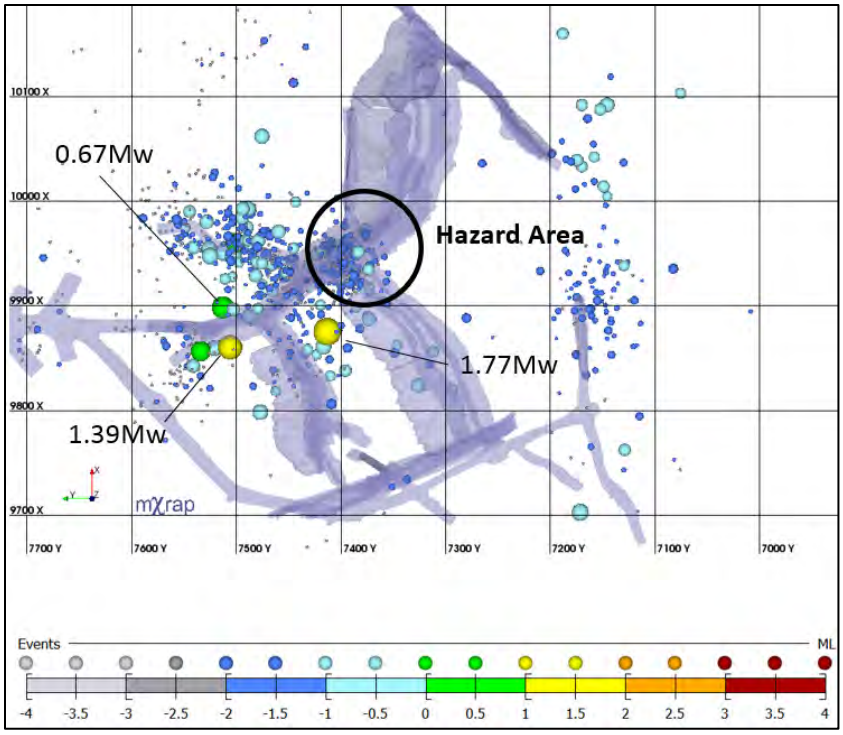

Figure 77 Plan View of Seismic Activity Occurring in the Forecast Period

In the forecast period, a very large event, the second largest at the mine to date occurred following a stope blast on the level above.

Conversely, if the threshold is exceeded and no e vent occurs, it is not considered a success. As well, if no threshold is exceeded and a large event occurs, it is not considered a success. Both cases are illustrated in the following two figure (see Figures 78, 79, 80 and 81):

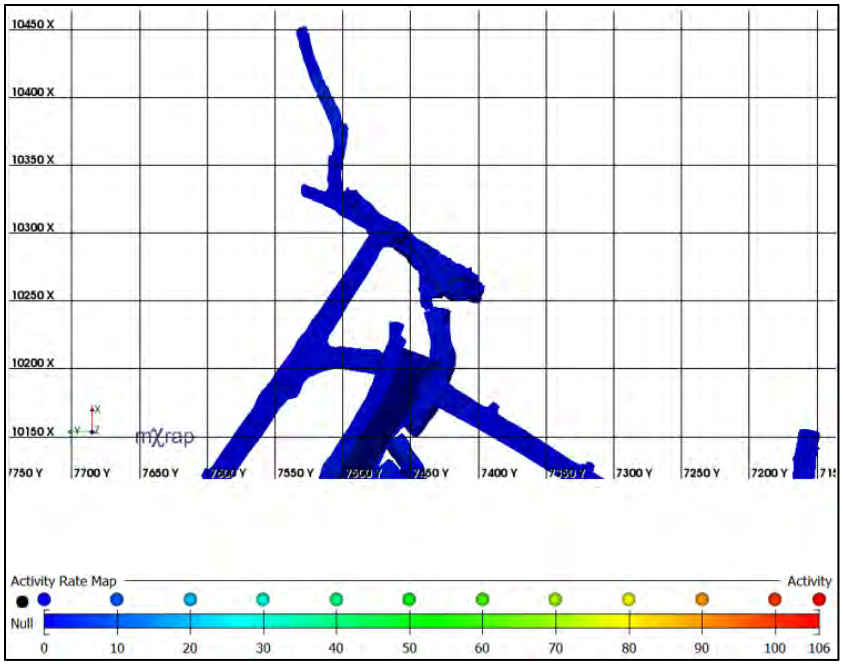

Figure 78 Plan View of an Unsuccessful Forecast Using the M > -1 Hazard Map

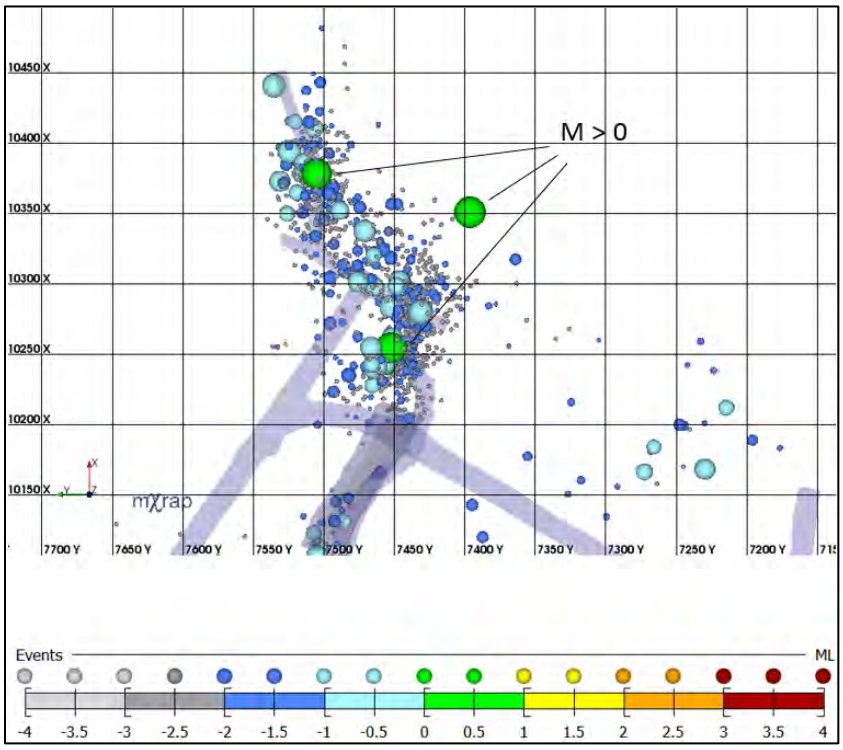

Figure 79 Plan View of Seismic Activity Occurring in the Forecast Period

In the above figure, the activity hazard map, using -1 M_w as a lower bound, was not above threshold, however in the following two months, three events above 0 M_w occurred due to cut-and-fill mining.

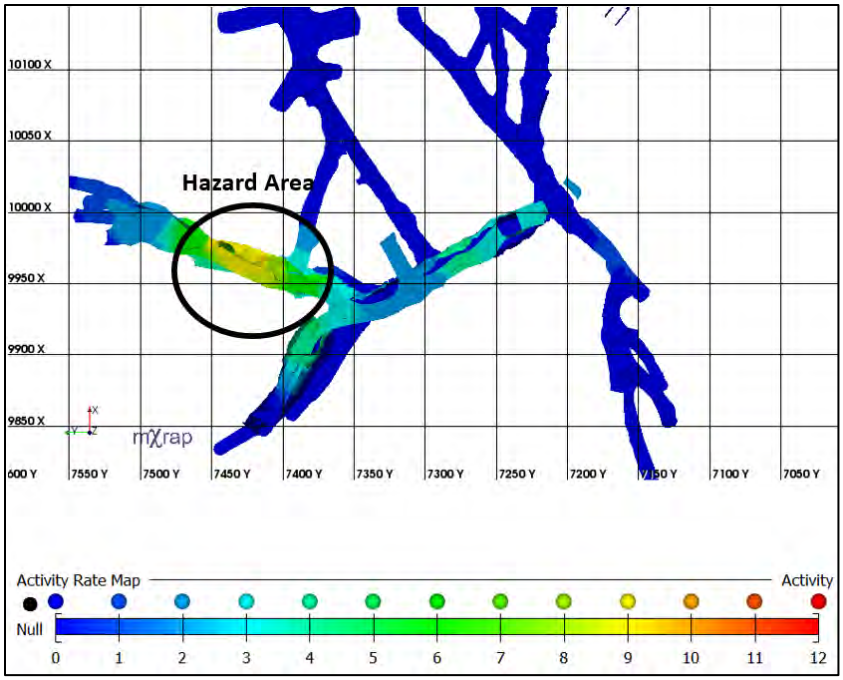

Figure 80 Hazard Map, Plan View of 4400L Using M > 0 as a Lower Bound

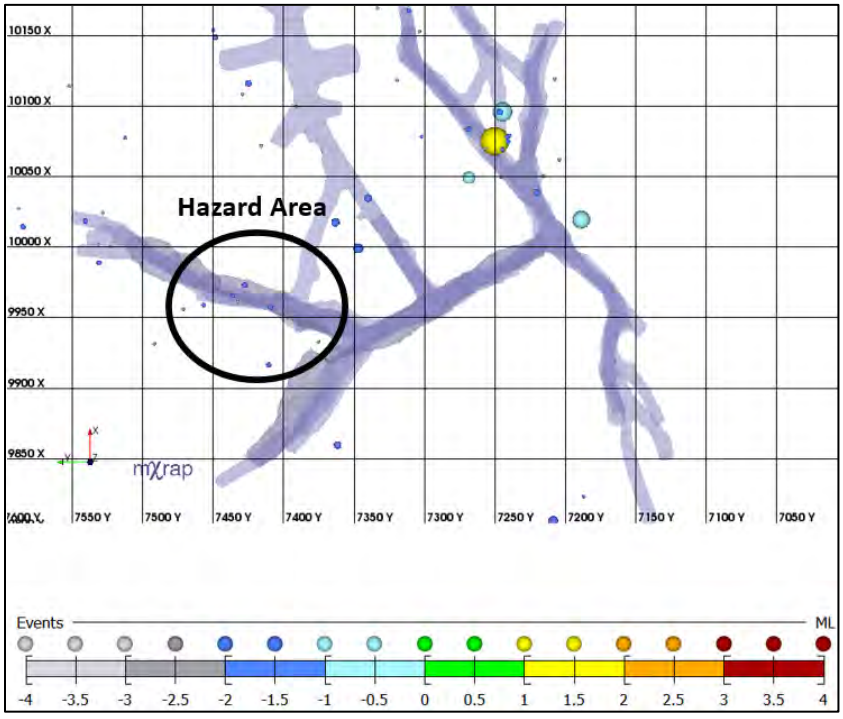

Figure 81 Plan View of Seismic Activity Occurring in the Forecast Period

In the last figure, using M > 0 as a lower bound, about nine events > 0 M_w occurred following a final sill stope blast. In the next two months, no large events occurred. What these two figures illustrate is the effect of mining activities on seismic activity, namely

large events. When assessing these hazard maps, these inconsistencies have been noted and are discussed in the following section (see Section 5.3.1). Success is depicted as a percentage of the total amount of large events occurring in the forecast period. The equation for success rate is given below:

$$Success\ Rate\ (\%) = \frac{N_{successes}\ in\ forecast\ period}{N_{M>0}\ in\ forecast\ period} \qquad (10)$$

Referring to the above equation, if 20 events > 0 M_w occurred in the forecast period and 10 were successfully forecasted by the hazard map, the success rate in that case would be 10/20 or 50%.

4.3.4 False Alarms

In the figurative ebb and flow of seismic activity that drives hazard levels, an alarm occurs when a defined, parametric hazard threshold is exceeded. For example, if the tolerance for seismic activity in a specific area, in the past 6 months, is no more than 3 events above 0 M_w, if 6 events > 0 M_w have occurred then this would constitute an alarm and the qualified mine personnel should at the very least, be cognizant of that alarm. If the area in question is above threshold for hazard, and no large event occurs in the forecast period, this is considered a false alarm.

The concept of incorporating alarms and alarm periods into hazard assessment was put forth by Young (2012) who used an apparent-stress-time-history as an alarm tool. In that regard, when the frequency of high apparent stress events exceeds a defined threshold it constitutes an alarm period. The nature of the result, be it false or successful, depends on whether or not a large event occurs during the alarm period. Brown (2015) also used alarms in forecasting large events using the ASR or Apparent Stress Ratio over time. This dimensionless metric is simply the 80^{th} percentile of apparent stress divided by the 20^{th} percentile. Increasing ASR values are indicative of increasing stress conditions in the rockmass. As ASR increases, the likelihood of large seismic events occurring may also increase (Brown, 2015). The evaluation of the hazard maps in this thesis incorporates a

false alarm rate which builds upon the concept of seismic hazard alarms as presented by Young (2012) and Brown (2015).

Essentially, a given hazard map will have any number of forecasted high hazard zones located around the mine solid model based on localized seismicity. Based on the rationale previously mentioned, the forecast is made that large events will occur in the near future in those areas. However, this is not always the case. The false alarm rate is a numeric value shown as a percentage being 100% minus the number of hazard areas that experienced a large event in the forecast period divided by the total number of hazard areas on the map using the data in the trailing period.

$$False\ Alarm\ Rate\ (\%) = \left[1 - \left(\frac{N_{hazard\ areas}\ that\ experienced\ M > 0}{N_{hazard\ areas}\ in\ trailing\ period}\right)\right] \times 100\% \qquad (11)$$

Referring to the above equation, if there were 20 areas on the hazard map using a defined trailing window, and 15 of the 20 areas experienced an event(s) > 0 M_w in the forecast period, then the false alarm rate in that case would be 1-(15/20) or 25%. Essentially, the lower the false alarm rate, the more accurate the hazard map is in regards to forecasting.

4.4 Examples of the Mapping Methods Used

In order to assess the effectiveness of these techniques, the following sections give examples of each hazard map along with the scorecard used for evaluation in regards to success rate and the false alarm rate. As mentioned in Section 2.5.5, mXrap is a useful program in the analysis of seismic data using a development platform-app format. Using the notion of a node-based, heat-map style, hazard map, six different hazard maps were created as new apps in mXrap™. Essentially, the program generates the maps based on the specific definition of each app and the user is left with the task of interpreting the results.

4.4.1 The Scorecard

As referenced in introduction to this chapter, there must be some level of constancy in the evaluation of the techniques. By doing so, one can see the effect of various conditions subject to what is constant. For example, in this research, the definition of success does not change. As well, the format of the scorecard that is discussed in this section is consistent in each type of hazard map.

The purpose of the scorecard is to record a number of data points in an organized way. This is also to eventually draw parallels between the successes of using one parameter when compared to others. The types of information recorded are shown below:

1. Level ID (the specific sub-level)
2. Location (the area on the specific sub-level)
3. Is the area accessible? Yes or No
4. Parametric value above threshold (be it the cumulative or incremental value)
5. Mining activity in the trailing period (Stope ID and/or heading developed)
6. Mining activity in the forecast period (Stope ID and/or heading developed)
7. Successfully forecasted $M > 0$ event(s) in the forecast period
    a. Date/time
    b. Location
    c. Magnitude
8. Success Rate & False Alarm Rate

Items 1 to 7 on the list describe the nature of the hazard map in relation to what hazard-defining seismicity occurred in the forecast period. Item 8 pertains to the calculated values of the success rate and false alarm rate. Descriptions of each have been discussed in the previous Sections (4.3.3 & 4.3.4).

Scorecards are given in Appendices B, C, and D. The approach taken in evaluating these maps was from the point of reference of a mine-site user. Essentially, in the interest of routine hazard analysis, one would evaluate the state of hazard in the mine continuously. One would go through the entire mine creating a catalogue of hazardous areas by recording the types of information listed previously. Then the accuracy of the hazard map

would be evaluated over the forecast period. In the interest of simplicity, the map would be considered 'valid' or 'current' over the entire forecast period after which another evaluation would be undertaken.

4.4.2 Cumulative Energy Hazard Map

The following section aims to give a practical example of the use of the cumulative energy hazard map. The example shown is an abutment on the western edge of the Morrison vein complex in middle of the mine. The following figure shows the cumulative energy map for the period from Dec-2015 to June-2016, approximately 6 months (see Figure 82):

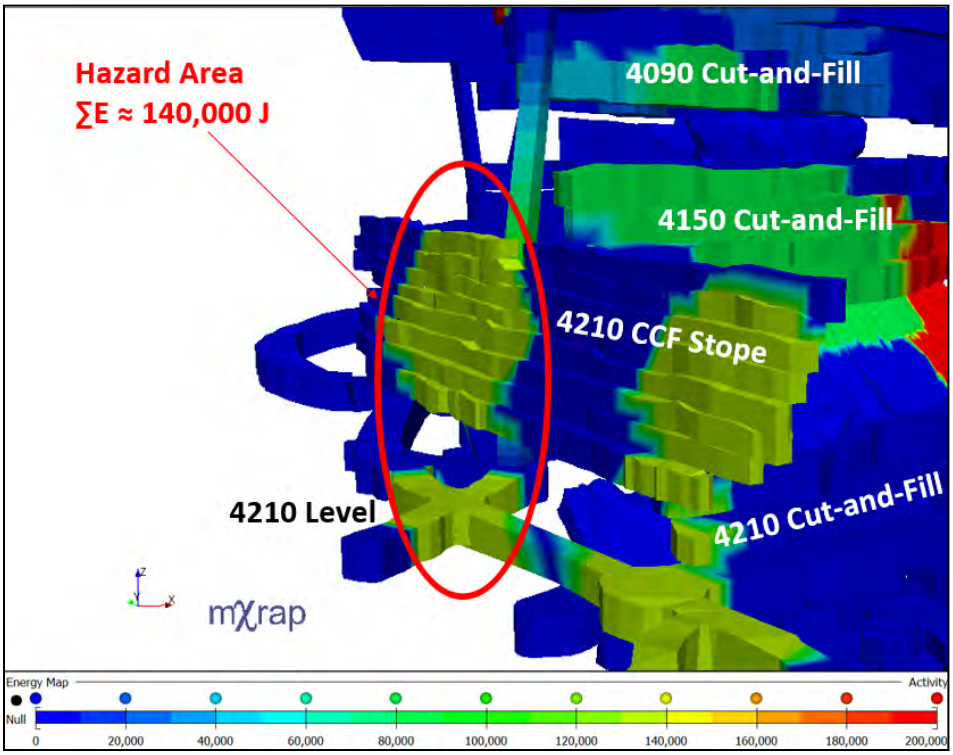

Figure 82 Cumulative Energy Hazard Map shown for a Western Abutment, Note that the Captive Stope, Previously Mined from 4210L, is Striking Orthogonally to the Current Vein being mined on 4150L

In the above figure, there are multiple areas above the hazard threshold. The one in question occurs on the hanging-wall of a previously mined captive cut-and-fill stope (CCF Stope). The vein mined by that stope is roughly orthogonal to the main vein system which was mined up to the vein in question (C-South Vein). Using the previous 6

months, a cumulative energy release of 140000 J, 14 x threshold, was calculated. This constitutes an area that would be part of the overall scorecard.

Once the hazard area has been defined, the mining activity in the trailing period that likely contributed to the elevated nature of hazard is catalogued. The stopes taken in the trailing period are shown in the following figure (see Figure 83):

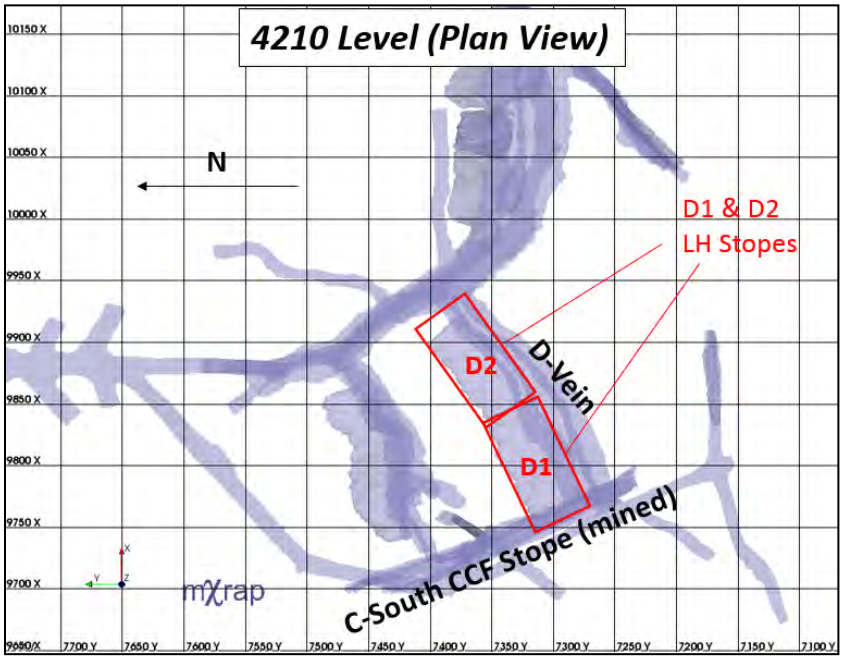

Figure 83 Plan view of 4210L Showing Stopes Mined in the Trailing Period

As can be seen, two long-hole stopes were mined in the 6 month trailing period in close proximity to the hazard area. Once the hazard level and previous mining activity have been established, the results in the forecast period can be evaluated (see Figure 84):

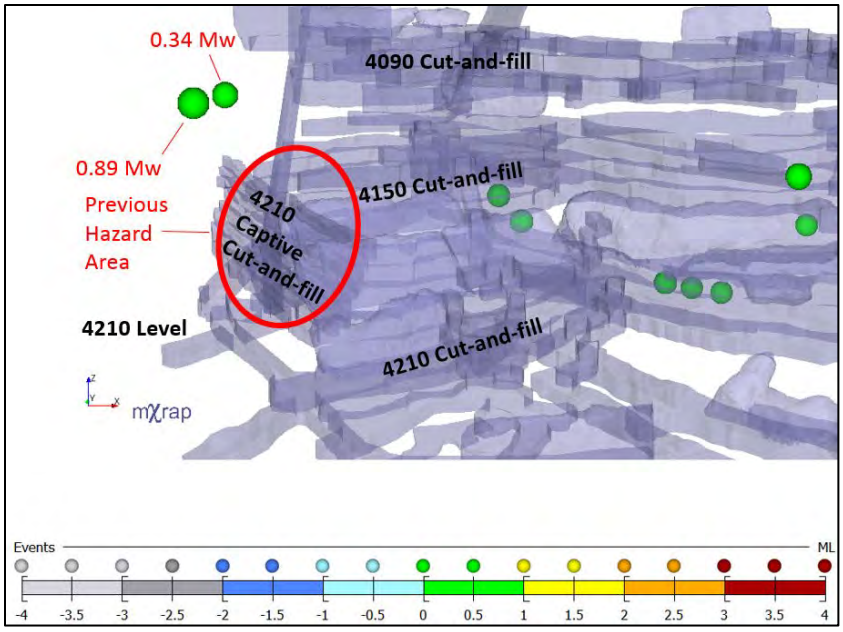

Figure 84 Seismic Activity Occurring in the Forecast Period, Note That This Figure is shown in Reference to Figures (79 & 80)

In the 2 month forecast period, 2 large events occurred following a stope blast on the level above (4150 Level). The scorecard for this instance is given in the table below (see Table 10):

Table 10 Scorecard shown for the Scenario Described Previously

Level	HazMap Results		Area Accessible	Past Activity	Planned activity	Forecast Period		
	Location	∑E				Date/Time	Location	Mag
4210	CCF (North)	140000	No	4210 D1 + D2 Stopes	4150 D1/D2 Stope	13/06/2016 4:35	4090/4150 D-Vein Abt.	0.34
						13/06/2016 4:36	4090/4150 D-Vein Abt.	0.89

4.4.3 Cumulative Moment Hazard Map

The methodology using the cumulative moment hazard map is identical to the energy hazard map discussed in the previous section. The first step is to catalogue the hazard areas on the current hazard map by sub-level and location on the level. The moment hazard map is shown in the following figure for the period from February-2016 to August-2016 (see Figure 85):

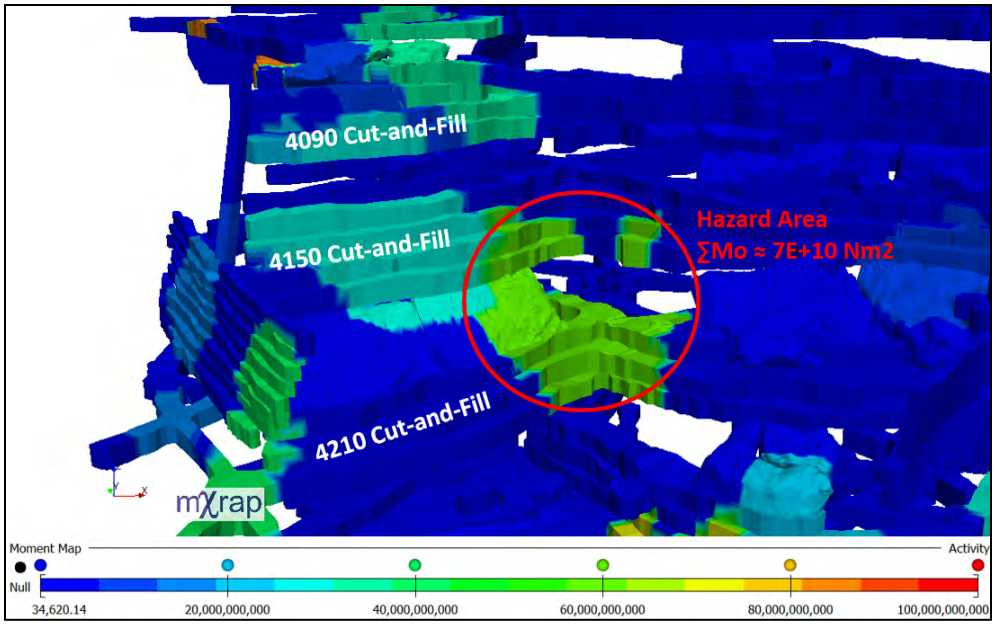

Figure 85 Isometric View of the Cumulative Moment Hazard Map in a Central Mining Pillar for the Period from Feb-Aug 2016

The area shown in the figure above is a central retreat pillar that is diminishing horizontally as long-hole stopes are taken toward the level center. As mentioned before, it is pertinent to record past mining activity in the trailing period (see Figure 86):

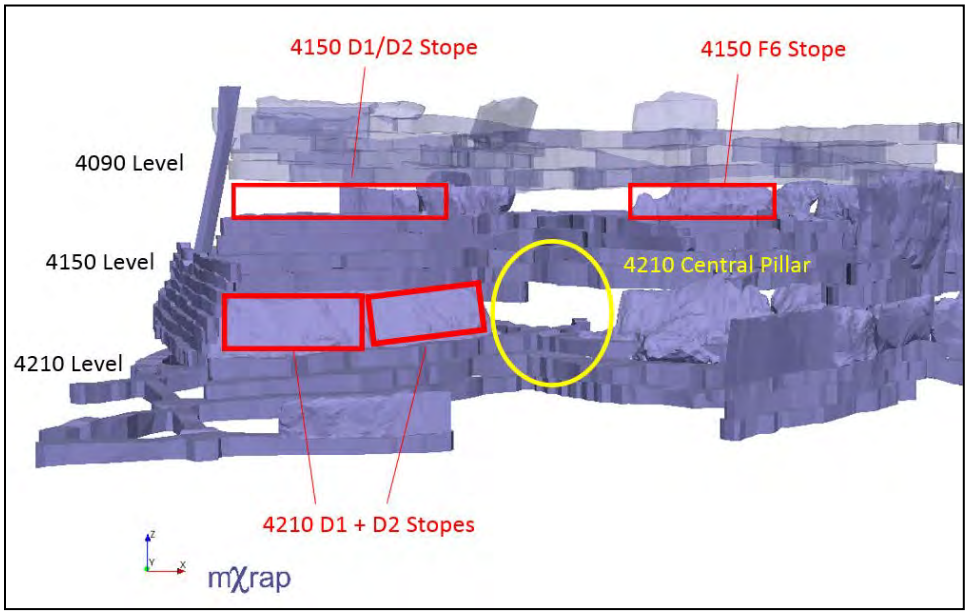

Figure 86 Mining Activity in the Trailing Period for the Corresponding Hazard Map in the Previous Figure (Figure 82), Note the Stopes Taken (in Red) Around the Hazard Area

As can be seen, 2 large long-hole stopes were taken in the trailing period. This is likely the cause of the large cumulative moment value. The following figure shows the seismic activity occurring in the forecast period (see Figure 87):

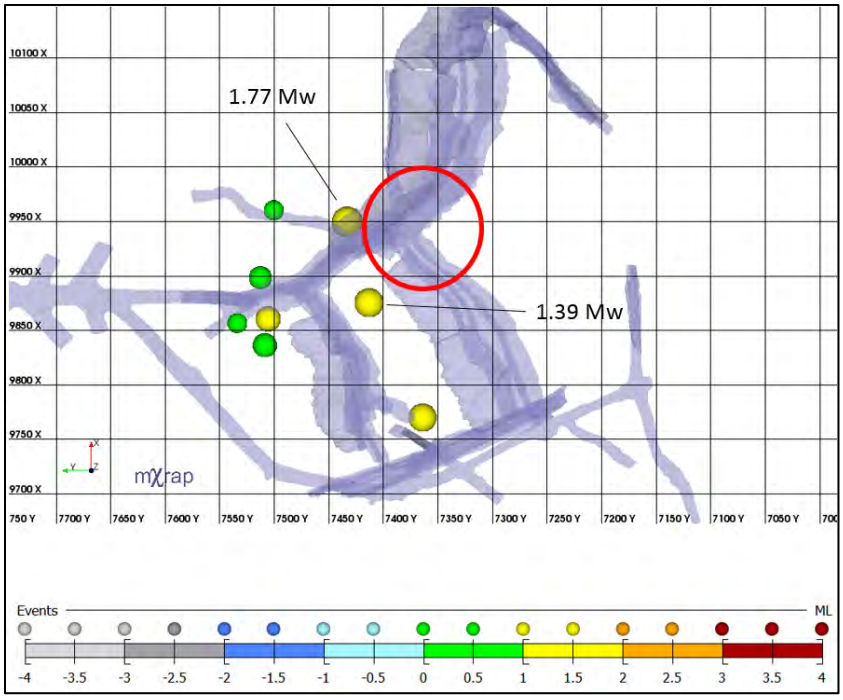

Figure 87 Plan View of 4210L Showing Seismicity Occurring in the Forecast Period from Aug-Oct 2016

As can be seen in the previous figure, 7 events > 0 M_w occurred in close proximity to the hazard area. Therefore, this was a successful forecast. An example scorecard for this example is shown in the following table (see Table 11):

Table 11 Scorecard Shown referencing Figures 82, 83 and 84

Level	HazMap Results		Area Accessible	Past Activity	Planned activity	Forecast Period		
	Location	∑Mo				Date/Time	Location	Mag
4150/4210	F/D Pillar	7E+10	Yes	4150 D1/D2 + F6 4210 F1/Frec Stopes	4210 F3 Stope	2016/09/17 04:41:54	4210 c3, B-West (HW) near F/B intersection	1.39
						2016/08/05 10:50:10	4280 c2, G-North, near G/F/B intersection	1.77

4.4.4 80th Percentile Apparent Stress Activity Hazard Map

The following is an example of the AS-80 hazard map. This is one of 2 types tested that use a count or incremental value above threshold rather than a cumulative one. The trailing period in this example is from February-2016 to August-2016, the forecast period is the following 2 months, from August-2016 to October-2016. Shown below is the AS-80 hazard map for 4340 Level, G-North Vein (see Figure 88):

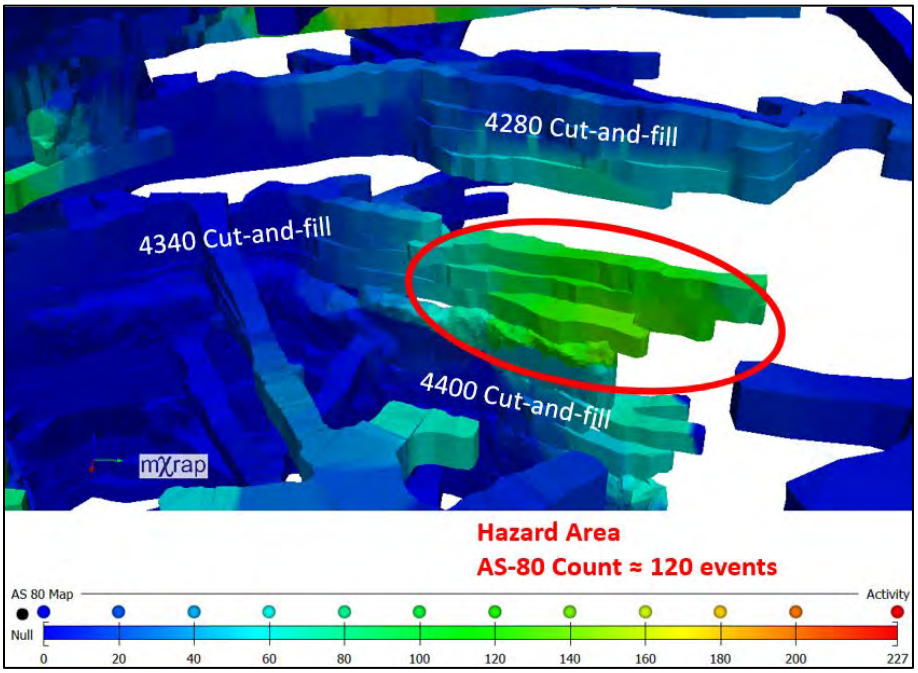

Figure 88 Isometric View of the AS-80 Hazard Map for the Period from Feb 2016 – Aug 2016 with the Hazard Area of Interest shown in Red

The mining activity accompanying the hazard map is shown in the following figure (see Figure 89):

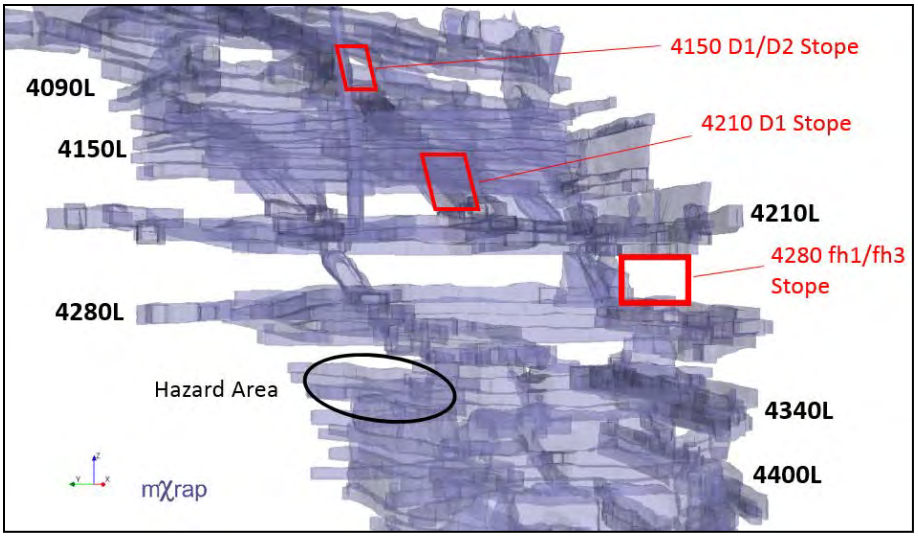

Figure 89 Section View (looking East) showing the Hazard Area with Past Stoping shown in Red

The figure above is a section view looking east. In the trailing period, 3 large stopes were taken which likely contributed to the level of hazard in the area shown in the black oval. The seismic activity occurring within the hazard area vicinity in the trailing period is shown in the following figure (see Figure 90):

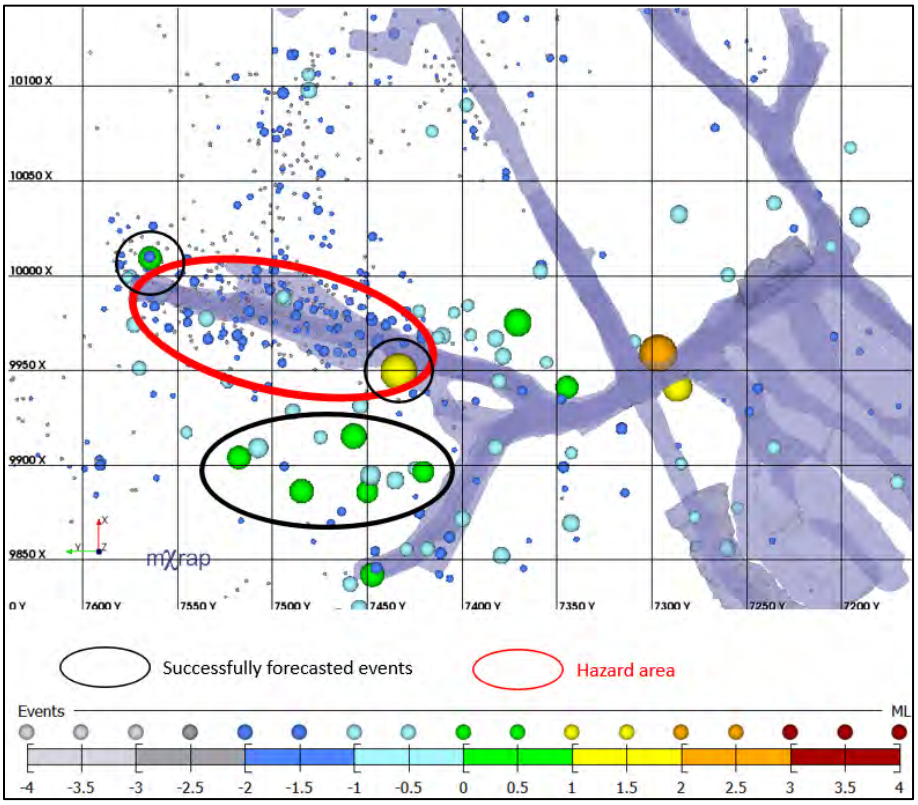

Figure 90 Plan View of Seismic Activity Occurring in the Forecast Period (referencing Figures 88 & 89)

Shown above, a large number of events > 0 M_w occurred. It should be noted that at least 3/7 events can be directly tied to stope blasting on the levels above. The stope in question, 4210-F3 Stope, was the final extraction of the diminishing pillar mentioned in the previous section (4.4.3).

4.4.5 Magnitude Activity Hazard Map

The magnitude hazard map, like the AS-80 map uses a counted value above threshold rather than a cumulative value. As mentioned in Section 4.3.2, 3 different lower-bounds were used: -1, -0.5, and 0. The following example shows the magnitude activity map using events above -1.0M_w for an abutment on the eastern edge of the Morrison orebody, this area has experienced large amounts of seismicity over the mine life so far (see Figure 91):

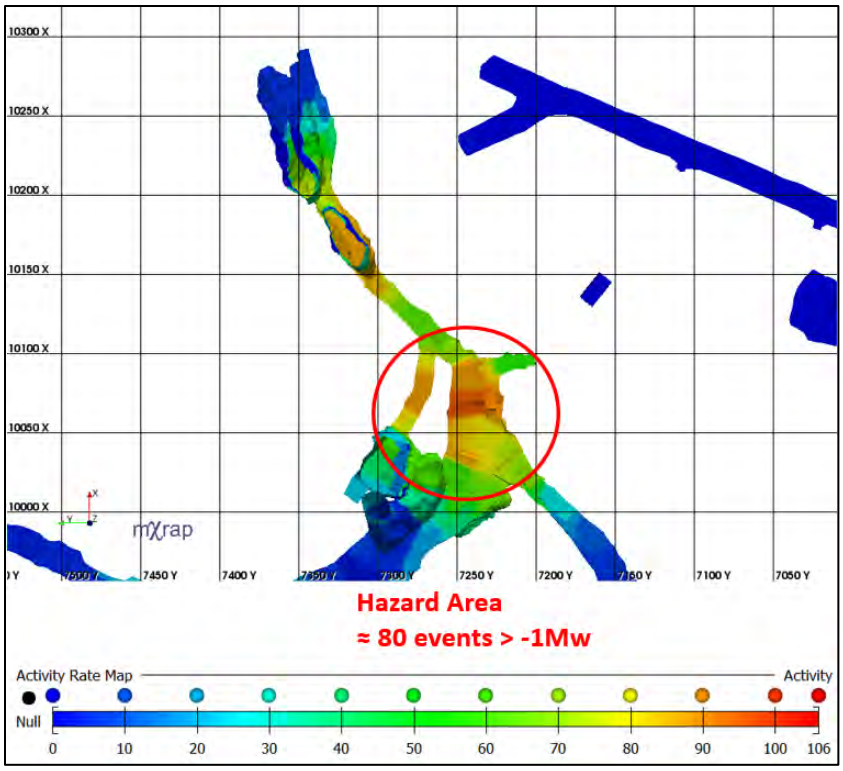

Figure 91 Activity Hazard Map using Events Above -1.0Mw for the Period of Dec 2015 - June 2016

In the previous figure, approximately 90 events above -1.0M_w occurred following 2 stope blasts, the locations of which are shown in the following figure (see Figure 92):

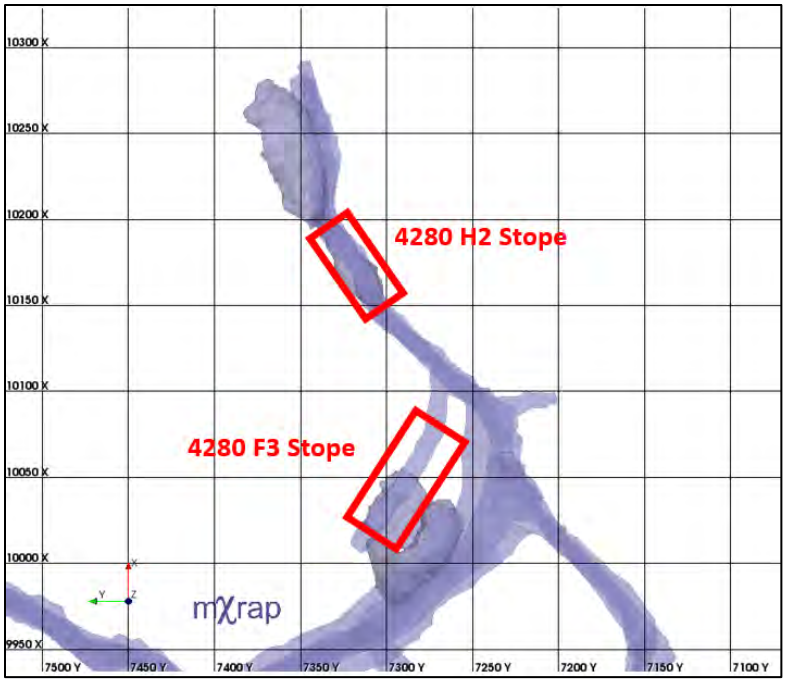

Figure 92 Stope Extraction in the Period from Dec 2015 - June 2016 with Stopes shown in Red

The following figure shows the seismic activity occurring in the forecast period (see Figure 93):

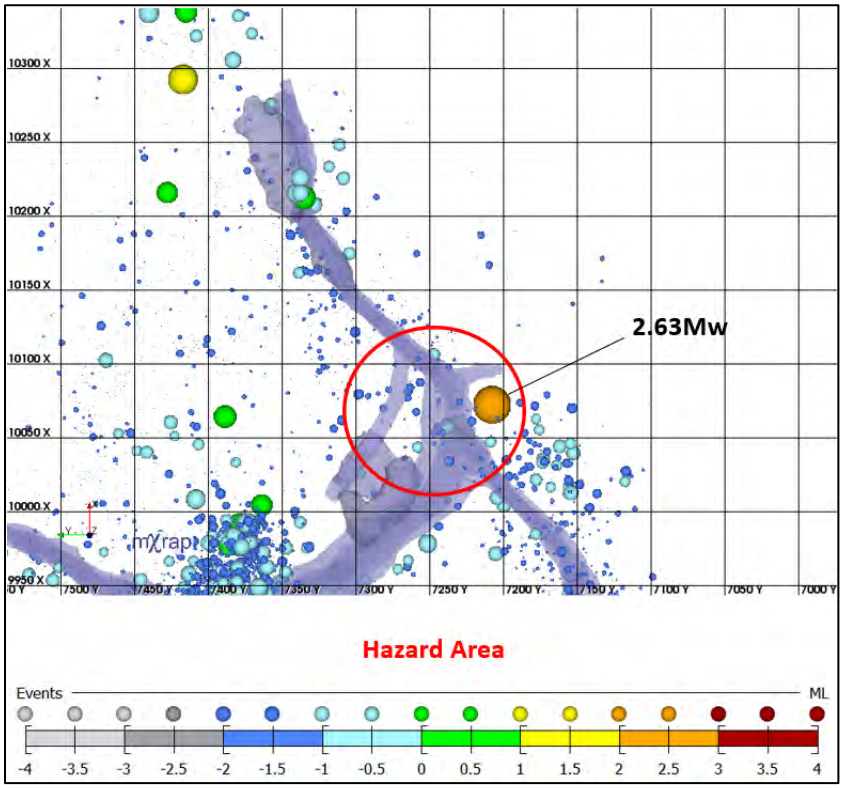

Figure 93 Plan View of Seismic Activity Occurring in the Period from June - Aug 2016

In the forecast window, a large event at 2.63M_w occurred following a stope blast on the level below. This is considered a successful forecast. The examples given in this section only show successful applications. Full scorecards for each hazard map over the time periods discussed in Section 4.1 can be found in appendices A, B and C. One concept that is absent in these hazard map applications is an estimation for how large the forecasted event may be. The standard set is simply that if the area is over threshold in the trailing period that an event above 0M_w 'will' occur in the forecast period. This is a binary model. Discussed in Chapter 5 is a possible synergy in using these hazard maps with what is called the Magnitude Hazard Map to give an indication of the size of the expected event.

5 Results and Discussion

5.1 Hazard Map Results

As discussed in the previous chapter, a scorecard format was used to evaluate the success and accuracy of each type of hazard map. The evaluations were done visually and are characteristic of empirical methodologies. The time periods used for hazard assessment are a 6 months trailing window to forecast the following 2 months. Additional work has been done in varying the trailing period and forecast period lengths. The results of which are further discussed in Section 5.2.4.

The utility of a hazard map is measured by how many large events were effectively forecasted compared to the total number of large events occurring in the forecast window. This is known as the success rate which is defined in Section 4.3.3. As well, the false alarm rate, which is the number of hazard areas that were identified as high hazard areas but did not record a large event, is used to determine the most effective hazard map. The success and false alarm rates are defined in Section 4.3.3 & 4.3.4. The following charts show the results in terms of success and false alarm rates for each technique over each of the three forecast time periods analyzed (see Figures 94, 95 & 96):

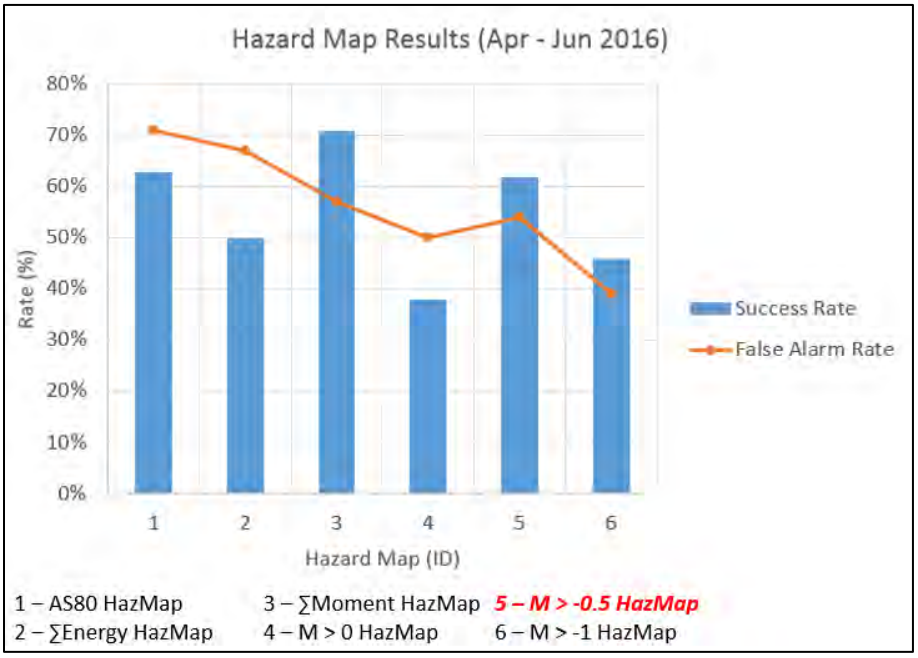

Figure 94 Hazard Maps Results for the First Forecast Period with Success Rate (in Blue) and False Alarm Rate (in Orange)

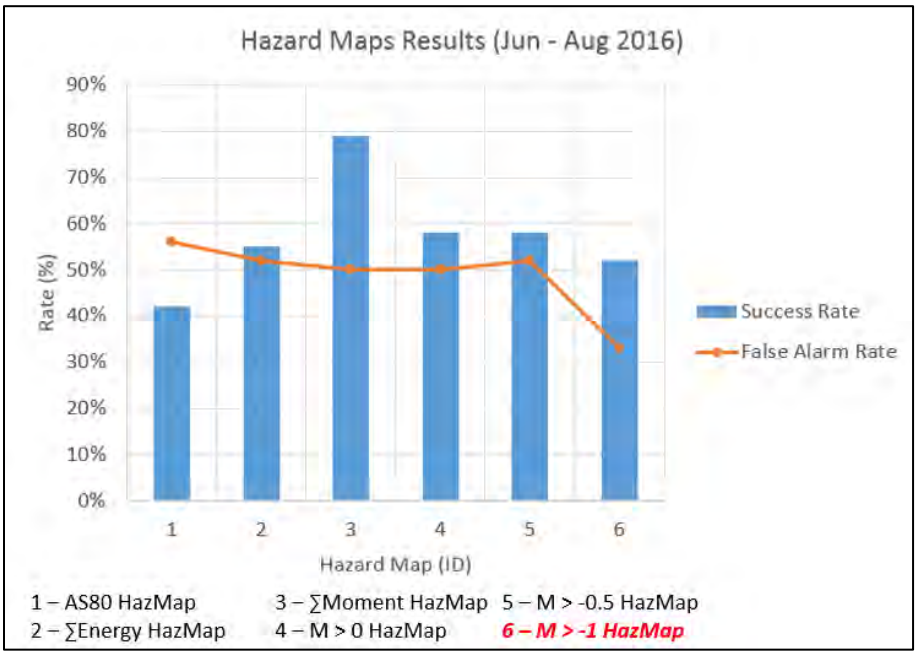

Figure 95 Hazard Maps Results for the Second Forecast Period with Success Rate (in Blue) and False Alarm Rate (in Orange)

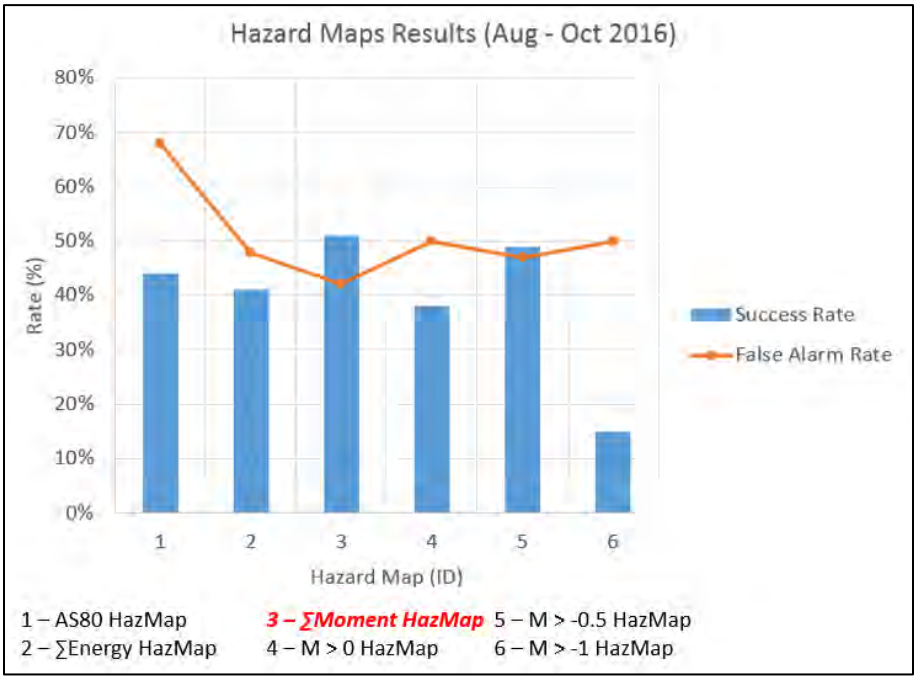

Figure 96 Hazard Maps Results for the Third Forecast Period with Success Rate (in Blue) and False Alarm Rate (in Orange)

Referring to the previous figures, in terms of success and false alarm rates, the most effective hazard map is one that minimizes the false alarm rate and maximizes the success rate. Previous work done by Simser (2008) suggests that approximately 30% of large events have some pre-cursory micro-seismic activity. In keeping with this finding, success rates higher than 30% are considered to be acceptable since they account for the events that had previous activity and are possibly forecastable. Brown (2015) concluded that success rates above 70% are ideal as they would include these events identified by previous activity as well as events triggered by blasting. Given the results shown in the previous figures, all of the hazard maps fall somewhere between acceptable and ideal.

In terms of success rate to false alarm rate, Young (2012) found that a ratio of successes to false alarms of 1:2 is relatively low. Using these rationales, the cumulative moment map achieved the best results. However, it was found that using cumulative parametric values subjects one to variability brought on b y seismic events with incredibly high seismic energy and moment. Due to this finding, the activity hazard map using -0.5 M_w as a lower bound yielded the best results in that they are more consistent. Although this map did not have the lowest false alarm rate, it had the highest success rate to false alarm ratio after the cumulative moment hazard map. The variability of cumulative hazard maps is discussed in the following subsection (5.1.1).

5.1.1 A Note on the Cumulative Hazard Maps

Judging only previous figure, it is fairly simple to assess which hazard map is best. The higher the success rate, and the lower the false alarm rate the better. Alcott (1998) found that rockburst hazard assessed from cumulative seismic parametric values is more susceptible to uncharacteristically high numeric values resulting from an incomplete data set. As well a cumulative approach to hazard assessment can be effected more by events that have an erroneously high seismic parameter or parameters associated with them. These rogue events occurring in the data set can vastly increase the cumulative hazard value. This behavior is shown in the following figure (see Figure 97):

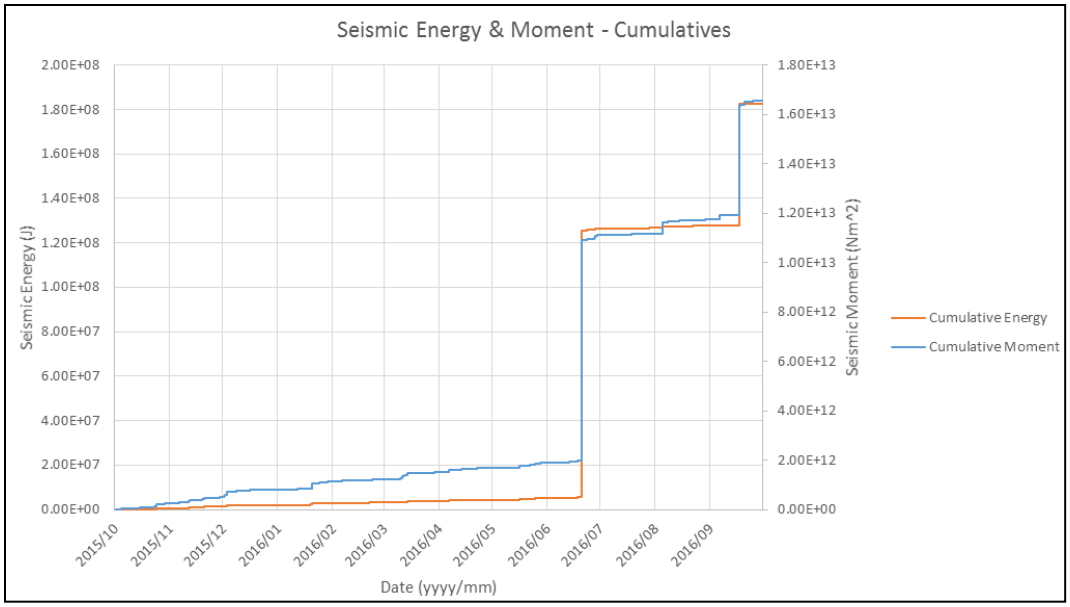

Figure 97 Time-History Chart of Cumulative Seismic Energy and Seismic Moment

Referring to the previous figure, there are two large steps in both distributions of energy and moment. The first occurs on June 20th, 2016 and is attributable to the occurrence of a 2.63 M_w event. The second occurs on September 17th, 2016 and is attributable to the occurrence of a 2.29 M_w event. It should be noted that the increase in cumulative values is almost an entire order of magnitude (10x). Preceding time windows inclusive up to June 2016, will not contain the 2.63 M_w and thus have smaller cumulative values. The same is true for time periods sufficiently far enough into the future that would not include this large step.

This susceptibility to rogue events reduces the utility of cumulative value hazard maps since the high hazard value could be either attributed to many events occurring with moderately high parametric value or simply one or two outlier events that may not be representative of the population. Essentially, hazard areas influenced in this way may not be accurate forecasts of future seismicity.

5.2 Hazard Mapping Analysis

5.2.1 Hazard Map Scaling

The hazard defining condition, as stated in the previous chapter, is the occurrence of an event above $0M_w$. What the hazard maps, in and of themselves, do not do is give an indication of exactly how large an event one can expect or how many events above a certain size will occur. The idea in hazard scaling is that the larger the hazard value, the larger the expected event size.

To investigate this notion, the successfully forecasted events > $0M_w$ have been graphed against the values of the hazard areas in the trailing period. The likelihood of an event above a certain size has been calculated for logical ranges for each hazard map. These ranges are defined by 'banding' or grouping in the data spread. To determine the likelihood for each defined hazard range, the number of events above a certain magnitude is counted then divided by the total number of events in the range. This is denoted by the following equation:

$$P > M(\%) = \frac{\Sigma(events > M)}{\Sigma(events)}$$

An example of this analysis is shown using colored segregation in the following figure for the AS-80 hazard map along with the results in the subsequent table (See Figure 98 & Table 12):

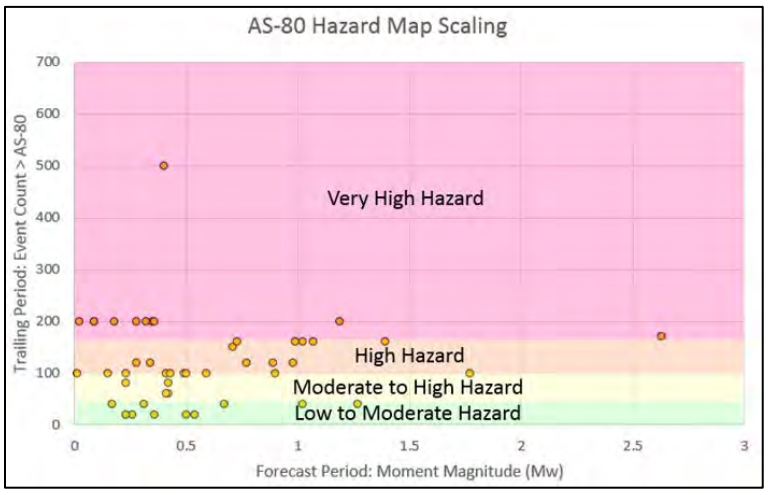

Figure 98 AS-80 Hazard Map Scaling Chart using a 60ft Search Radius

Table 12 AS-80 Hazard Map, Probability of Event Occurrence based on Magnitude

Range	P > 0.5	P > 1	P > 2
0 - 50	11%	5%	0%
50 - 100	14%	3%	0%
100 - 160	37%	11%	0%
> 160	33%	24%	5%

What is apparent from the above table and figure is that the likelihood of larger events increases with the hazard value. This trend can be seen in the other hazard maps. Graphs of likelihood vs hazard range are shown below for P > 0.5, P > 1, and P > 2 (see Figures 99, 100 and 101):

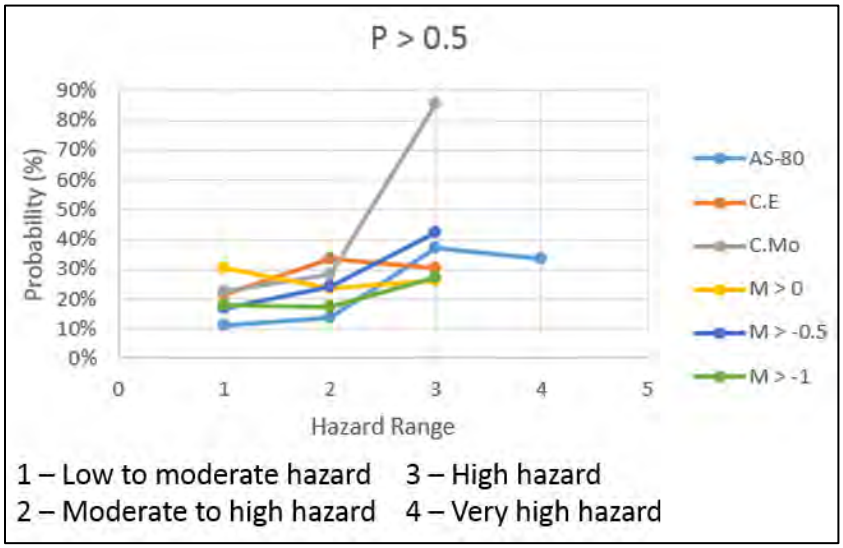

Figure 99 Probability of Event Occurrence above 0.5Mw

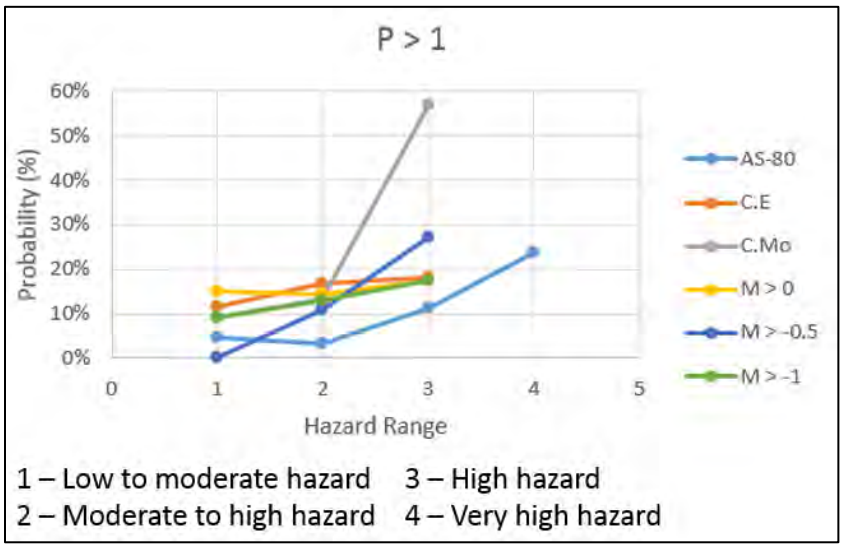

Figure 100 Probability of Event Occurrence above 1.0Mw

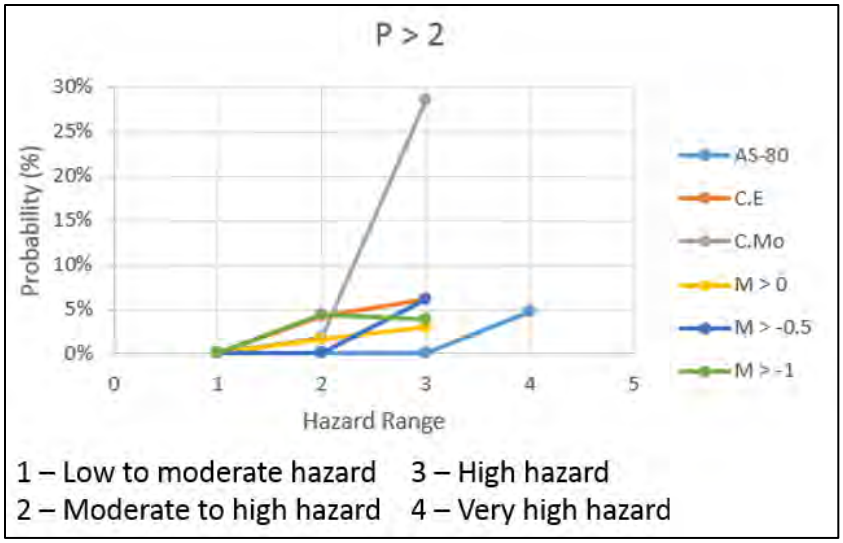

Figure 101 Probability of Event Occurrence above 2.0Mw

As seen in the previous figures, the likelihood of larger events occurring increases with an increasing hazard values. This is evident by the general upward trend of each series defined by a certain hazard map (see legend). A table to hazard map ranges for each map is shown below (see Table 13):

Table 13 Hazard Map Ranges

HazMap	Low	Moderate to High	High	Very High
M > -1	1 - 30 events	30 to 60 events	> 60 events	N/A
M > -0.5	1 - 2 events	2 to 5 events	> 5 events	N/A
M > 0	1 - 2 events	2 to 5 events	> 5 events	N/A
C.Moment	1e+9 - 1e+10N.m	1e+10 - 1e+11N.m	> 1e+11N.m	N/A
C.Energy	0 - 100000J	100000 - 200000J	> 200000J	N/A
AS-80	0 - 50 events	50 - 100 events	100 - 160 events	> 160 events

From these results it is reasonable to assume that an increase in hazard value, be it cumulative or counted, can increase the likelihood of larger events occurring. This notion is also subject to whether or not mining activities are occurring in the forecast period as is discussed in Section 5.3.

5.2.2 Hazard Map Triggering

The purpose of this section is to investigate precursory evidence for the occurrence of a large event. Hazard map triggering is the idea that there should be some commonality between the different maps in terms of hazard areas. For example, the 4210 Level, central

pillar or 'F/D' pillar is highly seismically active since the extraction sequence on that level is reducing its horizontal dimensions. One would expect that this hazard area should show up on most, if not all the hazard maps for a few reasons. First that there has been large amounts of seismic activity in that area in the past (including large events), and second that the planned stopes are large in comparison to the average size at the mine of about 5000tonnes. This is illustrated in the following figure (see Figures 102, 103 and 104):

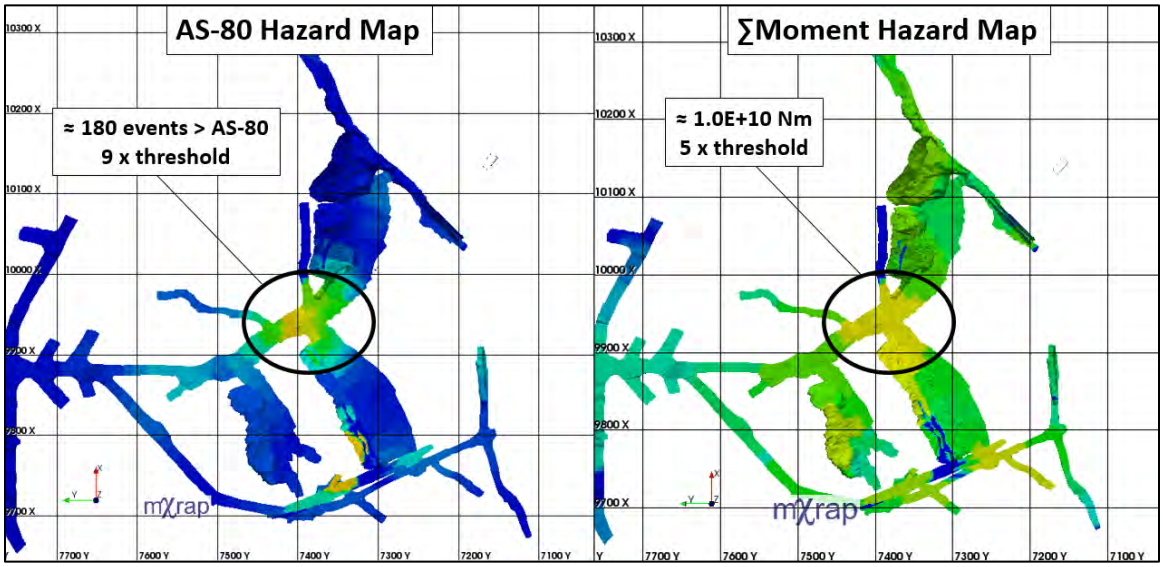

Figure 102 AS-80 and Cumulative Moment Hazard Maps for the 4210 F/D Central Pillar

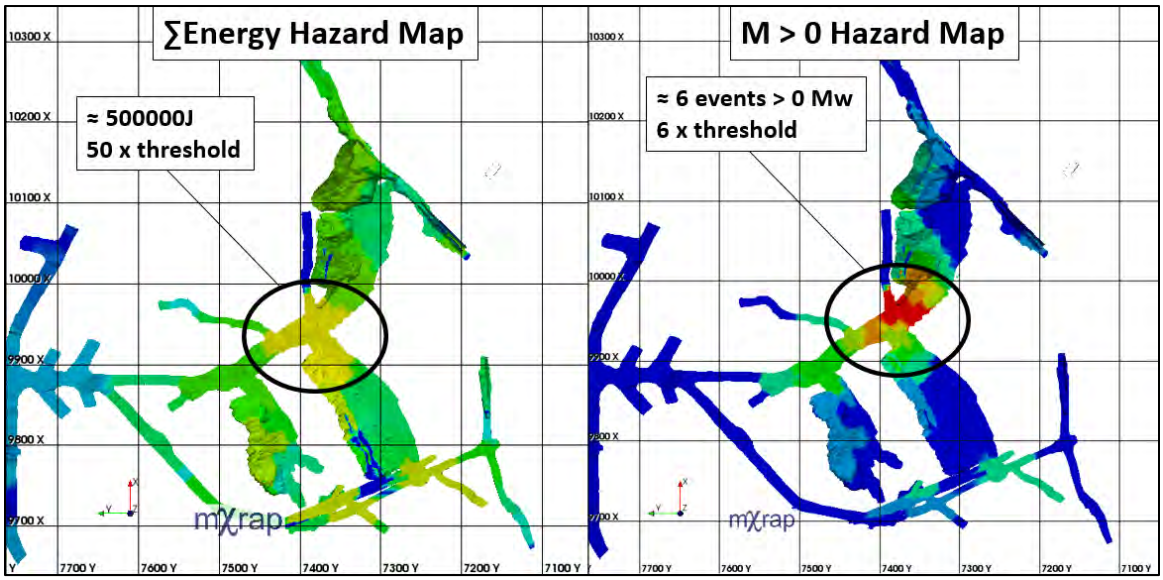

Figure 103 Cumulative Energy and M > 0 Hazard Map for the 4210 F/D Pillar

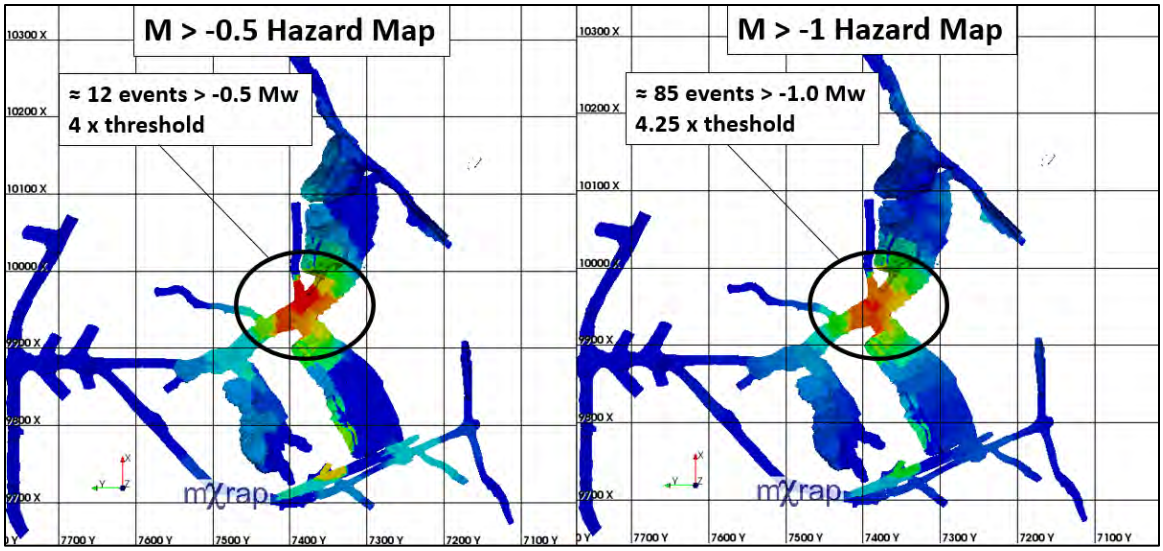

Figure 104 M>-0.5 and M>-1 Activity Hazard Maps for the 4210 F/D Pillar

Referring to the previous 3 figures, each hazard map shows a level above threshold in the 4210 central pillar. This is in keeping with the notion of triggering. In this case, one would expect there to be a larger event occurrence in this area in the forecast period provided there was sufficient mining activity in the vicinity. The seismicity occurring in the forecast period is shown in the following figure (see Figure 105):

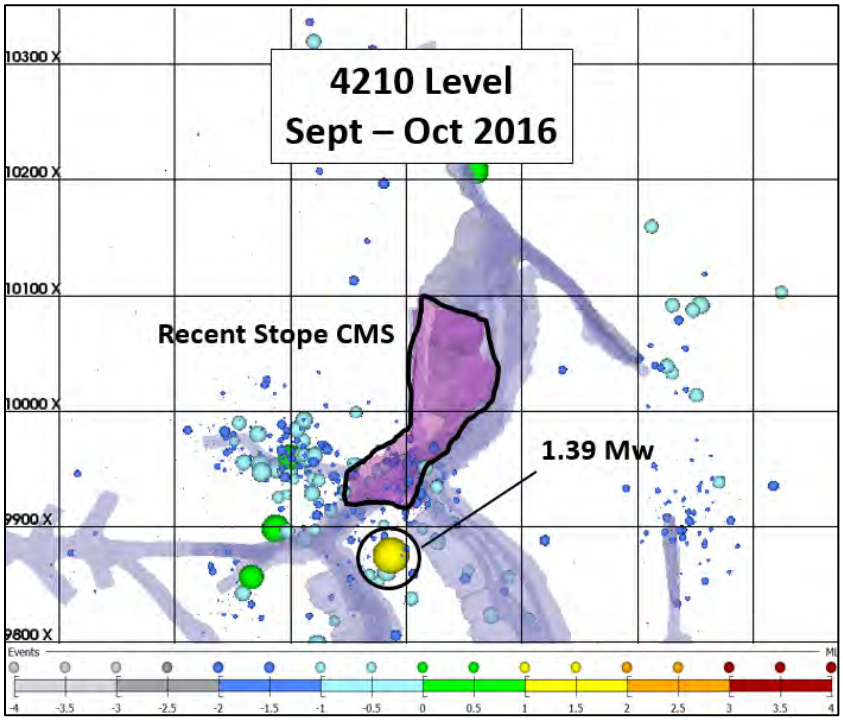

Figure 105 Plan View of Seismic Activity Occurring in the Forecast Period

One can see, from the previous 3 figures, all of the hazard maps were accurate in forecasting the occurrence of a large event. For each time period assessed, the events > 0 M_w were plotted against the hazard maps that showed a level greater than threshold. An example of this, in tabulated form is shown in below (see Table 14):

Table 14 Events > 0 Mw in the Forecast Period vs Hazard Maps in the Trailing Period > Threshold

Events > 0 in Forecast Period			Hazard Maps Triggered					
Date/Time	**Location**	**Mag**	**M > 0**	**M > -0.5**	**M > -1**	**AS-80**	**∑E**	**∑Mo**
2016/09/06 07:06:23	4090 c1, H-North, beneath LH stopes	1.27				Yes	Yes	
2016/09/17 04:40:15	4090 c3, B-West (HW)	1.27	Yes	Yes			Yes	Yes
2016/09/17 04:35:34	4090 c4, (FW) of F/D Veins	0.83	Yes	Yes				Yes

From the above table, the number of hazard maps triggered is counted. This has been graphed against the magnitude of the forecasted event. The idea is that more hazard maps would be triggered in the occurrence of a larger event. This graph is shown in the following figure (see Figure 106):

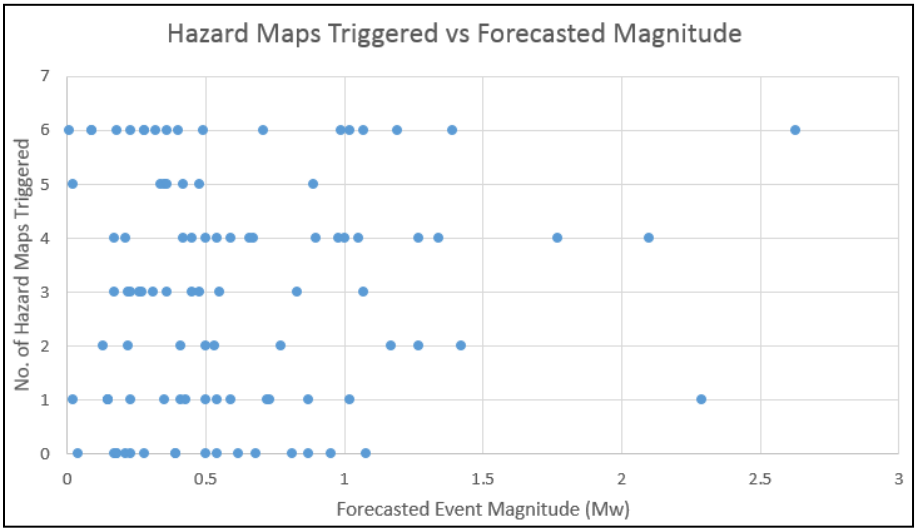

Figure 106 Event Magnitude versus How Many Hazard Maps Triggered in the Trailing Period

From the previous graph, the likelihood of occurrence of an event > 0.5, 1, and 2 has been calculated using the same method as discussed in the previous section and is summarized in the following graph (see Figure 107):

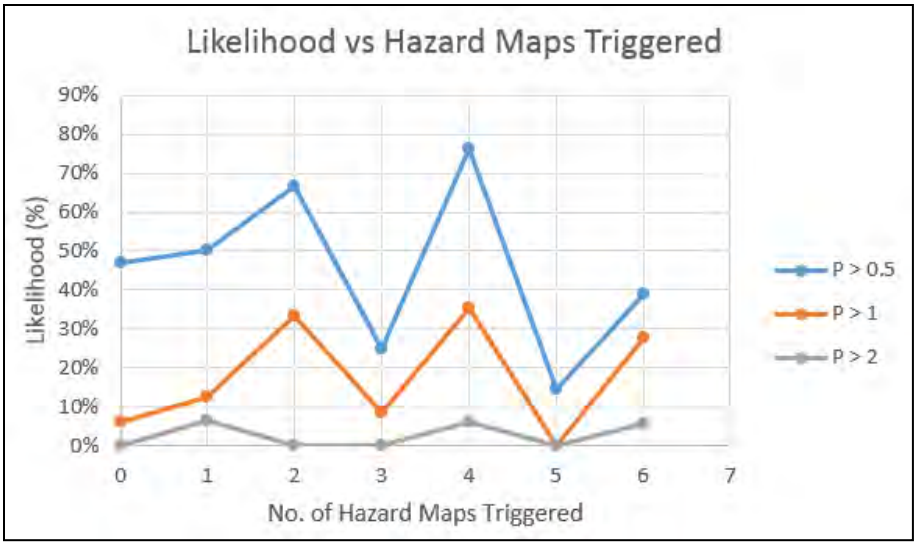

Figure 107 Likelihood of an Event > Mag Occurring vs Hazard Maps Triggered

From the above chart, it is obvious that the notion of hazard map triggering does not apply, that being that the larger the forecasted magnitude, the more hazard maps will have been triggered. This is evident in that there is no consistent upward or downward trend in the data.

5.2.3 Comparisons to the Magnitude Hazard Map

As stated in the previous section, the hazard assessing technique in this thesis is binary. While it is possible to determine roughly, where a large event will occur, the size of the event is unknown simply that it is above 0 M_w. Section 5.2.1 has shown that the likelihood of larger events can increase with increased parametric hazard values. To compliment the concept of scaling, a hazard map using a determination of M_{max} has been analyzed over the specified time periods used in this thesis and is compared to the forecasted magnitudes. The equation used to determine M_{max} was put forth by Kijko and Funk (1994) and is given by the following equation:

$$M_{max} = X_{max} + (X_{max} - X_{n-1}) \quad (12)$$

Where M_{max} = maximum expected magnitude, X_{max} = the largest event magnitude in the data set, X_{n-1} = the second largest event magnitude in the data set

This analysis, in terms of mapping can be done in a number of ways, however for the interests of this thesis, the nodal approach has been used. Essentially, one wants to see how well this hazard map estimates the expected size of events in the forecast period.

Shown below is a figure with the magnitude hazard map, the AS-80 hazard map and the seismicity occurring in the forecast period (see Figure 108):

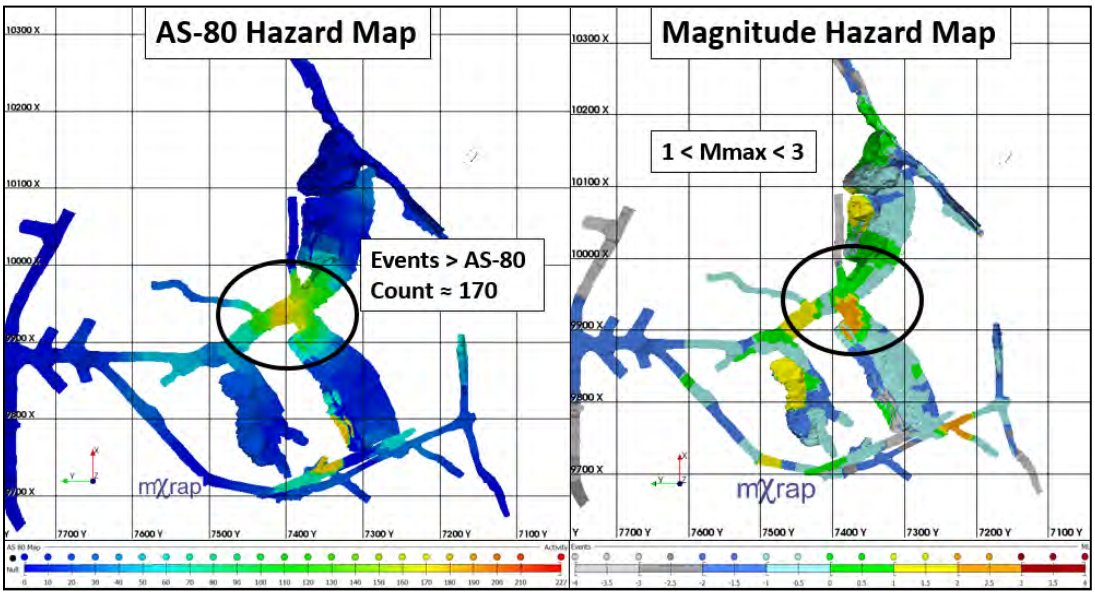

Figure 108 AS-80 Hazard Map Compared to the Magnitude Hazard Map

As seen in the previous figure, the hazard areas on the two different maps are similarly located. The following figure shows the seismicity occurring in the forecast period (see Figure 109):

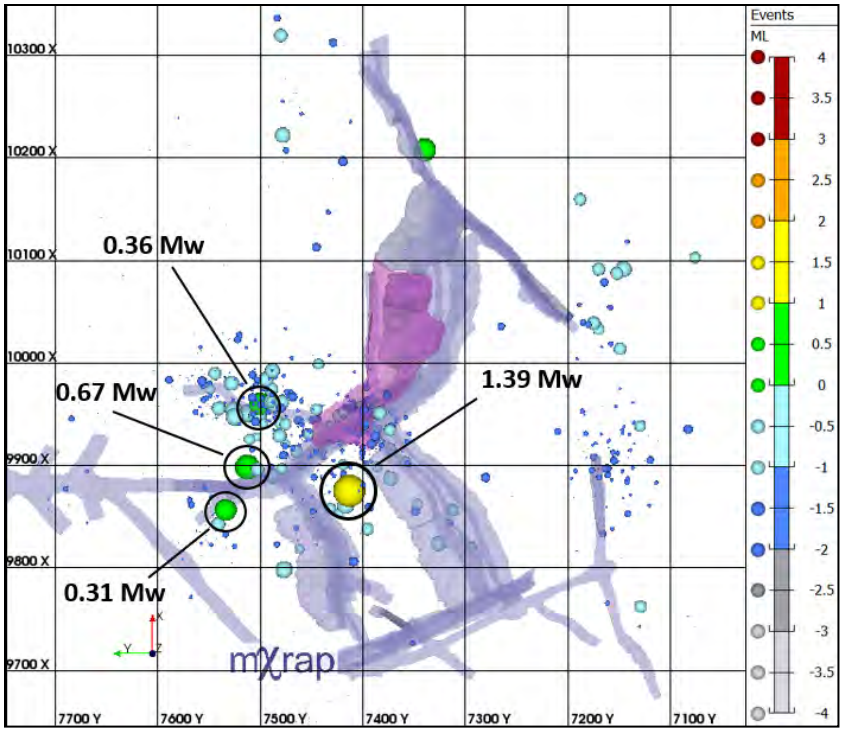

Figure 109 Plan View of Seismic Activity Occurring in the Forecast Period

In the forecast period, one can see the occurrence of 4 events > 0 M_w following a large stope blast. In this case, the successfully forecasted events using the AS-80 hazard map were compared to the corresponding estimate of M_{max} using the magnitude hazard map. This comparison is shown in the following table (see Table 15):

Table 15 Events Occurring in the Forecast Period vs Magnitude Hazard Map Mmax Estimations

Forecast Period: Events > 0 M_w			Magnitude Hazard Map Forecast	
Date/Time	**Location**	**Mag**	**M_{max} Estimate**	**Comments**
2016/09/17 04:41:54	4210 c3, B-West (HW) near F/B intersection	1.39	1 < M < 2	accurate hazard
2016/09/23 07:12:36	4210 c3, near F/B intersection	0.67	0 < M < 1	accurate hazard
2016/09/17 04:40:17	4210 c3, near main acc.	0.31	0 < M < 1	accurate hazard
2016/09/17 04:43:24	4210 c2, G-North	0.36	0 < M < 1	accurate hazard

This process was repeated for each hazard map for the successfully forecasted events. The results are shown in the following figures (see Figures 110, 111 and 112):

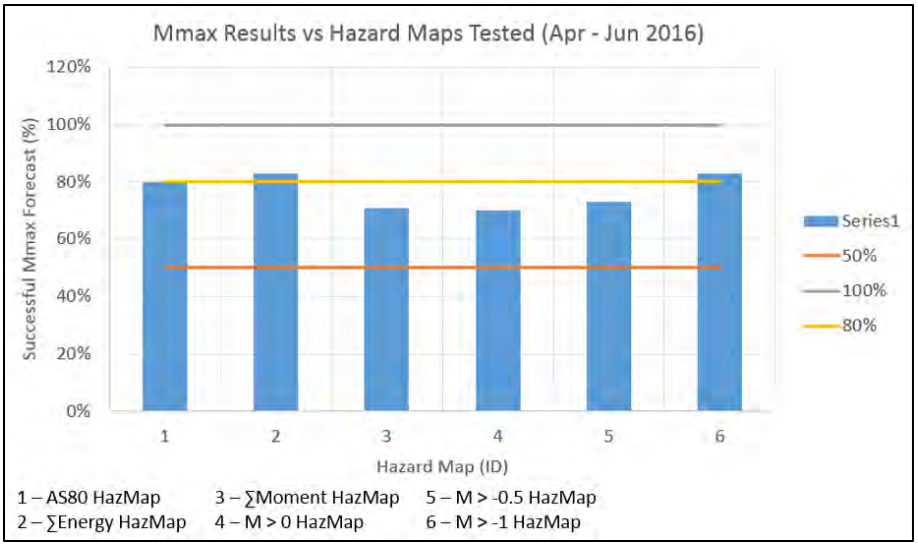

Figure 110 Successful Mmax Forecasts vs Hazard Maps Tested (Apr - Jun 2016)

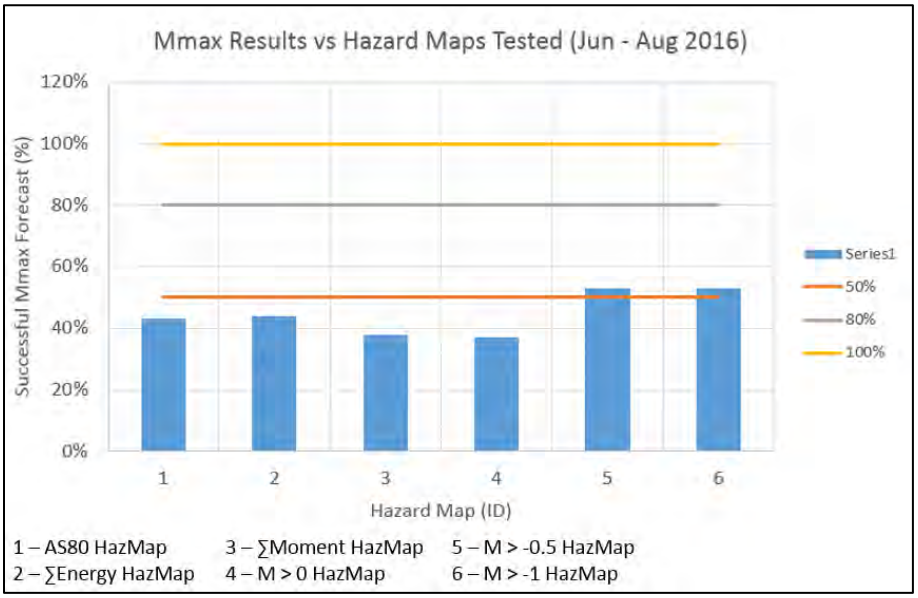

Figure 111 Successful Mmax Forecasts vs Hazard Map Results (Jun - Aug 2016)

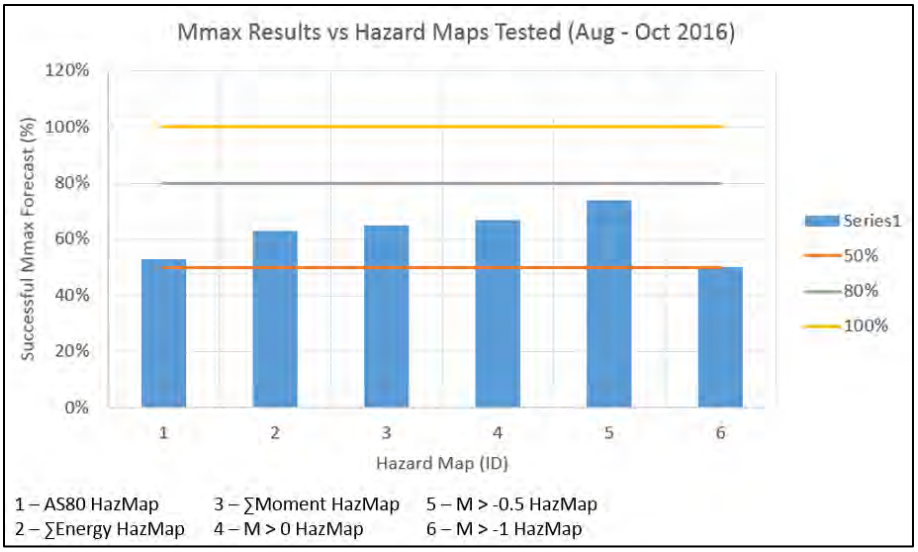

Figure 112 Successful Mmax Forecasts vs Hazard Map Results (Aug - Oct 2016)

From examining the above figures, it is clear that using the magnitude hazard map in conjunction with some of the hazard maps used in this thesis can give a reasonable estimation of the largest expected event size. For example, using the AS-80 hazard map, for the period from April – June 2016, the magnitude hazard map correctly estimated 80% of the successfully forecasted events. Due to the equation used to calculate the maximum event size (given previously), overestimates are common. This is especially true in cases where a large event occurs surrounded by comparatively smaller events since the difference between magnitudes is larger.

5.2.4 Variation in Time Windows

As stated in the previous chapter, the time periods used for hazard assessment are a 6 month trailing period to forecast the following 2 months. The 6-2 method is based on previous work done for Morrison Mine consisting of a retrospective analysis and a series of bi-monthly reports to track the changes in seismic hazard and seismic conditions at the mine. Both the trailing window and forecast window were chosen based on the bi-monthly reporting done for Morrison mine. It should be noted that a 6 month period is between medium and long term, referring to van Aswegen (2005). The 2 month forecast window was chosen because it is the length of the bi-monthly period. This makes the analysis simple and more organized.

Analyses were completed using different trailing and forecast periods. The activity magnitude hazard maps (M > 0, M > -0.5, and M > -1) were assessed using the following time regimes:

1. Medium – Long Term (6 month trailing, 2 month forecast)
2. Short – Medium Term (3 month trailing, 1 month forecast)
3. Short Term (1 month trailing, 1 week forecast)

The success and false alarm rates are expressed as average values over the whole forecast time period. The forecast time range for time regimes 1 and 2 covers April to September 2016 and 1 month to 1 week regime covers the month of September. The results are shown in the following chart (see Figure 113):

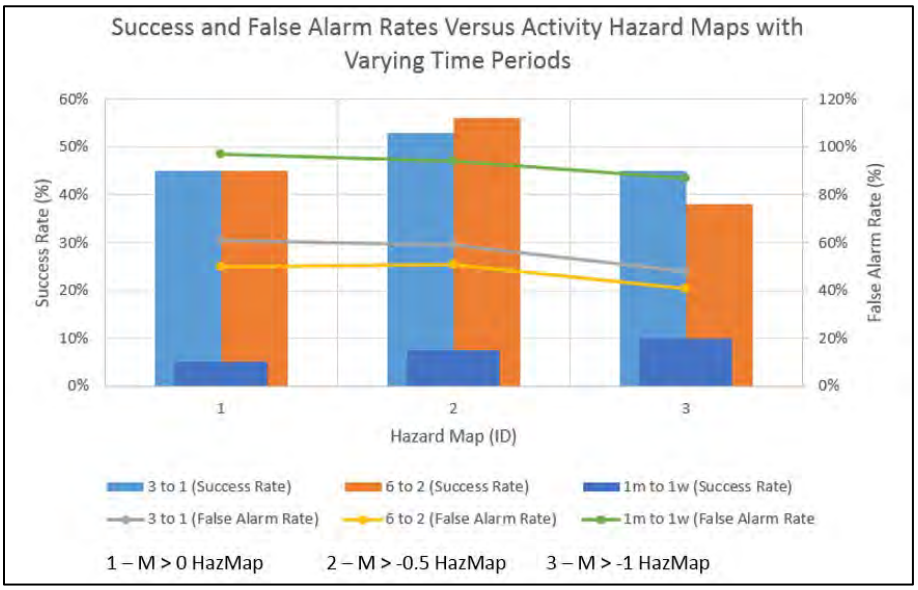

Figure 113 Success and False Alarm Rates vs Activity Hazard Maps with Varying Time Periods

Using a 3 month trailing window and 1 month forecast window is half of the time period regime used in this thesis. As mentioned previously, since seismicity at Morrison Mine is heavily predicated on mining activity, looking back 3 months instead of 6 months will certainly miss some past mining. This is evident by the higher average false alarm rates (seen in the grey trend-line).

Another variation of this method was using 1 month to forecast the following week. This was carried out in the interest of short-term scheduling/planning. The time period examined for forecasting was the month of September 2016 divided into week-long

segments. As is evident in the previous figure, the success and false alarm rates are much lower than the previously proposed time periods. This is likely due to insufficient mining activity captured in the trailing period. Therefore, using 1 month to forecast the following week is not a good estimate of seismic hazard. The success rates for the other two time periods are comparable to each other. It is fair then to say that variation in the time periods of 3 or 6 months does not have a major impact on success rate but rather has a higher impact on the false alarm rate.

5.2.5 Variation in Search Radius

As discussed in Section 4.1.3, the search radius used to generate the hazard maps was 60ft and the radius used in hazard forecasting was 100ft around the hazard area. This is based on the error residuals associated with recorded seismic events. The 60ft radius used in hazard map generation was chosen based on rule of thumb stating that the an adequate search radius is equal to the sublevel spacing so as to not have enormous hazard areas. The effect of changing the search radius size is shown in the following figures:

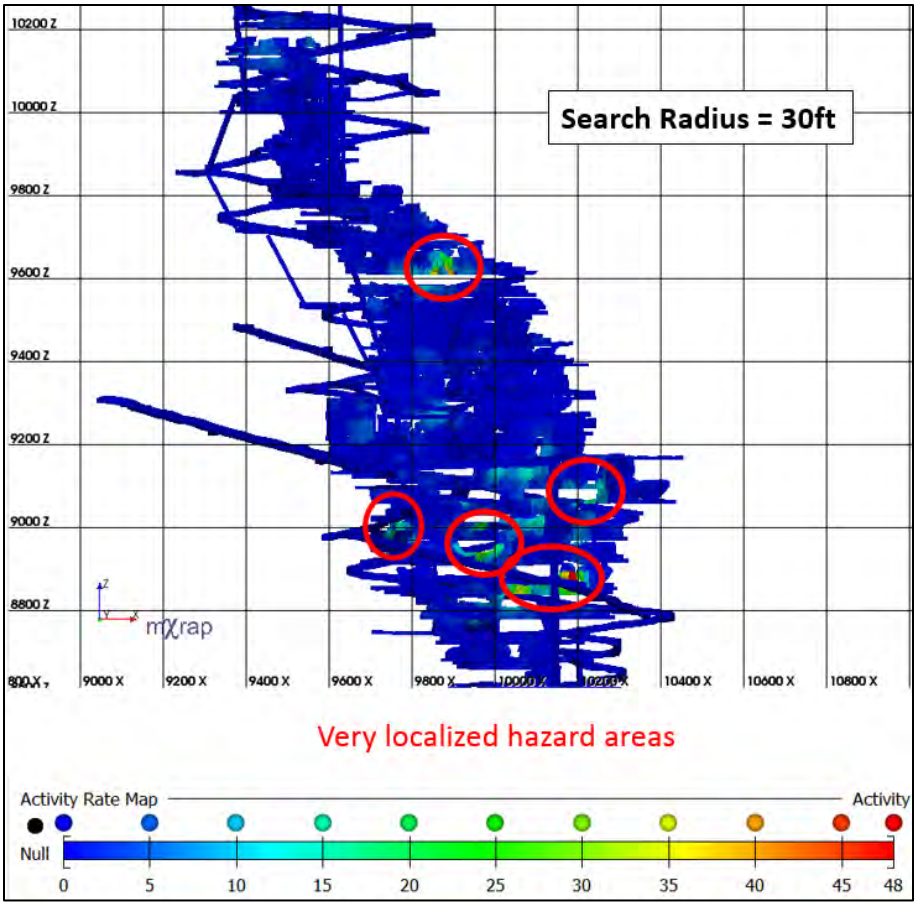

Figure 114 Activity Hazard Map using -1Mw as a Lower Bound; Section View looking North

As seen in the previous figure, there are 5 hazard areas on the map using a 6-month trailing period. These areas are quite localized in that they occupy specific areas on a certain sublevel i.e. a sill-drift intersection. With using a small search radius, the amount of data used in generating the hazard will be smaller, in this case 48 events above -1 M_w is the maximum amount of any hazard area on the map.

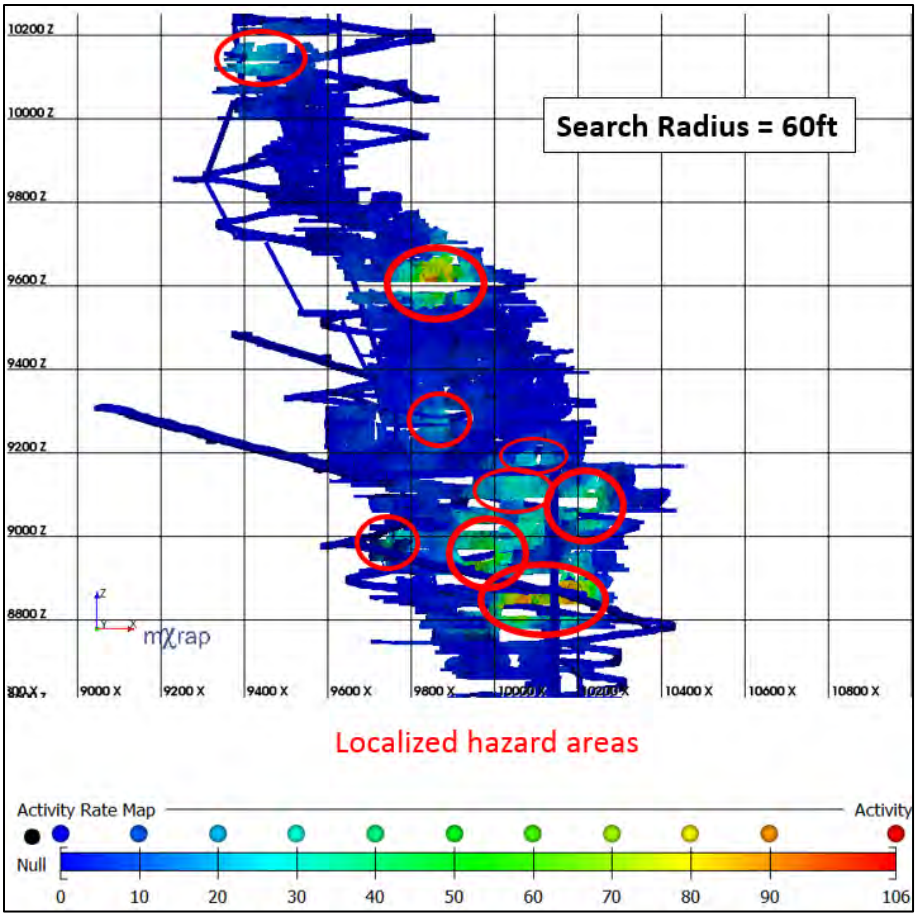

Figure 115 Activity Hazard Map using -1Mw as a Lower Bound; Section View looking North

Referring to Figure 115, using a 60ft search radius increases the size of the hazard areas. These areas, given their relative dimensions could be inclusive of a cluster of adjacent stopes rather than more localized zones as in figure. This is beneficial is determining seismic hazard moving forward in a retreat stope sequence as data is pulled from the surrounding stopes (provided they were mined in the trailing period) not just in the area on the sublevel itself but potentially on the level above and below. This is also pertinent data since Morrison Mine maintains a tighter sublevel spacing of 18m or 60ft.

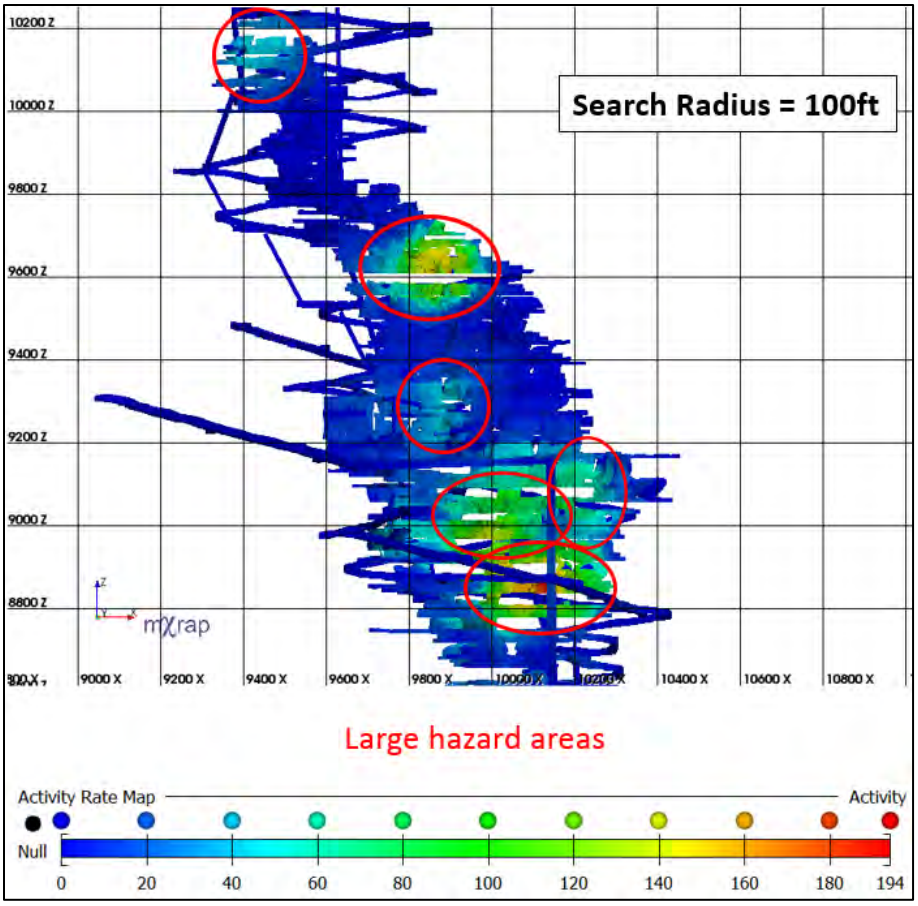

Figure 116 Activity Hazard Map using -1Mw as a Lower Bound; Section View looking North

A search radius of 100ft was used in the previous figure. What is evident is that the hazard areas become quite large, encompassing several sublevels. This large of a search radius may still be useful as it can pinpoint entire zones where the most seismicity above a certain size has occurred. However, in the interest of practicality to mine personnel, it becomes difficult to pinpoint specific hazard areas when entire sublevels are above threshold.

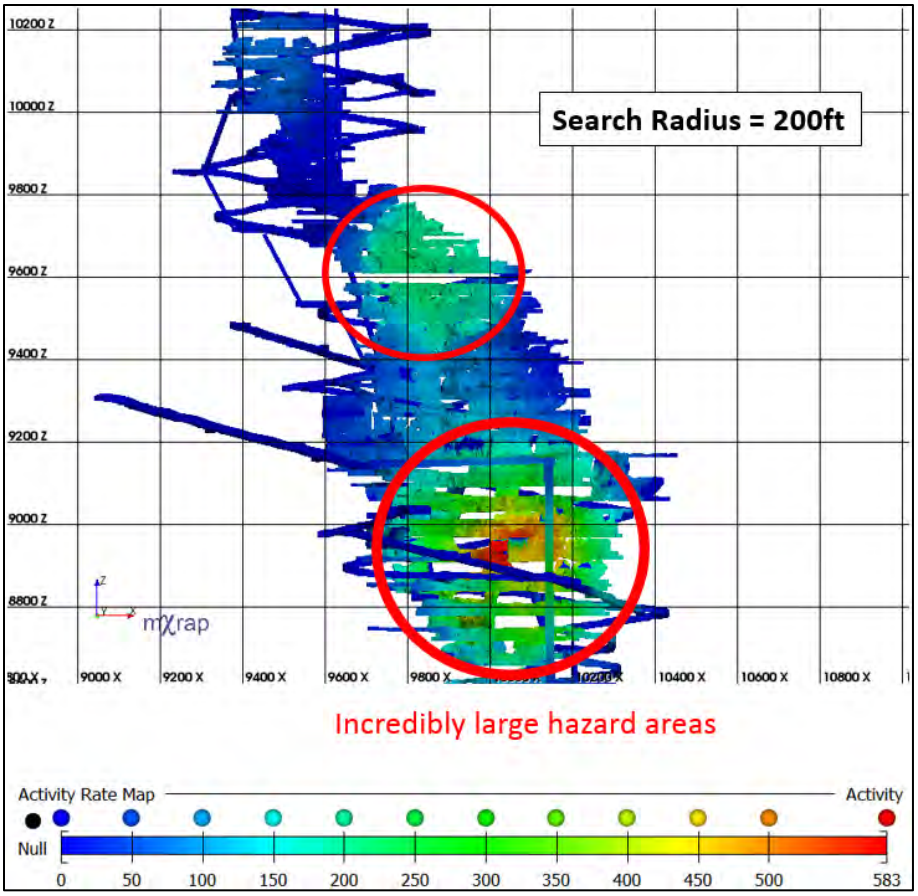

Figure 117 Activity Hazard Map using -1Mw as a Lower Bound; Section View looking North

Figure 116 was made using a search radius of 200ft. It is clear that the hazard areas are so large that it would be very difficult to pinpoint specific problem areas in the mine. Therefore, given the figures shown using a search radius of 30ft, 60ft, 100ft, and 200ft, the 60ft radius appears to be the most useful as it is not too localized that it misses important data but not to globular that it puts the entire mine on high-alert.

The following figures illustrate the impact that varying the search radius can have on seismic hazard forecasting in regards to future seismicity (see Figures 118, 119 and 120):

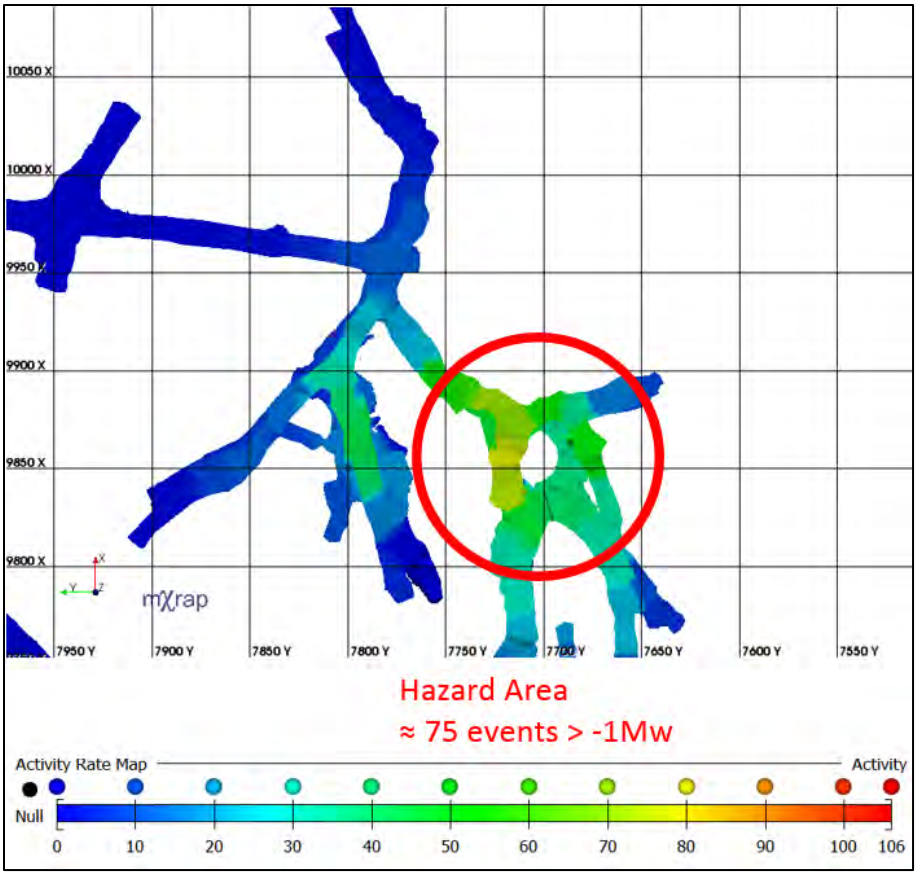

Figure 118 Activity Hazard Map using -1 Mw as a Lower Bound shown in Plan View for 3570 Level with Denoted Hazard Area using a 6month Trailing Period

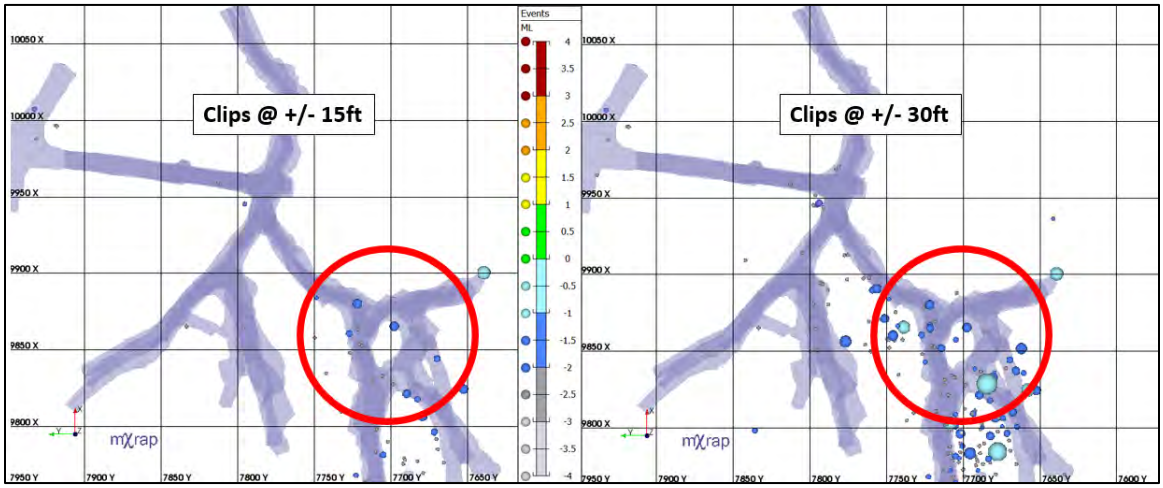

Figure 119 Plan view of seismic activity occurring in the 2month forecast period using both a 15ft and 30ft search radius

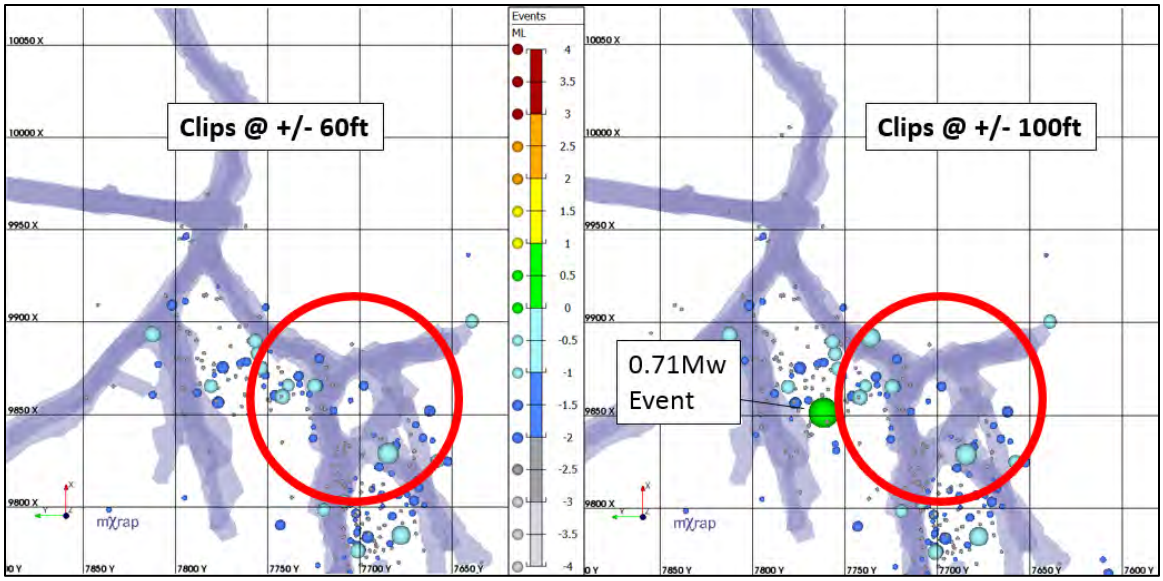

Figure 120 Plan view of Seismic Activity Occurring in the 2month Forecast Period using both a 60ft and 100ft Search Radius

What is apparent from the previous 2 figures is that varying the search radius can impact hazard forecasting by missing important large events. When the clips are set at +/- 100ft in the vertical direction, a large event is picked up at 0.71 M_w. Search radii less than 100ft would miss that event and thus the hazard forecast would not be accurate. It is for this reason that a search radius of 100ft is used in the forecast period.

5.2.6 Hazard Mapping in Relation to Fault-Slip Seismicity

In seismic data analysis, fault-slip seismic activity presents a unique challenge since these are larger and can occur at random times at distances far from the active mining area. This is because they often occur due to stress changes on a mine-wide or zone-wide scale (Gibowicz and Kijko, 1994).

As discussed previously, the hazard maps tested in this thesis are node-based meaning that a color scheme (cold to warm) is mapped onto a wireframe model of mine workings using a search radius around a node with X,Y,Z coordinates. This works well for using data from seismic events that occur close to mine workings. Although mine faults can be included as wireframe models, they have not been used as part of these hazard maps. This is mainly because they are interpretations and may not be entirely accurate whereas mine workings have been surveyed from known points. It stands to reason then that these

events may not be picked up by a hazard map meaning that there is not a hazard area corresponding to the location of a future event.

To assess the effectiveness of the hazard maps used in this thesis at forecasting fault-slip seismicity, all the events occurring in the three time periods that are suspected to be fault-slip have been analyzed based on whether or not they were included in the seismic hazard forecast from each of the hazard maps. The rationale for determining whether or not these events are fault-slip is listed below in order of importance:

1. If the event location is close to a known fault, i.e. within 100ft
2. If the event does not occur close to a blast in time, i.e. more than 12 hours after
3. If the S:P energy ratio is greater than 10

Using this rationale, 17 events have been identified over the period from April – October 2016. The following charts compare the events identified to the time from nearest blast and distance from nearest blast (see Figures 121 & 122):

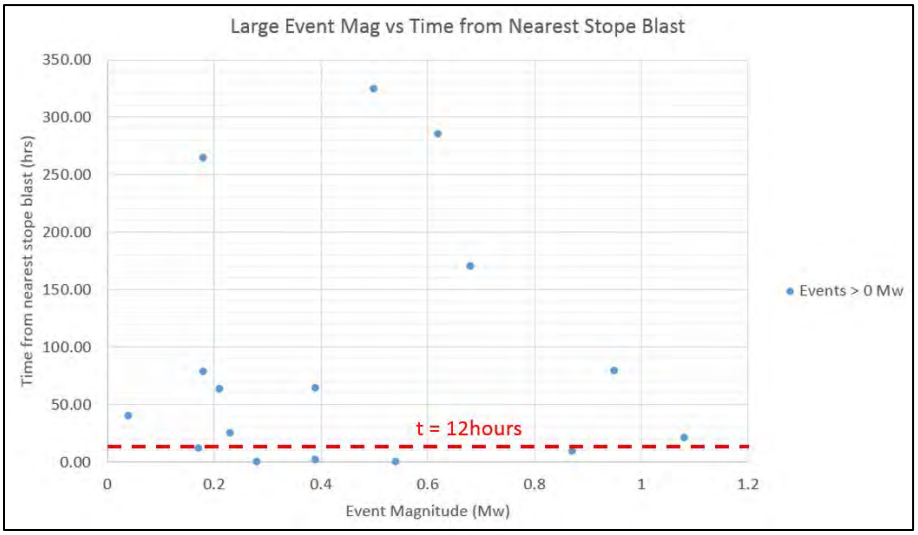

Figure 121 Time from Nearest Stope Blast vs Event Magnitude (Mw) of Fault-Related Events

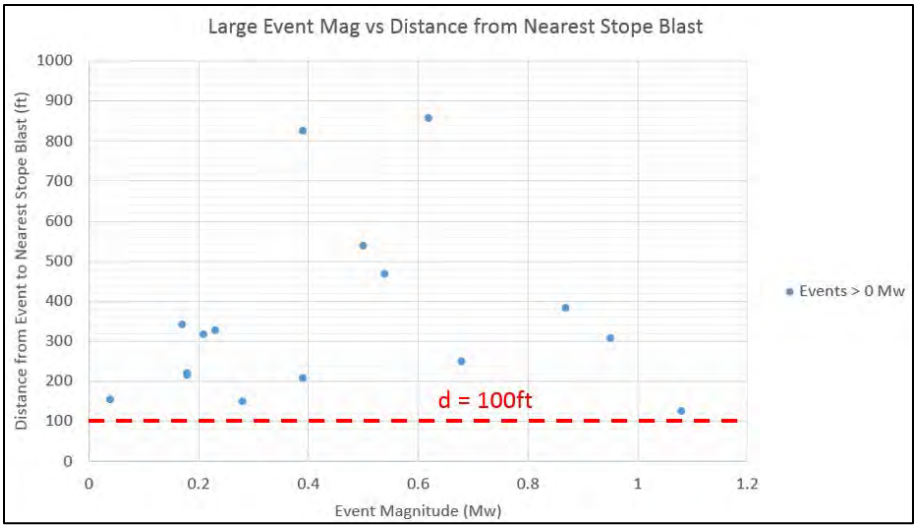

Figure 122 Distance from Nearest Stope Blast vs Event Magnitude (Mw) of Fault-Related Events

From the above charts, it is clear that most of the events occur more than 12 hours from a blast and at distances greater than 100ft. As well, 12 out of 17 events identified are located close to a mine fault and out of the 12 events, 8 occur more than 12 hours after a blast. It should also be noted that these 17 events were not forecasted by any of the hazard maps tested in this thesis. Given these results, unless events are occurring sufficiently close to mine workings, as in the case of some fault-slip events, they will not be accurately forecasted by node-based hazard maps.

5.3 Further Applications

5.3.1 Hazard Mapping as a Proxy for Blast Hazard Forecasting

When analyzing seismic data in a mining context, one would expect to be able to determine what is mining-induced and what is related to geometry and geological features. Since these hazard maps work off of a trailing period extending back in time in order to provide a hazard forecast, past mining-induced activity is included in the trailing data. Due to the way that Morrison Mine extracts stopes, along veins towards the central access point, if there is planned stoping in the forecast period, any past stoping in that area captured by the hazard map becomes part of the hazard forecast. Therefore, these hazard maps can be considered a stope forecasting tool to indicate how potentially 'bad' the seismic reaction to extraction will be.

It has been decided, for the purposes of this research, to quantify the statement that 'past seismicity is a good indicator of future seismicity'. To do this, the mining activity in the trailing period has been catalogued along with the mining activity that is planned in the forecast period. Using these two pieces of data, the mining influence on each hazard map can be determined. With each hazard map, all the successes that result from blasting in the forecast period subject to a hazard area defined by mining activity in the trailing period, are divided by the total number of successes. This is shown in the following equation:

$$Mining\ Influence\ (\%) = \frac{(N_{successes} | Past\ mining\ \propto Future\ Mining)}{N_{total\ successes}} \qquad (12)$$

The results are tabulated in the following table (see Figure 123):

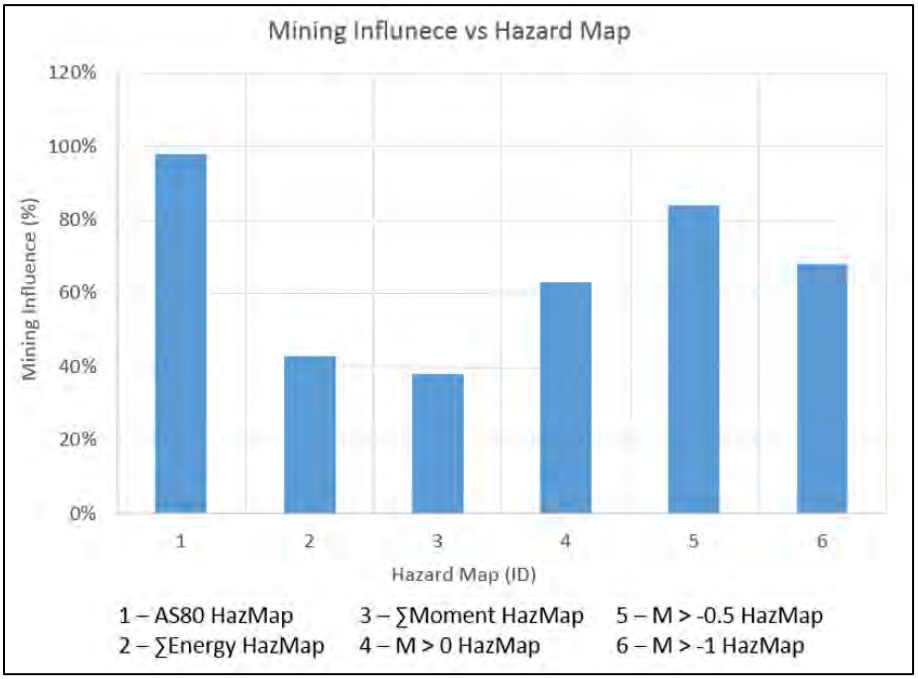

Figure 123 Mining Influence vs Hazard Map ID

Out of the 6 hazard maps, the event count above 80th percentile apparent stress map has the highest mining influence. This is likely due to the fact that large amounts of high apparent stress events occur after stopes blasts.

6 Thesis Summary

As stated previously, mining-induced seismicity has been and is becoming a pervasive issue in mines around the world. In this regard, the safety of personnel and longevity of mining operations is of high importance. Seismic hazard assessment is the means by which the likelihood of a large event occurring in space and time is estimated. Hazard can be either assessed probabilistically or empirically, the latter of which has been explored in this thesis through hazard mapping. Node-based hazard mapping techniques have been applied to a relatively deep, narrow-vein copper mine in Sudbury, Ontario. Hazard in this case is defined as whether or not an event above 0 moment-magnitude will occur in the near future. The structure of hazard assessment revolves around using a defined trailing period to provide a forecast of seismicity to a future time period.

6.1 Parametric Hazard Analysis Summary

For the hazard analysis carried out in this thesis, a series of seismic parameters were chosen and the rationale is outlined below:

Seismic Energy (E)

a) Independent seismic source parameter
b) Well correlated to moment magnitude (as $M_w \uparrow$ E ↑, generally)
c) Areas with high cumulative energy values are indicative of high stress conditions

Seismic Moment (M_o)

a) Independent seismic source parameter
b) Perfectly correlated with moment magnitude (as $M_w \uparrow$ Mo ↑)
c) Areas with high cumulative moment have experienced large amounts of deformation and are more likely to experience large seismic events

Moment Magnitude (M_w)

a) Dependent seismic source parameter
b) Well-known parameter describing the size of a seismic event
c) Practical and simple to use in hazard analysis

Apparent stress > 80th percentile (AS-80)

a) Dependent seismic source parameter
b) Values above the minewide 80th percentile are considered high apparent stress after Brown (2015)
c) Areas experiencing high apparent stress are indicative of increasing stress conditions in the local rock mass

6.2 Seismic Hazard Mapping Summary

In the interest of practical hazard analysis, seismic hazard mapping was chosen so that areas of the mine with elevated hazard can be easily identified. Two assessment techniques were tested which are summarized below:

1. Cumulative approach: Using seismic energy and seismic moment, the cumulative parametric values within a defined search radius, over a trailing period were mapped onto the solid model of mine workings. Essentially, areas with cumulative values above the defined threshold (see Section 4.3) will experience a large seismic event in the forecast period.
2. Counting approach: Using moment-magnitude and apparent stress above the mine-wide 80th percentile, the number (or counted value) of events based on each parameter were plotted as a hazard map onto a solid model of mine workings. Areas with counted values above the defined threshold will experience a large seismic event in the forecast period.

As discussed in Section 5.1.1, unlike the counting approach, the cumulative approach is susceptible to rogue events that have very high parametric values. As well, it has been shown in Section 5.2.1 that a weak scaling relationship exists between hazard value and forecasted seismic event magnitude; as hazard value ↑ M_w ↑, generally. This is more evident in events occurring above 1.0 M_w. With this in mind, these sizeable occurrences drive up the hazard value erroneously and would be indicative of a larger event occurring. This would create an overestimate of hazard and increase the false alarm rate. It is recommended, in using hazard maps for large event forecasting, that a counting approach be used as it is more robust than a cumulative approach.

6.2.1 Hazard Mapping Results

The hazard maps were evaluated using a trailing period of 6 months to provide a forecast for the following 2 months. The time periods used are summarized below:

1. April – June 2016 (Forecast Period) | October 2015 – April 2016 (Trailing Period)
2. June – August 2016 (Forecast Period) | December 2015 – June 2016 (Trailing Period)
3. August – October 2016 (Forecast Period) | February – August 2016 (Trailing Period)

Out of the 6 hazard maps tested, the one that yielded the best results in terms of success rate and accuracy was the cumulative moment map with an average success rate of 67% and a false alarm rate of 50%. Beyond that, the counted magnitude hazard map using -0.5 M_w as a lower bound was the most successful with an average success rate of 56% and an false alarm rate of 51%.

As discussed in Section 5.4, the hazard mapping methods outlined in this thesis do not give an indication of how large an expected event will be. To give an indication of the expected event size the results were compared to the magnitude hazard map where the maximum expected event size is found using an equation put forth by Kijko and Funk (1994). Correlations between this hazard map and the other ones developed in this thesis are, on average, between 50 and 70% with the M > -0.5 map having the highest correlation on average at 67%. Given these results, it is recommended that the Mmax determination be used to estimate the forecasted event size. This can be easily coupled with the M > -0.5 activity hazard map to give an indication of where the large event(s) may occur.

As discussed in Chapter 3 (Section 3.3) much of the seismicity at Morrison Mine is caused by blasting. There is also activity that likely a result of faulting due to the presence of major faults that crisscross the orebody. This seismic activity is very difficult to forecast, especially using node-based hazard maps since these fault-events occur far away from mine workings. Referring to Section 5.2.6, out of 17 identified fault-related

events, none of them were forecasted by any the hazard maps. Given these results, it is fair to assert that node-based hazard maps are not a reliable tool for forecasting fault-slip seismicity.

Finally, since the majority of seismicity at Morrison is driven by mining activity, these hazard maps can be used as a forecast for stope blasting as an indication of what seismicity could be expected from further mining. Of course this is predicated on the notion that future conditions will mimic current/past conditions. From analyzing each hazard map based on mining influence, or simply how many events were successfully forecasted in situations where past mining was proportional to future mining, it is evident that the AS-80 map provides the most consistently accurate results at 98% accurate.

6.3 Recommendations for Future work

It has been demonstrated, by this research that node-based hazard maps can be used as simple yet effective visual tools to determine which areas of the mine are experiencing and may experience dangerous levels of seismicity. This work should be treated as preliminary and further expansion upon the basic principles should be done. Suggestions for future work are listed below:

1. *Grid-based Hazard Maps*: While node-based hazard maps are limited to coordinates along mine workings, grid-based hazard maps are plotted based on a 3-dimensional grid. Areas experiencing seismicity away from workings can be seen using these maps. The rationale is that these types of maps could potentially be used to determine the seismic hazard for areas where workings may eventually be developed. It is recommended that the same hazard maps used in this thesis be applied using a grid-based approach.
2. *Same Hazard Maps, Different Mines*: These hazard maps have been tested at Morrison Mine only. The seismicity at the mine is mainly predicated on stope blasting with little-to-no, pure fault-slip seismicity. While the conditions at Morrison are relatively to other mines operating in Levack i.e. Vale's Coleman Mine and Glencore's Fraser Mine (formerly Strathcona Deep Copper), the nature of mining there is fairly unique; narrow-vein copper stringer mining. It is

recommended that these maps proposed in this thesis be tested at other mines in other jurisdictions that utilize different mining methods and mine different ores. This would serve as a test of this hazard mapping technique's overall applicability to Canadian underground hard-rock mines.

3. *Activity Hazard Map Optimization*: The purpose of using hazard maps in the context of this thesis was to show that they can be used to forecast future seismicity in terms of large events. A broad-brush approach was taken using 6 different hazard maps over the same time periods to compare each. Out of the maps used, the activity maps using a magnitude lower bound, and apparent stress over the mine-wide 80^{th} percentile, are simplest to understand and use. It is recommended that an optimization study be done on one of these activity maps. This would include determining an optimal search radius coupled with a trailing period and forecast period.

7 References

1. Abel, M.K. (1980). *The Structure of the Strathcona Mine Copper Zone*. CIM Bulletin 826(74), pp. 89-97
2. Alcott, J. (1998). *Rockburst Hazard Assessment: Integration of Micro-seismic Data into Ground Control Decision Making Process*. M.A.Sc. Laurentian University.
3. Boatwright, J., Fletcher, J.B. (1984). *The Partition of Radiated Energy between P and S Waves*. Bulletin of the Seismological Society of America 74(2), pp. 61-376
4. Brady, B.H.G., Brown, E.T. (2004). *Rock Mechanics for Underground Mining*. Dordrecht: Kluwer Academic Publishers
5. Brown, L.G. (2015). *Seismic Hazard Evaluation Using Apparent Stress Ratio for Mining-Induced Seismic Events*. M.A.Sc. Laurentian University. 160p.
6. Cook, N.G.W. (1976). *Seismicity Associated with Mining*. In: Engineering Geology, 10(2-4), pp. 99-122
7. ESG Solutions. (2017). *Mining*. [online] Available at: https://www.esgsolutions.com/mining-and-geotechnical/mining [Accessed 09-May-17]
8. FNX Mining Company Inc. (2009). *Technical Report on Mineral Properties in the Sudbury Basin*. Toronto: FNX Mining Company, pp.40-41
9. Gibowicz, S., Kijko, A. (1994). *Introduction to Mine Seismology*. San Diego: Academic Press
10. Gutenberg, B., Richter, C.F. (1944). *Frequency of Earthquakes in California*. Bulletin of the Seismological Society of America 34(4), pp. 185-188
11. Hanks, T.C., Kanamori, H. (1979). *A Moment Magnitude Scale*.
12. Harris, PH, Wesseloo, J (2015). mxrap software, version 5, Australian Centre for Geomechanics, The University of Western Australia, Perth, Western Australia, http://mxrap.com/
13. Heal, D., Mikula, P., Hudyma, M. (2008). *Generic Seismic Risk Management Plan for Underground Hard Rock Mines*. Broadway Nedlands: Australian Centre for Geomechanics
14. Hedley, D.G.F. (1992). *Rockburst Handbook for Ontario Hardrock Mines*. CANMET
15. Hoek, E., Brown E. (1980). *Underground Excavations in Rock*. London: Institution of Mining and Metallurgy
16. Hudyma, M. (2008). *Analysis and Interpretation of Clusters of Seismic Events in Mines*. Ph.D Thesis. University of Western Australia
17. Hudyma, M. (2010). *Applied Mine Seismology Concepts and Techniques*. Sudbury: Laurentian University
18. Hudyma, M. (2014). *Mine Seismic Systems*, ENGR 5336 Course Notes, Laurentian University

19. Hudyma, M. (2004). *Mining-Induced Seismicity in Underground, Mechanised, Hardrock Mines – Results of a World Wide Survey*. Australian Centre for Geomechanics
20. Hudyma, M. (1995). *Seismicity at Brunswick Mining*. In: Quebec Mining Association Ground Control Colloque Val d'Or: Quebec Mining Association
21. Hudyma, M. (2016). *Sudbury Regional Seismic Network – Quick User's Guide*. Laurentian University.
22. International Union of Pure and Applied Chemists (IUPAC). (2001). *Threshold limit value (TLV)*. [online] IUPAC Gold Book. Available at: https://goldbook.iupac.org/html/T/TT06915.html [accessed 29-mar-17]
23. Kijko, A., Funk, C.W. (1994). *The Assessment of Seismic Hazard in Mines*. The Journal of the South African Institute of Mining and Metallurgy, 94(7), pp. 179-185
24. Marshall, B. (2015). *Facts and Figures of the Canadian Mining Industry F&F 2015*. The Mining Association of Canada. Available at: http://mining.ca [accessed 17-Oct-2017]
25. Mendecki, A. (2013). *Mine Seismology – Glossary of Selected Terms*. In: The 8th Rockbursts and Seismicity in Mines Symposium Moscow: GS-RAS
26. Mendecki, A. (2016). *Mine Seismology Reference Book – Seismic Hazard.* Institute of Mine Seismology
27. Mendecki, A. (1993). *Real time quantitative seismology in mines*. In: 3rd International Symposium on Rockbursts and Seismicity in Mines. Rotterdam: Balkema, pp. 284-295.
28. Mendecki, A., Brink, A.van Z., Green, R.W.E., Mountfort, P., Dzhafarov, A., Niewiadomski, J., Kijko, A., Sciociatti, M., Radu, S., van Aswegen, G., Hewlett, P., de Kock, E., Stankiewicz, T. (1996). *Seismology for Rockbursts Prevention, Control, and Prediction.* GAP-017 Project Report, ISS International, pp. 3-9
29. Mendecki, A., Lötter, E. (2011). *Modelling Seismic Hazard for Mines*. In: Australian Earthquake Engineering Society Conference 2011. Barossa Valley:
30. Mendecki, A., Lynch, R., Malovichko, D. (2010). *Routine Micro-Seismic Monitoring in Mines*. In: AEES 2010 Conference Perth: Australian Earthquake Engineering
31. Michigan Technological University (MTU). (2007). *UPSeis - What is Seismology*? [online] Available at: http://www.geo.mtu.edu/UPSeis/waves.html [Accessed 13-Nov-16]
32. Milner, N., Larose, M., Switzer, D., Watson, J. (2013). *Application of Numerical Modelling to predict Seismic Probability and Mitigate Associated Risks during the Craig Pillar Extraction at Morrison Mine*, KGHM International [PowerPoint Slides]. Proceedings from the Vancouver 2014 Conference, Vancouver BC.
33. Morrison, R.K.G. (1970). *A Philosophy of Ground Control*. Toronto: Ontario Department of Mines

34. Morissette, P. (2015). *A Ground Support Strategy for Deep Underground Mines Subjected to Dynamic Loading Conditions*. Ph.D Thesis. University of Toronto.
35. Ortlepp, W.D. (1992). *The Design of Support for the Containment of Rockburst Damage in Tunnels.* In: Rock Support and Underground Construction, Rotterdam: Balkema, pp. 593-609
36. QuadraFNX Mining Ltd. (2011). *Analyst and Investor Tour – November 2011*. [PowerPoint] [Accessed 19-Apr-2017]
37. Reichl, C., Schatz, M., Zsak, G. (2017). *World Mining Data*. [online] Vienna: The Organizing Committee for the World Mining Congress. Available at: http://www.wmc.org.pl [Accessed 17-Oct-2017]
38. Rebuli, D., Goldswain, G., Lynch, R. (2016). *High Quality Microseismic Monitoring in Mines: Accelerometers or Geophones?* In: CIM MEMO 2016 Sudbury: Institute of Mine Seismology
39. Richter, C.F. (1935). *An Instrumental Earthquake Magnitude Scale*. Bulletin of the Seismological Society of America, 25(1-2), pp. 1-32
40. Richter, C.F. (1958). *Elementary Seismology*. San Francisco: W.H. Freeman & Co
41. Rousell, D.H. (1983). *Nature and Origin of Mineralization inside the Sudbury Basin*. Ontario Geologic Survey Open File Report 5443.
42. Simser, B., Falmagne, V., Gaudreau D., MacDonald, T. (2003). *Seismic Response to Mining at the Brunswick No. 12 Mine*. In: Canadian Institute of Mining and Metallurgy Annual General Meeting. Montreal: CIM
43. Smith, D.A., Bailey, J.M., Pattison, E.F. (2013). *Discovery of New Offset Dykes and Insights into the Sudbury Impact Structure*. In: Large Meteorite Impacts and Planetary Evolution V. Sudbury: USRA
44. Suorineni, F.T., Malek, F. (2014). *The Sudbury Basin stress tensor – myth or reality?* In: Deep Mining 2014 Sudbury: Australian Centre for Geomechanics
45. Taghipoor, S., Watson, J., Laing, D. (2016). *Numerical Investigation of Rockbursts at Morrison Mine*. [PowerPoint Slides]. In: 2016 Workplace Safety North Conference, Sudbury ON.
46. Taghipoor, S. (2013). *Microseismic Monitoring – Morrison Deposit*. [Internal Report] Sudbury: KGHM International, p.11.
47. Urbancic, T.I., Young, R.P., Bird, S., and Bawden, W. (1992). *Microseismic Source Parameters and their use in Characterizing Rock Mass Behaviour: Considerations from Strathcona Mine*. In: 94th Annual General Meeting of the CIM: Rock Mechanics and Strata Control Sessions, pp. 36-47
48. Van Aswegen, G. (2005). *Routine Seismic Hazard Assessment in some South African Mines*. In: The Sixth International Symposium on R ockburst and Seismicity in Mines. Perth: Australian Centre for Geomechanics, pp.437-444.
49. Wesseloo, J., Potvin, Y. (2012). *Advancing the Strategic Use of Seismic Data in Mines*. Perth: MERIWA, pp. 69-73

50. Wesseloo, J., Woodward, K., and Pereira, J. (2014). *Grid-based Analysis of Seismic Data*. The Journal of the South African Institute of Mining and Metallurgy, 114(10), pp. 815-821

51. Young, D. (2012). *Energy Variations in Mining-Induced Seismic Events using Apparent Stress*. M.A.Sc. Laurentian University

Appendix A: Hazard Map Threshold Calibrations

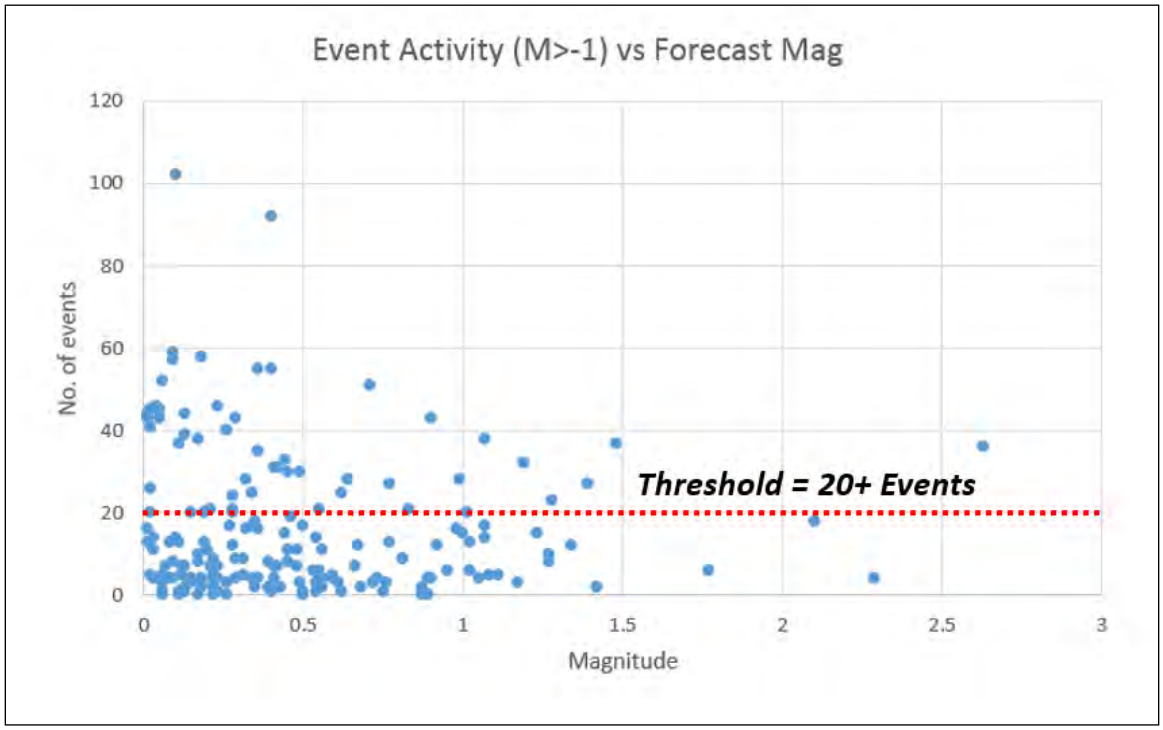

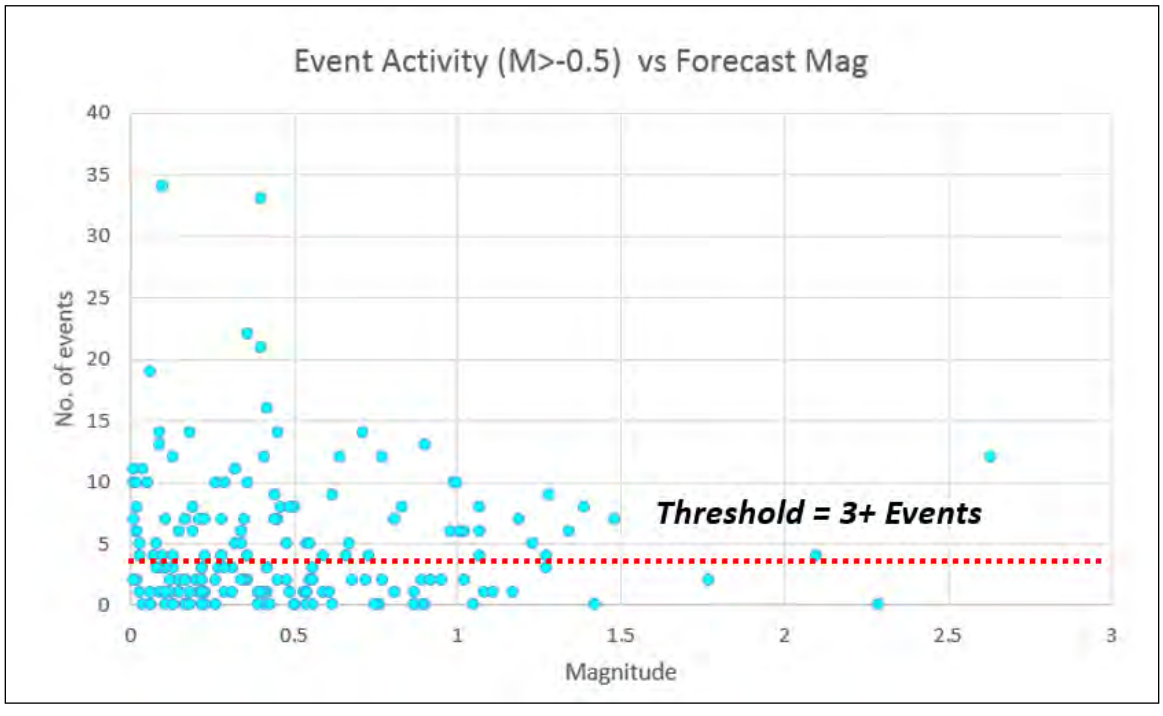

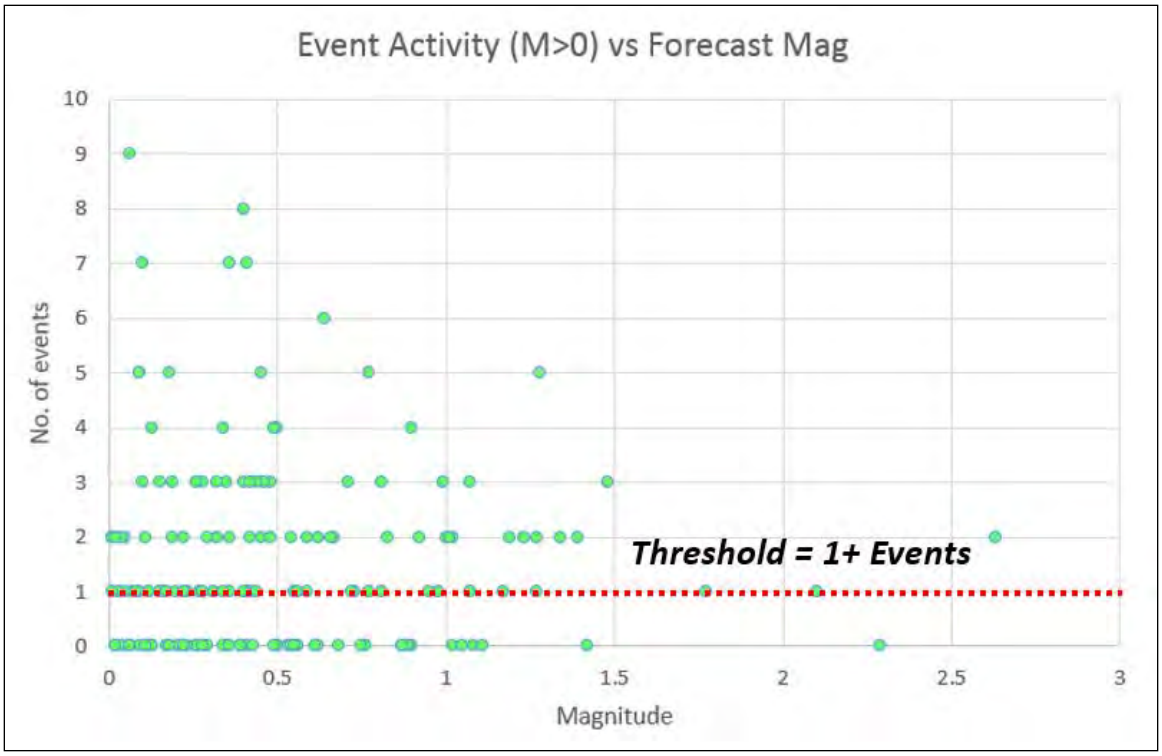
Event Activity (M>0) vs Forecast Mag
No. of events
Magnitude
Threshold = 1+ Events
0
1
2
3
4
5
6
7
8
9
10
0
0.5
1
1.5
2
2.5
3

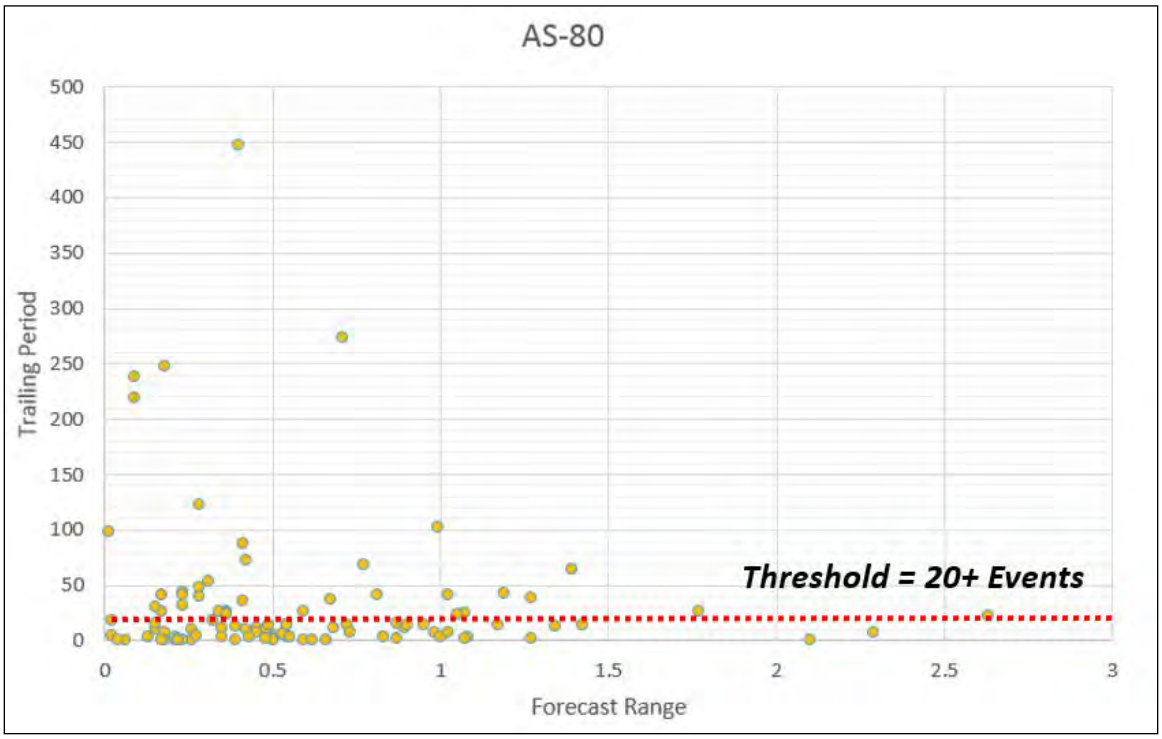
AS-80
Trailing Period
Forecast Range
Threshold = 20+ Events
0
50
100
150
200
250
300
350
400
450
500
0
0.5
1
1.5
2
2.5
3

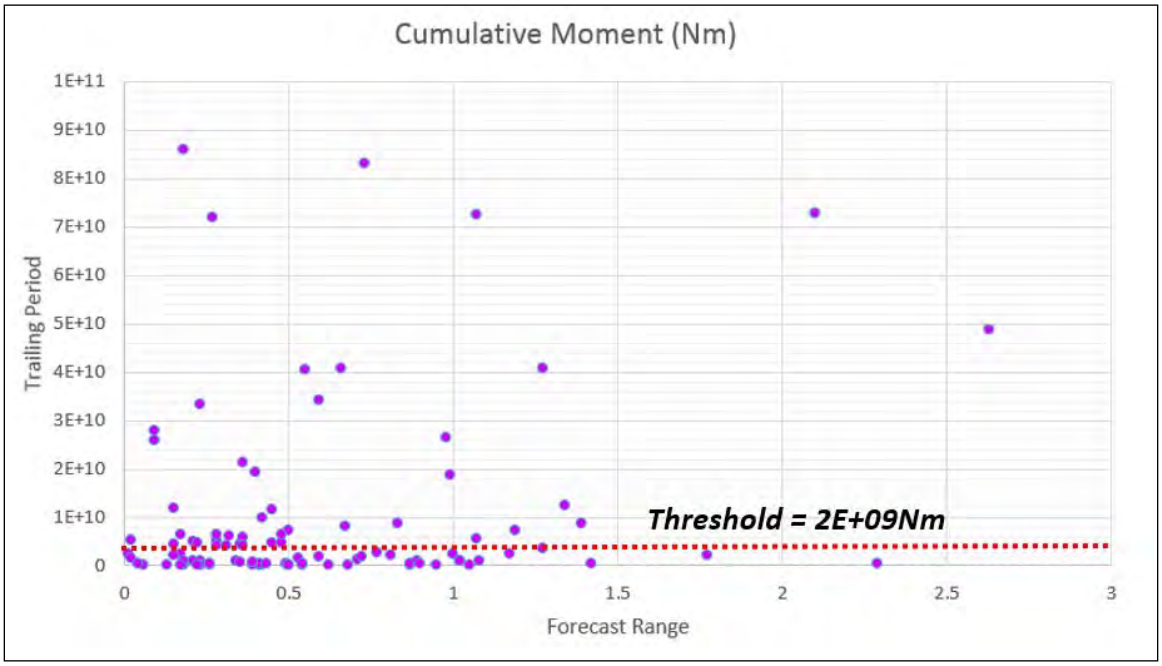
Cumulative Moment (Nm)
1E+11
9E+10
8E+10
7E+10
6E+10
5E+10
4E+10
3E+10
2E+10
1E+10
0
Trailing Period
0
0.5
1
1.5
2
2.5
3
Forecast Range
Threshold = 2E+09Nm

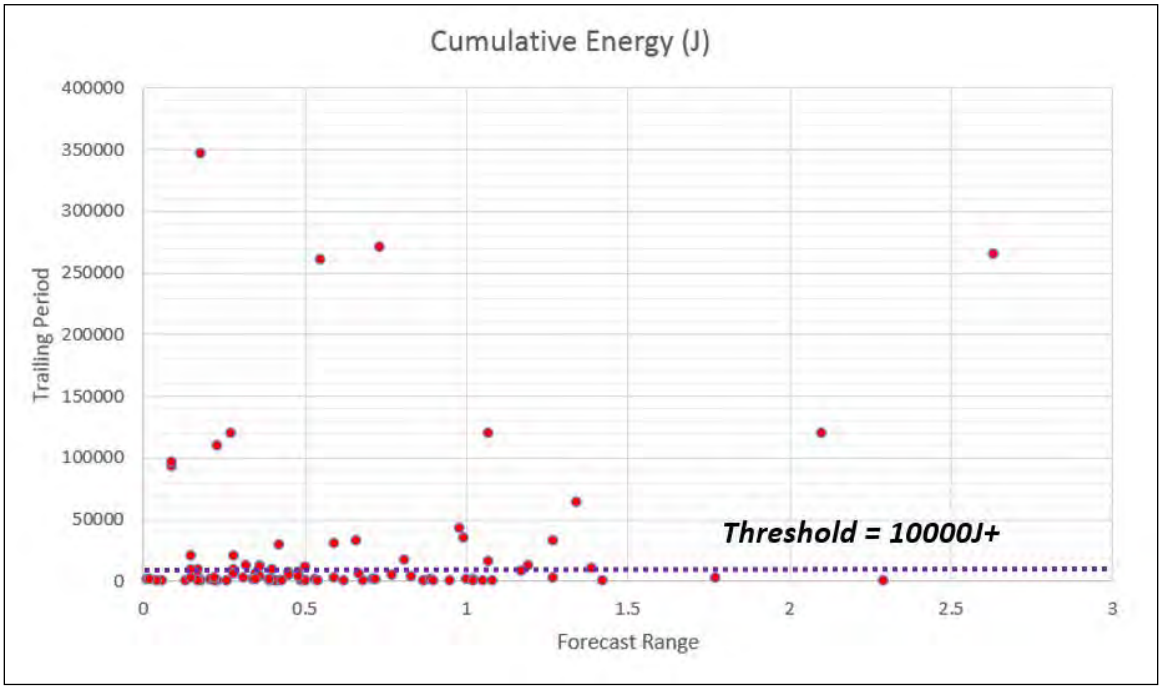
Cumulative Energy (J)
400000
350000
300000
250000
200000
150000
100000
50000
0
Trailing Period
0
0.5
1
1.5
2
2.5
3
Forecast Range
Threshold = 10000J+

Appendix B: Hazard Map Scorecards and Associated Figures (April – June 2016)

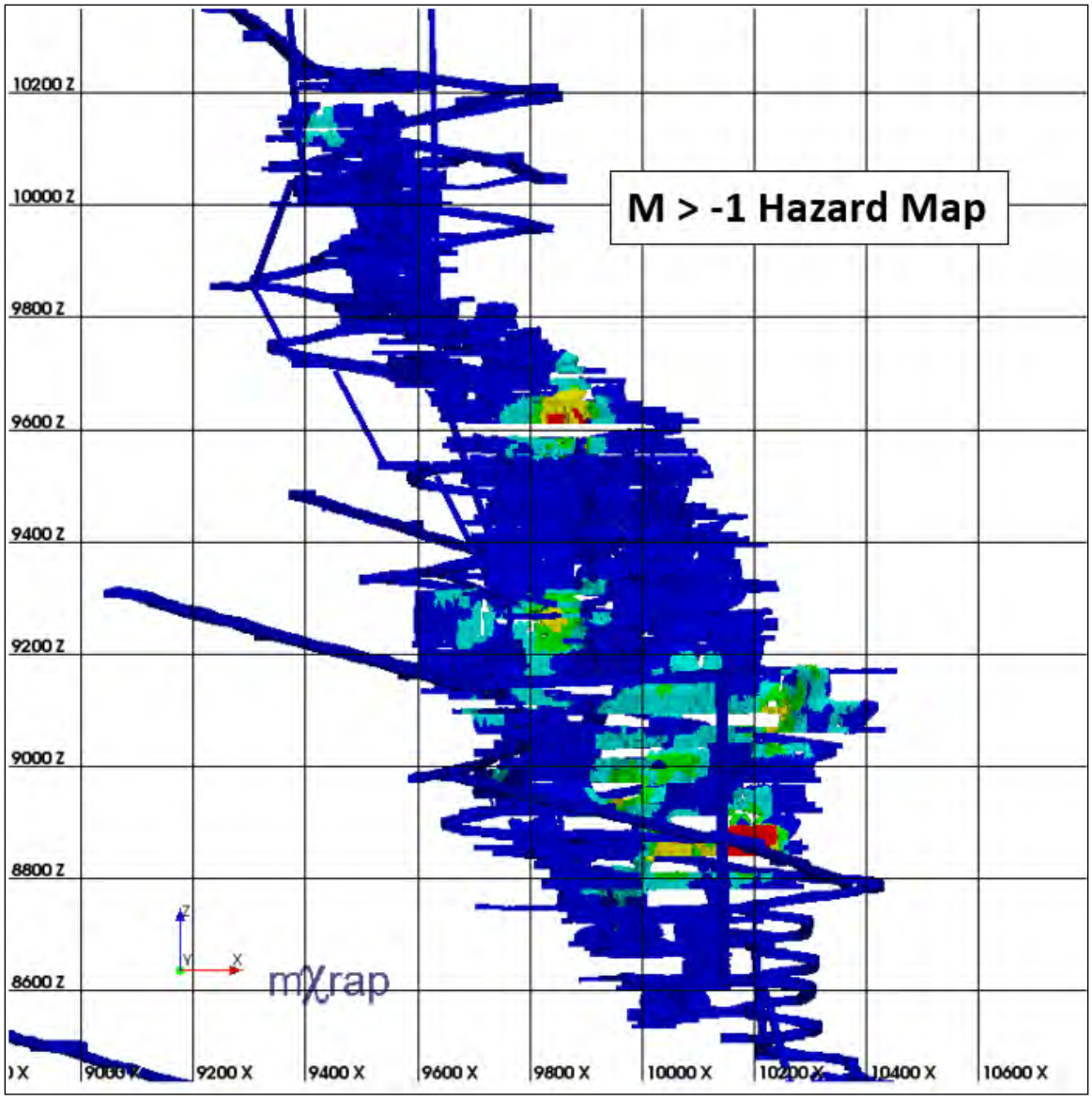

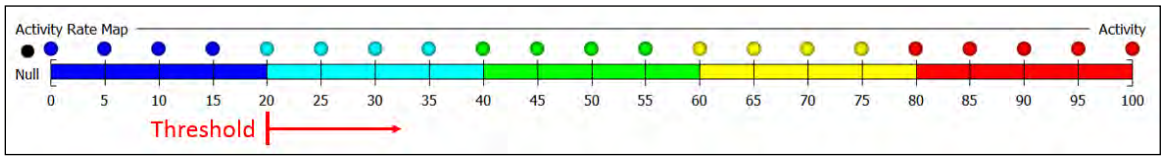

Level	Hazard Map Results		Area Accessible?	Past Activity	Planned activity	Forecast Period		
	Location	Number of events				Date/Time	Location	Mag
2950/3030	X-West	20	No	3050 XYZ1 + X2 Stopes	None			
3450/3510/3570	Z-East/A/DBZ Central	70	Yes	3690 A4 Stope	None			
3810	c1 BP Loop	20	Yes	3870/3920 BDE & 4030 B1 Stopes	None	22/05/2016 16:54	B-West Terminus	1.02
3870/3920	B-West Shrink	20	No	3870/3920 BDE & 4030 B1 Stopes	None	21/05/2016 2:36	B-West Shrink Stope (FW)	0.35
	B-West near Main acc.	55	No	3870/3920 BDE & 4030 B1 Stopes	3870 B1 + DE1 & 3810-6 BFG Stopes	09/05/2016 7:29	near main access	0.23
3970	H-Vein TDBs main acc.	40	Yes	4090 F2 & 4150 F6 Stopes	3970 H c2 dev			
3970/4030	F-East	30	Yes	4030 T3 + EF1 & 4150 F6 Stopes	4030 EF2 + EF3/EF4 Stopes			
	BCD 4030 acc.	30	yes	4030 T3 + EF1 & 4090 D1 + D2 Stopes	4030 EF2 + EF3/EF4 Stopes	13/04/2016 8:29	cut3 D-West	1
4030/4090	F/H	60	Yes	4090 F2 & 4150 F6 Stopes	None	25/05/2016 3:19	H-Vein Abutment	0.01
4090/4150	D-West abt.	20	yes	4150 c4 D-west dev.	None	06/04/2016 14:17	4210 CCF Stope (HW)	0.77
	F/D/E	30	Yes	4150 F6 Stope	None	16/05/2016 20:04	cut3 F-West near D-SW	0.02
	F-East/D	50	Yes	4150 F6 & 4210 F1 Stopes	None	16/05/2016 13:42	cut3 D-West	1.19
	F/B	20	Yes	4150 F6 & 4210 D1 + D2 + F1 Stopes	None	21/04/2016 15:38	cut2 F-East near B-West	0.28
4210/4280	H-North	126	Yes	4280 H2 + F3 Stopes	None	21/05/2016 20:38	H-North LH (FW)	0.4
4280/4340	F/H	70	Yes	4280 H2 + F3 Stopes	None	22/04/2016 11:34	H-North (HW)	0.99
						25/05/2016 2:27	cut1 H-North (FW)	1.07
4340	Main acc./F-Vein	20	Yes	4280 H2 + F3 Stopes	None			
4340/4400/4460	G-North	40	No	4400 F2 & 4460 G2 Stopes	None			
4460	F-Vein acc./Main TDBs	20	No	4400 F2 & 4460 G2 Stopes	None			

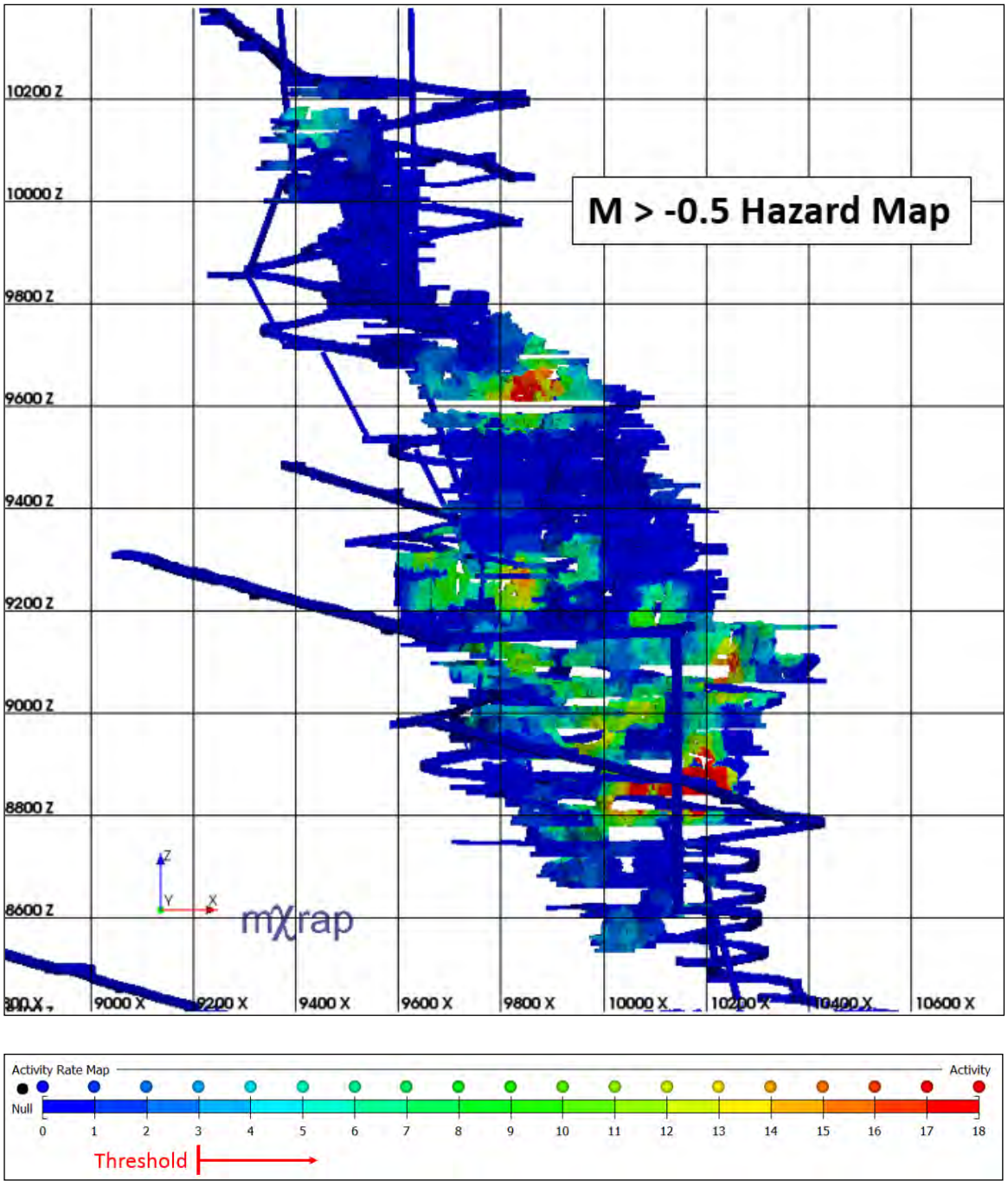
M > -0.5 Hazard Map
10200 Z
10000 Z
9800 Z
9600 Z
9400 Z
9200 Z
9000 Z
8800 Z
8600 Z
9000 X
9200 X
9400 X
9600 X
9800 X
10000 X
10200 X
10400 X
10600 X
Z
Y
X
mXrap

Activity Rate Map
Activity
Null
0
1
2
3
4
5
6
7
8
9
10
11
12
13
14
15
16
17
18
Threshold

Level	Hazard Map Results		Area Accessible?	Past Activity	Planned activity	Forecast Period		
	Location	Number of events				Date/Time	Location	Mag
2950/3030	X-West	3	No	3050 XYZ1 + X2 Stopes	None			
3450/3510	Main TDBs	20	No	3690 A4 Stope	None			
3510/3570	DBZ (Central)	10	Yes	3690 A4 Stope	None			
	Z-West/Z1	3	Yes	3690 A4 Stope	None			
3810	c6 AB acc.	8	Yes	3870/3920 BDE & 4030 B1 Stopes	None	22/05/2016 16:54	B-West Terminus	1.02
3810/3870	c1 BP loop/B-West Shrink	8	No	3870/3920 BDE & 4030 B1 Stopes	None	21/05/2016 2:36	B-West Shrink Stope (FW)	0.35
	G-North	3	Yes	3870/3920 BDE & 4030 B1 Stopes	None	23/05/2016 11:32	G-North Terminus	0.26
						21/05/2016 3:17	G-North Terminus	0.54
3870/3920	Main acc./B-West	12	No	3870/3920 BDE & 4030 B1 Stopes	None	09/05/2016 7:29	near main access	0.23
	BFE (Central-Right)	8	Yes	3870/3920 BDE & 4030 B1 Stopes	3870 B1 + DE1 & 3810-6 BFG Stopes			
3970/4030	F-East LHs	8	Yes	4030 T3 + EF1 & 4150 F6 Stopes	4030 EF2 + EF3/EF4 Stopes	12/04/2016 12:24	F-East LH (HW)	0.5
3970	H-Vein TDBs/H-North	8	Yes	4090 F2 & 4150 F6 Stopes	3970 H c2 dev			
3970/4030	C-South	10	Yes	4030 B1 Stope	None			
3970/4030/4090	F/H-South	12	Yes	4090 F2 & 4150 F6 Stopes	3970 H c2 dev	25/05/2016 3:19	H-Vein Abutment	0.01
4030/4090	BCD near main acc.	10	Yes	4030 c4 TDBs + B1 Stope	4030 EF2 + EF3/EF4 Stopes	13/04/2016 8:29	cut3 D-West	1
	F/D	8	Yes	4030 B1 & 4090 D1 + D2 Stopes	4030 EF2 + EF3/EF4 Stopes			
4090/4150	F-East + H	8	Yes	4090 F2 & 4150 F6 Stopes	None			
4150	D-West	3	Yes	4210 D1 + D2 Stopes	None	28/05/2016 4:00	cut4 D-Southwest	0.98

Level	Hazard Map Results		Area Accessible?	Past Activity	Planned activity	Forecast Period		
	Location	Number of events				Date/Time	Location	Mag
4150/4210	F/D	16	Yes	4150 F6 & 4210 D1 +D2 + F1 Stopes	None	16/05/2016 20:04	cut3 F-West near D-SW	0.02
						16/05/2016 13:42	cut3 D-West	1.19
	F/B	8	Yes	4150 F6 & 4210 D1 +D2 + F1 Stopes	None	21/04/2016 15:38	cut2 F-East near B-West	0.28
4210/4280	H-North	45	Yes	4280 H2 + F3 Stopes	None	21/05/2016 20:38	H-North LH (FW)	0.4
4280/4340	F/H	18	Yes	4280 H2 + F3 Stopes	None	22/04/2016 11:34	H-North (HW)	0.99
						25/05/2016 2:27	cut1 H-North (FW)	1.07
4340/4400/4460	G-North	18	No	4400 F2 & 4460 G2 Stopes	None			
4400/4460	F-Vein near acc.	3	No	4400 F2 Stope	None			
4520	I-North abt./Level acc.	3	Yes	4580 HI + G1 Stopes	None			
	Main TDBs	3	Yes	4580 HI + G1 Stopes	None			
4580	GHI	3	Yes	4580 HI + G1 Stopes	None			

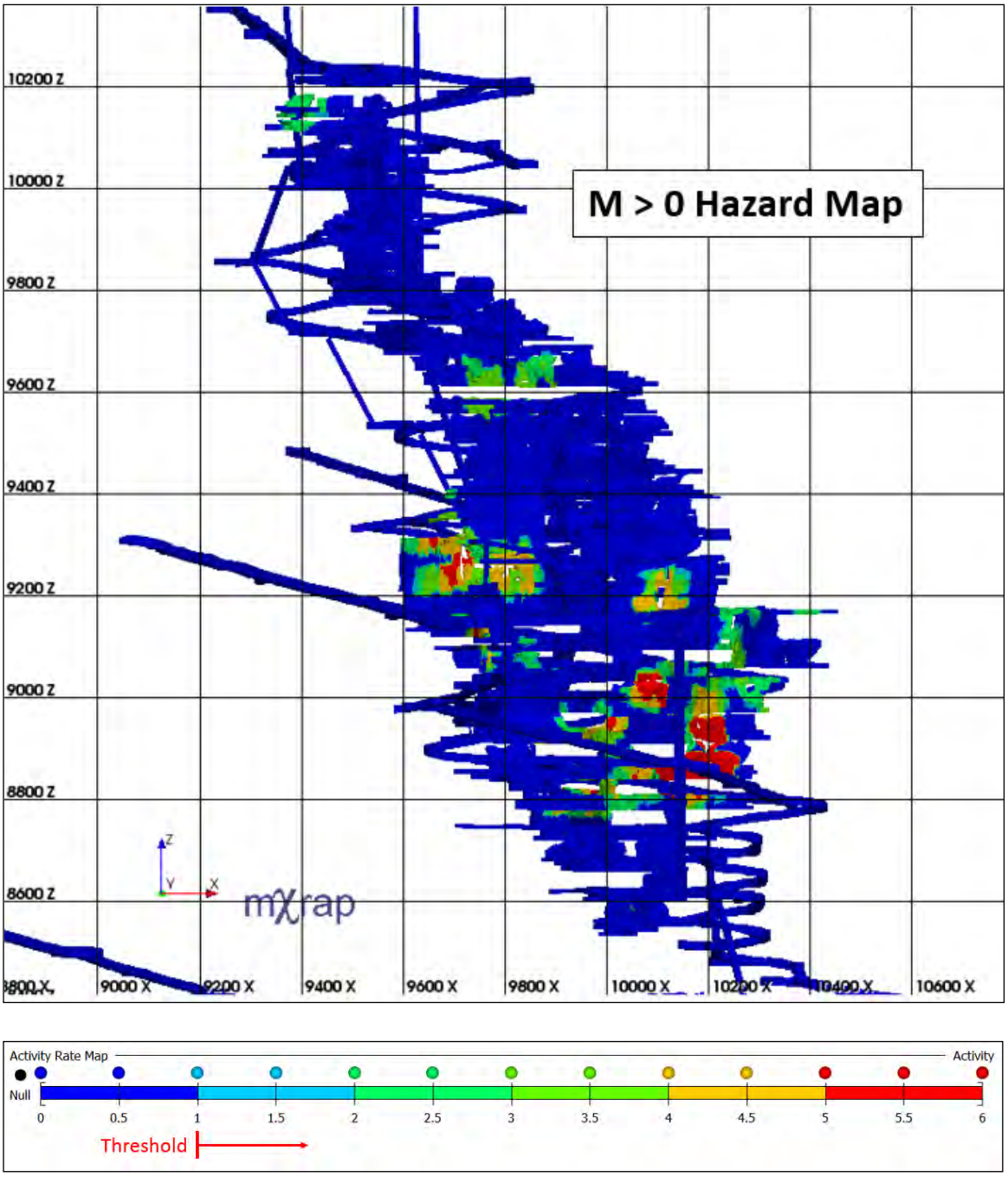
M > 0 Hazard Map
10200 Z
10000 Z
9800 Z
9600 Z
9400 Z
9200 Z
9000 Z
8800 Z
8600 Z
9000 X
9200 X
9400 X
9600 X
9800 X
10000 X
10200 X
10400 X
10600 X
Z
Y
X
mXrap

Activity Rate Map
Activity
Null
0
0.5
1
1.5
2
2.5
3
3.5
4
4.5
5
5.5
6
Threshold

Level	Hazard Map Results		Area Accessible?	Past Activity	Planned activity	Forecast Period		
	Location	Number of events				Date/Time	Location	Mag
3510	Main TDBs	4	Yes	3690 A4 Stope	None			
3510/3570	Z-West/Z1	2	Yes	3690 A4 Stope	None			
3810	c6 AB acc.	2	Yes	3870/3920 BDE & 4030 B1 Stopes	None	22/05/2016 16:54	B-West Terminus	1.02
3810/3870	c1 BP loop/B-West Shrink	5	No	3870/3920 BDE & 4030 B1 Stopes	None	21/05/2016 2:36	B-West Shrink Stope (FW)	0.35
3870/3920	B-West	5	Yes	3870/3920 BDE & 4030 B1 Stopes	None	09/05/2016 7:29	near main access	0.23
3970	F-East LHs	5	No	4030 T3 + EF1 & 4150 F6 Stopes	4030 EF2 + EF3/EF4 Stopes	12/04/2016 12:24	F-East LH (HW)	0.5
4030	C-South	5	Yes	4030 B1 Stope	None			
4090	D-West abt.	5	No	4090 D1 + D2 & 4030 B1 Stopes	None			
4090/4150	F/H	2	No	4090 F2 Stope	None	25/05/2016 3:19	H-Vein Abutment	0.01
	Main acc./FH	5	Yes	4090 F2 & 4150 F6 Stopes	None			
4210	F/D	5	Yes	4210 D1 + D2 + F1 & 4150 F6 Stopes	None	16/05/2016 13:42	cut3 D-West	1.19
	F/B	5	Yes	4210 D1 + D2 + F1 & 4150 F6 Stopes	None	21/04/2016 15:38	cut2 F-East near B-West	0.28
4210/4280	H-North	8	Yes	4280 H2 + F3 Stopes	None	21/05/2016 20:38	H-North LH (FW)	0.4
4280	F/H	7	Yes	4280 H2 + F3 Stopes	None	22/04/2016 11:34	H-North (HW)	0.99
						25/05/2016 2:27	cut1 H-North (FW)	1.07
4340	Main acc./F-Vein	5	Yes	4280 H2 + F3 Stopes	None			
	G-North/FNW	9	No	4400 F2 & 4210 F1 Stopes	None			
	H-North	5	No	4280 H2 + F3 Stopes	None			
4400/4460	G-North near acc.	7	Yes	4400 F2 Stope	None			

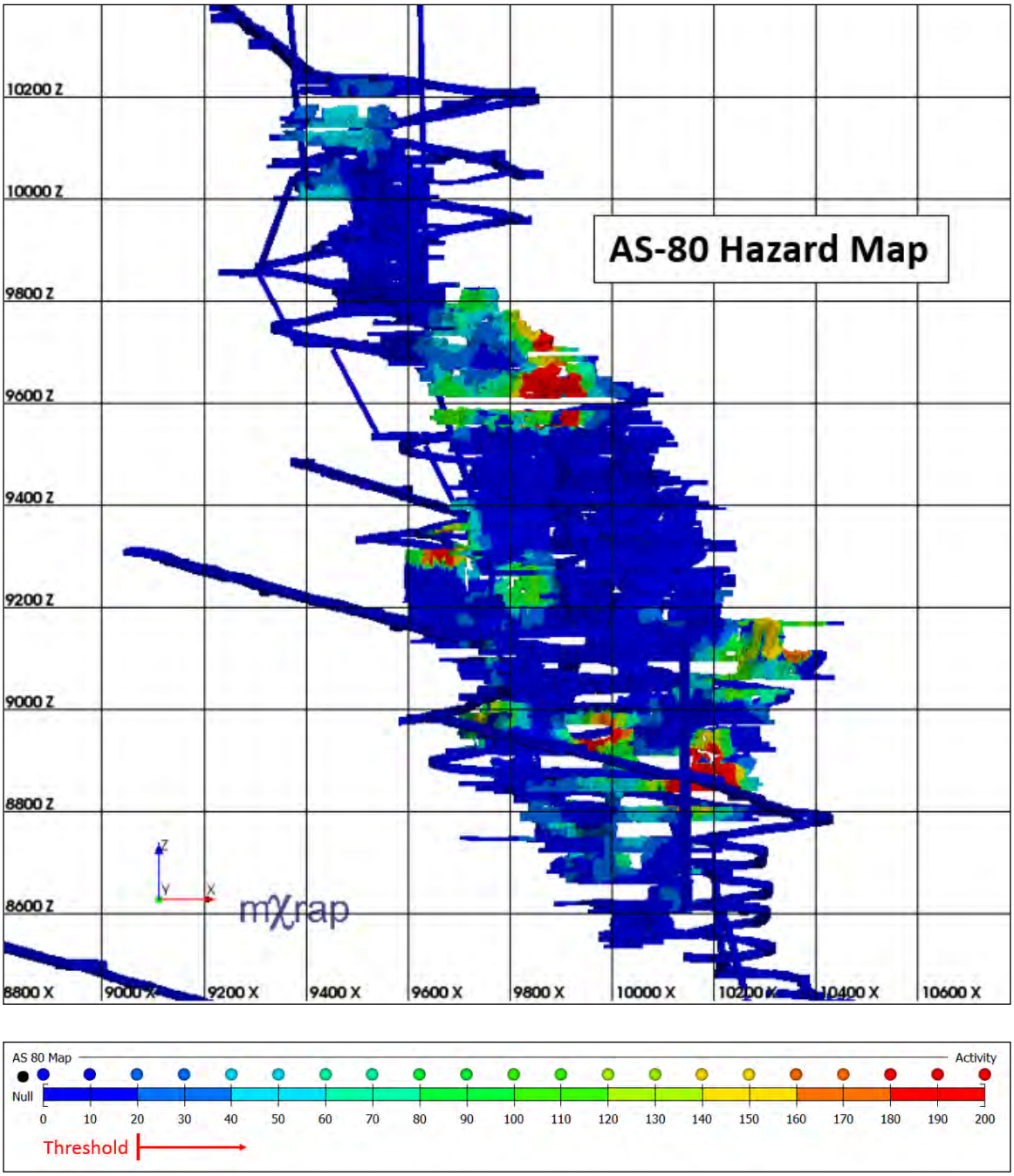
AS-80 Hazard Map
10200 Z
10000 Z
9800 Z
9600 Z
9400 Z
9200 Z
9000 Z
8800 Z
8600 Z
8800 X
9000 X
9200 X
9400 X
9600 X
9800 X
10000 X
10400 X
10600 X
Z
Y
X
mXrap

AS 80 Map
Activity
Null
0
10
20
30
40
50
60
70
80
90
100
110
120
130
140
150
160
170
180
190
200
Threshold

Level	Hazard Map Results		Area Accessible?	Past Activity	Planned activity	Forecast Period		
	Location	Number of events				Date/Time	Location	Mag
2900	Central	20	No	3050 XYZ1 + X2 Stopes	None			
2950/3030	X-West	40	No	3050 XYZ1 + X2 Stopes	None			
3090/3120	X-West	40	No	3050 XYZ1 + X2 Stopes	None			
3330/3390/3450	Z-West	80	No	3450 Z3 & 3690 A4 Stopes	None			
3450/3390	Z-East	150	Yes	3450 Z3 & 3690 A4 Stopes	None			
3510/3570	DBZ (Central)	650	Yes	3690 A4 Stope	None			
	Z1-Southwest	100	Yes	3690 A4 Stope	None			
3810	c6 AB acc.	160	Yes	3870/3920 BDE & 4030 B1 Stopes	3810-6 BFG & 3870 DE + B1 Stopes	22/05/2016 16:54	B-West Terminus	1.02
	G-North	20	No	3870/3920 BDE & 4030 B1 Stopes	3810-6 BFG & 3870 DE + B1 Stopes	23/05/2016 11:32	G-North Terminus	0.26
						21/05/2016 3:17	G-North Terminus	0.54
	c3 acc.	20	Yes	3870/3920 BDE & 4030 B1 Stopes	3810-6 BFG & 3870 DE + B1 Stopes			
3810/3870	B-West/BP Loop	200	Yes	3870/3920 BDE & 4030 B1 Stopes	3810-6 BFG & 3870 DE + B1 Stopes	21/05/2016 2:36	B-West Shrink Stope (FW)	0.35
3870	c1 acc.	40	Yes	3870/3920 BDE & 4030 B1 Stopes	3810-6 BFG & 3870 DE + B1 Stopes			
3870/3920	B-West/BDE	100	Yes	3870/3920 BDE & 4030 B1 Stopes	3810-6 BFG & 3870 DE + B1 Stopes	09/05/2016 7:29	near main access	0.23
3920	Main acc.	40	Yes	3870/3920 BDE & 4030 B1 Stopes	3810-6 BFG & 3870 DE + B1 Stopes			
3970	C-South Shrink/CRG Pillar acc.	20	Yes	4030 B1 Stope	None	09/05/2016 6:50	C-South LH Stope (FW)	0.23
	BP Dr.	20	Yes	H-Fault activity	None			
	H-North	100	Yes	3970 c2 dev. & 4090 H2 Stope	3970 c2 dev.			
3970/4030	H-Vein	140	Yes	3970 c2 dev. & 4090 H2 Stope	None			
	B-West	20	No	4030 B1 Stope	None			

Level	Hazard Map Results		Area Accessible?	Past Activity	Planned activity	Forecast Period		
	Location	Number of events				Date/Time	Location	Mag
4030/4090/4150	F/H	100	Yes	4090 H2 + F2 Stopes	None	25/05/2016 3:19	H-Vein Abutment	0.01
	H-North	160	No	4090 H2 Stope	None			
4150/4210	D-West abt.	120	Yes	4210 D1 + D2 Stopes	None	28/05/2016 4:00	cut4 D-Southwest	0.98
						06/04/2016 14:17	4210 CCF Stope (HW)	0.77
	F/D	200	Yes	4210 D1 + D2 + F1 Stopes	4150 F6 Stope	16/05/2016 20:04	cut3 F-West near D-SW	0.02
						21/04/2016 15:38	cut2 F-East near B-West	0.28
						16/05/2016 13:42	cut3 D-West	1.19
4210/4280	H-North LHs	500	Yes	4280 F3 + H2 Stopes	4280 Destress	21/05/2016 20:38	H-North LH (FW)	0.4
4280	H-south	40	Yes	4280 F3 + H2 Stopes	4280 Destress			
	G-North	100	No	4210 D1 + D2 & 4280 F3 Stopes	None			
4280/4340	F/H	160	Yes	4280 F3 + H2 Stopes	4280 Destress	22/04/2016 11:34	H-North (HW)	0.99
						25/05/2016 2:27	cut1 H-North (FW)	1.07
	G-North	300	No	4280 F3 & 4460 G2 Stopes	None			
	H-North	120	No	4280 F3 + H2 Stopes	4280 Destress			
4400/4460	G-North	100	Yes	4400 F2 & 4460 G2 Stopes	None			
	F-Vein	20	Yes	4400 F2 & 4460 G2 Stopes	None			
	F/H/I	20	Yes	4400 F2 Stope	None			
4460	I-North abt.	40	No	4580 HI Stope	None			
	Level Acc./TDBs	40	Yes	4460 G2 Stope	None			
4520	I-North/Fuel Bay	20	Yes	4580 HI Stope	None			

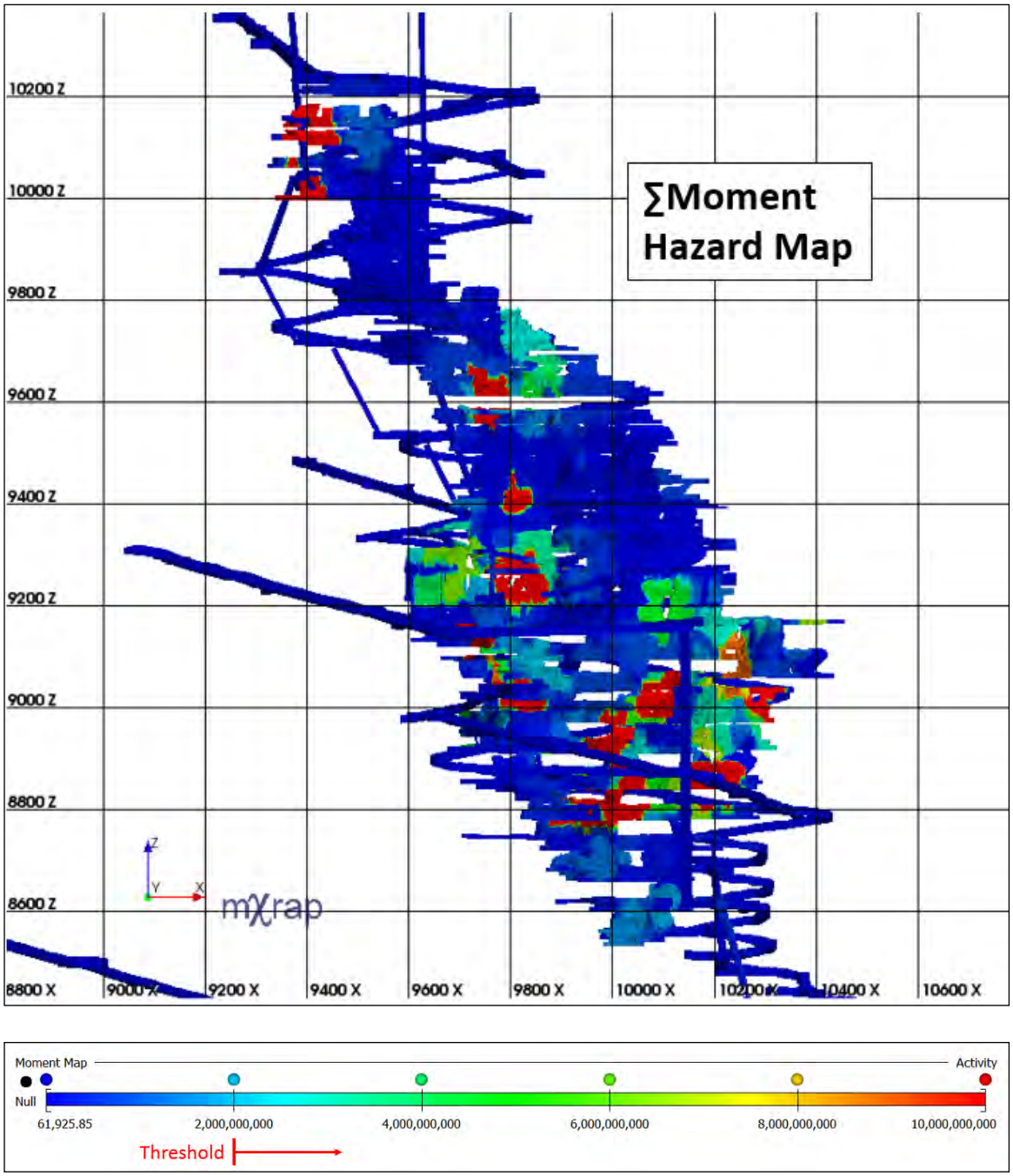
∑Moment
Hazard Map
10200 Z
10000 Z
9800 Z
9600 Z
9400 Z
9200 Z
9000 Z
8800 Z
8600 Z
8800 X
9000 X
9200 X
9400 X
9600 X
9800 X
10000 X
10200 X
10400 X
10600 X
Z
Y
X
mXrap

Moment Map
Activity
Null
61,925.85
2,000,000,000
4,000,000,000
6,000,000,000
8,000,000,000
10,000,000,000
Threshold

Level	Hazard Map Results		Area Accessible?	Past Activity	Planned activity	Forecast Period		
	Location	∑Mo (Nm)				Date/Time	Location	Mag
2950/3030	X-West	4.00E+10	Yes	3050 XYZ1 + X2 Stopes	None			
3050/3090/3120	X-West	2.20E+10	Yes	3050 XYZ1 + X2 Stopes	None			
3390/3450	Z-East	2.00E+09	No	3450 Z3 + 3690 A4 Stopes	None			
3510/3570	DBZ (Central)	5.00E+09	Yes	3690 A4 Stope	None			
	Z-West/Z1	1.60E+10	Yes	3690 A4 Stope	None			
3750/3810	B-West	2.00E+10	Yes	3810 F3 & 3870/3920 BDE + 3870 B2 Stopes	3810-6 BFG & 3870 DE + B1 Stopes			
3810/3870	B-West abt.	6.00E+09	Yes	3810 F3 & 3870/3920 BDE + 3870 B2 Stopes	3810-6 BFG & 3870 DE + B1 Stopes	22/05/2016 16:54	B-West Terminus	1.02
	G-North	8.00E+09	No	3810 F3 & 3870/3920 BDE + 3870 B2 Stopes	3810-6 BFG & 3870 DE + B1 Stopes	23/05/2016 11:32	G-North Terminus	0.26
						21/05/2016 3:17	G-North Terminus	0.54
3870	Main acc.	8.00E+09	Yes	3810 F3 & 3870/3920 BDE + 3870 B2 Stopes	3810-6 BFG & 3870 DE + B1 Stopes			
3870/3920	B-West	4.00E+10	Yes	4030 B1 Stope	3870 DE + B1 Stopes	09/05/2016 7:29	near main access	0.23
3920	B-West Shrink	5.00E+09	No	4030 B1 Stope	3870 DE + B1 Stopes	21/05/2016 2:36	B-West Shrink Stope (FW)	0.35
3970	F-East	5.00E+09	Yes	4030 T3 + EF1 Stopes	4030 EF2 + EF3/EF4 Stopes	12/04/2016 12:24	F-East LH (HW)	0.5
	BP Dr./H-South	2.00E+09	Yes	3970/4090 H1 & 4090 F2 Stopes	3970 c2 dev.			
	H-North	6.00E+09	Yes	3970/4090 H1 & 4090 F2 Stopes	3970 c2 dev.			

Level	HazMap Results		Area Accessible?	Past Activity	Planned activity	Forecast Period		
	Location	∑Mo (Nm2)				Date/Time	Location	Mag
3970/4030	C-South	1.50E+10	Yes	4030 B1 Stope	None			
4030/4090	F/H	1.00E+10	No	3970/4090 H1 & 4090 F2 Stopes	None	25/05/2016 3:19	H-Vein Abutment	0.01
	F/D	2.00E+09	Yes	4030 B1 & 4090 D1 + D2 Stopes	None	13/04/2016 8:29	cut3 D-West	1
4090	D-West abt.	5.00E+09	No	4030 B1 & 4090 D1 + D2 Stopes	None			
4090/4150	F-West	3.50E+10	Yes	4090 F2 & 4150 F6 Stopes	None			
	D-West	2.50E+10	Yes	4030 B1 & 4090 D1 + D2 Stopes & 4210 D1 + D2 Stopes	None	28/05/2016 4:00	cut4 D-Southwest	0.98
						12/04/2016 10:18	Far HW	0.54
4150	H-North abt.	1.50E+10	No	3970/4090 H1 & 4090 F2 & 4280 H2 Stopes	None			
4150/4210	CCF (North)	5.00E+09	Yes	4090 D1 + D2 & 4210 D1 + D2 Stopes	None	06/04/2016 14:17	4210 CCF Stope (HW)	0.77
	F/B	5.00E+09	Yes	4150 F6 & 4090 D1 + D2 & 4210 D1 + D2 Stopes	None	21/04/2016 15:38	cut2 F-East near B-West	0.28
	F-East	1.20E+10	Yes	4150 F6 & 4210 D1 + D2 + F1 Stopes	None	16/05/2016 13:42	cut3 D-West	1.19
						16/05/2016 20:04	cut3 F-West near D-SW	0.02
	F/H	3.00E+09	No	4280 H2 Stope	None			
4280/4340	H-North	1.20E+10	Yes	4280 H2 Stope	None	22/04/2016 11:34	H-North (HW)	0.99
						21/05/2016 20:38	H-North LH (FW)	0.4
	F/H	1.50E+11	Yes	4280 H2 + F3 Stopes	None	25/05/2016 2:27	cut1 H-North (FW)	1.07
	G-North	4.00E+10	No	4460 G2 Stope	None			
4400/4460	G-North	1.50E+10	No	4460 G2 Stope	None			

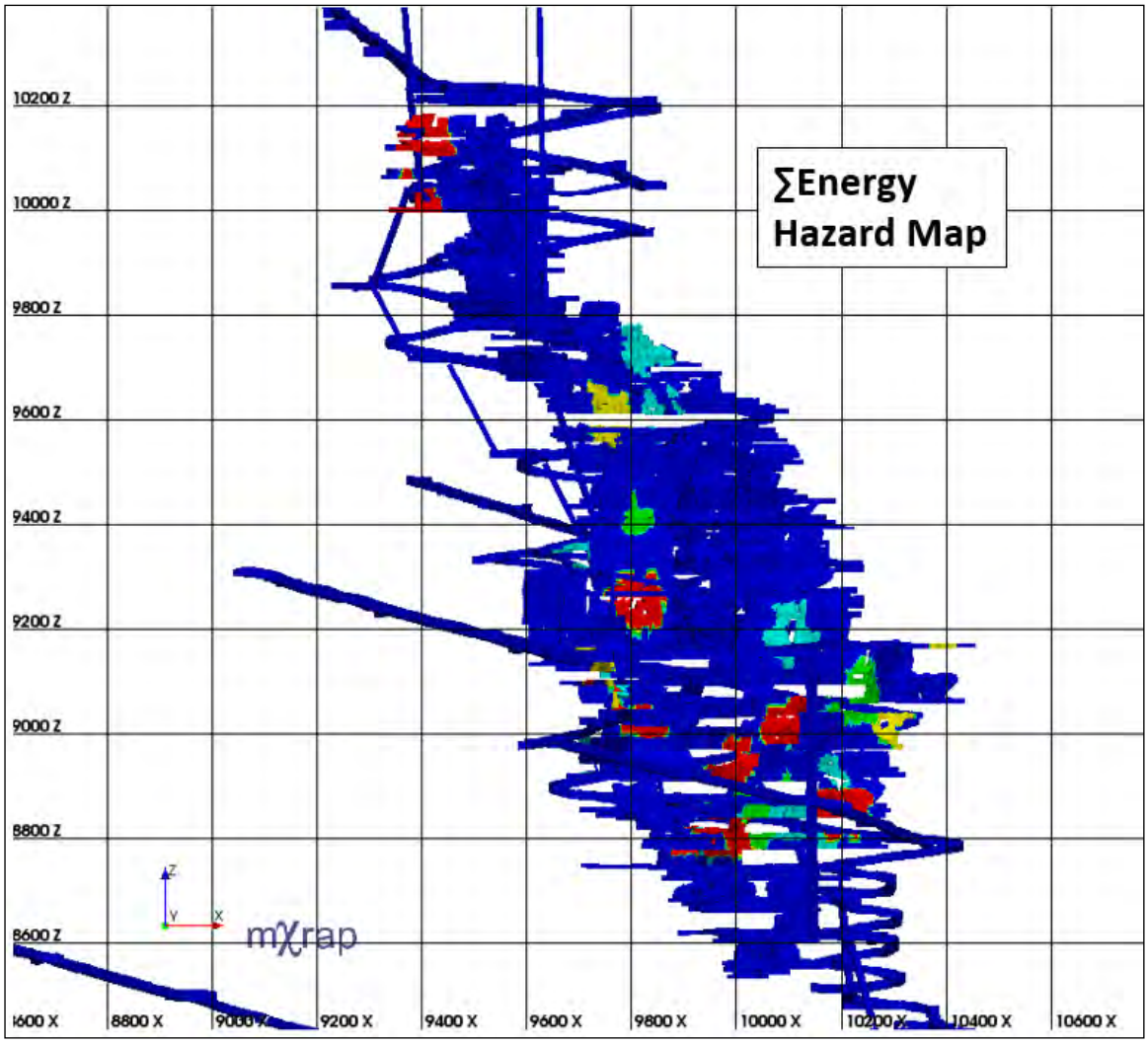
10200 Z
10000 Z
9800 Z
9600 Z
9400 Z
9200 Z
9000 Z
8800 Z
8600 Z
8800 X
9200 X
9400 X
9600 X
9800 X
10000 X
10400 X
10600 X
∑Energy
Hazard Map
Z
Y
X
mXrap

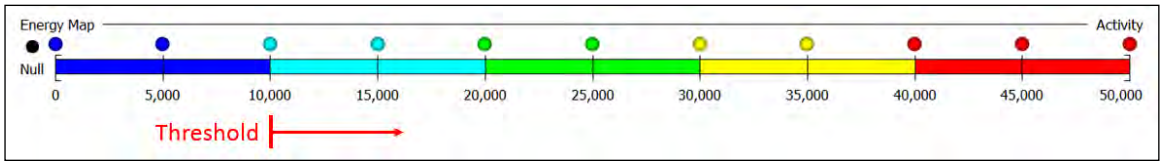
Energy Map
Activity
Null
0
5,000
10,000
15,000
20,000
25,000
30,000
35,000
40,000
45,000
50,000
Threshold

	HazMap Results		Area	Past Activity	Planned activity	Forecast Period		
Level	**Location**	**∑E**	**Accessible**			**Date/Time**	**Location**	**Mag**
2950/3030	X-West	70000	Yes	3050 XYZ1 + X2 Stopes	None			
3050/3090/3120	X-West	120000	Yes	3050 XYZ1 + X2 Stopes	None			
3390/3450	Z-East	10000	No	3690 A4 Stope	None			
3510/3570	DBZ (Central)	10000	Yes	3690 A4 Stope	None			
	Z-West/Z-Southwest	30000	Yes	3690 A4 Stope	None			
3750/3810	B-West	20000	Yes	3810 F3 & 3870/3920 BDE + 3870 B2 Stopes	3810-6 BFG & 3870 DE + B1 Stopes			
3810	B-West abt.	10000	Yes	3810 F3 & 3870/3920 BDE + 3870 B2 Stopes	3810-6 BFG & 3870 DE + B1 Stopes	22/05/2016 16:54	B-West Terminus	1.02
3870/3920	B-West	150000	No	4030 B1 Stope	3870 DE + B1 Stopes	09/05/2016 7:29	near main access	0.23
3970	F-East	10000	Yes	4030 T3 + EF1 Stopes	4030 EF2 + EF3/EF4 Stopes	12/04/2016 12:24	F-East LH (HW)	0.5
	H-North	30000	Yes	4090 F2 Stope	3970 c2 dev.			
3970/4030	C-South	30000	Yes	4030 B1 Stope	None			
4030/4090	D-West abt.	50000	No	4090 D1 + D2 Stopes	None			
	F/H	20000	Yes	4090 F2 Stope	None	25/05/2016 3:19	H-Vein Abutment	0.01
4090/4150	F-West	150000	Yes	4150 F6 & 4210 F1 Stopes	None			
	D-West	50000	Yes	4090 D1 + D2 & 4210 D1 + D2 Stopes	None	13/04/2016 8:29	cut3 D-West	1
						28/05/2016 4:00	cut4 D-Southwest	0.98
4150	H-North abt.	30000	No	3970/4090 H1 Stope	None			

Level	Hazard Map Results		Area Accessible?	Past Activity	Planned activity	Forecast Period		
	Location	∑E (J)				Date/Time	Location	Mag
4210	CCF (North)/c1 acc.	10000	No	4090 D1 + D2 & 4210 D1 + D2 Stopes	None			
	F/D	60000	Yes	4210 D1 + D2 + F1 Stopes	None	16/05/2016 20:04	cut3 F-West near D-SW	0.02
						21/04/2016 15:38	cut2 F-East near B-West	0.28
						16/05/2016 13:42	cut3 D-West	1.19
	B-Vein	50000	Yes	4090 D1 + D2 & 4210 D1 + D2 Stopes	None			
4210/4280	H-North LHs	120000	Yes	4280 H2 + F3 Stopes	4280 destress	22/04/2016 11:34	H-North (HW)	0.99
						21/05/2016 20:38	H-North LH (FW)	0.4
4280/4340	F/H	550000	Yes	4280 H2 + F3 Stopes	None	25/05/2016 2:27	cut1 H-North (FW)	1.07
	G-North/F-NW	150000	No	4460 G2 Stope	None			
4340/4400	G-North	30000	No	4460 G2 Stope	None			

Appendix C: Hazard Map Scorecards and Associated Figures (June – August 2016)

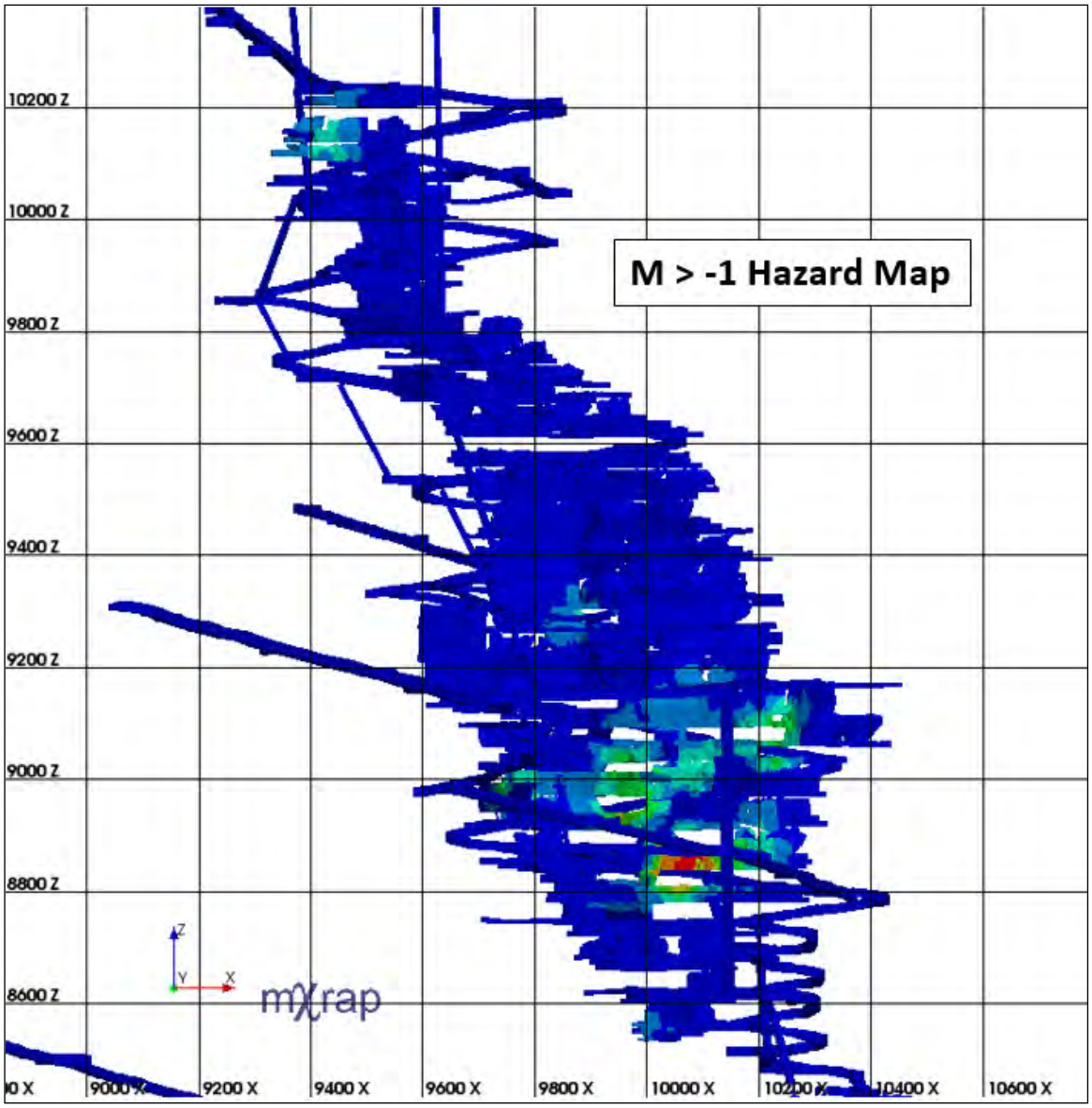

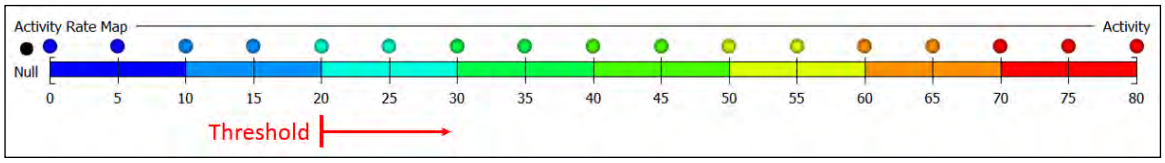

Level	Hazard Map Results		Area Accessible ?	Past Activity	Planned activity	Forecast Period		
	Location	Number of events				Date/Time	Location	Mag
2950/3030	X-West	20	No	3050 XYZ1 + X2 Stopes	None			
3450/3510/3570	Main TDBs & DBZ Central	80	Yes	3690 A4 Stope	None	28/07/2016 19:10	TDB c4 access	0.71
3810/3870	G-North abt.	20	No	3810-3 BFG + 3810-6 BFG & 3870 B1 Stopes	None	27/06/2016 13:20	Below G-North Shrink	0.49
3870	BDE	20	Yes	3810-3 BFG + 3810-6 BFG & 3870 B1 & 3870/3920 BDE Stopes	None			
3970/4030	F-East	20	Yes	4030 T3 + EF1 + EF2 + EF3/EF4 Stopes	None			
4030/4090	F/H	40	Yes	4090 F2 Stope	None	13/07/2016 0:35	4030/4090 F/H (along H-fault)	0.17
4090/4150	F-West	30	Yes	4150 F6 & 4210 F1 Stopes	4150 D1/D2 Stope	28/06/2016 5:13	4210 Recovery Dr.	0.15
	F/D	40	Yes	4150 F6 & 4210 F1 Stopes	4150 D1/D2 Stope	28/06/2016 6:32	4090 c3 E-West, near D Vein Acc	0.21
4150/4210	D-West abt.	30	Yes	4150 F6 & 4210 D1 + D2 + F1 Stopes	4150 D1/D2 Stope	13/06/2016 4:35	4090/4150 D-Vein Abt	0.34
						13/06/2016 4:36	4090/4150 D-Vein Abt	0.89
	F/D	60	Yes	4150 F6 & 4210 D1 + D2 + F1 Stopes	4150 D1/D2 Stope	22/06/2016 18:41	4210 Recovery Dr. Access	0.18
						24/06/2016 7:59	4210 Recovery Dr. Access	0.09
						28/06/2016 17:32	4210 Recovery Dr. Access	0.09
						16/07/2016 4:38	4210 Recovery Dr	0.17
	F/B	20	Yes	4150 F6 & 4210 D1 + D2 + F1 Stopes	4150 D1/D2 Stope	13/06/2016 18:21	4210 c3, F/B Intersection	0.32
						28/06/2016 9:25	4210 c3, F/B Intersection	0.36
4210/4280	H-North	80	Yes	4280 H2 + F3 Stopes	4280 fh1/fh3 Stope	20/06/2016 5:01	4280 c3 H-North Abt	1.05
						20/06/2016 19:48	4280 H-North LH (HW)	0.36
						03/07/2016 9:09	4280 along H-Fault (H-North Abt)	0.13
4280/4340	F/H	80	Yes	4280 H2 + F3 Stopes	4280 fh1/fh3 Stope	20/06/2016 4:55	4340 c3 H-North (along H-fault)	2.63
4340	F-Vein/Main acc.	20	Yes	4280 H2 + F3 Stopes	4280 fh1/fh3 & 4340 BWS Stopes			
	G-North	50	No	4280 H2 + F3 & 4210 F1 Stopes	None			

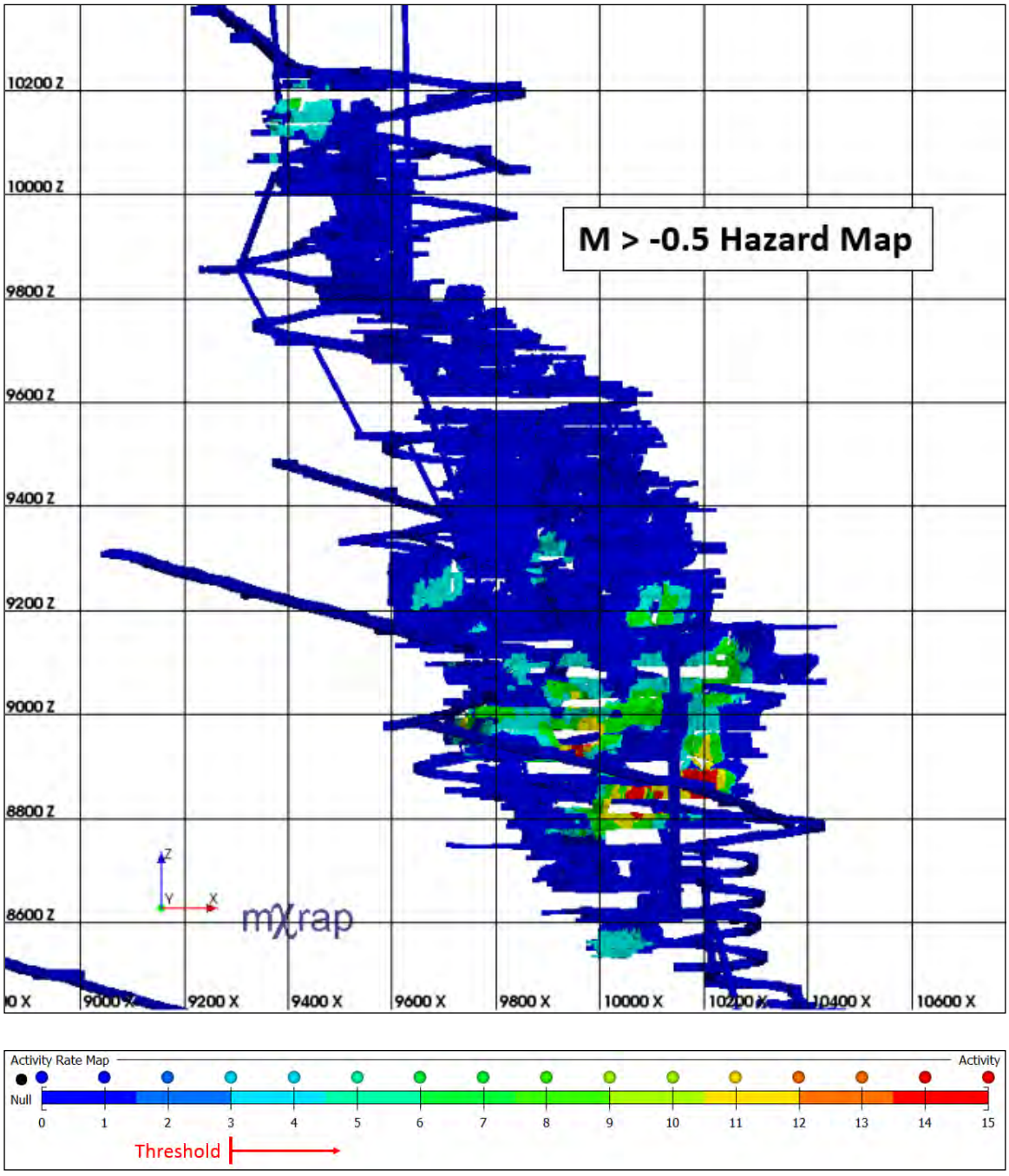
M > -0.5 Hazard Map
10200 Z
10000 Z
9800 Z
9600 Z
9400 Z
9200 Z
9000 Z
8800 Z
8600 Z
9200 X
9400 X
9600 X
9800 X
10000 X
10400 X
10600 X
Z
Y
X
mXrap
Activity Rate Map
Activity
Null
0
1
2
3
4
5
6
7
8
9
10
11
12
13
14
15
Threshold

Level	Hazard Map Results		Area Accessible?	Past Activity	Planned activity	Forecast Period		
	Location	Number of events				Date/Time	Location	Mag
2950/3030	X-West	3	No	3050 XYZ1 + X2 Stopes	None			
3450/3510	Main TDBs	20	Yes	3690 A4 Stope	None	28/07/2016 19:10	TDB c4 access	0.71
3510/3570	Z-West	3	Yes	3690 A4 Stope	None			
	DBZ (Central)	16	Yes	3690 A4 Stope	None			
3810/3870	G-North abt.	3	Yes	3810-3 BFG + 3810-6 BFG & 3870 B1 Stopes	None	27/06/2016 13:20	Below G-North Shrink	0.49
	BDE	8	Yes	3810-3 BFG + 3810-6 BFG & 3870 B1 & 3870/3920 BDE Stopes	None			
3920	B-West Shrink	3	No	3810-3 BFG + 3810-6 BFG & 3870 B1 & 3870/3920 BDE Stopes	None			
3970/4030	F-East	8	No	4030 T3 + EF1 Stopes	None			
4030/4090	F/H	8	Yes	4090 F2 & 4150 F6 Stopes	None	13/07/2016 0:35	4030/4090 F/H (along H-fault)	0.17
	D-West	3	Yes	4090 D2 Stope	4150 D1/D2 Stope	28/06/2016 4:48	4090 c4 D-West	0.59
4090/4150	F/D	8	Yes	4090 D2 Stope	4150 D1/D2 Stope	28/06/2016 6:32	4090 c3 E-West, near D Vein Acc	0.21
	F-West	8	Yes	4090 H2 & 4150 F6 & 4210 F1 Stopes	None	28/06/2016 5:13	4210 Recovery Dr.	0.15
4150	F/H	3	No	4090 H2 & 4280 H2 Stopes	None			
4150/4210	D-West abt.	8	Yes	4210 D1 + D2 Stopes	4150 D1/D2 Stope	13/06/2016 4:35	4090/4150 D-Vein Abt	0.34
						13/06/2016 4:36	4090/4150 D-Vein Abt	0.89
	F/D	16	Yes	4150 F6 & 4210 D1 + D2 + F1 Stopes	None	22/06/2016 18:41	4210 Recovery Dr. Access	0.18
						24/06/2016 7:59	4210 Recovery Dr. Access	0.09
						28/06/2016 17:32	4210 Recovery Dr. Access	0.09
						16/07/2016 4:38	4210 Recovery Dr	0.17

Level	HazMap Results		Area Accessible?	Past Activity	Planned activity	Forecast Period		
	Location	Number of events				Date/Time	Location	Mag
4210	F/B	8	Yes	4150 F6 & 4210 D1 + D2 + F1 Stopes	None	13/06/2016 18:21	4210 c3, F/B Intersection	0.32
						28/06/2016 9:25	4210 c3, F/B Intersection	0.36
4280	H-North	36	Yes	4280 H2 + F3 Stopes	4280 fh1/fh3 Stope	20/06/2016 5:01	4280 c3 H-North Abt	1.05
						20/06/2016 19:48	4280 H-North LH (HW)	0.36
						03/07/2016 9:09	4280 along H-Fault (H-North Abt)	0.13
	F/G	8	Yes	4150 F6 & 4210 D1 + D2 + F1 Stopes	None			
	F-North	3	Yes	4150 F6 & 4210 D1 + D2 + F1 Stopes	None			
4280/4340/4400	G-North	12	No	4280 H2 & 4210 F1 Stopes	None			
4280/4340	F/H	18	Yes	4280 H2 + F3 Stopes	4280 fh1/fh3 Stope	20/06/2016 4:55	4340 c3 H-North (along H-fault)	2.63
	F-Vein/Main acc.	8	Yes	4280 H2 + F3 Stopes	4340 BWS & 4280 fh1/fh3 Stopes			
4460	G-North acc.	3	No	4460 G2 Stope	None			
4520	I-North/Level acc.	3	Yes	None	None	28/06/2016 13:02	4520 near fuel bay	0.72
	Main TDBs	3	Yes	4580 G1	None			
4580	F/H	3	Yes	4580 G1	None			

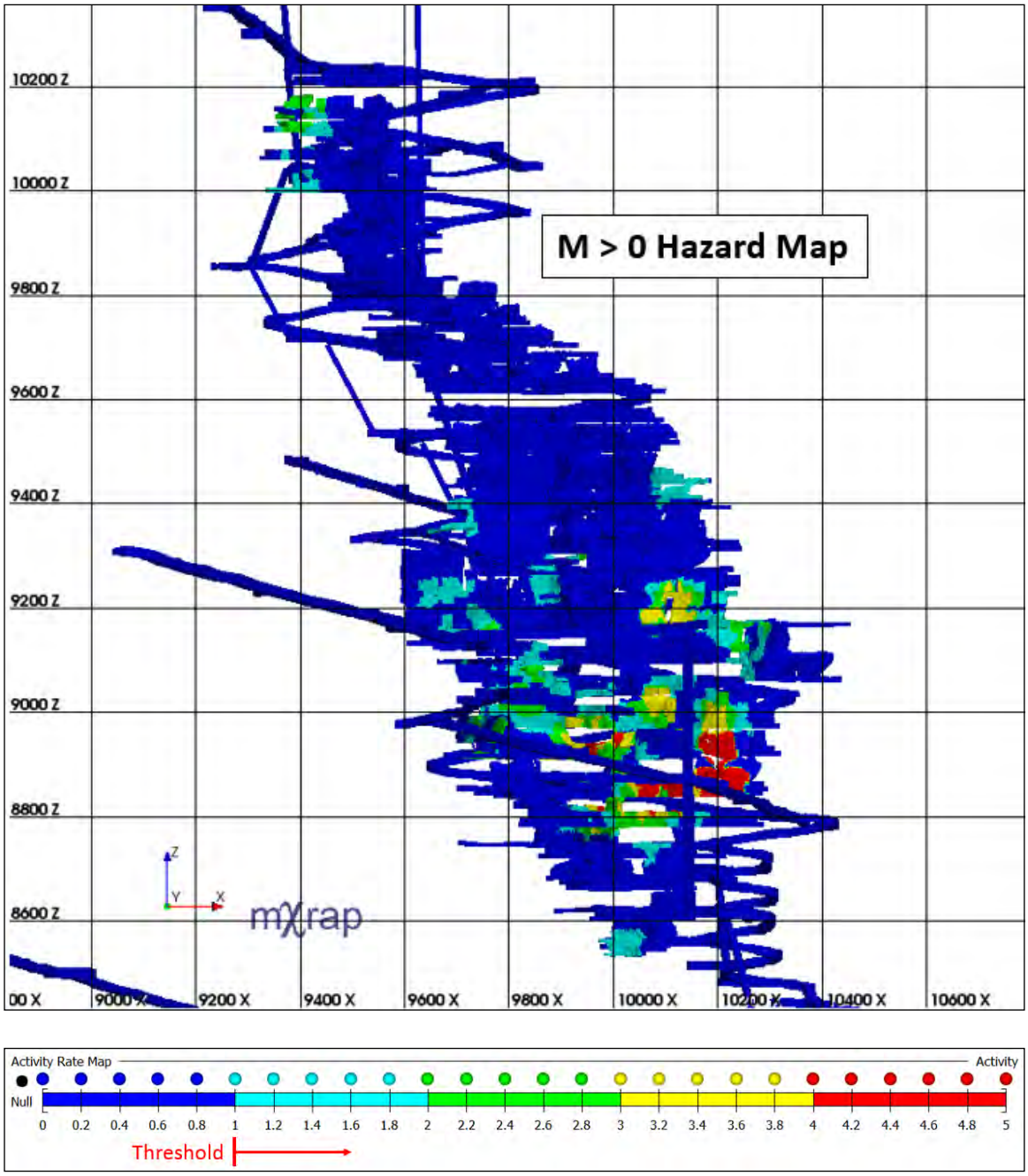
M > 0 Hazard Map
10200 Z
10000 Z
9800 Z
9600 Z
9400 Z
9200 Z
9000 Z
8800 Z
8600 Z
9000 X
9200 X
9400 X
9600 X
9800 X
10000 X
10200 X
10400 X
10600 X
Z
Y
X
mXrap

Activity Rate Map
Activity
Null
0 0.2 0.4 0.6 0.8 1 1.2 1.4 1.6 1.8 2 2.2 2.4 2.6 2.8 3 3.2 3.4 3.6 3.8 4 4.2 4.4 4.6 4.8 5
Threshold

Level	Hazard Map Results		Area Accessible?	Past Activity	Planned activity	Forecast Period		
	Location	Number of events				Date/Time	Location	Mag
3510	Main TDBs	6	Yes	3690 A4 Stope	None	28/07/2016 19:10	TDB c4 access	0.71
3570	Z-West loop	2	Yes	3690 A4 Stope	None			
3810/3870	G-North abt.	3	Yes	3810-1 BFG + 3810-6 BFG & 3870/3920 BDE Stopes	3870 DE1 + B1&Pillar Stopes	27/06/2016 13:20	Below G-North Shrink	0.49
3920	B-West Shrink	2	No	3810-1 BFG + 3810-6 BFG & 3870/3920 BDE Stopes	None			
3970	F-East LHs	2	Yes	4030 T3 + EF1 Stopes	None			
	H-South/BP Dr.	2	Yes	c2 TDB dev & 4090 F2 Stope	c2 TDB dev	29/06/2016 5:38	3970 H-Vein c2 (south side)	0.48
						18/07/2016 17:39	3970 H-Vein c2 (south side)	0.45
	H-North	2	Yes	c2 TDB dev & 4090 F2 Stope	c2 TDB dev	30/06/2016 19:39	3970 H-Vein c2 (north side)	0.42
	C-South/CRG Pillar acc.	2	Yes	None	None	13/06/2016 4:56	Near 3970 BP, below C-South CCF	0.53
						28/06/2016 4:39	3970 Craig Pillar Acc, near BP Dr.	1.17
4090	D-West	2	Yes	4090 D2 Stope	4150 D1/D2 Stope	28/06/2016 4:48	4090 c4 D-West	0.59
4090/4150	D-West	2	Yes	4090 D2 Stope	4150 D1/D2 Stope			
	F-West	5	Yes	4150 F6 & 4210 F1 Stopes	4150 D1/D2 Stope			
	F/H	3	No	4150 F6 & 4210 F1 & 4280 H2 (Blast 2)	None			

Level	Hazard Map Results		Area Accessible?	Past Activity	Planned activity	Forecast Period		
	Location	Number of events				Date/Time	Location	Mag
4150/4210	F/D	5	Yes	4150 F6 & 4210 F1 + D1 + D2 & 4280 F3 Stopes	None	22/06/2016 18:41	4210 Recovery Dr. Access	0.18
						24/06/2016 7:59	4210 Recovery Dr. Access	0.09
						28/06/2016 5:13	4210 Recovery Dr.	0.15
						28/06/2016 17:32	4210 Recovery Dr. Access	0.09
						16/07/2016 4:38	4210 Recovery Dr	0.17
	F/B	5	Yes	4150 F6 & 4210 F1 & 4280 F3 Stopes	None	13/06/2016 18:21	4210 c3, F/B Intersection	0.32
						28/06/2016 9:25	4210 c3, F/B Intersection	0.36
	CCF South abt.	2	Yes	4150 F6 & 4210 F1 + D1 + D2 & 4280 F3 Stopes	None			
4210/4280	H-North LHs	9	Yes	4280 H2 + F3 Stopes	4280 fh1/fh3 Stope	26/06/2016 4:13	4210 H-North Abt	0.15
						20/06/2016 5:01	4280 c3 H-North Abt	1.05
						20/06/2016 19:48	4280 H-North LH (HW)	0.36
4280/4340	H-North & F/H	5	Yes	4280 H2 + F3 Stopes	4280 fh1/fh3 Stope	20/06/2016 4:55	4340 c3 H-North (along H-fault)	2.63
4340	Main acc./FB	5	Yes	4210 F1 + D1 + D2 & 4280 F3 Stopes	4280 fh1/fh3 Stope			
4340/4400	G-North	5	No	4280 H2 & 4210 F1 Stopes	None			
4460	G-North	2	No	4460 G2 Stope	None			

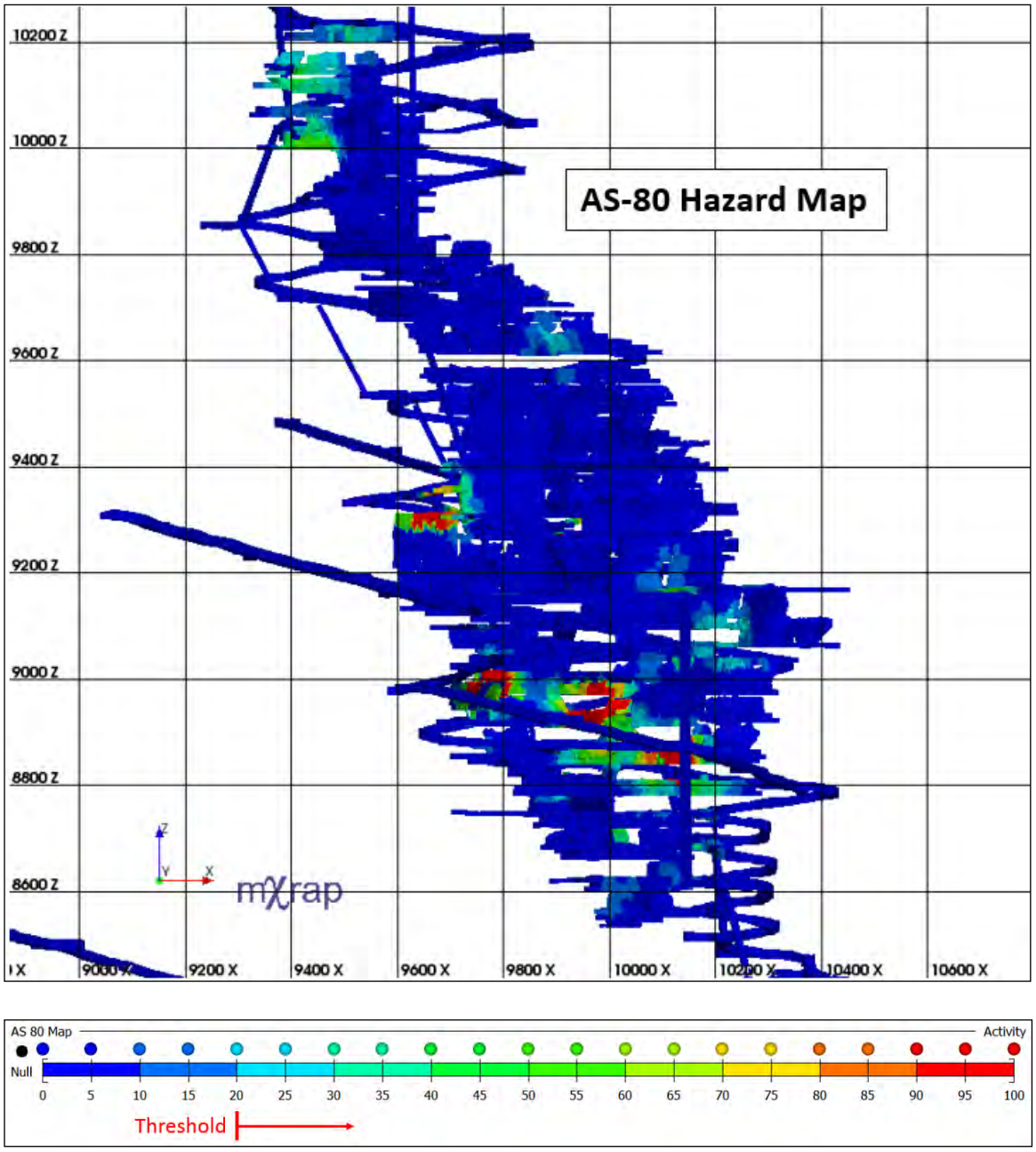
AS-80 Hazard Map
10200 Z
10000 Z
9800 Z
9600 Z
9400 Z
9200 Z
9000 Z
8800 Z
8600 Z
9200 X
9400 X
9600 X
9800 X
10000 X
10400 X
10600 X
Z
Y
X
mXrap

AS 80 Map
Activity
Null
0
5
10
15
20
25
30
35
40
45
50
55
60
65
70
75
80
85
90
95
100
Threshold

Level	Hazard Map Results		Area Accessible?	Past Activity	Planned activity	Forecast Period		
	Location	Number of events				Date/Time	Location	Mag
2900	central	20	Yes	3050 XYZ1 + X2 Stopes	None			
2950/3030	X-West	40	No	3050 XYZ1 + X2 Stopes	None			
3090/3120	X-West	40	No	3050 XYZ1 + X2 Stopes	None			
3390/3450	Z-East Abt.	120	No	3690 A4 Stope	None			
3510	Z-east	150	No	3690 A4 Stope	None	28/07/2016 19:10	TDB c4 access	0.71
	A1	120	No	3690 A4 Stope	None			
3510/3570	Z1-Southwest	60	No	3690 A4 Stope	None			
	DBZ Central	300	Yes	3690 A4 Stope	None			
3810	c6 AB acc.	80	Yes	3810-1 BFG + 3810-6 BFG & 3870/3920 BDE Stopes	3870 DE1 + B1&Pillar Stopes	17/06/2016 17:12	access rp c6	0.23
3810/3870	c1 BP loop	100	Yes	3810-1 BFG + 3810-6 BFG & 3870/3920 BDE Stopes	3870 DE1 + B1&Pillar Stopes			
	G-North abt.	100	Yes	3810-1 BFG + 3810-6 BFG & 3870/3920 BDE Stopes	3870 DE1 + B1&Pillar Stopes	27/06/2016 13:20	Below G-North Shrink	0.49
3870	c1 acc.	100	Yes	3870/3920 BDE Stopes	3870 DE1 + B1&Pillar Stopes			
3920	Main acc.	80	No	3870/3920 BDE Stopes	3870 DE1 + B1&Pillar Stopes			
3970	H-North	60	Yes	c2 TDB dev & 4090 F2 Stope	c2 TDB dev	30/06/2016 19:39	3970 H-Vein c2 (north side)	0.42
						18/06/2016 12:31	4090/4030 H-North (FW)	0.41
	BP Dr.	60	Yes	H-Fault activity	None			
4030/4090	F/H	40	No	4090 F2 Stope	None	13/07/2016 0:35	4030/4090 F/H (along H-fault)	0.17
4150	H-South	40	No	4210 F1 & 4150 F6 Stopes	None			

Level	Hazard Map Results		Area Accessible?	Past Activity	Planned activity	Forecast Period		
	Location	Number of events				Date/Time	Location	Mag
4150/4210	D-West Abt.	120	Yes	4210 D1 + D2 Stopes	4150 D1/D2 Stope	13/06/2016 4:35	4090/4150 D-Vein Abt	0.34
						13/06/2016 4:36	4090/4150 D-Vein Abt	0.89
	F/D	200	Yes	4210 D1 + D2 + F1 & 4150 F6 Stopes	4150 D1/D2 Stope	22/06/2016 18:41	4210 Recovery Dr. Access	0.18
						24/06/2016 7:59	4210 Recovery Dr. Access	0.09
						28/06/2016 17:32	4210 Recovery Dr. Access	0.09
						13/06/2016 18:21	4210 c3, F/B Intersection	0.32
						28/06/2016 9:25	4210 c3, F/B Intersection	0.36
4250	H-South acc.	60	Yes	4280 H2 + F3 Stopes	4280 fh1/fh3 Stope			
4280/4340	F/H	170	Yes	4280 H2 + F3 Stopes	4280 fh1/fh3 Stope	20/06/2016 4:55	4340 c3 H-North (along H-fault)	2.63
	G-North	200	No	4210 D1 + D2 & 4460 G2 Stopes	None			
4340	H-South abt.	20	No	4280 H2 + F3 Stopes	None			
4400	H-North abt.	40	No	None	None			
	Level acc.	40	Yes	4460 G2 Stope	None			
	G-North Abt.	40	No	4460 G2 Stope	None			

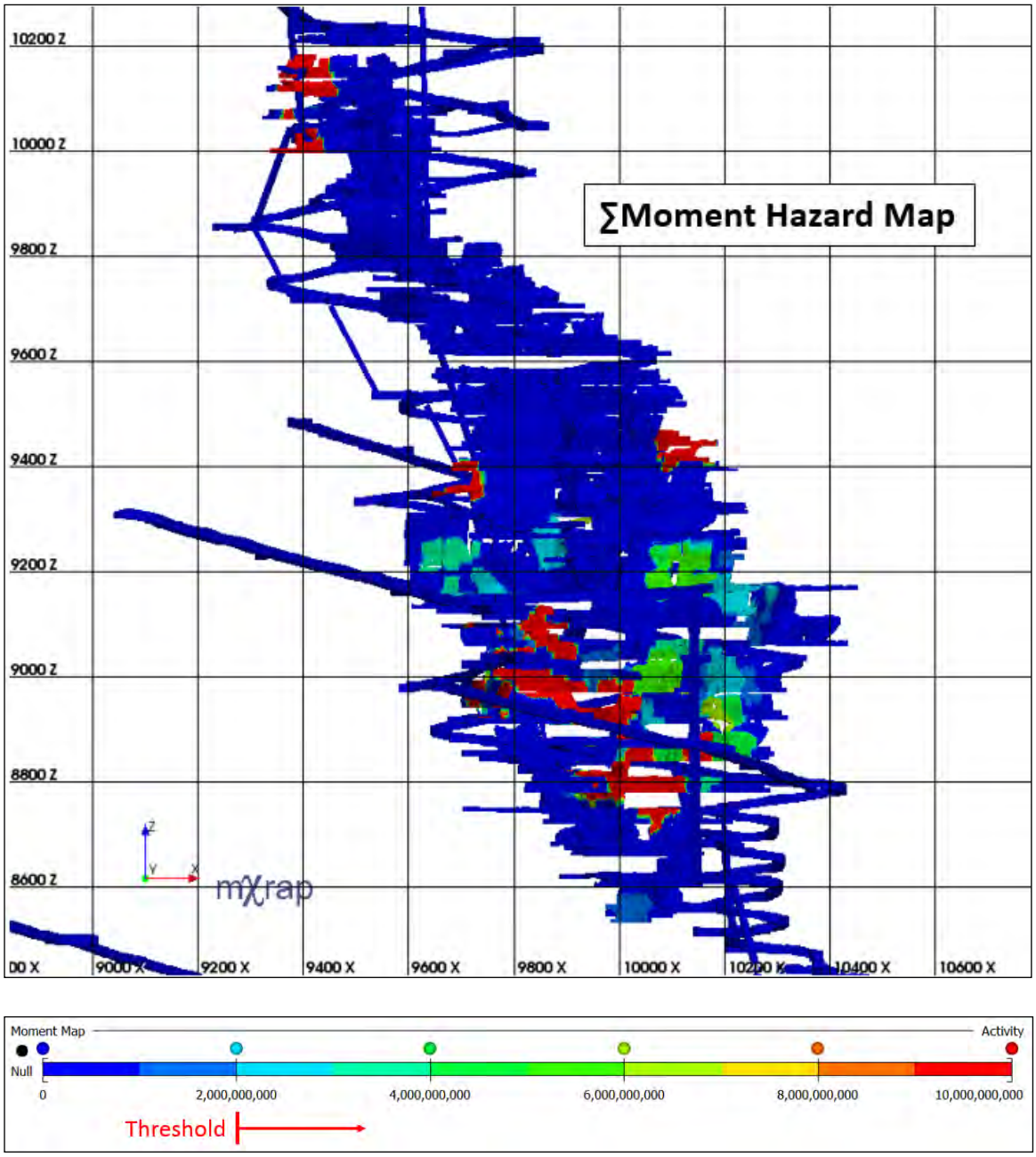
∑Moment Hazard Map
10200 Z
10000 Z
9800 Z
9600 Z
9400 Z
9200 Z
9000 Z
8800 Z
8600 Z
9000 X
9200 X
9400 X
9600 X
9800 X
10000 X
10400 X
10600 X
Moment Map
Activity
Null
0
2,000,000,000
4,000,000,000
6,000,000,000
8,000,000,000
10,000,000,000
Threshold

Level	Hazard Map Results		Area Accessible?	Past Activity	Planned activity	Forecast Period		
	Location	∑Mo (Nm2)				Date/Time	Location	Mag
2950/3030	X-West	4.00E+10	Yes	3050 XYZ1 + X2 Stopes	None			
3050/3090	X-West	3.00E+10	Yes	3050 XYZ1 + X2 Stopes	None			
3390/3450	Z-East	3.00E+09	No	3690 A4 Stope	None			
3510/3570	DBZ (North Central)	5.00E+09	Yes	3690 A4 Stope	None	28/07/2016 19:10	TDB c4 access	0.71
	Z-West/Z1	1.60E+10	Yes	3690 A4 Stope	None			
3690/3750	F-East	1.00E+10	No	None	None			
3750/3810	B-West	2.50E+10	Yes	3870/3920 BDE + 3870 B2 Stopes	3810-6 A1/A2 & 3870 DE/B&Pillar Stopes			
	B-West abt.	3.00E+10	Yes	3870/3920 BDE + 3870 B2 Stopes	3810-6 A1/A2 & 3870 DE/B&Pillar Stopes	17/06/2016 17:12	access rp c6	0.23
3810/3870	G-North	8.00E+09	Yes	3810-3 BFG + 3870 B1 + DE1 Stopes	3810-6 A1/A2 & 3870 DE/B&Pillar Stopes	27/06/2016 13:20	Below G-North Shrink	0.49
3870/3920	BDE (Central)	2.00E+09	Yes	3870/3920 BDE + 3870 B2 Stopes	3810-6 A1/A2 & 3870 DE/B&Pillar Stopes			
3920	B-West Shrink	5.00E+09	No	3870/3920 BDE + 3870 B2 Stopes	None			
3970	F-East Pillar	5.00E+09	Yes	4030 T3 + EF1 Stopes	None			
	H-North	6.00E+09	Yes	3970 c2 dev. & 4090 F2 Stope	3970 c2 dev.	30/06/2016 19:39	3970 H-Vein c2 (north side)	0.42
						18/06/2016 12:31	4090/4030 H-North (FW)	0.41
	C-South/BP Dr.	2.00E+09	Yes	H-Fault actvitity	None	13/06/2016 4:56	Near 3970 BP, below C-South CCF	0.53
						28/06/2016 4:39	3970 Craig Pillar Acc, near BP Dr.	1.17
3970/4030	F/H	2.00E+09	Yes	3970 c2 dev. & 4090 F2 Stope	3970 c2 dev.	29/06/2016 5:38	3970 H-Vein c2 (south side)	0.48
						18/07/2016 17:39	3970 H-Vein c2 (south side)	0.45
						13/07/2016 0:35	4030/4090 F/H (along H-fault)	0.17

Level	Hazard Map Results		Area Accessible?	Past Activity	Planned activity	Forecast Period		
	Location	∑Mo (Nm2)				Date/Time	Location	Mag
4030/4090	F/D	3.50E+10	Yes	4030 EF1 + EF2 + EF3/EF4 & 4150 F6 Stopes	4150 D1/D2 Stope	28/06/2016 4:48	4090 c4 D-West	0.59
						28/06/2016 6:32	4090 c3 E-West, near D Vein Acc	0.21
4090/4150	D-West	3.00E+10	Yes	4210 D1 + D2 Stopes	4150 D1/D2 Stope			
4150	H-North abt.	6.00E+09	No	4280 H2 Stope	None	21/06/2016 8:24	4150 H-North Abt	0.02
						27/06/2016 13:33	4150 H-North Abt	0.87
						26/06/2016 4:13	4210 H-North Abt	0.15
	F-West	3.50E+10	No	4150 F6 Stope	4150 D1/D2 Stope	28/06/2016 5:13	4210 Recovery Dr.	0.15
4210	CCF (North)	1.50E+10	No	4210 D1 + D2 Stopes	4150 D1/D2 Stope	13/06/2016 4:35	4090/4150 D-Vein Abt	0.34
						13/06/2016 4:36	4090/4150 D-Vein Abt	0.89
	F/D	6.00E+10	Yes	4210 D1 + D2 + F1 & 4150 F6 Stopes	4150 D1/D2 Stope	22/06/2016 18:41	4210 Recovery Dr. Access	0.18
						24/06/2016 7:59	4210 Recovery Dr. Access	0.09
						28/06/2016 17:32	4210 Recovery Dr. Access	0.09
						13/06/2016 18:21	4210 c3, F/B Intersection	0.32
						28/06/2016 9:25	4210 c3, F/B Intersection	0.36
	CCF (South)	4.50E+10	No	4210 D1 + D2 Stopes	4150 D1/D2 Stope			
4280	H-North	3.00E+10	No	4280 H2 + F3 Stopes	4280 fh1/fh3 Stope	20/06/2016 5:01	4280 c3 H-North Abt	1.05
						20/06/2016 19:48	4280 H-North LH (HW)	0.36
4340	G-North/F-NW	1.50E+10	No	4460 G2 Stope	None			
4280/4340/4400	F/H	1.50E+11	Yes	4280 H2 + F3 Stopes	4280 fh1/fh3 Stope	20/06/2016 4:55	4340 c3 H-North (along H-fault)	2.63
4460	G-North	8.00E+09	No	4460 G2 Stope	None			

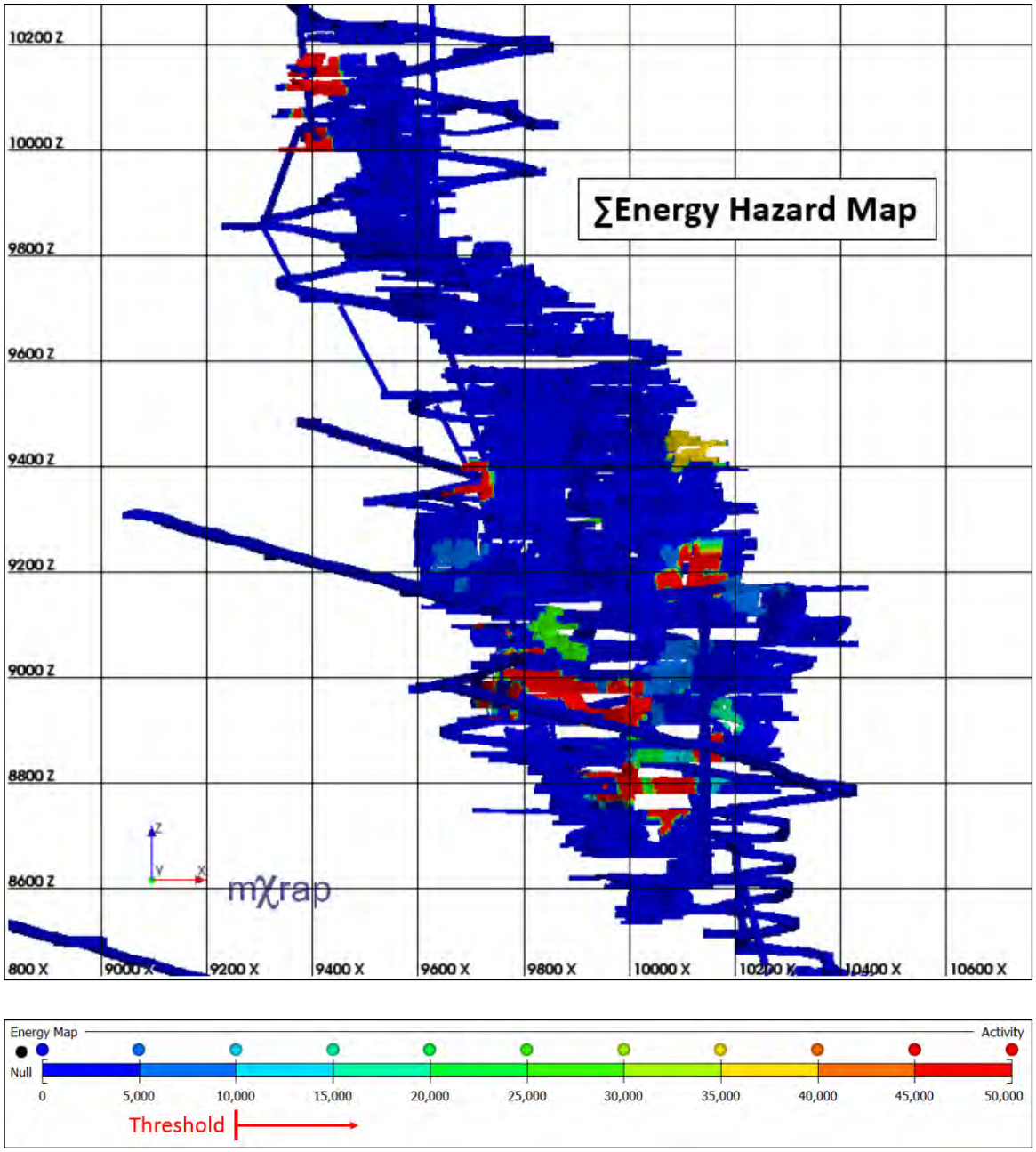
∑Energy Hazard Map
10200 Z
10000 Z
9800 Z
9600 Z
9400 Z
9200 Z
9000 Z
8800 Z
8600 Z
800 X
9000 X
9200 X
9400 X
9600 X
9800 X
10000 X
10200 X
10400 X
10600 X
mXrap
Energy Map
Activity
Null
0
5,000
10,000
15,000
20,000
25,000
30,000
35,000
40,000
45,000
50,000
Threshold

Level	Hazard Map Results		Area Accessible?	Past Activity	Planned activity	Forecast Period		
	Location	∑E				Date/Time	Location	Mag
2950/3030	X-West	70000	Yes	3050 XYZ1 + X2 Stopes	None			
3050/3090/3120	X-West	120000	Yes	3050 XYZ1 + X2 Stopes	None			
3390/3450	Z-East	10000	No	3690 A4 Stope	None			
3510/3570	DBZ (Central)	10000	Yes	3690 A4 Stope	None	28/07/2016 19:10	TDB c4 access	0.71
	Z-West/Z-Southwest	30000	Yes	3690 A4 Stope	None			
3690/3750	F-East	30000	No	None	None			
3810	B-West abt.	120000	Yes	3870/3920 BDE + 3870 B2 Stopes	3810-6 A1/A2 & 3870 DE/B&Pillar Stopes	17/06/2016 17:12	access rp c6	0.23
3870	G-North abt.	20000	Yes	3810-3 BFG + 3870 B1 + DE1 Stopes	3810-6 A1/A2 & 3870 DE/B&Pillar Stopes	27/06/2016 13:20	Below G-North Shrink	0.49
3970	F-East	50000	Yes	4030 T3 + EF1 Stopes	None	29/06/2016 5:38	3970 H-Vein c2 (south side)	0.48
						18/07/2016 17:39	3970 H-Vein c2 (south side)	0.45
	H-North	30000	Yes	3970 c2 dev. & 4090 F2 Stope	3970 c2 dev.	30/06/2016 19:39	3970 H-Vein c2 (north side)	0.42
4030/4090	F/D	20000	Yes	4030 EF1 + EF2 + EF3/EF4 & 4150 F6 Stopes	4150 D1/D2 Stope	28/06/2016 4:48	4090 c4 D-West	0.59
						28/06/2016 6:32	4090 c3 E-West, near D Vein Acc	0.21
4090/4150	F-West	130000	Yes	4150 F6 Stope	4150 D1/D2 Stope	28/06/2016 5:13	4210 Recovery Dr.	0.15
	D-West	100000	Yes	4210 D1 + D2 Stopes	4150 D1/D2 Stope			

Level	Hazard Map Results		Area Accessible?	Past Activity	Planned activity	Forecast Period		
	Location	∑E				Date/Time	Location	Mag
4210	CCF (North)	120000	No	4210 D1 + D2 Stopes	4150 D1/D2 Stope	13/06/2016 4:35	4090/4150 D-Vein Abt	0.34
						13/06/2016 4:36	4090/4150 D-Vein Abt	0.89
	CCF (South)	120000	No	4210 D1 + D2 Stopes	4150 D1/D2 Stope			
	F/D	240000	Yes	4210 D1 + D2 & 4150 F6 Stopes	4150 D1/D2 Stope	13/06/2016 18:21	4210 c3, F/B Intersection	0.32
						22/06/2016 18:41	4210 Recovery Dr. Access	0.18
						24/06/2016 7:59	4210 Recovery Dr. Access	0.09
						28/06/2016 9:25	4210 c3, F/B Intersection	0.36
						28/06/2016 17:32	4210 Recovery Dr. Access	0.09
	B-Vein	50000	Yes	4210 D1 + D2 & 4150 F6 Stopes	4150 D1/D2 Stope			
4210/4280	H-North LHs	10000	Yes	4280 H2 (Blast 2) + F3 Stopes	4280 fh1/fh3 Stope	20/06/2016 19:48	4280 H-North LH (HW)	0.36
	F/H	120000	Yes	4280 H2 (Blast 2) + F3 Stopes	4280 fh1/fh3 Stope			
4340	TDBs/FB	550000	Yes	4280 F3 + H2 Stopes	4340 BWS & 4280 fh1/fh3 Stopes			
4340/4400	H-North	300000	No	4280 F3 + H2 Stopes	4340 BWS & 4280 fh1/fh3 Stopes	20/06/2016 4:55	4340 c3 H-North (along H-fault)	2.63
	G-North	30000	No	4460 G2 Stope	None			
4460	G-North	15000	No	4460 G2 Stope	None			

Appendix D: Hazard Map Scorecards and Associated Figures (August – October 2016)

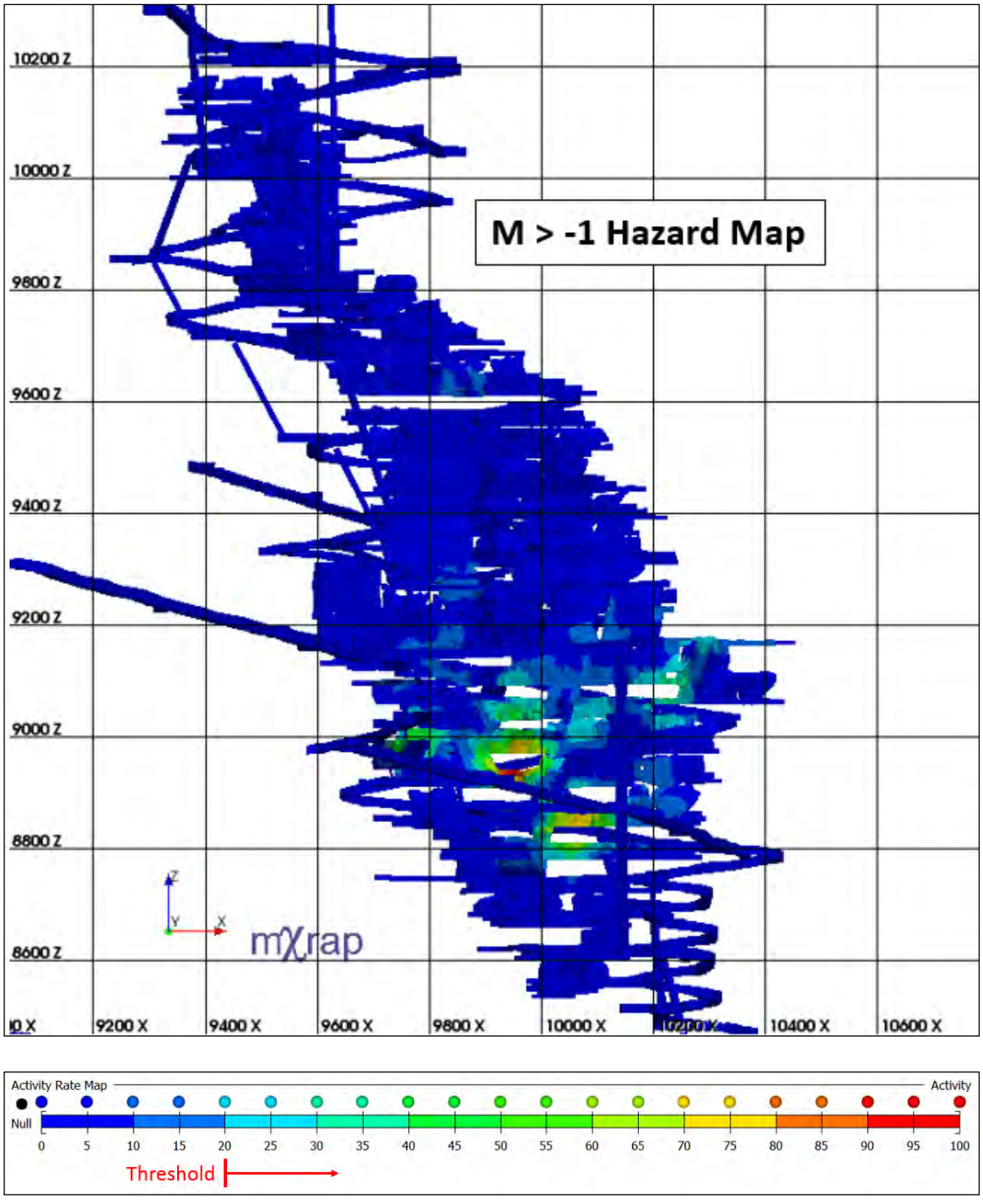

Level	Hazard Map Results		Area Accessible?	Past Activity	Planned activity	Forecast Period		
	Location	Number of events				Date/Time	Location	Mag
3870	c1 BDE Acc.	20	Yes	3870 DE1 + B1&Pillar Stopes	3810-3 A1 Stope			
3970	H-South/TDBs	20	Yes	H-Vein c2 dev & 4090 F2 Stope	3970 H1 Stope	2016/08/26 05:21:23	above 3970 H-North	0.28
4030/4090	F/H	35	No	4090 F2 Stope	3970 H1 Stope	2016/09/09 04:13:50	4150 c3, near H/F Intersection	0.48
4090	Main acc. F-Vein	35	Yes	4090 F2 Stope	3970 H1 Stope			
4090/4150	F/D	35	Yes	4150 D1/D2 + F6 Stopes	4150 EF Stope			
4150/4210	D-West abt.	50	No	4150 D1/D2 & 4210 D1 + D2 Stopes	4150 EF & 4210 F2rec Stopes			
	F/D	75	Yes	4150 D1/D2 & 4210 D1 + D2 Stopes	4150 EF & 4210 F2rec Stopes	2016/09/17 04:41:54	4210 c3, B-West (HW) near F/B intersection	1.39
						2016/09/23 07:12:36	4210 c3, near F/B intersection	0.67
						2016/08/05 10:50:10	4280 c2, G-North, near G/F/B intersection	1.77
4280/4340	F/H	60	Yes	4280 fh1/fh3 Stope	None	2016/09/17 15:08:26	4340 c4 F-Vein, near TDB acc	2.1

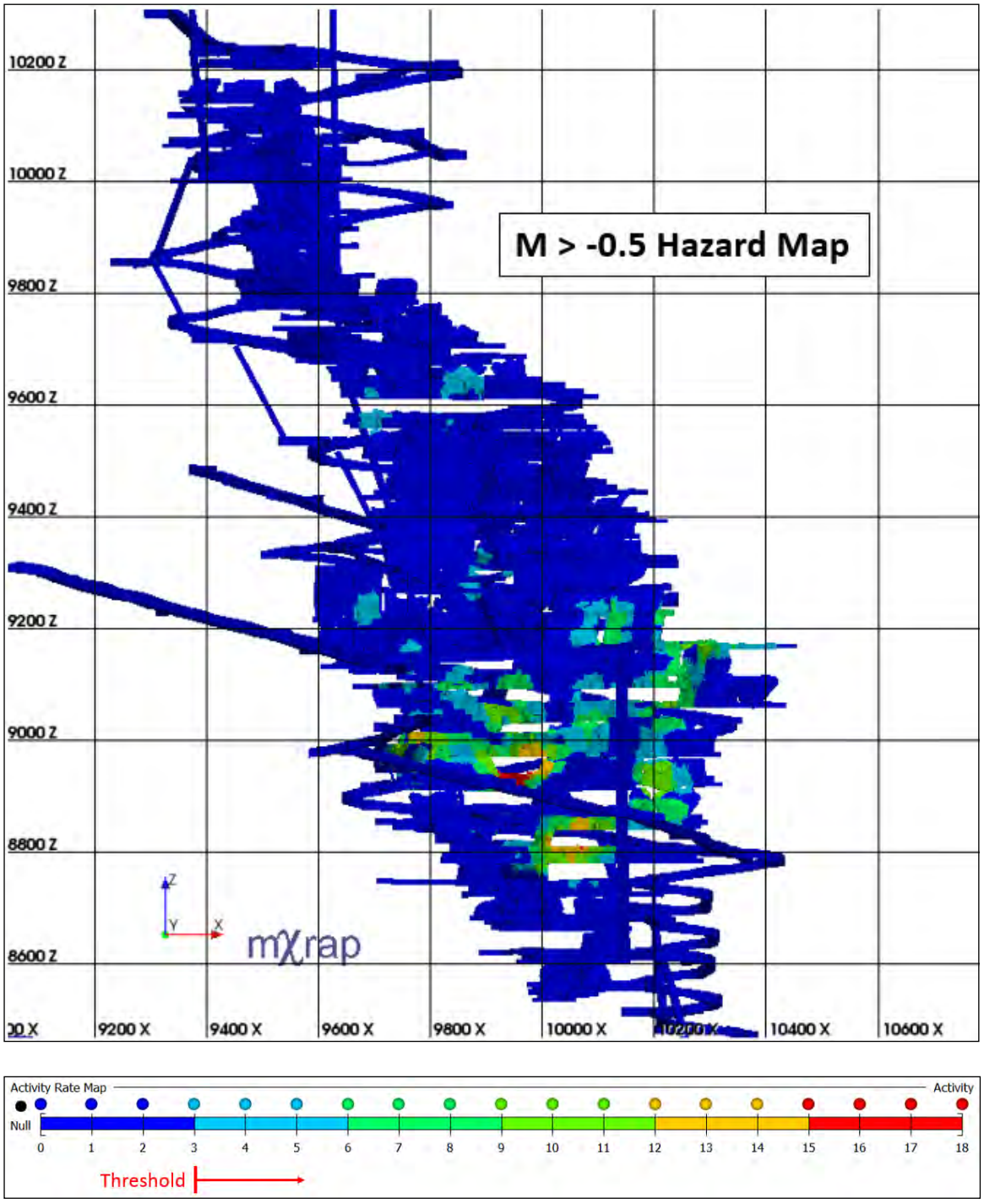
M > -0.5 Hazard Map
10200 Z
10000 Z
9800 Z
9600 Z
9400 Z
9200 Z
9000 Z
8800 Z
8600 Z
9200 X
9400 X
9600 X
9800 X
10000 X
10400 X
10600 X
Z
Y
X
mXrap
Activity Rate Map
Activity
Null
0 1 2 3 4 5 6 7 8 9 10 11 12 13 14 15 16 17 18
Threshold

Level	Hazard Map Results		Area Accessible?	Past Activity	Planned activity	Forecast Period		
	Location	Number of events				Date/Time	Location	Mag
3510/3570	Main acc./Central Veins	4	Yes	3570 BP dev	3570 BP dev			
	Z1-Southwest	4	Yes	3570 BP dev	3570 BP dev	2016/08/14 08:48:42	3570 c3, Z-Southwest; near bypass breakthrough	0.35
3810/3870	BDE	6	Yes	3870 DE1 + B1&Pillar Stopes	3810-3 A1 Stope			
3870	G-North abt.	5	Yes	3870 DE1 + B1&Pillar Stopes	3810-3 A1 Stope	2016/09/12 04:27:06	3810 c1, G-North abt.	0.42
3870/3920	B-West	3	No	3870 DE1 + B1&Pillar Stopes	3810-3 A1 Stope			
	B-West shrink	4	No	3870 DE1 + B1&Pillar Stopes	3810-3 A1 Stope			
3970	F-East LHs	7	No	3870 DE1 + B1&Pillar Stopes	None	2016/09/06 05:03:04	3970 F-East LH (FW)	1.34
	H-Vein Main acc./H-South	9	Yes	c2 dev. & 4090 F2 Stope	3970 H1 Stope			
	H-North	5	Yes	c2 dev. & 4090 F2 Stope	3970 H1 Stope	2016/08/26 05:21:23	above 3970 H-North	0.28
	C-South/CRG Pillar acc.	4	Yes	None	None			
4030/4090	F/H	9	Yes	4090 F2 Stope	3970 H1 Stope	2016/09/09 04:13:50	4150 c3, near H/F Intersection	0.48
	F/D	10	Yes	4150 D1/D2 & 4210 D1 + D2 Stopes	None	2016/08/06 22:42:00	4090 c1, B-West (HW); between B and D Veins	0.66
						2016/09/17 06:18:36	4090 c3, (FW) of F-Vein	0.22
						2016/09/17 04:40:15	4090 c3, B-West (HW)	1.27
						2016/09/17 04:35:34	4090 c4, (FW) of F/D Veins	0.83

Level	Hazard Map Results		Area Accessible?	Past Activity	Planned activity	Forecast Period		
	Location	Number of events				Date/Time	Location	Mag
4090/4150	F-West	5	No	4150 F6 Stope	4150 EF Stope			
4150/4210	D-West	12	No	4150 D1/D2 & 4210 D1 + D2 Stopes	None			
	F/D	15	Yes	4150 D1/D2 + F6 & 4210 D1 + D2 Stopes	4210 F2rec & 4150 EF Stopes	2016/09/17 04:41:54	4210 c3, B-West (HW) near F/B intersection	1.39
4210	F/B	6	Yes	4150 D1/D2 + F6 & 4210 D1 + D2 Stopes	4210 F2rec & 4150 EF Stopes	2016/09/23 07:12:36	4210 c3, near F/B intersection	0.67
						2016/09/17 04:40:17	4210 c3, near main acc.	0.31
						2016/09/17 04:43:24	4210 c2, G-North	0.36
4210/4280	H-North	9	No	4280 fh1/fh3 Stope	None	2016/09/23 17:29:47	4280 H-North, Between LHs	0.45
4280/4340	F/H	13	Yes	4340 BWS & 4280 fh1/fh3 Stopes	None	2016/08/08 16:58:55	4340 c2 F-Vein near main acc.	1.07
						2016/09/17 15:08:26	4340 c4 F-Vein, near TDB acc	2.1
						2016/09/17 06:05:02	4340 c1, G-North (FW) near main acc.	0.9
						2016/09/17 07:21:57	4340 c2, F-Vein; near main acc.	0.27
4400	H-North	4	No	4280 fh1/fh3 Stope	4460 HR1 Stope	2016/09/25 07:06:12	4400 c2, H-North (FW)	0.55
4520	Level acc.	4	Yes	None				

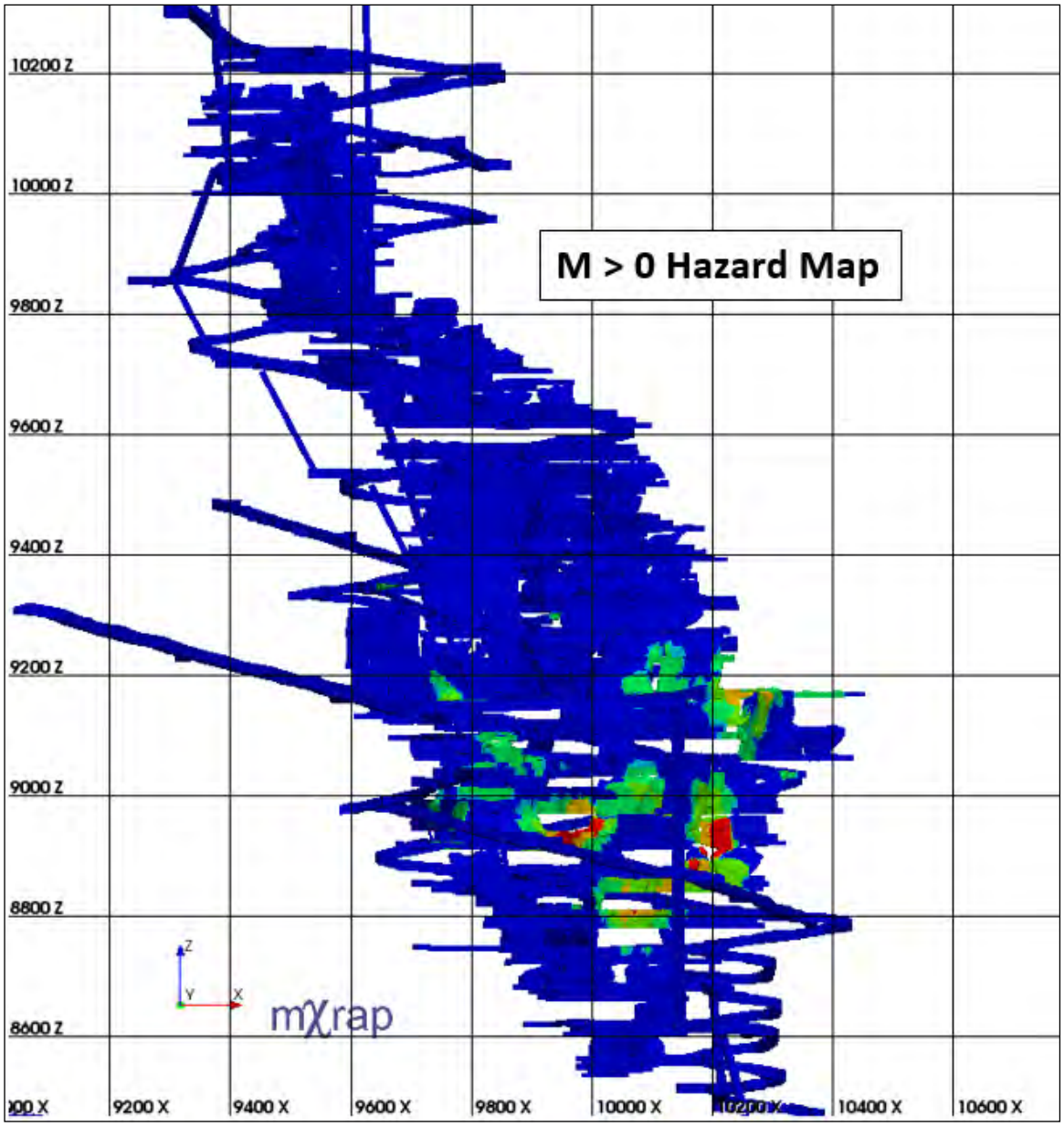
M > 0 Hazard Map
10200 Z
10000 Z
9800 Z
9600 Z
9400 Z
9200 Z
9000 Z
8800 Z
8600 Z
9200 X
9400 X
9600 X
9800 X
10000 X
10400 X
10600 X
Z
Y
X
mXrap

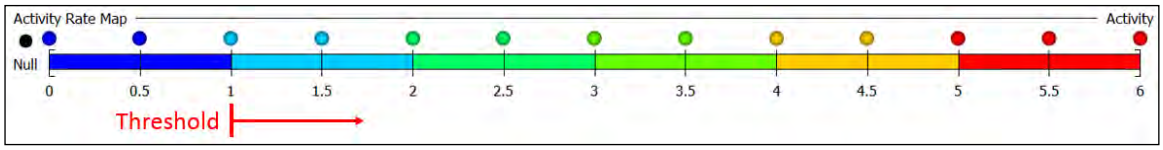
Activity Rate Map
Activity
Null
0
0.5
1
1.5
2
2.5
3
3.5
4
4.5
5
5.5
6
Threshold

Level	Hazard Map Results		Area Accessible?	Past Activity	Planned activity	Forecast Period		
	Location	Number of events				Date/Time	Location	Mag
3810	c6/AB acc.	2	Yes	3810-6 A1/A2 Stope	3810-3 A1 Stope			
3870	G-North abt.	2	Yes	3870 DE1 + B1&Pillar Stopes	3810-3 A1 Stope	2016/09/12 04:27:06	3810 c1, G-North abt.	0.42
3970	F-East LHs	2	No	4090 F2 Stope	3970 H1 Stope	2016/09/06 05:03:04	3970 F-East LH (FW)	1.34
	H-South/BP Dr.	5	Yes	4090 F2 Stope	3970 H1 Stope			
	H-North	2	Yes	4090 F2 Stope	3970 H1 Stope	2016/08/26 05:21:23	above 3970 H-North	0.28
	C-South/CRG Pillar acc.	2	Yes	None	None			
4030/4090	F/H	2	No	4090 F2 Stope	None			
	F/D	2	Yes	4150 D1/D2 Stope	None	2016/08/06 22:42:00	4090 c1, B-West (HW); between B and D Veins	0.66
						2016/09/17 04:40:15	4090 c3, B-West (HW)	1.27
						2016/09/17 04:35:34	4090 c4, (FW) of F/D Veins	0.83
						2016/09/17 06:18:36	4090 c3, (FW) of F-Vein	0.22
4090/4150	D-West	2	No	4150 D1/D2 Stope	None			
4150/4210	D-West abt.	2	No	4150 D1/D2 Stope	None			
	F-West	2	No	4150 F6 Stope	None			
	F/D	5	Yes	4210 D1 + D2 & 4150 D1/D2 + F6 Stopes	4210 F2rec Stope	2016/09/17 04:41:54	4210 c3, B-West (HW) near F/B intersection	1.39
						2016/08/05 10:50:10	4280 c2, G-North, near G/F/B intersection	1.77
	F/H	4	No	4150 F6 & 4280 fh1/fh3 Stopes	None	2016/09/09 04:13:50	4150 c3, near H/F Intersection	0.48

Level	Hazard Map Results		Area Accessible?	Past Activity	Planned activity	Forecast Period		
	Location	Number of events				Date/Time	Location	Mag
4210	F/B	2	Yes	4210 D1 + D2 & 4150 D1/D2 + F6 Stopes	4210 F2rec Stope	2016/09/17 04:40:17	4210 c3, near main acc.	0.31
						2016/09/23 07:12:36	4210 c3, near F/B intersection	0.67
						2016/09/25 21:40:12	4280 c4, F-North	1.02
	G-North	2	No	4210 D1 + D2 & 4150 D1/D2 + F6 Stopes	4210 F2rec Stope	2016/09/17 04:43:24	4210 c2, G-North	0.36
	CCF South abt.	2	No	4210 D1/D2 Stopes	None			
4280	H-North	4	No	4280 fh1/fh3 Stope	None	2016/09/23 17:29:47	4280 H-North, Between LHs	0.45
4280/4340	F/H	5	Yes	4280 fh1/fh3 Stope	None			

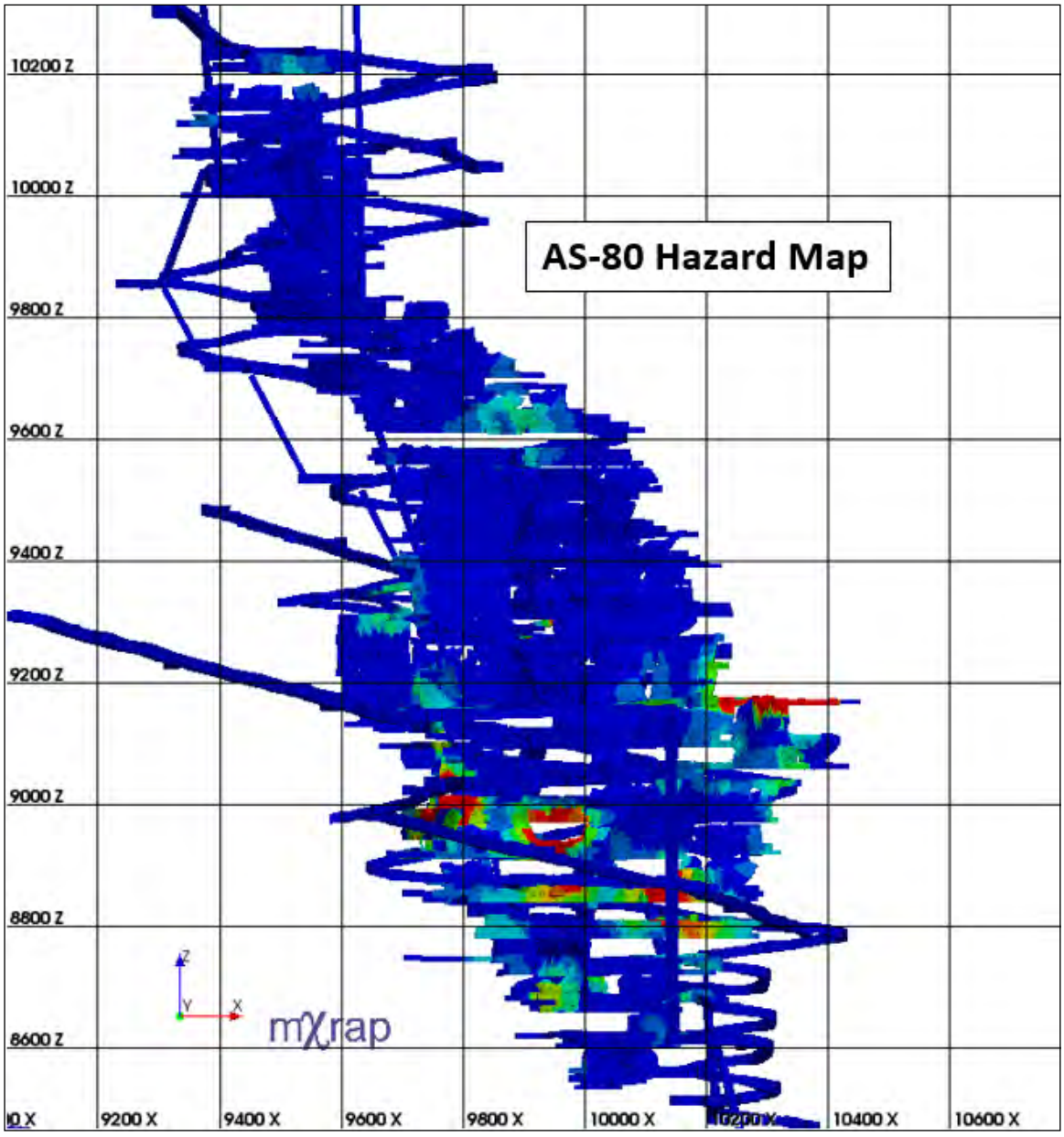
AS-80 Hazard Map
10200 Z
10000 Z
9800 Z
9600 Z
9400 Z
9200 Z
9000 Z
8800 Z
8600 Z
9200 X
9400 X
9600 X
9800 X
10000 X
10400 X
10600 X
Z
Y
X
mXrap

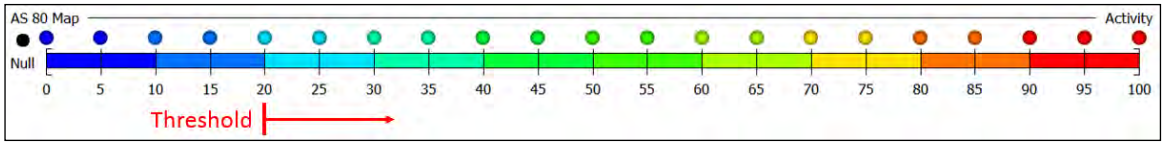
AS 80 Map
Activity
Null
0
5
10
15
20
25
30
35
40
45
50
55
60
65
70
75
80
85
90
95
100
Threshold

Level	Hazard Map Results		Area Accessible?	Past Activity	Planned activity	Forecast Period		
	Location	Number of events				Date/Time	Location	Mag
3510	Level acc./Remuck	20	Yes	None	None	2016/09/12 15:13:43	3450 c3, A-East/A1 far (FW)	0.5
3510/3570	DBZ (Central)	40	Yes	None	None			
3810	c3 acc.	40	Yes	3810 A1/A2 & 3870 DE1 + B1&Pillar Stopes	3810-3 A1 Stope			
	B-West abt.	20	Yes	3870 B1 Stope	3810-3 A1 Stope			
3810/3870	G-North Terminus	80	Yes	3870 DE1 + B1&Pillar Stopes	3810-3 A1 Stope	2016/09/12 04:27:06	3810 c1, G-North abt.	0.42
3870	c1 acc.	80	Yes	3870 DE1 + B1&Pillar Stopes	3810-3 A1 Stope			
3920	Level acc.	30	Yes	3870 DE1 + B1&Pillar Stopes	3810-3 A1 Stope			
3970	C-South Shrink	20	Yes	None	None			
	BP Dr.	40	Yes	None	None			
	H-South/BP Dr.	160	Yes	H-Vein c2 dev. & 4090 F2 Stope	3970 H1 Stope			
	H-North	120	Yes	H-Vein c2 dev.	3970 H1 Stope	2016/08/26 05:21:23	above 3970 H-North	0.28
4030/4090	F/H	20	No	4090 F2 Stope	3970 H1 Stope			
4090/4150	D-West abt.	160	No	4150 D1/D2 Stope & 4210 D1 + D2 Stopes	None	2016/09/17 08:11:56	4090 D-West abt.	0.73
	H-North abt.	40	No	4090 F2 Stope	3970 H1 Stope	2016/09/06 07:06:23	4090 c1, H-North, beneath LH stopes	1.27
4150/4210	F/D	160	Yes	4210 D1+D2 & 4150 D1/D2 + F6 Stopes	4210 F2rec & 4150 EF Stopes	2016/09/17 04:41:54	4210 c3, B-West (HW) near F/B intersection	1.39
	CCF South abt.	40	No	4210 D1+D2 & 4150 D1/D2 Stopes	4210 F2rec & 4150 EF Stopes			

Level	Hazard Map Results		Area Accessible?	Past Activity	Planned activity	Forecast Period		
	Location	Number of events				Date/Time	Location	Mag
4210	H-South	40	No					
	F/B	40	Yes	4210 D1+D2 & 4150 D1/D2 Stopes	4210 F2rec & 4150 EF Stopes	2016/09/23 07:12:36	4210 c3, near F/B intersection	0.67
						2016/09/17 04:40:17	4210 c3, near main acc.	0.31
						2016/09/25 21:40:12	4280 c4, F-North	1.02
	c1 H-South Acc.	20	Yes	4210 D1+D2 & 4150 D1/D2 Stopes	4210 F2rec & 4150 EF Stopes			
	G-North	20	No	4210 D1 + D2 & 4150 F6 + D1/D2 Stopes	4210 F2rec & 4150 EF Stopes	2016/09/17 04:43:24	4210 c2, G-North	0.36
4250	H-South	80	Yes	4280 fh1/fh3 Stope	None			
4280/4340	F/H	100	Yes	4280 fh1/fh3 Stope	None			
	G-North	100	No	4210 D2 Stope	None	2016/08/05 10:50:10	4280 c2, G-North, near G/F/B intersection	1.77
						2016/09/24 21:51:08	4340 c3, G-North terminus	0.41
						2016/09/17 06:05:02	4340 c1, G-North (FW) near main acc.	0.9
						2016/08/05 04:46:45	4340 above c3, F-Northwest near F/G intersection	0.15
						2016/09/17 05:46:26	4340, between F-Northwest and G-North	0.43
						2016/09/19 01:40:37	4340, between F-Northwest and G-North	0.5
						2016/09/17 12:36:27	above 4340, between F-Northwest and G-North	0.59
4340	H-South abt.	20	No	4280 fh1/fh3 Stope	4460 HR1 Stope			
4340/4400	Level acc.	20	Yes	4280 fh1/fh3 Stope	None			
4460	H-South abt.	60	Yes	4580 G1 Stope	4460 HR1 Stope			

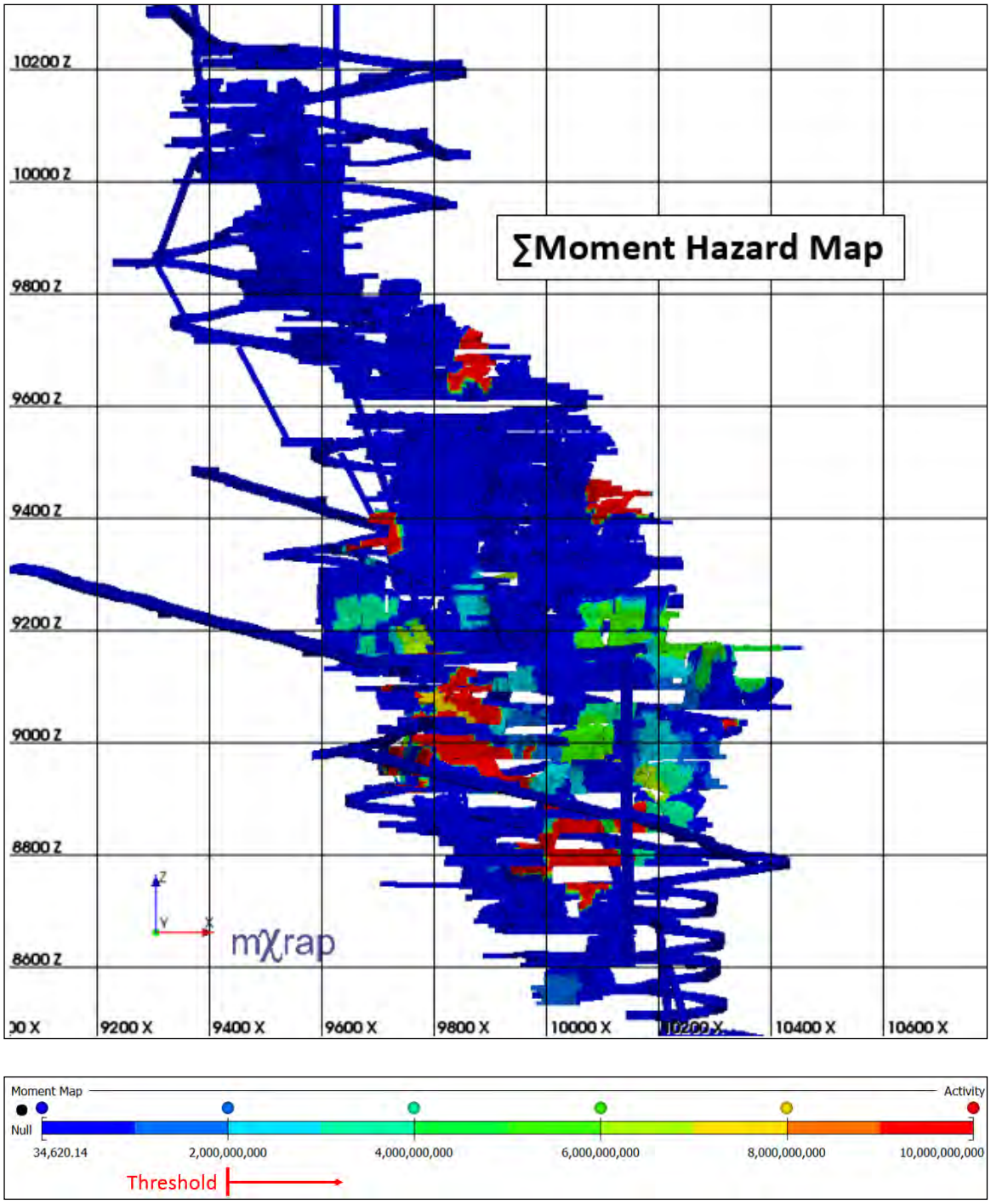
∑Moment Hazard Map
10200 Z
10000 Z
9800 Z
9600 Z
9400 Z
9200 Z
9000 Z
8800 Z
8600 Z
9200 X
9400 X
9600 X
9800 X
10000 X
10400 X
10600 X
Z
Y
X
mXrap

Moment Map
Activity
Null
34,620.14
2,000,000,000
4,000,000,000
6,000,000,000
8,000,000,000
10,000,000,000
Threshold

	HazMap Results		Area	Past Activity	Planned activity	Forecast Period		
Level	**Location**	**∑Mo (Nm2)**	**Accessible**			**Date/Time**	**Location**	**Mag**
3450/3510	TDBs/Z-East	1.20E+10	Yes	3810 A1/A2 Stope	None	2016/09/12 15:13:43	3450 c3, A-East/A1 far (FW)	0.5
3690/3750	F-East	1.20E+10	No	None	None			
3750/3810	B-West abt.	3.50E+10	Yes	3810 A1/A2 & 3870 B1 Stopes	3810 A3 Stope			
3870	G-North abt.	5.00E+09	No	3810 BFG & 3870 B1 Stopes	3810 A3 Stope	2016/09/12 04:27:06	3810 c1, G-North abt.	0.42
3870/3920	B-West Shrink	3.00E+09	No	3870 B1 Stope	None			
	BDE (Central)	2.00E+09	Yes	3870 DE + B1 Stopes	3810-3 A1 Stope			
3970	F-East Pillar	5.00E+09	Yes	4030 EF1 + EF2 + EF3/EF4 Stopes	3970 H1 Stope	2016/09/06 05:03:04	3970 F-East LH (FW)	1.34
						2016/09/17 10:43:55	3970 BP Dr. (FW) side of F-vein	0.22
	BP Dr./H-South	5.00E+09	Yes	3970 c2 dev. & 4090 F2 & 4280 fh1/fh3 Stopes	3970 H1 Stope			
	H-North	5.00E+09	Yes	3970 c2 dev. & 4090 F2 & 4280 fh1/fh3 Stopes	3970 H1 Stope	2016/08/26 05:21:23	above 3970 H-North	0.28
	C-South/BP Dr.	5.00E+10	Yes	H-Fault activity	None	2016/09/17 04:30:00	3970 Craig Pillar Acc, near H-Fault	2.29
4030/4090	F/D	3.50E+10	Yes	4030 EF2 & 4150 D1/D2 Stope	4150 EF Stope	2016/08/06 22:42:00	4090 c1, B-West (HW); between B and D Veins	0.66
						2016/09/17 04:40:15	4090 c3, B-West (HW)	1.27
						2016/09/17 06:18:36	4090 c3, (FW) of F-Vein	0.22
						2016/09/17 04:35:34	4090 c4, (FW) of F/D Veins	0.83

Level	Hazard Map Results		Area Accessible?	Past Activity	Planned activity	Forecast Period		
	Location	∑Mo (Nm2)				Date/Time	Location	Mag
4090/4150	D-West	3.00E+10	No	4150 D1/D2 & 4210 D1 + D2 Stopes	4210 F2rec Stope			
4150/4210	F-West	5.00E+09	No	4150 F6 & 4210 F2rec Stopes	4210 F3 Stope	2016/09/09 04:13:50	4150 c3, near H/F Intersection	0.48
	F/D	7.00E+10	Yes	4150 F6 & 4210 D1 + D2 + F2rec Stopes	4210 F3 Stope	2016/09/17 04:41:54	4210 c3, B-West (HW) near F/B intersection	1.39
						2016/08/05 10:50:10	4280 c2, G-North, near G/F/B intersection	1.77
4210	CCF (North)	1.50E+10	No	4150 D1/D2 & 4210 D1 + D2 Stopes	4210 F2rec Stope	2016/09/20 05:44:21	4280 c4, B-West	1.42
	CCF (South)	5.00E+10	No	4150 F6 & 4210 D1 + D2 + F2rec Stopes	4210 F3 Stope			
4210/4280	H-North LHs	6.00E+09	No	4280 fh1/fh3 Stope	None	2016/09/23 17:29:47	4280 H-North, Between LHs	0.45
4280/4340/4400	F/H	9.00E+12	Yes	4280 fh1/fh3 & 4340 BWS Stopes	None	2016/09/17 06:05:02	4340 c1, G-North (FW) near main acc.	0.9
						2016/08/08 16:58:55	4340 c2 F-Vein near main acc.	1.07
						2016/09/17 07:21:57	4340 c2, F-Vein; near main acc.	0.27
						2016/09/17 15:08:26	4340 c4 F-Vein, near TDB acc	2.1
						2016/09/25 07:06:12	4400 c2, H-North (FW)	0.55
4520	Fuel Bay	1.40E+10	Yes	4280 fh1/fh3 & 4150 D1/D2 Stopes	None			

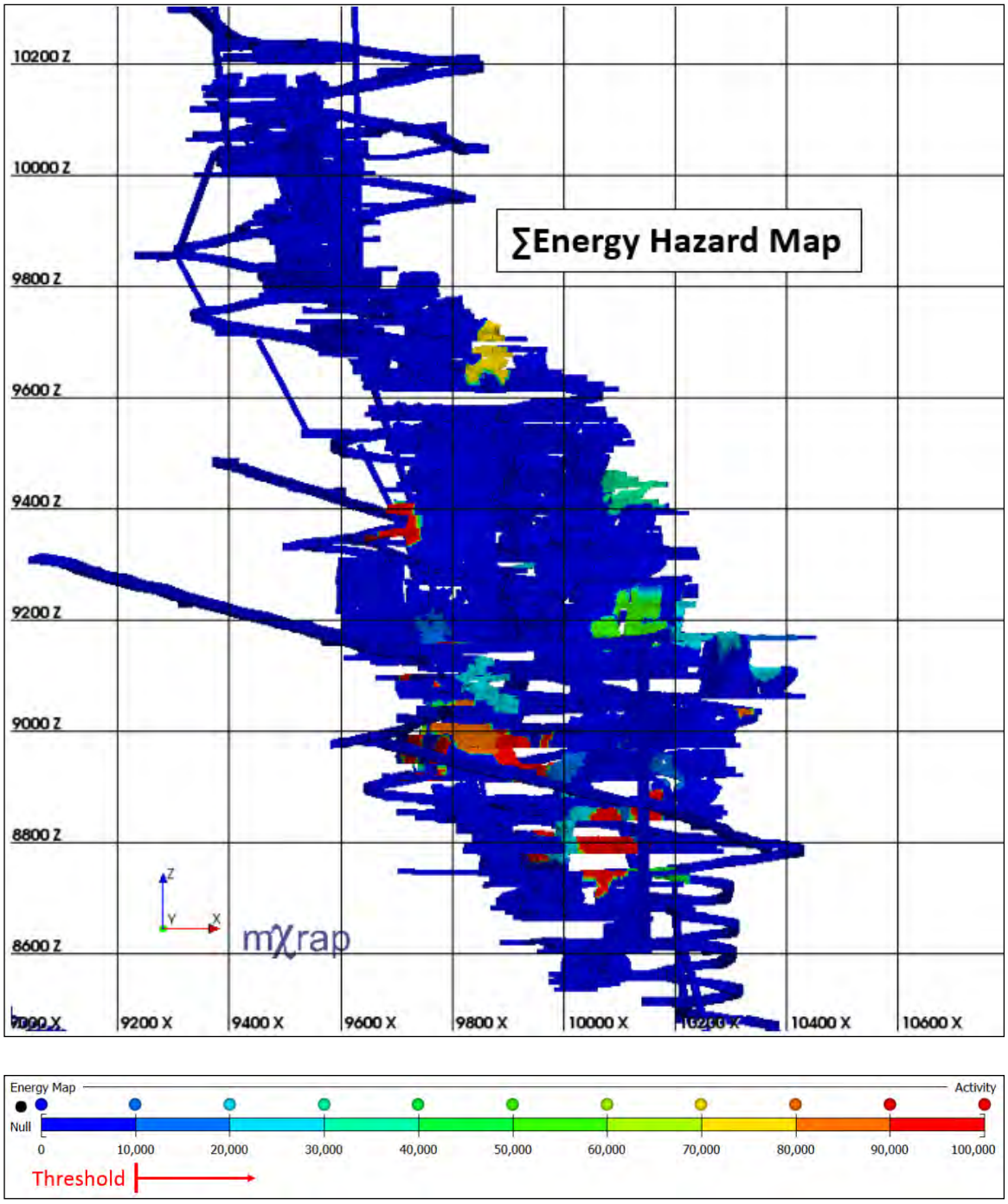
∑Energy Hazard Map
10200 Z
10000 Z
9800 Z
9600 Z
9400 Z
9200 Z
9000 Z
8800 Z
8600 Z
9200 X
9400 X
9600 X
9800 X
10000 X
10400 X
10600 X
Z
Y
X
mXrap

Energy Map
Activity
Null
0
10,000
20,000
30,000
40,000
50,000
60,000
70,000
80,000
90,000
100,000
Threshold

Level	Hazard Map Results		Area Accessible?	Past Activity	Planned activity	Forecast Period		
	Location	∑E (J)				Date/Time	Location	Mag
3450/3510	DBZ Central	70000	Yes	3810 A1/A2 Stope	None			
3690/3750	F-East	30000	No	None	None			
3810	B-West abt.	150000	Yes	3810 A1/A2 & 3870 B1 Stopes	3810 A3 Stope			
3870	G-North abt.	20000	No	3810 BFG & 3870 B1 Stopes	3810 A3 Stope	2016/09/12 04:27:06	3810 c1, G-North abt.	0.42
3970	F-East Pillar	50000	Yes	4030 EF1 + EF2 + EF3/EF4 Stopes	3970 H1 Stope	2016/09/06 05:03:04	3970 F-East LH (FW)	1.34
						2016/09/17 10:43:55	3970 BP Dr. (FW) side of F-vein	0.22
	BP Dr./H-South	20000	Yes	3970 c2 dev. & 4090 F2 & 4280 fh1/fh3 Stopes	3970 H1 Stope			
	H-North	10000	Yes	3970 c2 dev. & 4090 F2 & 4280 fh1/fh3 Stopes	3970 H1 Stope	2016/08/26 05:21:23	above 3970 H-North	0.28
	C-South/BP Dr.	300000	Yes	H-Fault activity	None			
4030/4090	F/D	20000	Yes	4030 EF2 & 4150 D1/D2 Stope	4150 EF Stope	2016/08/06 22:42:00	4090 c1, B-West (HW); between B and D Veins	0.66
						2016/09/17 04:40:15	4090 c3, B-West (HW)	1.27
4150	H-North abt.	80000	No	4150 D1/D2 & 4180 fh1/fh3 Stopes	4150 EF & 3970 H1 Stopes	2016/09/06 07:06:23	4090 c1, H-North, beneath LH stopes	1.27
	F/H	10000	No	4150 D1/D2 & 4180 fh1/fh3 Stopes	4150 EF & 3970 H1 Stopes	2016/09/09 04:13:50	4150 c3, near H/F Intersection	0.48
4150/4210	D-West	80000	No	4150 D1/D2 & 4210 D1 + D2 Stopes	4210 F2rec Stope			
	F/D	200000	Yes	4150 D1/D2 + F6 & 4210 D1 + D2 Stopes	4210 F2rec Stope	2016/09/17 04:41:54	4210 c3, B-West (HW) near F/B intersection	1.39

Level	Hazard Map Results		Area Accessible?	Past Activity	Planned activity	Forecast Period		
	Location	∑E (J)				Date/Time	Location	Mag
4210	CCF (North)	150000	No	4150 D1/D2 + F6 & 4210 D1 + D2 Stopes	4210 F2rec Stope	2016/09/20 05:44:21	4280 c4, B-West	1.42
	CCF (South)	150000	No	4150 D1/D2 + F6 & 4210 D1 + D2 Stopes	4210 F2rec Stope			
	B-Vein	50000	Yes	4150 D1/D2 + F6 & 4210 D1 + D2 Stopes	4210 F2rec Stope			
4280	H-North	150000	No	4280 fh1/fh3 Stope	None	2016/09/23 17:29:47	4280 H-North, Between LHs	0.45
4280/4340	F/H	115000000	Yes	4280 fh1/fh3 Stope	None			
4340	TDBs	150000	Yes	4280 fh1/fh3 Stope	4210 F2rec + F3 Stopes	2016/09/17 06:05:02	4340 c1, G-North (FW) near main acc.	0.9
						2016/08/08 16:58:55	4340 c2 F-Vein near main acc.	1.07
						2016/09/17 07:21:57	4340 c2, F-Vein; near main acc.	0.27
						2016/09/17 15:08:26	4340 c4 F-Vein, near TDB acc	2.1
4400	H-North	200000	No	4280 fh1/fh3 Stope	None	2016/09/25 07:06:12	4400 c2, H-North (FW)	0.55
	Level acc./I-North	50000	Yes	4280 fh1/fh3 Stope	None			

Appendix E: Hazard Map Scaling

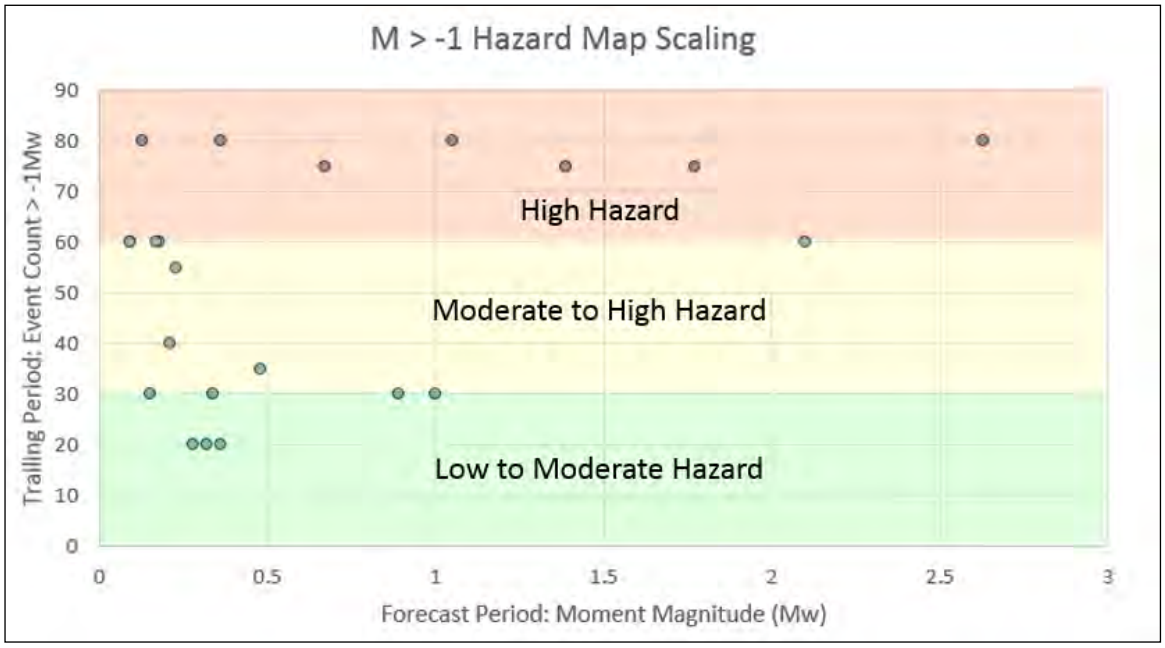

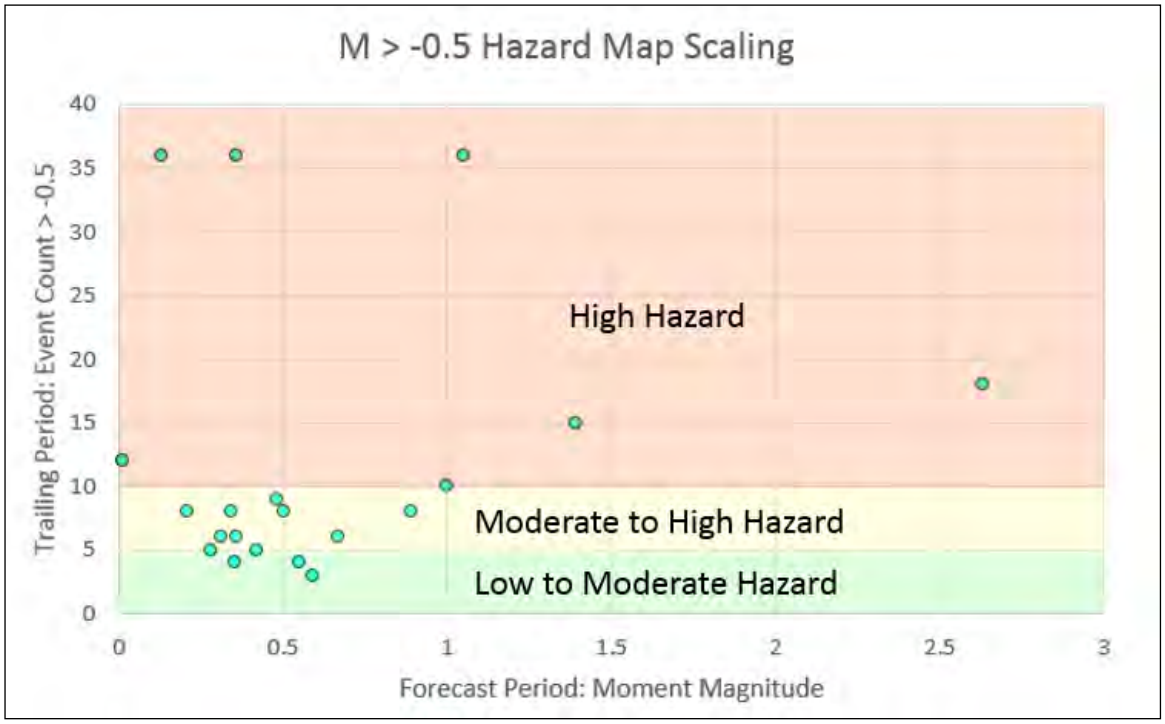

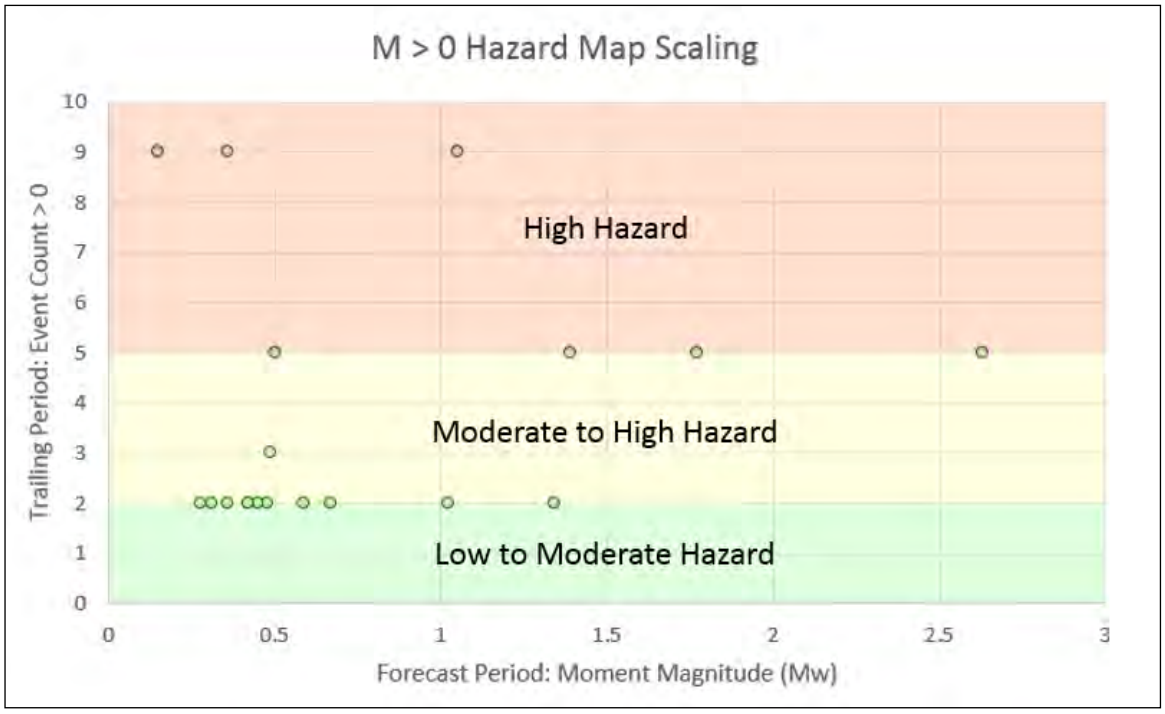
M > 0 Hazard Map Scaling
Trailing Period: Event Count > 0
Forecast Period: Moment Magnitude (Mw)
High Hazard
Moderate to High Hazard
Low to Moderate Hazard
0
1
2
3
4
5
6
7
8
9
10
0
0.5
1
1.5
2
2.5
3

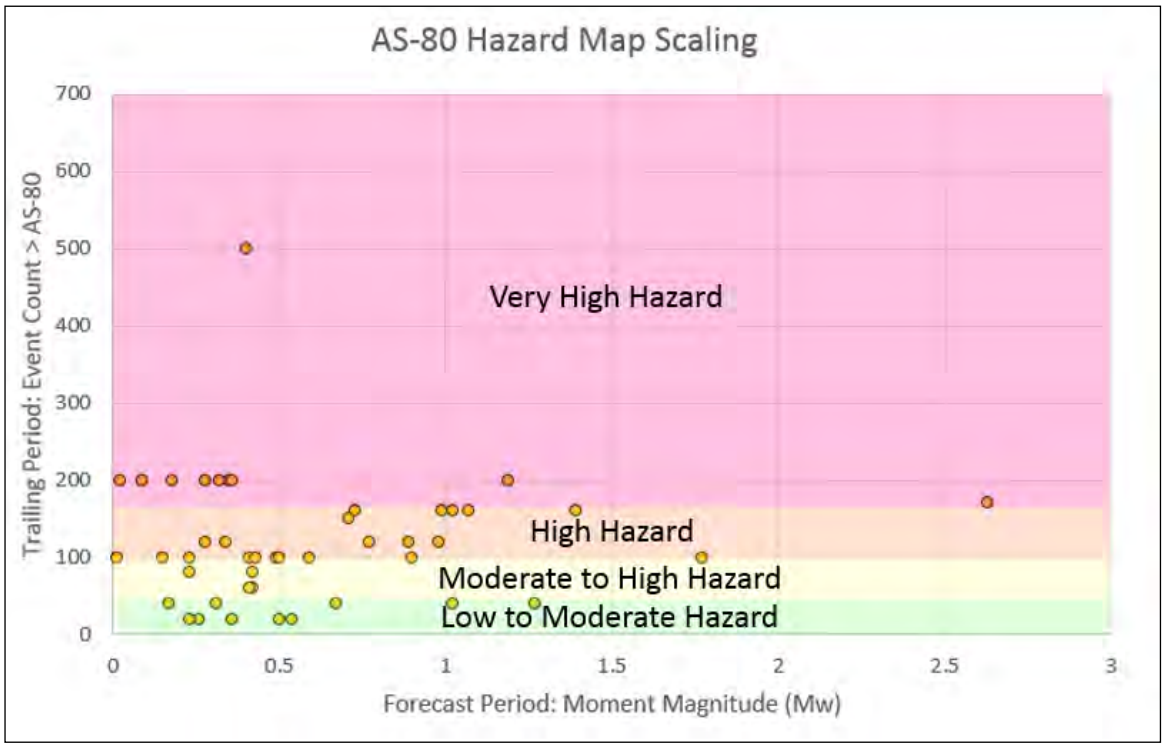
AS-80 Hazard Map Scaling
Trailing Period: Event Count > AS-80
Forecast Period: Moment Magnitude (Mw)
Very High Hazard
High Hazard
Moderate to High Hazard
Low to Moderate Hazard
0
100
200
300
400
500
600
700
0
0.5
1
1.5
2
2.5
3

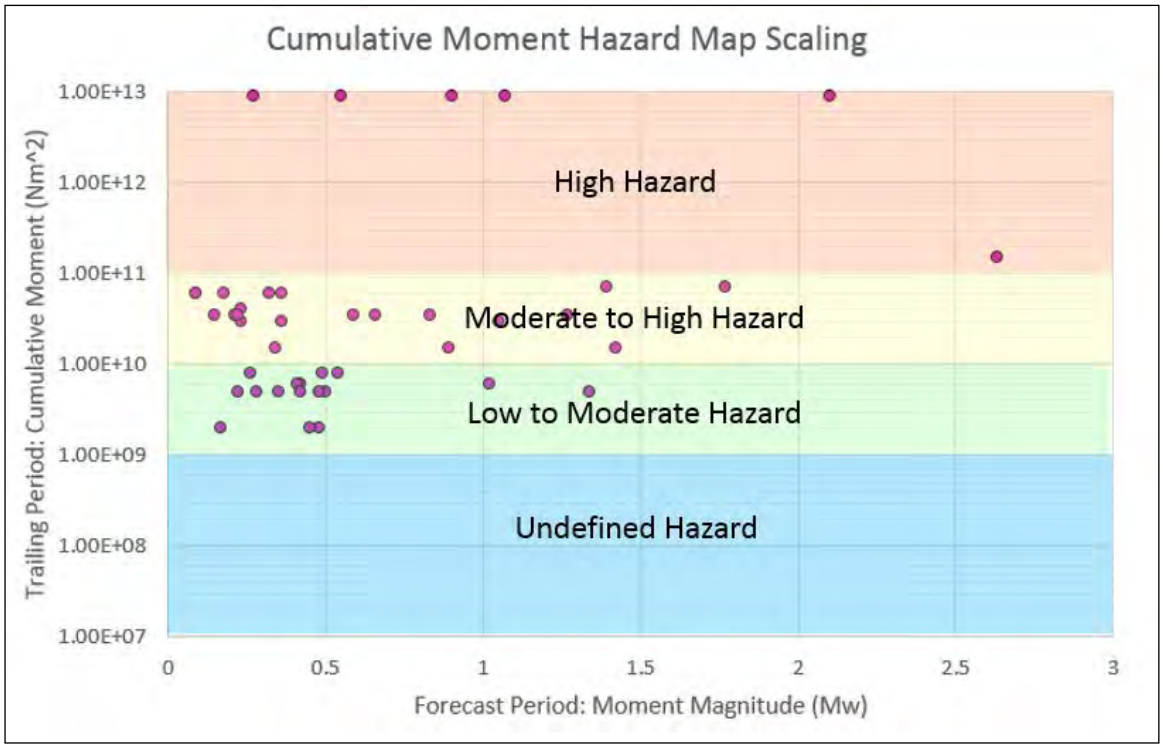
Cumulative Moment Hazard Map Scaling
Trailing Period: Cumulative Moment (Nm^2)
1.00E+13
1.00E+12
1.00E+11
1.00E+10
1.00E+09
1.00E+08
1.00E+07
High Hazard
Moderate to High Hazard
Low to Moderate Hazard
Undefined Hazard
0
0.5
1
1.5
2
2.5
3
Forecast Period: Moment Magnitude (Mw)

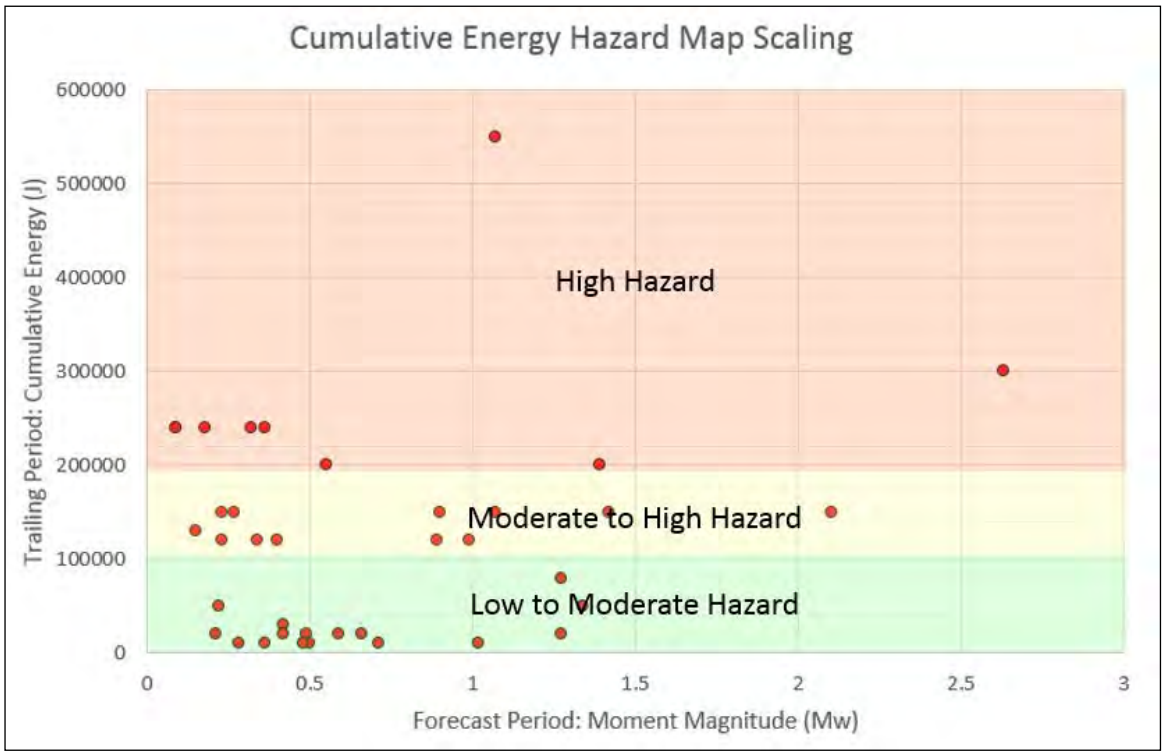
Cumulative Energy Hazard Map Scaling
Trailing Period: Cumulative Energy (J)
600000
500000
400000
300000
200000
100000
0
High Hazard
Moderate to High Hazard
Low to Moderate Hazard
0
0.5
1
1.5
2
2.5
3
Forecast Period: Moment Magnitude (Mw)